THE ROLE OF CALCIUM CALMODULIN KINASES IN MODIFICATION OF THE P53 SIGNALLING PATHWAY

Jennifer A. Faulkner

Thesis submitted for the degree of Doctor of Philosophy

at the University of Edinburgh

2009

ACKNOWLEDGEMENTS

Firstly, I would like to thank my supervisors, Ted Hupp and Ashley Craig, for their help, advice, patience and encouragement throughout my PhD studies. I would also like to thank Kathryn Ball for her helpful advice and guidance with my project. I would also like to thank all the members the lab, past and present, for their invaluable support and advice. Thanks to Jenny, Liz, Bart, Emma, Iro, Havi, Vikram, Mirjam, Lisa, Nicky, Ben, Madga, Sarah, David, Hannah, Euan, Susi, Angeli, Nathalie, Bodil, Erin, Craig, Jew Kwang, Yao, Ashley, Maura, Andrea, Angela, Ted, Kathryn, Lindsey, Lenny and Lee. Thanks to Nathalie for all her assistance and advice on all things cell culture related. A special thanks to Jenny and Lisa for sharing a bench with me, for 'keeping me right' and thanks to Jenny for all her technical help and advice. A special thanks to Lisa for being a great friend, fellow student and conference buddy. A huge thank you to Nicky and Ashley for proof-reading my thesis. A special thank you to Nicky for all her useful advice and technical assistance with all things science and IT related (and thanks too to Ross the master document creator!). I am also very grateful to all the support staff including wash-up and administration for all their help.

Many thanks to all my family and friends who have supported me throughout my studies. A special thank you to my Mum and late Dad, for all their love, support and encouragement, and especially to my Dad, who would have been so proud to see me complete my studies. Finally, a very special thank you to Graham, my best friend, for his endless love and support, and for always believing in me.

I am very grateful to Cancer Research UK for the funding I have received.

DECLARATION

I hereby declare that I am the author of this thesis and that I performed all the work described herein, except where specifically stated. All sources of information have been acknowledged by means of reference. The work described in this thesis has not been accepted in any previous application for a degree.

Jennifer A. Faulkner January 2009

ABSTRACT

P53 is a tetrameric transcription factor which exhibits DNA binding activity through its core domain which encompasses the conserved domains (known as Box II, III, IV and V). The N-terminal domain of p53 provides a scaffold for binding of components of the transcriptional machinery. Phosphorylation at residues within the N-terminal transactivation domain of p53 such as Serine 20 is a crucial event in the activation of p53. It stabilises the binding of the co-activator p300, reduces the binding of the inhibitory partner Mdm2 and enhances activation of p53 target genes. The identification of enzymes that phosphorylate p53 transactivation domain is an important development in the ongoing mapping of signaling pathways that control p53-dependent transcription and resultant tumour suppression. Environmental and physiological stresses activate p53 which has led to the creation of several hypothetical models in which tumour suppressor kinases mediate p53 activation by phosphorylation at Serine 20. Although much researched the identity of the main Serine 20 kinase in cells remains undefined. In this study we have identified Calcium Calmodulin kinase superfamily (CAMK) members as potent Serine 20 kinases in cells and show that the co-transfection of p53 peptides derived from the conserved domains can modify this response. Moreover, we show that the multi-protein docking site, p53 Box V domain, is required for Serine 20 phosphorylation and ubiquitination of p53. To further define the domains required for the interaction of p53 with CAMK superfamily members, mutagenesis of p53 was performed. Using transcriptional and binding based assays we were able to establish that p53 does indeed form an interaction with Chk1 and DAPK1. Development of cell models and gene expression studies demonstrated that depletion of Chk1 and DAPK1 results in activation of the p53 signalling pathway. There may therefore be a role for kinases as negative regulators of p53 and a potential for the development of kinases as drug targets for reactivation of the p53 pathway.

ABBREVIATIONS

aa	Amino acid
Ab	Antibody
AMP	Adenosine monophosphate
AMPK	5'AMP-activated protein kinase
ARF	ADP ribosylation factor
ASPP	Apoptosis-stimulatory protein of p53
A-T	Ataxia-telangiectasia
ATM	Ataxia-telangiectasia Mutated
ATP	Adenosine triphosphate
ATR	ATM and Rad-3 related
BER	Base excision repair
βGP	Beta Glycerol Phosphate
BAX	Bcl-2 associated protein X
Bcl-2	B-cell lymphoma-2
BSA	Bovine serum albumin
CAMK	Calcium Calmodulin kinase superfamily
C-terminus	Carboxy terminus of protein
CBP	CREB binding protein
Cdc	Cell division cycle
CDK	Cyclin dependent kinase
CHIP	Chaperone-associated ubiquitin ligase
Chk1	Checkpoint kinase 1
Chk2	Checkpoint kinase 2
CIP1	CDK interacting protein 1
CK	Casein kinase
DAPK1	Death-associated protein kinase 1
DBD	DNA binding domain

DMEM	Dulbecco's modified eagle's medium
DMSO	Dimethyl Sulfoxide
DNA	Deoxyribonucleic acid
DNA-PK	DNA-dependent protein kinase
DRP-1	DAPK related protein 1
DSB	Double strand break
dsRNA	Double stranded RNA
DTT	Dithiolthretiol
E2F-1	E2F transcription factor 1
E.Coli	Escherichia Coli
ECL	Enhanced chemiluminescence
EDTA	Ethylene diamine tetra-acetic acid
ERK	Extracellular single related kinase
FBS	Foetal bovine serum
FL	Full-length
G1	Gap phase 1
G2	Gap phase 2
GADD	Growth arrest and DNA damage gene
GST	Glutathione S-transferase
Gy	Gray
HAT	Histone acetyltransferase
HAUSP	Herpes virus-associated ubiquitin-specific protein
HDAC	Histone deacetylase
HEPES	N-(2-Hydroxethyl)piperazine-N'-(2-ethanesulfonic acid)
HIF-1	Hypoxia-inducible factor 1
HR	Homologous recombination
HRP	Horse radish peroxidase
HU	Hydroxyurea
IFN	Interferon
IP	Immunoprecipitation

IR	Ionising radiation
JNK	Jun NH_2-terminal kinase
kb	Kilo-base
kDa	Kilodalton
LB	Luria Bertani
LF 2000	Lipofectamine 2000
LFS	Li-Fraumeni syndrome
M	Mitosis
mA	Milli-amperes
MAPK	Mitogen-activated protein kinase
Mdm2	Mouse double minute 2
MEF	Mouse Embryonic Fibroblast
MMR	Mismatch repair
MRN	Mre11/Nbs1/Rad50
mTOR	Mammalian target of rapamycin
MTT	Methylthiazolylphenyl-tetrazolium bromide
NE	Nuclear extract
NER	Nucleotide excision repair
NES	Nuclear export signal
NFκB	Nuclear factor-kappa B
NHEJ	Non-homologous end joining
NHF	Normal Human Fibroblast
NLS	Nuclear localization signal
NO	Nitric oxide
NP40	Nonidet P40
N-terminus	Amino terminus of a protein
ORF	Open reading frame
PAGE	Polyacrylamide gel electrophoresis
PBS	Phosphate buffered saline

PBST	PBS-Tween 20 (0.01% v/v)
PCNA	Proliferating cell nuclear antigen
PI3-K	Phosphoinositide 3-kinase
PIKK	Phosphoinositide 3-kinase related kinase
PLB	Passive lysis buffer
PML	Promyelocytic leukaemia
PMSF	Phenylmethanesulphonyl fluoride
Pu	Purine
PUMA	p53 upregulated modulator of apoptosis
Py	Pyrimidine
REG	Regulatory domain
RLU	Relative light unit
RNA	Ribonucleic acid
RNAi	RNA interference
ROS	Reactive oxygen species
RT-PCR	Reverse transcriptase polymerase chain reaction
SDS	Sodium dodecyl sulfate
Ser	Serine
SH-3	Src homology domain 3
shRNA	Short hairpin RNA
siRNA	Small interfering RNA
SMG	Suppressor with morphogenetic effect on genitalia
SSB	Single strand break
SUMO	Small ubiquitin-like modifier
TA	Transactivation domains
TAF	TBP-associated factors
TBP	TATA box-binding protein
TET	Tetramerisation domain
Thr	Threonine

TK	Tyrosine kinase
TNF-α	Tumour necrosis factor alpha
Tris	Tris(hydroxymethyl)methylamine
TRRAP	Transformation/translation domain associated protein
TSC	Tuberous sclerosis
Tween 20	Polyoxyethylene sorbitan monolaurate
Ub	Ubiquitin
UV	Ultra violet light
v/v	Volume per volume
w/v	Weight per volume
WAF1	Wild-type p53 activated fragment
WT	Wild Type

LIST OF CONTENTS

LIST OF FIGURES

LIST OF TABLES

1 INTRODUCTION

1.1 The p53 tumour suppressor

The tumour suppressor gene *p53* is a key gene involved in the control of cancer progression. It has been described as the 'guardian of the genome' (Lane 1992) and in this report we will describe the function and activity of p53 as a tumour suppressor.

1.1.1 Discovery and Classification

The clarification of the role of p53 in carcinogenesis has been and continues to be a complex process. A protein, which was subsequently named p53, was initially identified in 1979 following the observation that antibodies against a SV40 large T antigen from tumours produced by SV-40 transformed cells coimmunoprecipitated a protein of molecular mass of 53kDa. It was concluded that p53 interacted with this SV40 large T antigen (Lane and Crawford 1979; Linzer and Levine 1979) and due to its high expression levels in transformed cells, p53 was termed a transformation-associated protein (Lane and Crawford 1979; Linzer et al. 1979; Rotter et al. 1980). Supporting this classification were the findings that transformed cells as well as cells from patients with various types of tumours contained elevated p53 levels, whereas in non-transformed cells p53 levels were negligible (Oren et al. 1982). Several studies then went on to examine the role of p53 as a cell-cycle dependent protein, and the results suggested that p53 was a regulator of growth (Milner 1984; Reich and Levine 1984). *p53* was subsequently classified as a proto-oncogene due to its apparent upregulation of expression in proliferating cells (Milner and Milner 1981; Milner 1984; Reich and Levine 1984). It was also demonstrated following exposure of non-transformed cells to UV irradiation, that there was accumulation of p53 due to post-translational stabilization suggesting that p53 may be involved in DNA synthesis (Maltzman and Czyzyk 1984).

The molecular cloning of the TP53 gene (Zakut-Houri et al. 1983; Zakut-Houri et al. 1985) and discovery of the sequence of the mouse wild-type TP53 gene led to the

revelation that previous experiments had employed mutant p53 variants (Eliyahu et al. 1988; Finlay et al. 1988) and that wild-type p53 actually suppressed oncogene-mediated transformation (Eliyahu et al. 1989; Finlay et al. 1989). This development clearly established *p53* as a bona fide tumour suppressor instead of the previous classification as an oncogene. Since then there has been significant development in the clarification of the role of p53 in carcinogenesis. P53 protein was shown to be lost or inactivated due to the presence of mutations in *p53* in about half of human cancers from a wide variety of tissues and it is now known to be the most commonly mutated gene in human cancer (Baker et al. 1989; Baker et al. 1990; Hollstein et al. 1994). These developments have provided a basis for elucidation of the various roles of p53 in carcinogenesis and have established distinct roles in which one of three events can occur; firstly, p53 loss of function, where the *p53* gene is mutated or there is complete loss of the gene; secondly, mutant p53 dominant-negative function, where there is promotion of tumourigenesis due to the mutant p53 inactivating WT p53 in cells by oligomerisation; and finally, mutant p53 gain of function, where expression of mutant p53 in cells lacking WT p53 enhances their tumourigenic potential (Weisz et al. 2007). p53 has been identified as a key regulator in a wide variety of cellular processes such as cell-cycle control, DNA repair, genome stability, senescence and programmed cell death, most of which will be discussed in this report (see below).

1.1.2 Structure of p53

The human *p53* gene was shown to be localized to the short arm of chromosome 17 (17q13), spanning approximately 20kb of DNA and composed of 11 exons the first of which is non-coding, localized 8 -10 kb away from exons 2 through 11 (Benchimol et al. 1985). An extensive phylogenetic study revealed that p53 has been conserved throughout evolution and by cross-species comparison of amino-acid sequences, the existence of five highly conserved domains (within amino acid residues 13 – 23, 117 – 142, 171 – 181, 234 – 250 and 270 – 286) was revealed (Soussi et al. 1990; Soussi and

May 1996). These domains were subsequently termed domains I to V or Box I to V (see Figure 1.1) and shown to be crucial for p53 functions (Soussi and May 1996).

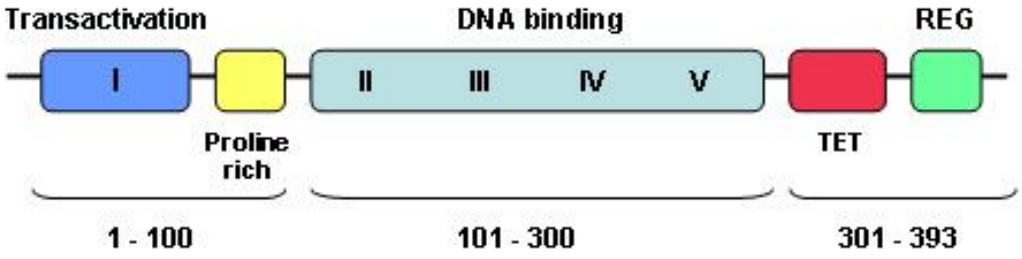

Figure 1.1 The protein structure of p53.
The amino terminus (1 to 42) contains the transactivation domain and the highly conserved region I (Box I). The proline rich region is adjacent to the transactivation domain and forms part of the N-terminal region. The central region contains the DNA-binding domain (101 to 300). The C-terminal negative regulatory region (301 to 392) contains the oligomerisation domain and a nuclear export signal.

The human p53 protein (as shown in Figure 1.1) consists of 393 amino-acids and consists of four major functional domains. The N-terminal region contains a transcriptional activation domain (amino-acids 1 - 42) and a proline rich domain (amino-acids 62 -92) , the central region contains the DNA-binding domain (amino-acids 102 –

292) and the C-terminal region contains both the oligomerisation domain (amino-acids 323 – 356) and a regulatory domain (amino-acids 360 – 393) (May and May 1999). These four domains modulate the activity of p53 as a stress-induced sequence-specific DNA-binding protein and transcription factor. The detail of each structure and the relation to function will be discussed in the following sections.

1.1.2.1 The amino terminus

The amino terminal region of p53 (amino-acids 1 - 42) contains the transactivation domain through which p53 interacts with components of the transcriptional machinery and a smaller highly conserved domain known as Box-I. This Box-I domain directs the binding of p53 to proteins such as p300 (a positive regulator of p53 required to drive p53-dependent gene expression) and the components of the basal transcription complex TFIID, TATA box binding protein (TBP) and TBP-associated factors (TAF) (Lu and Levine 1995). The regulation of protein-protein interactions can be modulated by phosphorylation within the Box-I domain or by protein-protein interactions which compete with p300 docking. Phosphorylation within the Box-I region at sites Ser 15, Thr 18 and Ser 20 stabilizes the binding of the co-activator p300 (Lambert et al. 1998; Dornan and Hupp 2001; Dornan et al. 2003).

In contrast to these positive regulatory binding factors, negative regulation of p53 occurs following the binding of Mdm2 or adenovirus E1B-55kDa which bind to amino acid residues 19, 22 and 23 within the transactivation domain (Momand et al. 1992; Lin et al. 1994; Levine 1997). The binding of Mdm2 inhibits the transcriptional function of p53 by competing with p300 and by promoting ubiquitination of p53 in the nucleus and the subsequent export of p53 to the cytoplasm for degradation by the 26S proteasome (Honda et al. 1997; Kubbutat et al. 1997; Michael and Oren 2003).

The N-terminal region also contains a proline rich region (also known as the Src homology 3-like or SH3 domain) which is characterized by the recurrence of proline residues in the form of PXXP (where X is any amino acid). This region, which includes five repeats of the PXXP motif, has similarity to the SH3-binding proteins. In addition, this motif is often required for p53-mediated apoptosis in conjunction with proteins such as ASPP (Trigiante and Lu 2006). It has also been shown that this domain may be important for p300 binding and furthermore it can allosterically control DNA-dependent acetylation of p53, thus controlling p53 activity (Dornan et al. 2003).

1.1.2.2 The Central domain

The central region from amino-acids 102 – 292 contains the sequence specific DNA-binding domain which consists of the four highly conserved regions Box II – V. The consensus DNA-binding site contains two copies of the 10bp motif 5' – PuPuPuCWWGPyPyPy – 3' (Pu is a purine base, Py is a pyrimidine base and W means A or T) which p53 recognizes and binds to (el-Deiry et al. 1992). The central region also functions as a protein binding domain, interacting with proteins such as ASPP2 (Gorina and Pavletich 1996). Elucidation of the crystal structure of the core domain allowed the identification of a large β sandwich that forms a scaffold for a loop-sheet-helix and two loops that coordinate a zinc ion (Cho et al. 1994). The scaffold anchors the loops and participates in head-to-tail dimerisation, loop L1 binds to DNA within the major groove, loop L2 binds to DNA within the minor groove and loop L3 packs against L1, stabilizing it. The zinc atom stabilizes the structure of the loops and the loop-sheet-helix motif form the DNA binding surface of p53 (Cho et al. 1994) (also see Figure 4.6 for details of this structure). The central region contains 80 - 90% of the mutations within p53 found in human cancers, the majority of mutations residing within the three loops. These mutations result in either prevention of DNA binding or destabilisation of the protein (May and May 1999).

1.1.2.3 The Carboxy terminal

The C-terminal region (residues 300 – 393) includes a flexible linker region connecting the central core domain and the C-terminal region, and a tetramerisation domain from amino-acids 323 – 356, which is also known as the oligomerisation domain responsible for tetramerisation of the p53 structure (Johnson et al. 1995). The tetramerisation domain forms a highly symmetrical tetramer composing of 4 monomers each of which contains a turn, a β-strand, a second turn and an α-helix. Two monomers form a dimer and two dimers interact through their α-helices to form a four-helix bundle (May and May 1999). Tetramerisation is important for modulation of p53's tumour suppressor activity and efficient transactivation (May and May 1999). The C-terminal region is also thought to be important for nuclear localization and is known to contain three nuclear localization signals, which when altered leads to cytoplasmic localization of p53, thus affecting the tumourigenesis activity of p53 (Shaulsky et al. 1990; Shaulsky et al. 1991).

The C-terminal region also contains a basic region (amino-acids 363 – 393), known as the regulatory domain which is adjacent to the oligomerisation domain. This region acts as a negative regulator of specific binding by p53, which due to the allosteric regulation of the DNA-binding domain, maintains the p53 tetramer in an inactive state (Hupp et al. 1992). Post-translational modification alters the specific activity of p53. Phosphorylation of Ser 392 within this domain is thought to regulate the stabilization of the tetramerisation domain and it has been shown that mutation of a site adjacent to Ser 392 (Lys 386) can increase p53's activity, most likely due to the neutralization of the negative-regulatory motif (Hupp et al. 2000).

1.1.3 Isoforms and family members of p53

Although originally p53 was thought to possess just one active promoter that transcribed three mRNA splice variants (FLp53, p53i9 and Δ40p53), the recent discovery that p53

actually possesses two promoters has led to the identification of several new alternatively spliced isoforms of p53 (Bourdon et al. 2005). This group used a technique that ensured only full-length, capped p53 mRNA molecules were analysed, which allowed the identification of mRNA species initiated from different start sites in exon 1 (P1 and P1'), and one mRNA species from derived from the novel promoter 2 (P2) within intron 4. Further cloning and sequencing of RT-PCR products led to the identification of three different splice variants involving intron 9: an α form terminating at amino-acid 393 and two variants lacking amino acids 323 – 392 (p53 β and p53 γ). This group therefore concluded that this and previously reported data suggested that p53 was capable of producing nine different transcripts. They also went on to demonstrate that these nine isoforms show different patterns of expression within tissues and cell lines and that the alternative promoter (P2) is conserved through evolution from *Drosophila* to mammalian species (Bourdon et al. 2005).

A recent study by Dornreiter and colleagues described another novel p53 variant which originated in primates and is derived from alternative splicing (Rohaly et al. 2005). This isoform (named Δp53 or as in this report p53 ΔV) lacks 66 internal amino-acids (residues 257 -322) which removes a significant C-terminal portion of the DNA-binding domain, including the conserved Box-V region. This study demonstrated that p53 ΔV can induce the transcription of a subset of p53 targets such as p21 and was shown to associate with p21 in S phase after UV irradiation (Rohaly et al. 2005).

Family members of p53 include p63 and p73. The three family members share significant homology at the amino-acid level within the three domains (the transcriptional activation domain, the sequence-specific DNA binding domain and the tetramerisation domain) (Yang et al. 2002). As homologues of p53, p63 and p73 have similar structural and functional characteristics, enabling them to bind p53 DNA-binding sites, to transactivate p53 target genes, and to induce cell cycle arrest and apoptosis. There are, however slight differences in structure, regulation and activity of p63 and p73

compared to p53, which means that these isoforms perform biological tasks which are not performed by p53 and vice versa (Blandino and Dobbelstein 2004). Whereas p53 is mutated in approximately 50% of all human cancers, mutation of its family members, p63 and p73 is rare. Disruption of p73 expression is thought to lead to defects in neuronal development and homeostasis, and loss of p63 in mice leads to the loss of squamous epithelia (Blandino and Dobbelstein 2004).

1.1.4 Activation of p53

The activation of different stress-induced signaling pathways leads to posttranslational modifications or groups of modifications on the p53 protein that modulate p53 activity, and ultimately regulate cell fate (see section 1.1.5). Activation of p53 can occur following genotoxic stresses such as ionizing radiation, UV light and cancer drugs (including Adriamycin and etoposide) which lead to DNA damage normally in the form of double strand breaks or bulky lesions. Alternatively, p53 can also be activated following non-genotoxic stresses such as hypoxia, oncogene activation and nutrient deprivation.

1.1.4.1 Genotoxic Stresses

The activation of p53 following DNA damage such as double strand breaks has led to p53 being regarded as the 'guardian of the genome' (Lane 1992). Damage insults such as ionizing radiation result in the formation of DNA backbone changes such as single strand breaks (SSB) or double strand breaks (DSB) and activate a signaling cascade which involves major molecular sensors such as ATM, ATR and DNA-PK (DNA protein kinase) (Efeyan and Serrano 2007). These sensor proteins are recruited to sites of damage, forming nuclear 'foci'. Signaling molecules such as Chk1 and Chk2 are then recruited and activated, and they inturn activate p53 by phosphorylation at various sites (Sancar et al. 2004; Efeyan and Serrano 2007). Phosphorylation of p53 following DNA damage ultimately leads to stabilization and accumulation of the protein in the nucleus

through inhibition of the binding of the negative regulator Mdm2. In addition, phosphorylation leads to the activation of p53 by stabilisation of the binding of co-activators such as p300 (Meek 2004) (see section 1.1.2.1). The sensor protein ATM, which is mutated in the cancer-prone disease ataxia telangectasia (AT) (Kastan et al. 1992), directly phosphorylates p53 at Ser 15 as well as activating other protein kinases such as Chk1 and Chk2, which can phosphorylate the N-terminal domain of p53 at sites such as Ser 15, Thr 18, Ser 20 and Ser 46 (Shieh et al. 1997; Chehab et al. 1999; Craig et al. 1999; Unger et al. 1999; Appella and Anderson 2001; Saito et al. 2002). It has been shown that cells lacking ATM and Chk2 are defective in their ability to stabilize p53 following ionizing radiation, thus highlighting the role of ATM and Chk2 in p53 stabilisation following damage (Vousden 2002). It is also thought that phosphorylation of p53-binding pocket on Mdm2 at residue Ser 17 by DNA-PK may inhibit Mdm2 binding, and therefore contribute to the activation of p53 following damage (Vousden 2002).

A second DNA damage response pathway is activated following UV-C radiation, which causes bulky lesions such as pyrimidine dimers and photoproducts that crosslink DNA bases. This pathway is thought to involve sensing a block to transcriptional elongation, thereby leading to the activation of ATR (Appella and Anderson 2001; Latonen and Laiho 2005). This damage-response pathway is also thought to be less rapid and more long-lived than that following ionising radiation (Appella and Anderson 2001; Latonen and Laiho 2005). In general a UV damage signal sensed by ATR is transduced by Chk1 to p53, but there can be some cross-talk between the pathways that lead to p53 activation. UV damage is thought to lead to the activation of kinases such as Chk1, p38, MAPK (mitogen-activated protein kinase), CK2 and HIPK2 (homeodomain-interacting protein kinase 2) which phosphorylate multiple sites across p53 including N-terminal sites (Ser 20, Ser 33, Ser 37 and Ser 46) and C-terminal sites (Ser 315 and Ser 392) (Appella and Anderson 2001).

Many other environmental, physiological and therapeutic agents also cause genotoxic stress leading to the activation of p53 through different signaling pathways. These agents include cancer drugs such as Adriamycin, topoisomerase inhibitors such as etoposide, DNA synthesis and transcription inhibitors such as aphidicoline, and DNA cross-linking agents such as cisplatinin. It is thought that most of these agents cause accumulation of p53 and its phosphorylation on Ser 15 (Appella and Anderson 2001). A recent report described a critical role for ATR, and not ATM or DNA-PK in mediating damage response to cisplatin treatment of renal cells and tissues (Pabla et al. 2008). They showed that ATR activated Chk2, which in turn induced p53 activation and apoptosis (Pabla et al. 2008).

1.1.4.2 Non Genotoxic Stresses

Activation of p53 can also occur following physiological processes such as hypoxia, oncogene activation, microtubule disruption and nutrient deprivation that are not associated with DNA damage. Hypoxia can be a feature of both solid tumours and ischemic disorders. Hypoxia also activates hypoxia-inducible factor-1 (HIF-1) which is a master regulator of cellular responses to hypoxia. The accumulation and dimerisation of HIF-1 results in the activation of target genes (Wang and Semenza 1995). It has been shown that hypoxia can induce p53 accumulation as a result of downregulation of Mdm2 (Alarcon et al. 1999; Koumenis et al. 2001; Wang et al. 2002). Moreover, in contrast to genotoxic insults such as IR, hypoxia does not induce the transcription of target genes such as *GADD45*, *Bax* and $p21^{WAF1,}$ suggesting that p53-dependent transactivation requires a DNA damage signal that is lacking following hypoxia treatment (Koumenis et al. 2001). Hypoxia primarily caused p53 to associate with the corepressor mSin3A rather than the co-activator p300 leading to p53-mediated transrepression (Koumenis et al. 2001). Although most data supports a role for p53 in the inhibition of the HIF system thereby inhibiting tumourigenesis, it has been demonstrated recently that Mdm2 can positively activate HIF-1α in hypoxic tumour cells in a p53-independent manner that

promotes tumour development (Nieminen et al. 2005). This recent data would suggest the existence of a negative feedback loop, whereby Mdm2 activates HIF-1, and HIF-1 downregulates Mdm2.

Stabilisation of p53 can occur following the activation of the p53-p14-Mdm2 pathway whereby p14 is activated by oncogenic stress signals (such as E2F), which inhibits Mdm2, and thereby stabilises p53. The presence of oncogenes such as c-myc and E2F-1 in cells can promote malignant transformation under certain conditions. However, oncogenes such as c-myc also activate p53. Raveh and colleagues investigated whether death-associated protein kinase (DAPK), a tumour suppressor which sensitises cells to apoptotic signals, could affect the initial steps of oncogenesis (Raveh et al. 2001). They found that DAPK suppresses oncogene-induced transformation of primary embryonic fibroblasts by activating p53 in a $p19^{ARF}$ (the murine equivelent of p14) – dependent manner. This led to induction of apoptosis in order to eliminate the pre-malignant cells. More recently it has been demonstrated that ATM plays a critical role in inhibiting the development of cancer by responding to oncogenic stress and inducing the accumulation and phosphorylation of p53 in response to deregulated Myc expression (Hong et al. 2006). In support of this, the group demonstrated that inactivation of ATM led to reduced apoptosis and increased tumourigenesis in Myc transgenic mice, suggesting that ATM is critical for the activation of p53 to allow apoptosis to proceed (Hong et al. 2006).

Activation of p53 can also occur in response to anti-cancer agents such as colcemid, nocodazole and taxol that deregulate cell adhesion, microtubule architecture or dynamics. Taxol, the first identified microtubule stabilizing drug has been used to treat solid tumours of the breast, ovary, head and neck (Bergstralh and Ting 2006). Taxol, but not nocodazole, was found to induce multi-site phosphorylation of p53 in several tumour cell lines. However, the pattern of phosphorylation was distinct from that observed after DNA damage induced by IR (Stewart et al. 2001). P53 activation after

colcemid treatment was accompanied by an increase in Ser 15 phosphorylation, which correlated with the activation of ERK1/2 MAP kinases and the development of focal adhesions, rather than the disruption of the microtubule system (Sablina et al. 2001).

Nutrient deprivation can also lead to the activation of p53 which will be discussed in more detail in the following section (see 1.1.5.4).

1.1.5 Function of p53

As a stress-induced sequence-specific DNA-binding protein and transcription factor, p53 plays a crucial role in the cellular response to genotoxic and non-genotoxic stresses. In unstressed cells, p53 is maintained at very low levels. However, following stresses such as double strand breaks induced by genotoxic agents, hypoxia or oncogene expression, the p53 protein becomes activated and accumulates rapidly (Lu and Lane 1993; Vousden 2002). In response to such stress signals, p53 becomes activated in a specific manner by post-translational mechanisms leading to either cell cycle arrest or cellular apoptosis (Jin and Levine 2001). This is achieved by p53's ability to regulate target genes, thereby allowing the cell to arrest temporarily to repair the damage or to activate apoptosis to eliminate the damaged cell. The decision to activate either cell cycle arrest of apoptosis depends on the type or degree of damage and the subsequent differential phosphorylation. The specific roles of p53 in the cellular responses to damage will be discussed below.

1.1.5.1 Cell cycle arrest and Senescence

Cell cycle checkpoints are activated following damage to delay progression from G1 to S phase, to inhibit DNA synthesis as part of the intra-S phase checkpoint, and to prevent passage of cells from G2 into mitosis (Lavin and Gueven 2006). Following stress signals p53 induces cell cycle arrest which can occur in either the G1, G2 or S phases of the cell cycle (Agarwal et al. 1998). p53-induced G1 arrest is mediated by

phosphorylation at multiple sites, which involves ATM, Chk1 or Chk2 (see section 1.1.4.1). This stabilises the binding of the co-activator p300 (Dornan and Hupp 2001), reduces the binding of the inhibitory partner Mdm2 (Unger et al. 1999), and thereby enhances activation of p53 target genes such as $p21^{WAF1/CIP1}$ (Jabbur et al. 2000). p21 inhibits the phosphorylation of Rb by the cyclin E-Cdk2 or cyclin D-Cdk4/6 complexes ultimately leading to hypophosphorylation of Rb which sequesters E2F family members. This prevents E2F from activating the transcription of genes necessary for S phase entry, and thereby causes G1 arrest. p21 can therefore prevent progression into S phase and allow sufficient time for any damage to be repaired (Nyberg et al. 2002; Jackson et al. 2004).

p53-induced G2 arrest is mediated in part by the synthesis of 14-3-3 sigma which binds to Cdc25C and keeps it in the cell cytoplasm, thus preventing Cdc25C from activating cyclin B-Cdc2 (a complex essential for G2 to M phase transition) (Iliakis et al. 2003). *14-3-3 sigma*, like $p21^{WAF1}$, is a p53 target gene. It has been shown that in colorectal cancer cells exposure to ionizing radiation leads to significant upregulation of *14-3-3 sigma* in a p53-dependent manner resulting in G2 arrest (Hermeking et al. 1997).

Cellular senescence appears to be an irreversible form of cell cycle arrest that is a potent barrier to tumourigenesis (Chen et al. 2005; Collado and Serrano 2005). It can be triggered by the oncogene Ras or excessive P13K signaling (Collado and Serrano 2005). The activation of cellular senescence is thought to occur in a p53-dependent manner. A recent report has examined the effect of loss of p53 in aggressive carcinomas (Xue et al. 2007). They showed that following reactivation of p53 *in vivo*, hepatocarcinomas expressing either Ras or Akt showed clear signs of senescence, including the accumulation of senescence-associated-β-galactosidase activity and the senescence markers $p16^{INK4a}$, DrR2 and $p15^{INK4b}$ (Xue et al. 2007). Cellular senescence has also been shown to trigger the upregulation of inflammatory cytokines and other immune modulators (Shelton et al. 1999). Xue and colleagues reported the upregulation of

inflammatory cytokines following p53 reactivation which led to targeting of the tumour cells and therefore contributed to tumour clearance (Xue et al. 2007). p53 can therefore play a crucial role in the control of tumour development by activating a program of cellular senescence.

1.1.5.2 Apoptosis

In contrast to cell cycle arrest that prevents cell cycle progression to allow the repair of damage, apoptosis (or programmed cell death) allows the complete elimination of the damaged cell, which promotes tissue homeostasis and tumour prevention. p53 can induce apoptosis through an extrinsic or receptor-mediated pathway, or through an intrinsic or mitochondrial-mediated pathway. The latter shifts the balance in the Bcl-2 family towards pro-apoptotic members, thus promoting the formation of the apoptosome and consequently caspase-mediated apoptosis via caspase 9 (Haupt et al. 2003). The receptor mediated apoptotic pathway also triggers the activation of a caspase cascade, but via caspase 8. External signaling molecules such as tumour-necrosis factor-α (TNFα) and CD95 ligand (also known as Fas ligand) bind to their receptors TNFR and CD95 (also known as Fas or Apo-1), respectively and convey signals to the cell causing the activation of caspase 8 which results in apoptosis (Haupt et al. 2003). The intrinsic pathway is considered to be the main cellular protection mechanism against damage of various types. Cell fate is determined by a balance between pro-apoptotic (BAX, Bid, Bim and BAK) and anti-apoptotic (BCL2 and BCL-X_L) members of the BCL-2 family at the mitochondrial membrane. A dominance of pro-apoptotic members leads to the release of cytochrome c from the mitochondria, which together with apoptosis peptidase-activating factor 1 (APAF1) and caspase 9 form a complex known as the apoptosome. The apoptosome activates downstream caspases ultimately leading to apoptosis (Haupt et al. 2003).

Many members of the BCL-2 family including both pro-apoptotic (e.g. *Bax*, *Bak*, *Bok* and *BAD*) and anti-apoptotic (e.g. *Bcl-2* and *BCL-X_L*) representatives are all transcriptional targets of p53. In addition, it has been shown that p53 can localize to the mitochondria and bind to pro-apoptotic genes such as *Bak*, leading to the release of cytochrome c from the mitochondria. P53 can therefore have a direct effect on apoptosis as well as transcription-dependent effects (Leu et al. 2004). In addition, a role for p53 in formation has been suggested whereby p53 induces *APAF-1* expression (Haupt et al. 2003). Uniquely, the pro-apoptotic gene, Bid, seems to be capable of connecting the extrinsic and intrinsic pathways by firstly being activated by caspase-8 in the cytoplasm and translocating to the mitochondria to activate BAX and BAK (Haupt et al. 2003).

Manipulation of the apoptotic functions of p53 could provide an attractive target for cancer therapy, whereby directly activating p53 pro-apoptotic targets in tumours could provide an effective anti-tumourigenic therapy.

1.1.5.3 DNA Repair and Recombination

A role for p53 in DNA repair and recombination has been suggested. The five main DNA repair processes are nucleotide-excision repair (NER), base-excision repair (BER), mismatch repair (MMR), non-homologous end joining (NHEJ) and homologous recombination (HR). Although the transactivation-independent function of p53 is involved in HR regulation, the other DNA repair processes involve both the transactivation-dependent and independent activities of p53 (Sengupta and Harris 2005). The transcription-independent roles of p53 contribute to the control and efficiency of DNA repair and recombination which cooperate with its function in transcription. P53 is thought to be involved in the multi-step process of HR by binding to HR specific proteins such as RAD51 and RAD54 or by directly checking the fidelity of HR events (Sengupta and Harris 2005). p53 may also have a role to play in the regulation of the proteins that are involved in the NER process (Sengupta and Harris 2005).

Transcription-dependent effects of p53 can occur following exposure to nitric oxide (NO), which causes the p53-dependent transcriptional repression of the *3-methyladenine DNA-glycosylase (MPG)* gene that functions in the BER pathway (Sengupta and Harris 2005).

P53 and MMR positively affect each other's activity, whereby the stabilization of a mismatch repair protein heterodimer augments p53 activation during DNA damage (Sengupta and Harris 2005). It is also thought that p53 functions as a sequence-dependent transactivator by binding to response elements in the promoter region of MMR proteins such as MutS homologue-2 (MSH2). It is thought that MMR proteins and p53 may cooperate in the repair process (Sengupta and Harris 2005). A role for p53 in NHEJ has been suggested whereby p53 may interact with NHEJ proteins such as DNA-PK which leads to stabilization of p53 and ultimately apoptosis (Sengupta and Harris 2005). P53 may also have a direct transactivation-independent role in NHEJ whereby it is capable of rejoining DNA after DSBs or can facilitate precise ligation (Sengupta and Harris 2005).

The role of p53 in modulation of several DNA repair processes by both transactivation-dependent and transactivation-independent pathways has led to the idea that p53 may function as a 'molecular node' whereby it operates at the intersection of upstream signaling cascades and downstream DNA-repair and -recombination pathways (Sengupta and Harris 2005).

1.1.5.4 Cell survival and autophagy

A novel role for p53 function in metabolism has recently been reported in several studies whereby p53 either drives cells to undergo apoptosis or controls how cells use nutrients to preserve their survival (Jones et al. 2005; Bensaad et al. 2006; Crighton et al. 2006; Matoba et al. 2006). A report demonstrated that glucose (a direct energy source for

mammalian cells) availability directly regulates cell proliferation (Jones et al. 2005). They showed that cells arrest in the G1 phase of the cell cycle under low glucose conditions and this arrest is p53-dependent. When the cell is glucose deprived, AMPK is activated leading phosphorylation of p53 at Ser15 and activation of p53. Thus, implicating both AMPK and p53 as proteins required to promote cell cycle arrest and allow the cell to survive the unfavourable glucose deprived conditions (Jones et al. 2005)

P53 has also been reported to play a direct role in metabolism. In a study by Bensaad and colleagues, a product of a p53 target gene, *TIGAR* (*TP53-induced glycolysis and apoptosis regulator*) was identified, which functions to regulate glycolysis and protect cells against oxidative stress (Bensaad et al. 2006). *TIGAR* is thought to inhibit glycolysis by causing a decline in fructose-2,6-biphosphate which leads to the formation of fructose-6-phosphate and NADPH. This increased NADPH generation is thought to increase glutathione levels which promotes the scavenging of reactive oxygen species (ROS) thereby protecting cells from ROS and DNA damage-induced apoptosis (Bensaad et al. 2006).

In addition, p53 may modulate the balance between the utilization of respiratory and glycolytic pathways (Matoba et al. 2006). Cancer cells often use energy derived from glycolysis to sustain their growth and therefore their survival advantage (known as the Warburg effect) (Vousden and Lane 2007). The report by Matoba and colleagues suggested that p53 modulates the balance between the utilization of respiratory and glycolytic pathways and identified SCO2 (synthesis of cytochrome c oxidase 2) as a downstream mediator of this effect. They showed that disruption of SCO2 in cells wild-type for p53 caused a similar metabolic switch to glycolysis as that observed in p53 deficient cells. SCO2 therefore couples p53 to mitochondrial respiration (Matoba et al. 2006).

P53 is also thought to play a role in the autophagy pathway. Autophagy is an evolutionary conserved membrane-trafficking process that operates at basal levels to degrade cytosolic proteins and organelles by engulfing them in autophagosomes. It is thought to contribute to cell survival when nutrients are limiting (Crighton et al. 2006). This recent report demonstrated that the p53 target DRAM (damage regulated autophagy modulator) engages autophagy by the accumulation of autophagosomes in a p53-dependent manner. In addition, DRAM is required for p53-induced apoptosis as DRAM-dependent autophagy operates upstream of cytochrome c release from the mitochondria and is required for apoptosis to proceed (Crighton et al. 2006).

1.2 Regulation of p53 transcriptional activity

The activity of p53 is controlled by cellular levels of p53, its DNA-binding ability, its subcellular localization and the recruitment of transcriptional activators and repressors.

1.2.1 Protein stabilization

The regulation of cellular levels of p53 can be controlled by several proteins which by interacting with p53 can either positively or negatively control its level of expression. Mdm2, an E3 ubiquitin ligase, is thought to be one of the main proteins involved in control of p53 stability. It has been shown to bind to the transactivation domain of p53, repressing transcription but also promoting its ubiquitination and export to the cytoplasm for degradation by the 26S proteasome (Momand et al. 1992; Lu and Levine 1995; Thut et al. 1995; Chen et al. 1996; Haupt et al. 1996; Honda et al. 1997; Kubbutat et al. 1997; Thut et al. 1997; Michael and Oren 2003). p300 forms part of a positive regulatory pathway which facilitates induction of p53 dependent gene expression (Goodman and Smolik 2000). The interaction of p53 with CBP/p300 results in acetylation and transcriptional activation of p53 (Goodman and Smolik 2000). The roles of both Mdm2 and p300 in regulation of p53 transcriptional activity will be discussed in detail in section 1.3, and the role of ubiquitination and acetylation will be discussed in sections 1.2.2.2 and 1.2.2.3.

Although Mdm2 was thought to be the major p53 E3 ubiquitin ligase, several other E3 ligases that mediate p53 ubiquitination and degradation have recently been identified. These include Pirh2, constitutively photomorphogenic 1 (COP1), chaperone-associated ubiquitin ligase (CHIP), human topoisomerase I- and p53-binding protein (topors) and ARF-binding protein (ARF-BP1) (Liu and Chen 2006). In addition to its role as a ubiquitin ligase, inactivation of endogenous ARF-BP1 is crucial for ARF-mediated p53 stabilisation (Chen et al. 2005). COP1 has been shown to inhibit p53-dependent transcription and apoptosis as well as target p53 for degradation by the proteasome (Dornan et al. 2004). CHIP was also described to induce proteasomal degradation of

p53 (Esser et al. 2005). Finally, *Pirh1*, a gene that encodes a RING-H2 domain-containing protein with intrinsic ubiquitin ligase activity, interacts with p53 and promotes p53 ubiquitination and represses p53 functions (Leng et al. 2003).

Stabilisation of p53 can also occur by removal of the ubiquitin modification. Recently a novel p53-interacting protein was identified, herpes virus-associated ubiquitin-specific protease (HAUSP), which has intrinsic enzymatic activity that specifically deubiquitinates p53, therefore stabilizing p53 and promoting p53-dependent growth suppression (Li et al. 2002). HAUSP has also been shown to deubiquitinate and stabilise Mdm2, suggesting that Mdm2 is directly regulated by the deubiquitinase function of HAUSP (Li et al. 2004). Therefore HAUSP may play a crucial in the regulation of the p53-Mdm2 pathway. However, other proteins such as NAD(P)H quinone oxidoredectase (NQO1) can influence the degradation of p53 in an Mdm2- and ubiquitin-independent manner (Asher and Shaul 2005). The interaction of p53 with NQO1 leads to the degradation of p53 by the 20S proteasome (Asher and Shaul 2005).

A number of protein kinases influence the stabilization of the p53 protein by phosphorylation. The CAMK superfamily plays an important role in this process and is discussed in section 1.3.3. The role of phosphorylation is discussed in section 1.2.2.1. Other examples of kinases include homodomain-interacting protein kinase 2 (HIPK2), which is thought to increase p53 stability by phosphorylation of p53 on Ser 46, leading to the dissociation of p53 from Mdm2 and decreased shuttling of p53 from the nucleus (Di Stefano et al. 2004); and Jun NH_2-terminal kinase (JNK), which has been suggested to be an Mdm2-independent regulator of p53 in unstressed cells (Fuchs et al. 1995).

1.2.2 Post-translational modification

Control of p53 function can also be exerted via post-translational modifications such as phosphorylation of Serine and Threonine residues and acetylation, ubiquitination and

sumoylation of lysine residues. These post-translational modifications influence the interaction between Mdm2 and p53, the major mechanism for controlling p53 stability, as well as the interaction with p300, the major mechanism for controlling p53's activity as a transcription factor.

1.2.2.1 Phosphorylation

Phosphorylation is a reversible mechanism which is crucial for the regulation of the biological activity of protein. Protein kinases phosphorylate target proteins leading to their activation or inactivation (Bode and Dong 2004). Phosphorylation of p53 is one of the major mechanisms of post-translational modification that influences the stability of p53. Phosphorylation of p53 can occur at multiple sites across the protein although the majority of sites are located within 100 amino acids of the N-terminus or within the C-terminus. Following DNA damage, phosphorylation of p53 is thought to change the conformation of p53, preventing the binding of Mdm2 and therefore leading to the accumulation of p53 (Xu 2003; Bode and Dong 2004). The activation of various protein kinases such as ATM, ATR, Chk1, Chk2 and CK2 upon stress leads to the phosphorylation of multiple residues such as Ser 6, 9, 15, 20, 33, 37, 46, 149, 315 and 392, and Thr 18, 81, 150 and 155. Moreover, residues Thr 55, Ser 376 and Ser 378 are phosphorylated in unstressed cells (Xu 2003; Bode and Dong 2004). There is often overlap between sites of phosphorylation by the various different kinases and this can often be attributed to the type of stress signal which the cell is exposed to (Lavin and Gueven 2006). The most frequently described residue is the Ser 15 site which is phosphorylated by ATM as a result of DNA damage such as double-strand breaks (Banin et al. 1998; Khanna et al. 1998). Phosphorylation of Ser 15 results in reduced binding of Mdm2 and the subsequent stabilization of p53 (Shieh et al. 1997). ATM can phosphorylate multiple sites such as Ser 6, 9, 15, 20 and 46 as well as Thr 18 following ionizing radiation (Saito et al. 2002).

Other commonly described N-terminal sites of phosphorylation include Thr 18, Ser 20, Ser 33 and Ser 46. Phosphorylation at residues Thr 18 and Ser 20, which are within the Mdm2 binding region, stabilises the binding of the co-activator p300 (Dornan and Hupp 2001), reduces the binding of the inhibitory partner Mdm2 (Unger et al. 1999) and enhances activation of p53 target genes (Jabbur et al. 2000). This is supported by studies which demonstrated that Asp substitution (mimics phosphorylation due to the introduction of a negative charge within the functional group) at the two phosphoacceptor sites reduces the interaction of p53 with Mdm2 and increases the transactivation of the p53 target genes, $p21^{WAF1/CIP1}$ and *Fas* (Jabbur and Zhang 2002). In addition, mutation of the Ser 20 site in mice (Ser 23) leads to the formation of spontaneous B-cell lymphoma (MacPherson et al. 2004). Phosphorylation of Ser 20 in stressed cells was thought to be predominantly mediated by Chk1 and by ATM-activated Chk2, resulting in the alleviation of the inhibition mediated by Mdm2 (Shieh et al. 1997; Khanna et al. 1998; Chehab et al. 1999; Unger et al. 1999; Shieh et al. 2000). However, it has been shown that disruption of Chk2 did not affect p53 stabilization, phosphorylation or transcriptional activation of downstream targets (Ahn et al. 2003; Jallepalli et al. 2003), suggesting that Chk2 may play a less important role in p53 activation. Phosphorylation at Ser 33, Ser 46 and Thr 81 have also been suggested to lead to p53 stabilisation (Bode and Dong 2004).

The C-terminal region of p53 is a target for phosphorylation by casein kinase 2 (CK2) and protein kinase C which stimulate the binding of p53 to DNA (Hupp et al. 1993). The C-terminal region is thought to be key in regulating p53's DNA binding ability. In support of this, the phosphorylation of Ser 392 is thought to regulate the stability of the tetramerisation domain. It has been shown that mutation of a site adjacent to Ser 392 (Lys 386) can increase p53's activity, likely due to the neutralization of the negative-regulatory motif (Hupp et al. 2000). It has also been shown that phosphorylation of p53 at this CK2 site (Ser 392) leads to sequence-specific DNA binding stimulated by allosteric mechanisms that converts p53 protein from a low affinity to a high affinity

DNA-binding form by a conformational change (Lane and Hupp 2003). More recently, both Chk1 and Chk2 have been shown to phosphorylate p53 at multiple sites in both the N- and C-termini of p53 leading to its stabilization (Ou et al. 2005). This group identified several sites in the C-terminus including Ser 366, Ser 378 and Thr 387, which were damage inducible. Abrogation of either Chk1 or Chk2 prevented phosphorylation of two of these sites, which led to reduced induction of p53 downstream target genes (Ou et al. 2005).

Therefore the phosphorylation of several residues across the p53 protein plays a role in the modulation of its activity. The most extensively studied damage response pathways being the IR-ATM-Chk2-Ser20 and the UV-ATR-Ser15/Ser20 axes. The role of Ser 20 phosphorylation in assembly of the transcription complex and therefore the control of p53 activity will be discussed in more detail in section 3.1.1.

1.2.2.2 Acetylation

Phosphorylation stabilizes not only the p53:DNA complex but also the protein-protein interactions with the co-activator and acetyltransferase, p300. Acetylation is thought to be important for p53 stability and transcriptional activation (Bode and Dong 2004). Both p300 and CREB-binding protein (CBP) are histone acetyltransferases (HAT)-containing proteins that can coactivate transcription factors such as p53 (Chan and La Thangue 2001). It has been shown that p300/CBP interact with and acetylate p53 in the C-terminal domain, a region critical for the regulation of p53:DNA binding, thus suggesting that acetylation of p53 can stimulate DNA binding activity (Gu and Roeder 1997). Following the report by Gu and Roeder, the ability of p53 to be acetylated by p300 *in vivo* was confirmed using acetylation specific antibodies (Sakaguchi et al. 1998). PCAF and p300 can acetylate p53 at Lys 320 and Lys 372, 373, 381 and 382, respectively, and these lysine residues can be phosphorylated in response to DNA damage (Gu and Roeder 1997; Lill et al. 1997; Sakaguchi et al. 1998). Studies have

supported a role for DNA-damage induced phosphorylation of p53 as a modification which regulates the interaction between PCAF/p300 and p53 (Moll and Petrenko 2003; Xu 2003). These reports have shown that phosphorylation of p53 at Ser 15 or Ser 33/37 promotes the interaction with p300/CBP (Xu 2003). Acetylation of p53 may also regulate p53 stability. Studies have shown that the C-terminal lysine residues acetylated after DNA-damage are also residues ubiquitinated by Mdm2 (Moll and Petrenko 2003; Xu 2003). This would suggest that acetylation of these lysine residues after DNA damage could prevent ubiquitination by Mdm2, thereby promoting p53 stabilisation.

A recent report has shown that the native conformation of the p53 tetramer is critical to restrain acetylation in the absence of consensus site DNA (Ceskova et al. 2006). They developed a model whereby DNA binding in the core domain of p53 simultaneously stabilizes p300 docking to N-terminal p53 and exposes an acetylation motif within the C-terminal and thereby removes any conformational restraints to acetylation (Ceskova et al. 2006). The identification a novel site of acetylation within the DNA-binding domain of p53 (K120) that proteins of the MYST family of acetyltransferases directly acetylate has been described in a recent report (Sykes et al. 2006). Mutation of this site (to arginine) occurs in human cancer and leads to inhibition of acetylation, which prevents p53-mediated apoptosis by blocking transcription of pro-apoptotic genes BAX and PUMA (Sykes et al. 2006). Therefore acetylation has several functions in regulating the DNA-binding activity and stabilization of p53, as well as its ability to regulate the induction of apoptosis.

Histone acetylation by p300/CBP can be reversed by histone deacetylases (HDACs) which act as p53 corepressors (Liu and Chen 2006). P53 can transcriptionally repress target genes such as Myc, Nanog and HSP90 beta by recruitment of HDACs to promoters through interaction with mSin3a and other DNA-binding proteins (Liu and Chen 2006). A balance between p53 acetylation and deacetylation may allow the

activation and stabilization of p53 upon damage and once the damage is repaired the acetylated p53 may be inactivated by deacetylation (Liu and Chen 2006).

1.2.2.3 Ubiquitination

Ubiquitination of proteins is controlled by a series of enzymatic reactions catalysed by enzymes known as E1 (ubiquitin-activating enzyme), E2 (ubiquitin-conjugating enzyme) and E3 (ubiquitin protein ligase) (Bode and Dong 2004). Ubiquitination can either occur in the form of monoubiquitination, whereby the ubiquitin monomer conjugates with one or more lysines within the target protein, or alternatively polyubiquitination, whereby a polymeric ubiquitin chain conjugates with one or more lysines within the target protein (Bode and Dong 2004). Monoubiquitination is thought to regulate the function of target promoters, whereas polyubiquitination marks the protein for degradation by the 26S proteasome. Mdm2 was one of the first E3 ubiquitin ligases identified to mediate p53 degradation (Momand et al. 1992; Lu and Levine 1995; Thut et al. 1995; Chen et al. 1996; Haupt et al. 1996; Thut et al. 1997) (see section 1.2.1 for details on other E3 ligases). Upon binding to the Box-I region of p53, Mdm2 transfers ubiquitin tags onto lysine residues in the C-terminus of p53. It is thought that different levels of Mdm2 can induce either mono- or polyubiquitination of p53 in a dose-dependent manner, thereby controlling the fate of p53 (Li et al. 2003). Indeed, mono-ubiquitination is thought to act as a nuclear export signal for p53 whereas polyubiquitination marks p53 for degradation.

In unstressed cells, p53 is maintained at low levels by continuous ubiquitination and subsequent degradation by the 26S proteasome, which is primarily due to the interaction of p53 with the ubiquitin E3 ligase, Mdm2. It is only upon stress that this negative repression of p53 is released, allowing stabilization of p53 which accumulates in the nucleus (Shieh et al. 1997; Chehab et al. 1999; Craig et al. 1999; Unger et al. 1999). These reports demonstrate that DNA damage such as IR and UV lead to phosphorylation

of the N-terminal domain of p53 at sites such as Ser 15, Thr 18 and Ser 20, reducing the binding of Mdm2 and leading to the stabilization of p53. Mdm2 seems to play a role in controlling both the localization and degradation of p53. Overexpression of Mdm2 has been observed in many tumour types and can lead to complete deactivation of p53 (Bode and Dong 2004). The specific role of Mdm2 in control of ubiquitination of p53 will be discussed in more detail in section 1.3.2.

Histone ubiquitination is also able to regulate the transcription of p53 target genes and this ubiquitination mainly occurs on histones H2A and H2B. Although little is known about the regulation of p53-mediated transcription by histone ubiquitination, Mdm2 has been shown to bind histones H2A and H2B (Minsky and Oren 2004). This group showed that Mdm2 overexpression enhanced histone ubiquitination close to the p53 binding site within the $p21^{WAF1}$ promoter, suggesting that ubiquitination of H2A and H2B by Mdm2 may represent another mechanism by which Mdm2 negatively regulates p53 activity. This work also suggests that Mdm2 may drive gene silencing via chromatin modification (Minsky and Oren 2004).

A recent report described the analysis of enzymes required for the ubiquitination of p53 and identified UbcH5B/C as an E2-like protein involved in controlling levels of p53 and Mdm2 (Saville et al. 2004). This group showed that depletion of UbcH5B/C inhibited p53 ubiquitination and degradation, but that this p53 was transcriptionally inactive as it remained bound to Mdm2 (that was not ubiquitinated either). Activation of the stabilized p53 therefore required complete removal of the bound Mdm2 (Saville et al. 2004). It has also been reported that both p53 and Mdm2 can be modified by the ubiquitin-like proteins NEDD8, a well characterized regulator of $p27^{kip1}$, IκBα and SUMO (Watson and Irwin 2006). There are therefore several pathways involved in the ubiquitination and inactivation of p53.

1.2.2.4 Other modifications

Other post-translational modifications involved in the control of p53 transcriptional activity include sumoylation, glycosylation and ribosylation (although little is known about the role of the latter two in carcinogenesis) (Bode and Dong 2004). Sumolytion is similar to ubiquitination in that an iso-peptide bond is formed between the C-terminal group of a the small ubiquitin-like molecule, SUMO1 and the ε-amino group of lysine residues within transcription factors (Bode and Dong 2004). The sumoylation-specific E2 conjugating enzyme for p53 is Ubc9 and the sumoylation specific E3 ligase for p53 is protein inhibitor of activated STAT1 (PIAS-1) (Liu and Chen 2006). The target site for sumoylation in p53 is K386 and it was shown that sumoylation stimulates p53 transcriptional activity, but does not affect p53 ubiquitination (Liu and Chen 2006). Sumoylation of p53 appears to be regulated by Mdm2- and p14 ARF- mediated nuclear targeting and sumoylation may also have a repressive effect (Chen and Chen 2003). The debate over whether sumoylation of p53 results in the activation or the repression of p53 is still to be settled. The regulation of p53 activity therefore occurs as the result of several modifications and by the intervention of several proteins. The following section will examine in detail the regulators of p53 function.

1.3 Regulators of p53 function

Modulation of p53 activity depends on docking of several regulators, most of which have already been mentioned in previous sections. Two regulators, Mdm2 and p300 play crucial roles in regulating p53. Mdm2 is a negative regulator which facilitates p53 degradation via the proteasome (Oren 1999), whereas P300 is a positive regulator that facilitates p53-dependent gene expression (Goodman and Smolik 2000). These two components compete for binding to the N-terminal Box-I domain of p53 resulting in the modulation of the specific activity of p53 as a tumour suppressor (Dornan and Hupp 2001). Members of the Calcium Calmodulin kinase superfamily such as Chk1, Chk2 and DAPK1, also play an important role in the control of p53 activity by altering p53's interactions with p300 and Mdm2. This is achieved by phosphorylation in the Box-I domain. P300, Mdm2 and CAM kinases will therefore be discussed in this section.

1.3.1 P300

P300 forms part of a positive regulatory pathway which facilitates induction of p53 dependent gene expression (Goodman and Smolik 2000). P300 as well as CREB binding protein (CBP) were initially identified in protein-interaction studies. CBP was found to associate with CREB and p300 was shown to interact with the adenoviral-transforming protein E1A (Stein et al. 1990; Eckner et al. 1994). Eckner and colleagues cloned and analysed the 300 kDa protein, p300, and mapped the gene encoding p300 to chromosome 22q13. p300 contains 3 cysteine and histidine rich regions and a carboxy-terminal region which interacts specifically with E1A (Eckner et al. 1994). They also described how p300 may function as a transcriptional adaptor protein for transcriptional regulatory elements.

The link between p53 function and p300 was described in a report by Lill et al 1997. They showed that p300 and p53 colocalise in the nucleus in a stable DNA binding complex. Furthermore, p53's ability to mediate functions such as G1 checkpoint

activation was shown to be p300/CBP dependent (Lill et al. 1997). The discovery that p53 can be acetylated by p300 (Gu and Roeder 1997) provided an insight into the aspects of p300/CBP function. They showed that p53 was acetylated by p300 in the C-terminal domain, a region critical for the regulation of binding of the p53 to DNA. This acetylation was shown in both *in vitro* and *in vivo* assays and was shown to be evolutionary conserved (Gu and Roeder 1997; Sakaguchi et al. 1998). It is now known that p53 interacts with the carboxy-terminal region of CBP/p300 resulting in transcriptional activation of p53 responsive promoters such as *p21* and *Bax* (Goodman and Smolik 2000).

Phosphorylation of p53 at Thr 18 and Ser 20 stabilises the binding of the co-activator p300 (Dornan and Hupp 2001). Further studies defined the interaction of p53 with p300 In particular, comparison of p53 Box I phosphorylation sites revealed that Chk2 mediated phosphorylation at Ser 20 had the most stabilizing effect on p53:p300 complex formation compared to other phosphorylation sites (Dornan et al. 2003). This study mapped two consensus p53 binding sites within p300; the C-terminal Interferon-binding domain (IBiD) and the N-terminal domain which has homology to IBiD, IHD. Consensus site binding of p300 to p53 is essential for sequence specific DNA acetylation of p53, which results in stabilization of the p53:p300 acetyl-complex (Dornan et al, 2003). Dornan and collaegues identified three stages in the assembly of the p53:p300 complex: firstly, as a result of phosphorylation at Ser20 or Thr18 by Chk2, p300 docks stably to the phosphorylated – Box-I transactivation domain of p53 via the IBiD and IHD domains of p300; secondly, p300 docking leads to DNA dependent acetylation of p53; and finally leading to the acetyl-co-A dependent stabilization of the p300:p53 complex is achieved. Therefore, the complementary role of phosphorylation and acetylation is essential in assembly the p53-p300 transcription complex.

Dornan and colleagues also identified a further p300-binding motif which exists within the proline repeat region within the N-terminal domain of p53 (Dornan et al. 2003).

Using a technique which can define novel protein-protein interfaces, p300 was subjected to a peptide selection from a phage-peptide display library. PXXP-containing peptides derived from the p53 transactivation domain were identified and p300 was shown to bind to the PXXP containing peptides. In addition, deletion of the proline rich region destabilised the p53-p300 complex and prevented acetylation of p53. Furthermore, PXXP containing peptides inhibited sequence-specific DNA-dependent acetylation of p53, suggesting that p300 docking to both the Box-I (LXXLL) and the PXXP motifs of p53 is essential for p53 acetylation (Dornan et al. 2003).

Other reports have examined how p53 acetylation by p300 may be controlled *in trans* by other regulatory factors. A report by Dornan and colleagues focused on interferon regulatory factor 1 (IRF-1) binding to p300. They describe a crosstalk mechanism between the two transcription factors, p53 and IRF-1, in which IRF-1 binding to p300 results in stabilization of p300 binding to the LXXLL domain of p53. This in turn, leads to DNA-dependent acetylation of p53 and therefore stimulation p53 activity (Dornan et al. 2004).

The role of p300 as a scaffold for binding of components of the transcriptional machinery can be partly attributed to the presence of three broad functional domains: an acetyltransferase domain that mediates substrate acetylation; a bromodomian which is implicated in binding to acetylated amino acids; and transactivation peptide-binding domains such as LXXLL and PXXP. Further definition of the nature of the p300:p53 complex was described in a report by Finlan and collaegues. They characterized the IBiD homology domain (IHD) and defined the minimal IHD scaffold as a 75 amino acid fragment. This fragment displayed similar characteristics to full-length p300 including affinity for LXXLL-containing peptides. The minimal IHD scaffold was shown to interact with the LXXLL activation domain of p53 and stimulated the binding to Ser 20 phosphorylated tetramers to DNA (Finlan and Hupp 2004). These results therefore

demonstrate that the minimal IHD scaffold forms a transcriptionally active complex with p53.

1.3.2 Mdm2

Mdm2 (mouse double minute 2) is a key player in the negative regulation of p53 tumour suppressor protein (Oren 1999). Mdm2 is an oncogene product which was found to be amplified in mouse tumour cell lines in the form of 'double minutes', small acentromeric, extrachromosomal nuclear bodies (Fakharzadeh et al. 1991). It was later found to be amplified in human sarcomas (Oliner et al. 1992). A 90kDa protein was shown to form complexes with mutant and wild-type p53 and was subsequently identified as Mdm2 (Momand et al. 1992). Furthermore, this group showed that Mdm2 inhibited p53 mediated transactivation (Momand et al. 1992).

The relationship between Mdm2 and p53 was subsequently described in several reports Mdm2 was shown to bind to p53's transactivation domain, repressing transcription, and thereby inactivating p53. The reports also described how Mdm2 binding led to the subsequent degradation of p53 (Momand et al. 1992; Lu and Levine 1995; Thut et al. 1995; Chen et al. 1996; Haupt et al. 1996; Thut et al. 1997). Chen and colleagues described how Mdm2 binding could reverse p53 mediated cell cycle arrest and apoptotic functions (Chen et al. 1996). Mdm2 was also shown to contain an autoinhibitory domain which directly represses basal transcription in the absence of p53 (Thut et al. 1997). Using in vitro binding assays, a direct interaction between Mdm2 and two components of the transcriptional machinery, TFIIE and TBP was identified. p53 and Mdm2 therefore have a unique relationship, whereby binding of Mdm2 to p53 leads to inhibition of transcription functions and therefore inactivation of p53.

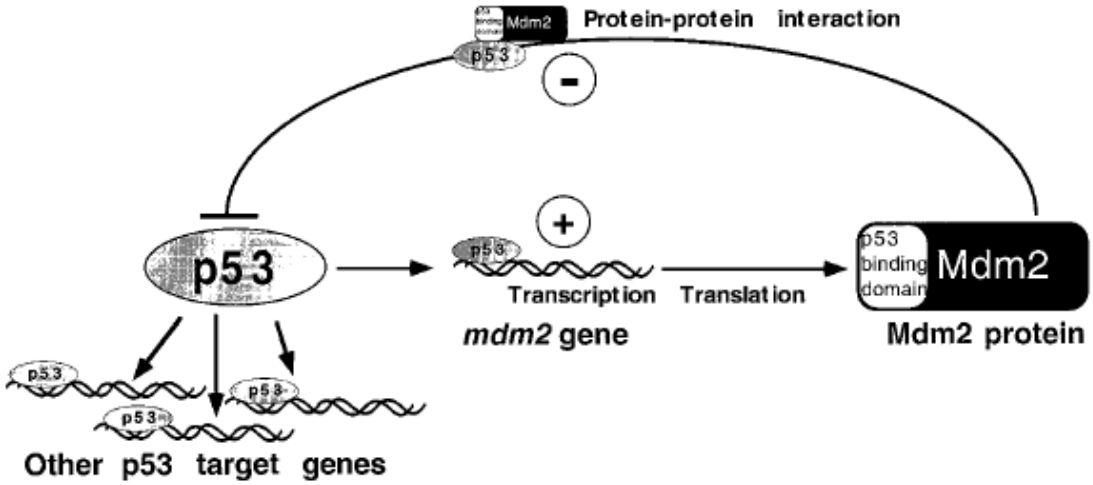

Figure 1.2 The p53-Mdm2 autoregulatory feedback loop.
This regulates the activity of the p53 protein and the expression of the *Mdm2* gene (Oren 1999).

The relationship between Mdm2 and p53 is even more unique given that p53 can bind to the *Mdm2* gene and stimulates its transcription (Barak et al. 1993; Wu et al. 1993). Barek and colleagues initially described how Mdm2 expression is induced by wild type p53 activity (Barak et al. 1993). A report by Wu and colleagues then examined the p53-Mdm2 interaction and demonstrated that the p53 protein regulates the *Mdm2* gene at the transcription level, suggesting that the *Mdm2* gene is autoregulated. A feedback loop (as shown in Figure 1.2) therefore regulates both the activity of the p53 protein and the expression of the *Mdm2* gene (Wu et al. 1993).

Mdm2 consists of an N-terminal domain which contains the p53 binding region; a central acidic domain which is capable of interacting with p14 ARF tumour suppressor and ribosomal protein L5; a zinc finger motif which is located downstream of the acidic domain; a RING finger domain at the C-terminus; and finally a nuclear localization signal (NLS) and nuclear export signal (NES) (Michael and Oren 2003) (see Figure 1.3).

Figure 1.3 The domain regions of the Mdm2 protein.
This includes the p53 binding domain, acidic domain, Zinc finger and RING finger domains (Ma et al. 2006).

The ability of Mdm2 to inactivate p53 requires direct binding of the two proteins. One of the key mechanisms for the regulation of p53 activity by Mdm2 indeed occurs when Mdm2 competes with p300 for binding to the N-terminal transactivation domain of p53. This results in the repression of p53-dependent transcription. The Mdm2-mediated negative regulation of p53 is also the result of the E3-ligase function of Mdm2, which can catalyse ubiquitination and the subsequent export of p53 to the cytoplasm for degradation by the 26S proteasome (Honda et al. 1997; Kubbutat et al. 1997; Michael and Oren 2003). The negative effect of Mdm2 is dependent on the relative amount of Mdm2, whereby when Mdm2 is abundant it promotes p53 polyubiquitination and degradation. However, lower levels of Mdm2 lead to p53 monoubiquitination and export to the cytoplasm (Li et al. 2003).

For the ubiquitination (and degradation) of p53 by Mdm2 to occur, a highly conserved region within the N-terminal activation domain (Box-I) of p53 interacts with a hydrophobic pocket in the N-terminal domain of Mdm2 (Bottger et al. 1997). Studies have shown that small peptide ligands designed to mimic the activation domain of p53 disrupt the p53-Mdm2 complex and stimulate p53-dependent gene expression (Bottger et al. 1997). Moreover, small-molecule antagonists of Mdm2 that mimic the p53 activation domain contact with Mdm2 can also activate p53 in cells (Vassilev et al. 2004). Together these results suggested that the activation domain of p53 was required for Mdm2-mediated inhibition of p53. However, it has since been demonstrated that the oligomerisation domain in the C-terminal region of p53 also contributes to efficient

Mdm2 binding and degradation (Kubbutat et al. 1998). In addition, the DNA-binding domain of p53 has been identified as a secondary binding site for Mdm2 (Shimizu et al. 2002; Wallace et al. 2006).

The regulation of ubiquitination of p53 by Mdm2 can occur by a variety of mechanisms such as phosphorylation and acetylation (see sections 1.2.2.1 and 1.2.2.2), but also by protein-protein interactions. These ultimately result in the inhibition of complex formation between Mdm2 and p53 thus preventing ubiquitination (Michael and Oren 2003). Abrogation of Mdm2 expression can also inhibit p53 ubiquitination. One such study demonstrated that treatment of cells with nitric oxide led to the accumulation of transcriptionally active p53, which was preceded by a downregulation of Mdm2 protein and a reduction in levels of ubiquitination. This therefore allowed p53 to avoid the inhibitory effects of Mdm2 (Wang et al. 2002). Phosphorylation of Mdm2 also controls the negative interaction with p53. For example, damage induced phosphorylation of Mdm2 at Ser 395 by ATM leads to accumulation of p53 (Maya et al. 2001). In addition, Mdm2 can itself be regulated by ubiquitination (see section 1.2.2.3). Protein-protein interactions also control the activity of Mdm2. The tumour suppressor p14 ARF has been shown to bind tightly to Mdm2, preventing Mdm2-mediated degradation of p53 (Kamijo et al. 1998). In addition p14 ARF is able to prevent Mdm2 from shuttling between the nucleus and the cytoplasm where it targets p53 for degradation (Tao and Levine 1999). TSG101 has also been shown to interact with p53 and Mdm2, leading to an increased half-life of Mdm2, elevated Mdm2 levels and decreased levels of p53 (Li et al. 2001)

Family members such as MdmX (Mdm4), a protein with structural homology to Mdm2, have been shown to increase the levels of both p53 and Mdm2, which is partly due to it forming a complex with p53 (Wang et al. 2001). Although Mdmx appears to compete with Mdm2 for binding to p53, it has no E3 ligase activity, and therefore cannot target p53 for degradation (Wang et al. 2001). This in turn, leads to the upregulation of Mdm2

levels via the feedback loop. MdmX has been shown to be overexpressed in tumours and tumour-derived cell lines where it coexists with wild-type p53 (Michael and Oren 2002).

Although *Mdm2* gene amplifications occur at relatively low frequencies in human cancer (Momand et al. 2000), Mdm2 is a potent oncogene product whose excess activity can lead to the development of cancer. Indeed, Mdm2 is frequently overexpressed at the protein level in human cancer. Strategies which can inhibit Mdm2 activity have therefore been investigated. Anti-Mdm2 therapy could allow reactivation of p53 activity in tumours with overexpressed Mdm2, but could also promote p53 activity in tumour which express wild-type p53 and normal levels of Mdm2 (Momand et al. 2000). More recently, the development of small molecules which interfere with the p53-Mdm2 complex has proved an interesting development. In particular, Nutlin-3 was identified in a screen for small-molecule antagonists of Mdm2 (Vassilev et al. 2004). This study demonstrated that Nutlin-3 binds to Mdm2 in the p53-binding pocket, therefore competing with p53 for binding to Mdm2. Nutlin-3 was therefore able to activate the p53 pathway to eliminate the cancer cell (Vassilev et al. 2004).

Thus, Mdm2 may inhibit transcription from p53 responsive promoters by four distinct mechanisms: (i) direct competition for binding to the activation domain of p53 with p300; (ii) direct inhibition of basal transcriptional machinery (Thut et al. 1997); (iii) indirectly affecting p53's activity by affecting p53's stability (see section 1.2.1); and (iv) nuclear export of p53 (see section 1.2.2.3)

1.3.3 The Calcium Calmodulin Kinase Superfamily

The Calcium Calmodulin Kinase (CAMK) superfamily form part of the human kinome, and are a complete family of protein kinases which are related based on their catalytic domains. The categorization of protein kinases demonstrated that there are seven major family groups, which include CAMK as well as families such as casein kinase-1 (CK-1), tyrosine kinases (TK) and tyrosine-like kinase (TLK) (Manning et al. 2002). For the purpose of this report we will focus on four members of the CAMK superfamily; Chk1, Chk2, DAPK1 and AMPK. Figure 1.4 shows the protein structure of Chk1 and Chk2.

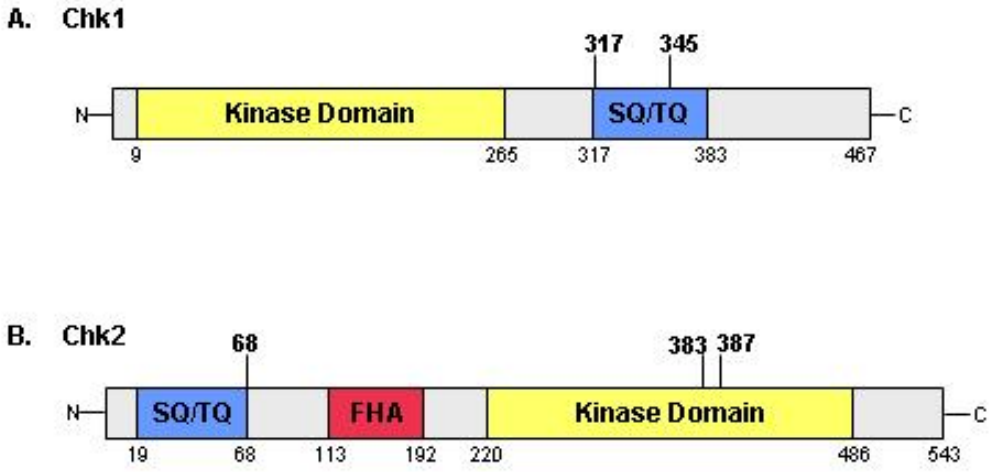

Figure 1.4 A schematic diagram of the protein structures of Chk1 and Chk2.

A. Chk1 is comprised of a kinase domain (shown in yellow) at the N-terminus and a regulatory domain at the C-terminus which contains the SQ/TQ domain (blue), the site of phosphorylation by ATM/ATR. B. In contrast to Chk1, the kinase domain (yellow) of Chk2 is located at the C-terminus of the protein. The N-terminal regulatory domain contains a fork-head associated domain (FHA) and an SQ/TQ domain (blue) at which phosphorylation by ATM occurs at Thr 68.

1.3.3.1 Chk1

Checkpoint kinase 1 (Chk1), a member of the CAMK superfamily, is a classical serine/threonine kinase that plays a major role in cell cycle checkpoint control. It is an evolutionary conserved protein kinase which was first identified in fission yeast as a gene product which functioned as a DNA damage checkpoint (Walworth et al. 1993). Chk1 homologues have since been identified in mammals, *Drosophila*, *Xenopus* and chicken, and the checkpoint function is thought to be largely conserved (Chen and Sanchez 2004). Chk1 is essential for embryonic development and studies in mammals have shown early embryonic lethality in Chk1-deficient mice and acute lethality of Chk1-deficient embryonic cells (Liu et al. 2000; Takai et al. 2000). However, Chk1 is dispensable in chicken DT40 B-lymphoma cells (Zachos et al. 2003). Zachos and colleagues showed that although Chk1 was not universally essential for vertebrate cell survival, Chk1 deficient cells failed to arrest in G2/M in response to ionizing radiation (IR) and failed to maintain viable replication forks. This led to decreased cell survival (Zachos et al. 2003).

Chk1 has a well conserved primary structure (Figure 1.4 A). Chk1 is composed of an N-terminal kinase domain and a C-terminal regulatory domain that contains the serine/glutamine rich SQ/TQ domain, which itself contains multiple phosphorylation sites (Bartek and Lukas 2003). Chk1 is activated through phosphorylation by both ATR and ATM at Serine/Threonine residues that are followed by glutamine (SQ/TQ) (Chen and Sanchez 2004). There are several SQ/TQ motifs found in the C-terminal regulatory domain, including two conserved sites: S345/Q346 and S317/Q318 which are important in the damage response (Chen and Sanchez 2004). Human Chk1 has been shown to be phosphorylated at S345 in response to IR, UV and hydroxyurea (HU) (Liu et al. 2000) and at S317 in response to UV and HU (Zhao and Piwnica-Worms 2001). Mutation of the conserved S345 motif in yeast results in a defective checkpoint response and renders the cell sensitive to IR, UV and other DNA damaging agents (Lopez-Girona et al. 2001).

The clarification of the crystal structure of recombinant human Chk1 revealed an open-kinase conformation, suggesting that the kinase domain itself is catalytically active without any modification (Chen et al. 2000). The role of the C-terminus of Chk1 in the regulation of Chk1 activity is beginning to be defined. It is thought to play an inhibitory role, and phosphorylation at the conserved sites (S317 and S345) within the SQ/TQ domain is thought to be required to release this inhibition (Chen and Sanchez 2004). For example, reports have shown that human and *Xenopus* truncated C-termini demonstrate much higher kinase activity than the full-length proteins (Chen et al. 2000; Oe et al. 2001), suggesting that the C-terminal region may have an autoinhibitory sequence that may interact with and inhibit the kinase domain. To address this issue, a group investigated the effects of mutation and phosphorylation of the SQ/TQ motifs on the domain-domain interaction and the kinase activity of Chk1 (Katsuragi and Sagata 2004). They showed that the C-terminal region does indeed contain an autoinhibitory region (AIR) that can bind to and inhibit the kinase domain of Chk1. Mutation or phosphorylation of the SQ/TQ motifs prevented this AIR-kinase domain interaction and inhibition (Katsuragi and Sagata 2004). Moreover, a report demonstrated that disruption of the C-terminal regulatory domain in truncation mutants of Chk1 activated Chk1 even in the absence of stress, and that full-length Chk1 had comparitivity low basal activity (Ng et al. 2004).

The phosphorylation of SQ/TQ motifs is therefore essential for the activation of Chk1 at the DNA damage/replication checkpoints. However, several other proteins are required for the activation of Chk1 by ATR/ATM. These 'adaptor proteins' function to either recruit Chk1 to ATR/ATM or to provide a platform on which phosphorylation can take place (Chen and Sanchez 2004). In yeast (*Saccaromyces cerevisae*), Rad9 (scRad9) has been shown to interact with scChk1 and scChk2 (Rad53) (Schwartz et al. 2002). Claspin also associates with Chk1, regulating Chk1 activation in response to replication stress. This study in mammalian cells found that Claspin coimmunoprecipitated with Chk1 after UV and HU treatment and that Claspin was hyperphosphorylated (Chini and

Chen 2003). Proteins such as replication protein A (RPA) which interacts with single stranded DNA are also required for Chk1 activation. RPA is recruited by ATR and the ATR interacting protein, ATRIP, to sites of DNA damage, and depletion of RPA results in reduced Chk1 activation (Zou and Elledge 2003).

Chk1 is a key regulator of the G2/M checkpoint of the cell cycle, and when activated Chk1 targets key cell cycle factors. Chk1 is one of several regulators (along with ATR, ATM, Chk2 and Pik1) involved in the blocking of activity of Cdc25C, a phosphatase which promotes mitosis by removing phosphates from cyclin B-Cdc2 complexes (see section 1.1.5.1). Activated Chk1 negatively regulates Cdc25C by phosphorylation at Ser216, which creates a binding site for 14-3-3 proteins, rendering Cdc25C catalytically inactive (Nyberg et al. 2002). It has been shown using a Chk1-deficient ES cell line that Chk1 is regulated by ATR and that Chk1 deficient cells are defective for the G2/M DNA damage checkpoint (Liu et al. 2000).

The intra-S phase checkpoint protects the integrity of replication forks, facilitates the recovery of DNA replication, and ensures that cells do not divide before the entire genome is duplicated (Bartek et al. 2004). The role of Chk1 at the intra-S phase checkpoint was investigated by the Carl Smythe group. They showed that treatment with HU led to significant phosphorylation and activation of Chk1, suggesting that Chk1 was necessary for the intra-S phase checkpoint (Feijoo et al. 2001). The role of Chk1 during replication arrest has been investigated by Zachos and colleagues. They showed that DT40 cells in which the *Chk1* gene has been disrupted (but remain viable) entered mitosis with incompletely replicated DNA when DNA synthesis was blocked, but only after an initial delay (Zachos et al. 2005). They proposed a role for Chk1 at the replication checkpoint in the maintenance of viable replication structures, and it is the continued presence of these structures which delays mitosis until DNA replication is complete (Zachos et al. 2005). A report also described Chk1's involvement in normal S phase to prevent increased initiation of DNA replication. They demonstrated that Chk1

inhibition led to increased initiation of DNA replication and DNA breakage (Syljuasen et al. 2005). More recently it has been shown that Chk1 is required for spindle checkpoint function, which delays the onset of anaphase in cells with mitotic spindle defects (Zachos et al. 2007). In addition, Chk1 catalytic activity is involved in DNA damage induced centrosome amplification (Bourke et al. 2007).

These studies combined demonstrate that Chk1 plays a crucial to promote cell survival during DNA damage by inhibiting of DNA replication and cell cycle progression. Many tumour cells suffer defects in p53 pathways and are therefore defective in G1 arrest. Indeed they rely on the p53-independent components of the S and G2 checkpoints to repair DNA damage and maintain a degree of genome integrity. By targeting components of the G2 pathway such as Chk1, it has been proposed that normal cells will arrest in G1, whereas tumour cells will undergo mitotic catastrophe and apoptosis (Zhou and Bartek 2004). Therefore reports have examined the targeting of Chk1 to improve the effectiveness of anti-cancer treatments in p53-deficient tumours. A report has described the development Chk1 inhibitors which abrogate cell cycle checkpoints and enhance the cytotoxicity of DNA-damaging agents in p53-deficient cells, but not p53 wild type cells (Chen et al. 2006). It has also been shown that when Chk1 is depleted in p53 and p21 null cells, there is abrogation of the G2 checkpoint and increased sensitization to DNA damaging agents. This suggests that G2 checkpoint abrogation in a G1 checkpoint deficient situation would favour cell death, and that targeting Chk1 may be a strategy to increase selectivity of anti-cancer treatment (Carrassa et al. 2004). Moreover, a cooperation between Chk1 and p21 has been proposed, whereby depletion of Chk1 and p21 following replication fork arrest eliminates the protection of G1 phase cells and leads to significant apoptosis in the cell population (Rodriguez and Meuth 2006). They propose that Chk1 inhibitor based therapies may be enhanced by inhibition of p21 function in the treatment of p53 deficient tumours (Rodriguez and Meuth 2006). Therefore Chk1 is a putative target for

pharmacological manipulation of checkpoint pathways, which could enhance the efficiency of anti-cancer therapies.

1.3.3.2 Chk2

Checkpoint 2 (Chk2), also a member the CAM kinase superfamily, is a nuclear serine threonine kinase that plays a key role in cell cycle arrest, activation of DNA repair pathways, maintenance of telomeres, as well as the induction of cell death by apoptosis (Zhou and Elledge, 2000). The first homologue of the Chk2 family, Rad 53, was identified in 1994 and was shown to be involved in checkpoint responses in budding yeast (Allen et al. 1994). In the following years several groups identified the mammalian homologue of Chk2 (Matsuoka et al. 1998; Blasina et al. 1999; Brown et al. 1999; Tominaga et al. 1999), and when the human homologue was identified by the Elledge group, it was named Chk2 (Matsuoka et al, 1998). Along with yeast homologues *Saccaromyces cerevisae* Rad 53 and *Schizosaccharomyces pombe* Cds1, homologues have also been identified in nematode *Caenorhabdatis elegans* and fruit fly *Drosophila melanogaster* (Bartek et al. 2001). The overall structure of Chk2 proteins is similar in all eukaryotes. Human Chk2 has ~82% homology with rat and mouse kinases and shares 34% homology with zebrafish. There are however functional differences between homologues: mammalian kinases seem to mainly respond to lethal DNA damage breaks, whereas yeast respond to various types of DNA damage (Bartek et al. 2001).

Although both Chk1 and Chk2 share functional similarities, there is no sequence homology outside the kinase domain. Chk2 consists of three functional domains (as shown in Figure 1.4 B): an amino terminal domain, rich in Serine or Threonine residues followed by glutamine (SQ/TQ; a consensus site for regulators such as ATM and ATR); the fork head associated (FHA) domain, which modulates protein-protein interactions as well as interactions with other domains within the protein itself (Ahn et al. 2004); and the kinase domain, which shares homology with other Ser/Thr kinases and occupies

almost the entire carboxyl terminal half of Chk2 (Bartek et al. 2001). A recent report compared the functions of the regulatory kinase domains of Chk1 and Chk2. Chk2 was able to inhibit cell cycle progression but the disruption of the regulatory kinase domain abolished kinase activity (Ng et al. 2004).

The mission of Chk2 is to relay signals from ATM to the cell cycle machinery. Chk2 is a stable protein, expressed throughout the cell cycle in an inactive form and becomes activated by ATM as a result of DNA damage such double strand breaks (DSB's) (Bartek and Lukas 2003). Damage signals are then propagated by ATM phosphorylation of the N-terminal region of Chk2, specifically threonine 68, which promotes Chk2 homodimerisation (Bartek et al. 2001). Homodimerisation of Chk2 leads to intermolecular transphorylation of C-terminal residues Thr 383 and Thr 387 within the auto-inhibitory loop, thus leading to the full activation of Chk2. Autophosphorylation of Ser 516 within the kinase domain has been described and has also been shown to be required for full activation of Chk2 (Wu and Chen 2003).

Other checkpoint proteins thought to be involved in the dynamics of Chk2 activation include the DNA ends processing MRN complex, and the DSB interacting proteins 53BP1 and MDC1 (Bartek and Lukas 2003). The MRN (Mre11/Rad50/Nbs1) nuclease complex is involved in sensing DNA damage, checkpoint activation and DNA damage repair (Buscemi et al. 2004). A recent report demonstrated that ATM is stimulated *in vitro* by MRN toward substrates such as p53, Chk2 and H2AX (Lee and Paull 2004). 53BP1 binds to p53 and has been shown to be a key inducer of the DNA damage checkpoint signal (Wang et al. 2002). Mdc1 was identified as a novel protein which works with H2AX to recruit repair proteins to sites of DNA damage and control damage induced checkpoint proteins such as Chk2 (Lou et al. 2003; Stewart et al. 2003). The suppression of Mdc1 leads to defective S phase checkpoint and reduced apoptosis in response to DNA damage (Lou et al. 2003).

Upon activation, Chk2 signals to a number of effectors which promote cell cycle arrest and apoptosis. Chk2 effector proteins include: BRCA1, a breast cancer susceptibility gene product; p53; and Cdc25C and Cdc25A, cell cycle phosphatases. In the cell cycle an initial, short-lived response to damage in G1 phase leads to the ATM-dependent, p53-independent activation of Chk2 (Nyberg et al. 2002). Chk2 phosphorylates Cdc25A at Ser 123, which in turn triggers ubiquitylation and proteasome-dependent degradation of Cdc25A (Bartek et al, 2001). The loss of Cdc25A consequently regulates Cdk2 by maintaining its inhibitory phosphorylation and thereby preventing its association with cyclin E, a necessary step for progression into S phase (Nyberg et al. 2002). A second stage in the G1 phase takes several hours to initiate, is p53-dependent and regulates a block to prevent entry into S phase. This involves the ATM/ATR and Chk2/Chk1 activation of p53, which leads to the transcriptional activation of p21 that in turn inhibits the Cdk2-cyclin E complex (Nyberg et al. 2002). This phase of G1 also involves the phosphorylation of Cdc25C by Chk2 at Ser 216, which inhibits the phosphatase activity of Cdc25C and promotes association with 14-3-3 proteins. This leads to sequestration of phosphorylated Cdc25C in the cytoplasm, maintaining the inhibitory phosphorylation on Cdk1 and thus maintaining a block at the G2/M phase of the cell cycle (Bartek et al, 2001).

BRCA1 has been identified as a substrate of Chk2 and a key regulator in the cell cycle (Bartek et al. 2001). Following DNA damage, BRCA1 is phosphorylated at Ser 988 by Chk2, which leads to the release of BRCA1 from Chk2 and the former thus is able to perform repairs which are essential for cell survival (Lee et al. 2000). The modulation of E2F1 by Chk2 may also regulate DNA damage-induced apoptosis. It has been shown that damage leads to accumulation of E2F1, and that E2F1 null thymocytes are resistant to etoposide-induced apoptosis (Lin et al. 2001). It has also been shown that Chk2 phosphorylates E2F-1 at Serine364 as a result of DNA damage leading to regulation of E2F-1 stability and transcriptional activity (Stevens et al. 2003). P53 is also a target of Chk2. Following DNA damage such as IR, the activation ATM/ATR and Chk2/Chk1

pathways leads to the phosphorylation of p53 at sites such as Ser 15 and Ser 20, resulting in the transcriptional activation of p53 and a reduction of the binding of the negative regulator, Mdm2. ATM can regulate p53 stability independently of Chk2, therefore Chk2 is not necessarily a component of ATM mediated death (Keramaris et al. 2003). There is, however, cooperativity in p53 activation, as ATM phosphorylates p53 Ser15 and Chk2 phosphorylates p53 Ser 20 (Nyberg et al. 2002). The role of p53 phosphorylation by kinases such as Chk2 will be discussed in more details in later sections (see 3.1.1 to 3.1.5).

Different classes of Chk2 mutation result in lack of Chk2 activity by different mechanisms, such as protein instability and cytoplasmic sequestration. Somatic mutations of the human Chk2 gene have been identified in sporadic human malignancies such as carcinoma of the breast, lung, bladder, ovary and vulva as well as in osteosarcinomas and lymphomas (Bartek and Lukas 2003). These mutations occur throughout the three functional domains of Chk2 and cause varying characteristics such as protein instability and kinase inactivity (Bartek and Lukas 2003). A report by Wu and colleagues characterized tumour-associated Chk2 mutants. They showed that frameshift mutations at the C-terminus (T366FS and R475FS) led to loss of Chk2 kinase activity and a mutation within the FHA domain (R145W) resulted in reduced catalytic activity of Chk2 (Wu et al. 2001). This is important as the FHA domain is involved in protein-protein interactions and Chk2 homodimerisation, and suggests that this domain is essential for Chk2 activation following DNA damage (Wu et al. 2001).

Several germ-line mutations of *Chk2* have also been identified in patients with Li-Fraumeni syndrome (Bell et al. 1999). Li-Fraumeni syndrome (LFS) is a rare, highly penetrant familial cancer syndrome that is characterised by multiple tumours at a young age, which are often genetically linked to a mutation in the *p53* gene (Bartek and Lucas, 2003). A study by Bell and colleagues (Bell et al. 1999) found germline mutations in the *Chk2* gene (I157T, 1100delC and 1442delT) in patients with LFS which lacked a

mutation in TP53, suggesting that genetic alteration in Chk2 may indeed predispose to cancer. This also suggested that Chk2 and p53 function in the same tumour suppression pathway (Bell et al. 1999). However, it was subsequently reported that I157T and 1100delC mutations are found at varying frequencies in normal healthy individuals, and therefore cannot predispose to the highly penetrant LFS (Antoni et al. 2007). Chk2 has since been described as a cancer susceptibity gene, whereby mutations such as I157T and 1100delC confer an increased risk to cancers such as breast and prostrate, and that these mutations are likely to act in synergy with other factors to cause cancer (Antoni et al. 2007).

A role for functional Chk2 as a putative target in the treatment of cancers that harbour the wild-type form of the kinase has been discussed. Groups have examined both inhibition and activation of Chk2 in order to treat human cancers. For example, one group demonstrated that siRNA to Chk2 prevented the release of the anti-apoptotic protein survivin from the mitochondria, which resulted in increased apoptosis following IR and doxorubicin treatment (Ghosh et al. 2006). The inhibition of Chk2 may also have a valuable role in radioprotection, whereby targeting Chk2 with small molecule inhibitors, such as the selective ATP-competitive 2-arylbenzimidazole Chk2 kinase inhibitor, protects normal proliferating cells from the side effects of radiotherapy (Arienti et al. 2005). Alternatively the activation of Chk2 may have useful therapeutic value to induce cell cycle arrest or apoptosis in tumour cells. A recent report used a tetracycline inducible form of Chk2 in p53 null cell lines and showed that when Chk2 is induced, it becomes activated by phosphorylation at Thr 68 leading to decreased cellular proliferation, G2 arrest and increased apoptosis (Chen et al. 2005). These studies combined suggest that the targeting of Chk2 either by inhibition or activation may have some therapeutic value. However, it is likely that Chk1 is a superior therapeutic target, with one report suggesting that it is a highly relevant drug target (Xiao et al. 2006).

1.3.3.3 DAPK1

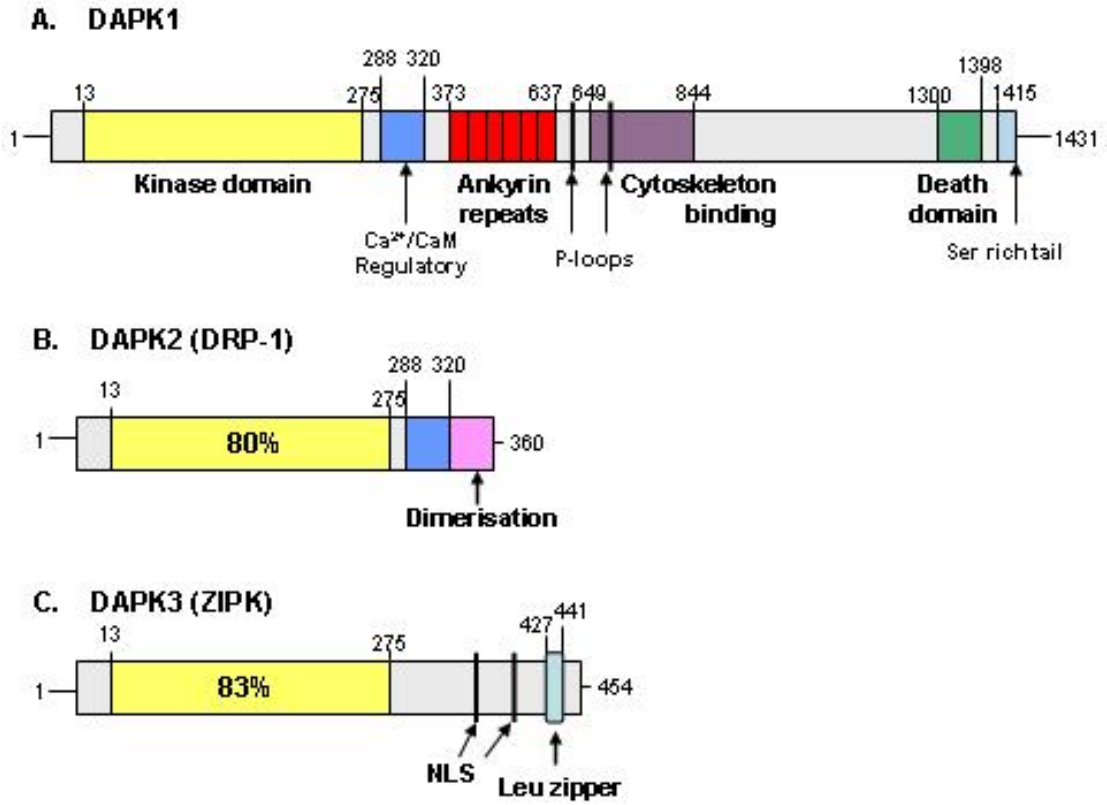

Figure 1.5 A schematic diagram of the DAPK family.

A. DAPK1, B. DAPK2 (DRP-1) and C. DAPK3 (ZIPK) each showing the domains within each family member. The numbers above represent the amino-acid position of each domain and the percentages within the kinase domain represent the degree of amino-acid homology to the kinase domain of DAPK1.

Death-associated protein kinase 1 (DAPK1) is a Calcium-Calmodulin regulated Ser/Thr kinase that mediates cell death. DAPK1 is a member of the DAPK family of three closely related kinases which also include DAPK2 or DRP-1 (DAPK related protein -1) and DAPK3 (also known as ZIPK) which share approximately 80% and 83% homology, respectively, to the kinase domain of DAPK1 as shown in Figure 1.5 (Gozuacik and Kimchi 2006). DAP kinases were first identified as a large group of genes which

function as positive mediators of cell death pathways. The identification of this group of genes involved the use of a technique known as 'technical knock-out' (TKO), which selects for clones that survive cytotoxic signals induced by interferon (IFN)-γ (Deiss and Kimchi 1991; Kimchi 1998). The genes identified were subsequently termed death-associated protein kinases. DAPK1 (which we will focus on in this report) has since been shown to be involved in apoptotic and autophagic cell death, tumour suppression and metastasic suppression (Gozuacik and Kimchi 2006).

The DAPK family of related CAM kinases is grouped as a subfamily due to the high degree of conservation within their catalytic domains, although outwith the kinase domain they vary greatly in their size and structure. DAPK1 is a 160-kDa protein (Figure 1.5A) that consists of an N-terminal catalytic kinase domain, which is composed of 11 subdomains found in all Ser/Thr kinases, and contains a stretch of basic amino acids (residues 45 – 47) known as the basic loop (Tereshko et al. 2001). This basic loop is considered a fingerprint of the DAPK family, as it is conserved among family members. Because of its proximity to the substrate binding site, this basic loop may play an important role in substrate phosphorylation, which in turn may regulate kinase activity (Tereshko et al. 2001). The Cal/CAM autoregulatory segment is found adjacent to the catalytic kinase domain and functions to suppress catalytic activity by binding to the catalytic cleft and acting as a pseudosubstrate (Shohat et al. 2001). Inhibitory autophosphorylation at Ser 308 within this autoregulatory domain reduces the binding affinity to CAM and further stabilizes the docking within the substrate binding site (Shohat et al. 2001). DAPK1 also has a large C-terminal extension that contains multiple functional domains: ankyrin repeats, which are necessary for localization of the kinase to actin stress fibres, necessary for cell death (Bialik et al. 2004); two P loops at residues 639-646 and 695-702, which are of unknown function; and a cytoskeletal interacting domain which directs the kinase to the actin cytoskeleton (Cohen et al. 1997). The extreme C-terminus contains two regulatory elements: a death domain followed by a Ser-rich tail. It has been shown that expression of the death domain protects cells

from tumour necrosis factor α (TNF α) and Fas induced apoptosis (Cohen et al. 1999). Two proteins, extracellular signal-regulated kinase (ERK) and UNC5H2 (a death domain protein that induces cell death when unbound from its ligand) have been shown to interact with the death domain, leading to the activation of DAPK1 (Chen et al. 2005; Llambi et al. 2005) (will be discussed in detail below).

DAPK2 (DRP-1) and ZIPK are comparatively smaller proteins (42-kDa and 52-kDa respectively) that differ in structure to DAPK1 outwith the kinase domain, lacking many of the component structures characteristic of DAPK1. DAPK2 does contain the Cal/CAM autoregulatory segment (which is lacking in ZIPK), followed by a 40aa C-terminal extension which is essential for homodimerisation of the protein. ZIPK contains a C-terminal leucine zipper motif, which mediates homodimerisation and interactions with other leucine zipper containing proteins (Bialik and Kimchi 2006).

Two important factors are proposed to activate DAPK1: firstly, the elevation of intracellular calcium, which is often observed in programmed cell death, and secondly, the dephosphorylation of DAPK1 at Ser 308 by a death-regulated phosphatase, which often occurs in response to cell death stimuli. These two mechanisms operate in combination to allow the activation of DAPK1 in specific circumstances (Bialik and Kimchi 2006). Moreover, additional phosphorylation events involving ERK and mitogen-activated protein kinase (MAPK) signaling pathways have been shown to regulate DAPK1 activity. It has been shown that DAPK1 and ERK binding *in vitro* and *in vivo* is mediated by a docking sequence in the death domain of DAPK1. This interaction promotes the pro-apoptotic function of DAPK1 through two mechanisms (Chen et al. 2005): ERK phosphorylation of DAPK1 on Ser 735 leads to the stimulation of DAPK1 catalytic activity; and furthermore DAPK1 promotes cytoplasmic localization of ERK. This leads to either the activation of cytoplamic localized DAPK1 by phosphorylation or impairment of ERK survival signals. These events are thought to constitute a feedback loop that promotes the apoptotic effect of DAPK1 (Chen et al.

2005). In addition to this study, it was shown that a downstream effector of ERK, the p90 ribosomal S6 kinase (RSK), inhibited exogenous DAPK1 cellular activity by phosphorylation at Ser 289 within the CaM-autoregulatory binding segment (Anjum et al. 2005). This correlated with the suppression of apoptotic activity of DAPK1 and identified DAPK1 as a novel target of the p90 ribosomal S6 kinases (RSK1/2) (Anjum et al. 2005).

It has also been shown that the Netrin-1 receptor, UNC5H2 (thought to trigger apoptosis in the absence of its ligand, Netrin-1), interacts with DAPK1 through their respective death domains. This interaction reduces DAPK1 autophosphorylation at Ser 308, thereby regulating the kinase activity of DAPK1 (Llambi et al. 2005). Netrin-1 has also been shown to interact with UNC5H2 to block activation of DAPK1, suggesting that UNC5H2 and Netrin-1 work together to control the pro-apoptotic activity of DAPK1 (Llambi et al. 2005). Together these studies suggest that phosphorylation of DAPK1 is a cellular event that controls the regulation of DAPK1 activity and therefore the apoptotic potential of this kinase.

DAPK1 has also been shown to interact with the cytoskeleton, which is often manifested by the formation of membrane blebs at the cell surface, leading to loss of adherence to the matrix (Inbal et al. 2002). Membrane blebbing is a common morphological feature of apoptosis and DAPK1 has been shown to phosphorylate the regulatory light chain of myosin II (MLC) on Ser 19, activating myosin contractility and subsequent formation of membrane blebs (Bialik et al. 2004). DAPK1 is also necessary for the full extent of blebbing that accompanies caspase-dependent TNFα-induced apoptosis (Inbal et al. 2002). When overexpressed, DAPK1 has also been shown to be involved, under certain cellular and experimental contexts, in non-apoptotic cell death (also referred to as Type-II cell death) with the accumulation of autophagic vesicles (Gozuacik and Kimchi 2006). The overexpression of DAPK1 leads to features characteristic of apoptotic and non-apoptotic cell death, such as formation of autophagic vesicles, membrane blebbing and

extensive cell rounding in a caspase-independent cell manner (Inbal et al. 2002). DAPK1 has been shown to be necessary for IFNγ-induced autophagy, but not for starvation or rapamycin induced autophagy (Gozuacik and Kimchi 2007). These reports together suggest that DAPK1 may act as a 'molecular switch' between apoptotic and autophagic cell death pathways.

A common epigenetic change in human cancer is reduced gene expression as a result of methylation. Many cell lines have been shown to have lost DAPK1 expression as a result of methylation, and not due to deletion or rearrangement of the gene (Kissil et al. 1997). A report described how DAPK1 expression was restored when some cell lines were treated with an agent (5-azadeoxycytidine) which removes the methyl groups from the CpG nucleotides (Kissil et al. 1997). *DAPK1* gene methylation has been observed in many human cancers originating from many different tissue types (Gozuacik and Kimchi 2006) suggesting a role for DAPK1 function in the control of biological properties associated with tumour progression. There may also be a role for *DAPK1* gene methylation as a diagnostic follow-up test for different types of cancer, whereby downregulation of the *DAPK1* gene may be used specifically to detect malignant cells (Gozuacik and Kimchi 2006).

A role for DAPK1 as a metastasis suppressor protein has also been suggested. One report examined DAPK1 expression in lung tumour growth and metastasis. They showed that DAPK1 expression was absent in highly metastatic mouse lung cell cancers and present in low metastatic variants of the same cell line. Following the reintroduction of DAPK1 there was attenuation of metastasis (Inbal et al. 1997). They also showed that DAPK1 expressing clones were sensitive to TNFα treatment, but that the highly metastatic clones were resistant to this treatment (Inbal et al. 1997). Other studies demonstrate that the loss of DAPK1 correlates with a more malignant phenotype and increased metastatic capacity, which is normally the result of DAPK1 hypermethylation (Gozuacik and Kimchi 2006). There may therefore be a role for DAPK1 as a metastatic

tumour suppressor protein, where it functions to increase sensitivity of tumour cells to programmed cell death during metastasis.

The molecular mechanisms involved in mediation of DAPK1 tumour suppression have suggested a role for p53. One study showed that the coexpression of DAPK1 with oncogenes Myc and Ras, or E1A and Ras led to the suppression of transformation mediated by these pairs of oncogenes. However, the combination of Ras and SV40 large T-antigen, which is known to promote p53 degradation was refractory to DAPK1. The deletion of the p53-binding C-terminal portion of the T-antigen, thereby restoring p53 function, enabled the restoration of DAPK mediated tumour suppression (Raveh et al. 2001). This study went on to show that DAPK1 counteracts oncogene-induced transformation by activating the $p14^{ARF}$-Mdm2 pathway (see section 1.1.4.2), which leads to the stabilization of p53 by inactivating the negative regulator Mdm2 (Raveh et al. 2001). Crosstalk between DAPK interacting proteins and the p53 pathway has been suggested. In addition to these studies, a report suggested that a positive feedback loop may operate between DAPK1 and p53. This hypothesis was suggested due to the presence of p53-binding sites on the DAPK1 promoter sequence, and the fact that p53 can induce the expression of DAPK1 (Martoriati et al. 2005). Therefore DAPK1 and p53 may operate in co-ordination to regulate cell death pathways. One such report suggested a connection between p53 and mammalian target of rapamycin (mTOR), a protein kinase central in nutrient and growth factor signalling. It was shown that p53 activation stimulated autophagy in an AMP-activated kinase (AMPK) and tuberous sclerosis complex (TSC)1/TSC2 dependent manner, both of which respond to energy deprevation in cells (Feng et al. 2005). More recently it has been demonstrated that DAPK1 can positively regulate mTOR by forming an interaction with TSC1/2 complex in cells. This interaction neutralises TSC1/2 mediated suppression of the mTOR translation pathway leading to stimulation of mTOR and mTOR targets: the translational regulators p70 S6 kinase and S6 kinase (C. Stevens et al, in press).

A role for DAPK1 as a novel therapeutic modality in the treatment of cancers has been suggested in several reports. The inactivation of DAPK1 in many human cancers and the fact that reactivating or reintroducing the kinase mediates events such as apoptosis or autophagy suggest that DAPK1 could be a good therapeutic target. DAPK1 has also been shown to play a role in pathologies of the nervous system and has been shown to target neuronal apoptotic regulators to block the destruction of cells after events such as stroke or neuronal cell death. DAPK1 may therefore may be a useful target protein in otther conditions (Bialik and Kimchi 2004). In light of the fact that DAPK1 expression is suppressed by methylation in many cancers, the development of demethylating agents may be a crucial approach for the reactivation of DAPK1 in cancers to promote cell death and elimination of the tumour.

1.3.3.4 AMPK

Mammalian AMP-activated protein kinase (AMPK) is another member of the CAM kinase superfamily, which is related to checkpoint kinases and death-associated protein kinases based on their catalytic kinases domains. The protein, which was subsequently named AMPK, was originally identified by two independent groups who showed that the protein could be regulated by both phosphorylation and by AMP. The protein appeared to be a physiological substrate of AMP and was therefore named AMPK (Hardie et al. 1998). AMPK forms a heterotrimeric complex whose components include three subunits: the catalytic α subunit (63 kDa), the β subunit (38kDa) and the γ subunit (35kDa) (Hardie et al. 1998). It is within the catalytic domain of the α subunit that AMPK becomes activated after phosphorylation at Thr 172 by an upstream kinase of AMPK (AMPK kinase; AMPKK) (Hawley et al. 1996). The α subunit demonstrate close homology to the related *S. cerevisae* gene product, *SFN1*, and contains a typical protein Ser/Thr kinase domain in the N-terminus (Hardie et al. 1998). Isoforms of the three subunits have been identified: α can exist as α1 or α2 isoforms; β can exist as β1

and β2 isoforms; and γ can exist as γ1, γ2 or γ3 isoforms (Hardie et al. 1998). However, isoforms α1, β1 and γ1 are most commonly expressed in cells (Stapleton et al. 1996).

AMPK acts as a metabolic sensor or 'fuel gauge' regulating several intracellular systems including the cellular uptake of glucose, the β oxidation of fatty acids, and the biogenesis of glucose transporter 4 (GLUT4) and the mitochondia. Deviations within the ADP: ATP ratio lead to the rise in AMP, which stimulates a pathway of energy conservation by activating AMPK. AMPK in turn, switches off ATP-consuming anabolic pathways and switches on ATP-producing catabolic pathways to conserve energy (Hardie et al. 1998). AMPK is regulated *in vivo* by an increase in AMP and phosphorylation at Thr 172 by a complex of AMPKK and the tumour suppressor LKB1 (Hawley et al. 2003; Shaw et al. 2004). Upon activation, AMPK phosphorylates metabolic enzymes or alters gene expression to activate the catabolic pathways and inhibit the anabolic pathways (Carling 2004). AMPK can also be activated by a calcium-dependent, AMP-independent process which involves phosphorylation by an upstream kinase, CAMKK β (Towler and Hardie 2007).

AMP accumulation has also been shown to have effects on cell growth and proliferation, whereby treatment of cells with AMP analogs induces cell cycle arrest (Imamura et al. 2001). Moreover, following energy starvation, AMPK has been shown to phosphorylate TSC2, leading to the dephosphorylation of S6K that is required for regulation of translation. This also leads to the inhibition of mTOR (Inoki et al. 2003). This report therefore implicated TSC2 in the coordination of cellular energy levels and cell growth or survival (Inoki et al. 2003). As mentioned in section 1.1.5.4, glucose availability directly regulate cell proliferation, and AMPK is thought to be the mediator of this process (Jones et al. 2005). When the cell is glucose deprived, AMPK is activated, leading phosphorylation of p53 at Ser15 and activation of p53. Thus, implicating AMPK as a intrinsic regulator of the cell cycle, promoting cell cycle arrest to allow the cell to survive the unfavourable glucose deprived conditions (Jones et al. 2005). A

recent report examined the role of a set of p53-regulated gene products including the β subunits of *AMPK*, which are shown for the first time to be regulated by the p53 protein as well as *PTEN* (phosphatase and tensin homologue), *TSC2* and *IGF-BP3*. Each of these genes is upregulated following stress and negatively regulates the IGF-1-AKT-mTOR pathways in a p53-dependent fashion (Feng et al. 2007). They showed that the genes were expressed under p53 control in a cell type and tissue-specific fashion, that mTOR communicates with the p53 pathway, and that AMPK β1 is a p53 regulated gene which is transcriptionally upregulated by a wide variety of stress signals (Feng et al. 2007). These results therefore suggest that p53 regulates AMPK and that AMPK is an essential component of the mTOR signaling pathway.

1.4 Project Aims

In this project we will examine the role of specific members of the Calcium Calmodulin kinase superfamily in the modification of the p53 signaling pathway. Phosphorylation of p53 at specific sites such as Ser 20 is crucial in the activation of p53 and is thought to involve CAM kinases such as Chk2. Although much researched the identity of the main Ser 20 kinases in cells remains undefined. To this end we will firstly set out to examine specific members of the CAMK superfamily and to confirm the identity of the main p53 Ser 20 kinase, thereby partially resolving the contraversy in the field.

P53 is a tetrameric transcription factor which exhibits DNA binding activity through the conserved domains, Box I to V. It is well established that the N-terminal Box-I domain domain of p53 provides a scaffold for binding of components of the transcriptional machinery. To futher elucidate specific regions where kinases may bind and/or phosphorylate, we will examine the role of the Box-V domain. Mutagenesis of p53 will also be performed to further define the sites of interaction and develop of understanding of the molecular mechanisms of the activation of p53.

Cell models and gene expression studies will be used to clarify the effect of depletion of CAM kinases on activation of p53. This will allow us to determine the role of kinases such as Chk1 and DAPK1 on activation status of p53 and allow us to determine kinase-dependent changes in p53 target gene expression. This may provide putative drug targets in which to allow manipulation of the p53 pathway.

Overall the report will therefore provide insight into the role of kinases in the modification of the p53 signalling pathway.

2 MATERIALS AND METHODS

2.1 General

2.1.1 Reagents and Materials

All chemicals were purchased from Sigma or BDH unless otherwise stated. Tissue culture and other general use plasticware were obtained from Nunc or TPP.

2.1.2 Buffers and Stock Solutions

Recipes for stock solutions are listed in section 2.8.

2.1.3 Plasmid DNA

Plasmid DNA for use in transient transfection assays, gene reporter assays, site directed mutagenesis and in vivo coimmunoprecipitation assays was either sourced commercially or kindly donated by colleagues. pcDNA3.1 was purchased from Invitrogen. pcDNA3-p53 was a kind gift from Prof. Sir David Lane. pcDNA3 p53 ΔV was a kind gift from Dr. I. Dornreiter (University of Hamburg, Germany). Other plasmids for transfection based assays were pDEST 3.2 Chk1 and pDEST 12.2 Chk2 which were kindly donated by Dr. Ashley Craig and pDEST GST-DAPK1 and DAPK3 which were a kind gift from Dr. Jennifer Fraser. HA-DAPK1 was kindly donated by Adi Kimchi (Weizmann Institute, Israel). FLAG Chk1 was a kind gift from KL Ball Laboratories. Gene reporter assay constructs pGL3-$p21^{WAF1}$-Luc and pCMV-β Gal were kind gifts from M.Oren (Weizmann Institute, Israel) and M.G. Luciani (University of Dundee) respectively. EGFP peptide constructs were constructed (D.Dornan) by ligating double-stranded oligonucleotides encoding Box-I, Box-V and NS into a XhoI-XbaI-digested EGFP-C3 plasmid (Clontech).

2.2 Cell Culture

2.2.1 Cell lines

Cells were maintained in a humidified CO_2 incubator (Hera) at 37^oC.

Table 2.1 Cell Lines

Cell Line	Source/Description	Medium	Growth conditions
H1299	Human lung carcinoma, p53 null	RPMI	5% CO_2
SAOS-2	Human osteosarcoma, p53 null	D-Mem	5% CO_2
A375	Human malignant melanoma, p53 WT	D-Mem	10% CO_2
A549	Human lung carcinoma, p53 WT	D-Mem	10% CO_2

2.2.2 Media and Sub-culturing of Cells

Cell stocks were maintained in medium (Invitrogen) as stated (Table 2.1) supplemented with 10% foetal calf serum (Invitrogen). Media was stored at 4^oC and warmed to room temperature before use. Cells were maintained in 10cm tissue culture dishes and were subcultured 2 – 3 times a week dependent on cell line. Media was removed and cells were washed using sterile 1x PBS to remove any remaining media. Cells were then trypsinised using 1x trypsin-EDTA solution (Invitrogen; 3ml per 10cm plate) and returned to incubator until cells detached. Medium was added up to 10ml and cells were then split into new tissue culture dish at a seeding density of 2.2×10^6 cells per 10cm dish.

2.2.3 Storage and Recovery of Cells

Cells were stored in liquid nitrogen for long term storage. To freeze cells, a confluent 10cm dish was trypsinised as above and cells were collected by centrifugation (1000rpm, 5 minutes, room temperature). The cell pellet was then resuspended in 1.5ml fresh medium and an equal volume of freezing medium (20% DMSO: 80% FCS). 1ml

cell suspension was frozen in cryogenic freezing vials within Nalgene™ Cryo 1ºC freezing containers before being transferred into liquid nitrogen.

To recover cells, cells were thawed rapidly in a waterbath (37^{o}C). To remove any potential cytotoxic effect of DMSO, the cell suspension was added to 9ml fresh medium in a falcon tube and cells were collected by centrifugation (as above). The cells were then resuspended in medium and transferred to a fresh tissue culture dish. Cells were allowed to grow until confluency and were then subcultured as normal.

2.2.4 Transient transfection of plasmid DNA

In preparation for transfection, cells were plated out into 6 well dishes at 2 – 4 × 10^5 cells per well, dependent on growth rate of the cell line. Medium was added up to 2ml per well and cells were cultured for 24 hours or until 70% confluent. Cells were transfected using Lipofectamine 2000™ (LF 2000; Invitrogen) according to manufacturer's instructions. Essentially, plasmid DNA was diluted in 200µl Optimem (Invitrogen) and total amounts were normalized using empty vector; pcDNA 3.1 (Invitrogen). For each transfection, 5µl of LF 2000™ was diluted in 200 µl Optimem and incubated for 5 minutes at room temperature. The diluted DNA was then combined with the diluted LF2000 and incubated at room temperature for 20 minutes to allow DNA-Lipofectamine complexes to form. The 400µl mixture was then added to cells and gently mixed. Cells were then incubated for 24 hours before harvest unless otherwise stated.

2.2.5 Transient transfection of siRNA

siRNA to target specific genes was obtained from Dharmacon (see Table 2.2). Prior to transfection, siRNA pellets were resuspended in 1 × siRNA buffer to a final concentration of 20µM. The solution was then placed on an orbital shaker for 30min at

room temperature to ensure efficient RNA resuspension. The 20 µM stock solution was aliquoted and stored at -20°C.

Table 2.2 Dharmacon siRNA products

Target Gene	Accession Number	Origin	Product	Catalogue number
Control	N/A	N/A	Non-targeting siRNA pool	D-001206-14-20
Chek1	NM_001274	Human	siGENOME SMARTPOOL	M-003255-02-0010
Chek2	NM_007194	Human	siGENOME SMARTPOOL Upgrade	M-003325-05-0010
DAPK1	NM_004938	Human	siGENOME SMARTPOOL Upgrade	MU-00417-02-0010
DAPK2	NM_014326	Human	siGENOME SMARTPOOL Upgrade	MU-004418-02-0010
DAPK3	NM_001348	Human	siGENOME SMARTPOOL Upgrade	MU-004947-00-0010
TP53	NM_000546	Human	siGENOME set of 4	MQ-003329-01-0010

Transfection of cells with siRNA was performed using DharmaFECT ® Buffer 4 which is provided at 1mg/ml. Cells were plated out in 6 well tissue culture dishes 24 hours prior to transfection as described (2.2.4). Firstly, a 1µM siRNA solution was prepared by adding 10µl stock solution (20µM) to 190µl Optimem. In a separate tube, 4 µl DharmaFECT ® Buffer 4 was added to 200 µl Optimem, mixed and incubated for 5 minutes at room temperature. The contents of the two tubes were then mixed and incubated for 20 minutes at room temperature. The mixture was then added to the cells by mixing gently to give a final working concentration of 100nM siRNA. Cells were

then incubated for 48 hours (unless otherwise stated) before harvesting or further treatment.

2.2.6 Cell treatments

Following transfection of cells with siRNA products and the subsequent incubation period, cells were either harvested (see section 2.3.1) in an undamaged state or treated with genotoxic agents as detailed in Table 2.3. Following the treatment, cells were either harvested immediately or incubated further.

Table 2.3 Cell treatments

Treatment	Dose Range	Incubation time post treatment
X-Ray irradiation	0.5 – 10 Gy γ	0 – 24hr
UV (shortwave cross-linker)	10 – 80 J/m^2	0 – 24hr

2.2.7 MTT: Cell viability assay

MTT is a standard colourimetric assay (an assay which measures changes in colour) used to determine changes in cell death under normal and cytotoxic conditions. The yellow methylthiazolyldiphenyl-tetrazolium bromide (MTT) is reduced to purple formazan in the mitochondria of living cells. A soluble solution such as DMSO is then added to dissolve the insoluble purple formazan product into a coloured solution. The absorbance of this coloured solution can then be quantified by spectrophotometry. The reduction reaction only takes place in living cells where the mitochondrial reductase enzymes are active and therefore a direct correlation can be made between the absorbance to the number of living cells.

2.2.7.1 Transient Transfection and Damage Treatment of Cells

Firstly, cells were prepared for the cell viability assay by transient transfection with siRNA (see 2.2.5). Following an incubation period of 48 hours, cells were treated with X-ray or UV damage as described in Table 2.3 and returned to the incubator for a further incubation period as described in the results section.

2.2.7.2 MTT treatment and measurement

A stock solution of methylthiazolyldiphenyl-tetrazolium bromide (MTT) reagent was prepared by dissolving 100mg MTT in 20ml sterile PBS to give a final stock concentration of 5mg/ml. The solution was filtered sterilized using a 0.2µM filter and stored at 4^{o}C in the dark for up to four weeks. In preparation for use a working concentration of 0.25µg/ml was prepared by diluting MTT in warm medium. The diluted MTT solution was added directly to the cells, leaving two wells as a blank (DMSO). Cells were returned to the incubator for 4 hours at 37^{o}C, then MTT was removed from the cells and DMSO (ACS spectrophotometric grade) was added to dissolve formazan crystals. The absorbance was then read by spectrophotometry at 570nm using PowerWaveXS™ Microplate Spectrophotometer (BioTek) and readings were collated using KC Junior package.

2.2.8 Gene reporter assay

2.2.8.1 Transient Transfection

Two types of gene reporter assay systems were performed; β-Galactosidase Enzyme Assay System with Reporter Lysis Buffer™ (Promega) and the Dual-Luciferase® Reporter Assay System (Promega). Readings were normalised to transfection efficiency using β-Gal (assay system) or a Renilla (Dual-Luciferase® Reporter Assay System).

2.2.8.2 Luciferase/ β-Gal assay system

For the Luciferase/β-Gal assay system cells were transiently transfected (see section 2.2.4) with 1µg of PGL3 luciferase reporter construct, 0.25µg pCMVβ-Gal construct and other constructs as required to a total plasmid concentration of 4µg. Twenty four hours following transfection cells were harvested for analysis by firstly washing each well in 2ml ice cold PBS. 70 µl of Reporter Lysis Buffer™ from the β-Galactosidase Enzyme Assay System (Promega) was added to each well and incubated for 10 min on ice. Cells were scraped into microcentrifuge tubes and debris was pelleted by centrifugation at 13000 rpm for 2 min at 4 ºC and lysates were then transferred to fresh microcentrifuge tubes.

For the luciferase assay, 20 µl of lysate was added to an opaque Microlite 2™ 96 well ELISA plate (CoStar; Corning Inc.) on ice. 50µl of luciferase substrate was then added and allowed to reach room temperature. Light emission was quantified using Fluroskan Ascent F1™ (Labsystems) luminometer.

The β-Galactosidase Assay™ (Promega) was carried out by the addition of 20 µl of lysate to a clear 96 well plate on ice. 20 µl β-Galactosidase 2x assay buffer was then added and incubated for 20 min at 37^{o}C. The reaction was terminated by the addition of 50µl sodium bicarbonate and absorbance at 405nm was read using the PowerWaveXS™ Microplate Spectrophotometer (BioTek).

The results were normalized by dividing the Luciferase readout by the β-Galactosidase readout to give a value of Relative Light Units. Unless otherwise stated each data point is the average of two replicates, therefore confidence intervals have not been included as such statistical parameters are not valid.

2.2.8.3 Dual-Luciferase Reporter Assay System

Dual luciferase assay system involved the transient transfection (see section 2.2.4) of 0.14µg PGL3 luciferase reporter construct, 0.06µg *Renilla* luciferase reporter construct (pRL CMV) along with other constructs as required to a total concentration of 1.6µg. Twenty four hours following transfection cells were processed for analysis using the Dual-Luciferase® Reporter Assay System (Promega). Cells were harvested by firstly washing in 2ml ice cold PBS before the addition of 100 µl 1x passive lysis buffer (PLB). The plate was then incubated with gentle agitation for 15 min at RT. Cells were then collected into a microcentrifuge tube and debris was pelleted by centrifugation (13000rpm, 30 sec, 4^{o}C). Lysate were retained in a fresh microcentrifuge tube.

The assays for firefly luciferase activity and *Renilla* luciferase activity were performed in one tube format using the Dual-Luciferase® Reporter Assay System (Promega). Firstly, 5 µl of lysate was added to a Microlite 2™ 96 well ELISA plate on ice. 25 µl of Luciferase Assay Reagent II was added to the plate and allowed to reach room temperature. Light emission was quantified using the Fluroskan Ascent F1™ (Labsystems). When the maximum signal of firefly luciferase activity was reached, *Renilla* luciferase activity was quantified by adding 25 µl of Stop & Glo® Reagent (prepared immediately before assay according to manufacturer's instruction; Promega) and light emission was measured using the Fluroskan Ascent F1™.

The results were normalized by dividing the maximum firefly luciferase readout by the maximum *Renilla* luciferase activity readout to give a value of Relative Light Units. Unless otherwise stated each data point is the average of two replicates, therefore confidence intervals have not been included as such statistical parameters are not valid.

2.3 SDS-PAGE

2.3.1 Preparation of Cell lysates

Cells were harvested on ice by firstly removing media and washing with ice cold 1x PBS (see section 2.8). Cells were then scraped into a small volume of PBS and collected in a microcentrifuge tube. Cells were pelleted by centrifugation (3000rpm, 3min, 4^{o}C) and the cell pellet was snap frozen in liquid nitrogen.

Frozen cell pellets were lysed in 2-3 x volume urea lysis buffer (unless otherwise stated; see section 2.8) by pipetting up and down several times until no particles were seen. Lysates were then incubated on ice for 30 minutes, followed by centrifugation (13000g, 10min, 4^{o}C) to obtain a supernatant from which any cell debris had been removed. The lysate was then snap frozen and stored at -80^{o}C.

2.3.2 Protein Quantification

Protein was quantified using the Bradford assay. Bradford reagent was prepared according to the original published recipe (Analytical Biochemistry 72, 248-254, 1976; see section 2.8). Prior to use, the reagent was filtered using 0.45µM filter to remove any precipitate.

The protein concentration of the cell lysate (see section 2.3.1) was determined by diluting 1µl of the lysate in 200 µl Bradford reagent (pre-warmed to room temperature) in a 96 well plate. The plate was incubated for 5 minutes at room temperature and then read using PowerWaveXS™ Microplate Spectrophotometer (BioTek) and readings were collated using KC Junior software programme package. Readouts were converted to concentrations in mg/ml by creating a standard curve taken from the BSA standards values (from 0 to 8 µg).

2.3.3 Preparation of gels and separation of proteins by SDS-PAGE

SDS polyacrylamide gels were prepared using 10-15% polyacrylamide as described (Laemmlli et al, 1970; see section 2.8) using Mini-Protean3™ (Biorad) gel casting modules. Firstly, the separating gel was poured and was overlayed with water to allow the gel to polymerise. Once polymerization was completed, the stacking gel was added along with the 10 or 15 well Teflon comb. This again was allowed to polymerise. The comb was then removed and wells were washed out with water to remove any residual APS.

4 × SDS sample buffer was then added to lysates. Samples were then heated for 5 minutes at 95^{o}C and 10-30µg samples were loaded. 5µl of Biorad protein standards were loaded into the first well as molecular weight markers. Proteins were then separated by electrophoresis in running buffer at 180V until the Bromophenol dye front reached the bottom of the gel.

2.3.4 Detection of fractionated proteins

2.3.4.1 Coomassie brilliant blue staining

SDS-PAGE (section 2.3.3) gels were fixed for coomassie staining (see section 2.8) for 5 min and stained with Coomassie Blue Stain for 5 min to 12 h at room temperature with agitation. Gels were destained until the bands were clearly visible and the background staining was removed. Gels were then dried by placing on Waltmann blotting paper and were covered with Saran Wrap and were then placed in a DryEase Gel Drying™ system (Invitrogen).

2.3.4.2 Immunoblotting

Transfer of separated proteins (see section 2.3.3) to Hybond-C Extra nitrocellulose membranes (Amersham Biosciences) was carried out electrophoretically in tanks

containing transfer buffer (see section 2.8) at 300mA for 60min or at 20mA overnight. Transferred proteins were stained with 25ml Pelikan ink (diluted 1/300 in PBS-Tween) for 5 minutes. The membrane was then rinsed twice in PBS-Tween (see section 2.8) to remove excess stain. Non-specific protein binding sites were blocked by incubating the membrane in PBS-Tween containing 5% (w/v) non-fat dried milk (Marvel), for 1 hour at room temperature. For phospho-specific antibodies, non specific binding was blocked using TBS-Tween (see section 2.8) containing 3% BSA and 1mM β-glycerophosphate. The phosphatase inhibitor, β-glycerophosphate, was added to preserve phosphorylation of proteins. The membranes were then incubated overnight at 4^{o}C with primary antibody (see Table 2.4) diluted in blocking buffer. The antibody was then removed and membranes were washed using either PBS-Tween or TBS-Tween (3 x 5 minute). The binding of mouse monoclonal antibodies was detected by adding anti-mouse IgG secondary antibody and detection of rabbit polyclonal bound antibodies was performed using anti-rabbit IgG secondary antibody (both conjugated to horse radish peroxidase; DAKO). Secondary antibodies were diluted 1/1000 in blocking buffer before adding to the membrane for incubation for 1.5 h at RT. Following 3 x 20 minute washes, specific bands were detected by enhanced chemiluminescence (ECL). Membranes were overlaid with ECL solution 1 and 2 (mixed 1:1; see section 2.8) for 1 min, blotted dry and exposed to X-ray film (SLS), which was then developed (X-ray Imaging Equipment™, Fuji).

2.3.4.3 Stripping Nitrocellulose membranes

To reprobe a membrane, membrane bound antibodies (see section 2.3.4.2) were removed using stripping buffer (see section 2.8). A fresh solution of 10ml of stripping buffer containing 70µl β-mercaptoethanol was added to the membrane which was then incubated at 50^{o}C for 30-45 minutes with occasional agitation. The membrane was then rinsed several times in ddH_2O and then processed for immunoblotting as normal.

Table 2.4 Antibodies

Antibody	KDa	Type	Company	Dilution
Chk1 (G-4)	56	Mouse monoclonal	Santa Cruz	1/1000
Chk2 (A-12)	66	Mouse monoclonal	Santa Cruz	1/500
DAP Kinase 1	160	Mouse monoclonal	BD	1/1000
DAP Kinase 2	42	Rabbit polyclonal	Abcam	1/500
DAP Kinase 3 (ZIPK)	52	Rabbit polyclonal	Abcam	1/500
GFP	27	Rabbit polyclonal	Abcam	1/2000
IRF1	48	Mouse monoclonal	BD	1/500
IRF2	50	Rabbit polyclonal	Santa Cruz	1/100
$p21^{WAF1}$	21	Mouse monoclonal	Oncogene	1/1000
PTEN	57	Mouse monoclonal	Cell Signaling	1/1000
p53 (DO1)	53	Mouse monoclonal	B. Vojtesek*	1/1000
p53 (DO12)	53	Mouse monoclonal	B. Vojtesek*	1/1000
p53– P (Ser 15)	53	Mouse monoclonal	Cell Signaling	1/1000
p53– P (Ser 15)	53	Rabbit monoclonal	Cell Signaling	1/1000
p53– P (Ser 20)	53	Rabbit monoclonal	Santa Cruz	1/200
p70-P S6 Kinase (Thr 389)	70	Mouse monoclonal	Cell Signaling	1/1000
S6 Ribosomal-P (Ser 235/236)	32	Rabbit polyclonal	Cell Signaling	1/1000

* A kind gift from B. Vojtesek, Dept. of Experimental Oncology, Masaryk Memorial Cancer Institute, Brno, Czeck Republic.

2.4 Microbiological Techniques

All microbiological techniques were carried out under aseptic conditions.

2.4.1 Preparation of competent cells

A starter culture of E. coli strain DH5α cells was set up in a 15ml sterile tube by inoculating a 2ml culture of LB with a colony of bacteria from a stock plate. The culture was incubated overnight at 37°C with rotation at 225rpm. The culture was diluted 1/100 in 200ml of LB and incubated at 37°C with agitation at 225rpm until the OD_{600nm} reached 0.3-0.5. The cells were collected by centrifugation (10min, 8000rpm, 4°C) and resuspended in 80ml ice-cold TFBI (see section 2.8). After 10 min incubation on ice the cells were again centrifuged (5min, 2500rpm, 4°C) and gently resuspended in 8ml of TFBII (see section 2.8). The cells were incubated on ice for 15 min and 200µl aliquots were added to pre-chilled microcentrifuge tubes. The aliquots were snap frozen on dry ice and stored at -80°C.

2.4.2 Agar bacterial culture dishes

LB agar was liquefied by heating in a microwave for 2 minutes. The liquid agar was then allowed to cool to hand-warm temperature, poured into 90mm Petri dishes (Sterlin) which were allowed to cool at room temperature. Antibiotic was added immediately prior to pouring the plates. Agar plates were then stored at 4°C.

2.4.3 Transformation of plasmid DNA by heat shock

50µl of competent DH5α cells (see section 2.4.1) were defrosted on ice and mixed with 1µl of plasmid DNA. The cells were then incubated on ice for 30 min and heat-shocked at 42°C for 45sec. The cells were returned to ice for 2 min before the addition of 500 µl LB. The culture was then incubated at 37°C, 225rpm for 45min. Cells were then plated onto LB agar bacterial culture plates containing appropriate selective antibiotic and incubated overnight at 37°C.

2.4.4 Amplification of plasmid DNA

A starter culture was initiated by inoculating a 5ml LB culture (see section 2.8) containing selective antibiotic with a single bacterial colony from a stock plate (see section 2.4.3) or a glycerol stock (see section 2.4.5). This was then incubated for 6-8hrs at 37^{o}C (225rpm). At this stage the 5ml culture could be processed for mini-prep isolation of plasmid DNA (see section 2.4.6) by centrifugation (4000rpm, 10min, 4^{o}C). Alternatively, for maxi-prep isolation of plasmid DNA (see section 2.4.6) the starter culture was transferred to a large culture flask containing 200ml LB (with appropriate antibiotics) and incubated overnight under the same conditions. The culture flask was at least 5x volume of culture being grown to allow for aeration.

2.4.5 Glycerol stocks

Glycerol stocks of bacterial cultures were prepared by adding 875µl starter bacterial culture to 125µl sterile 80% glycerol in a cryovial (Nunc). This was then snap frozen and stored at -80^{o}C.

2.4.6 Purification of plasmid DNA

Cells grown for amplification were collected by centrifugation (6000rpm, 15min, 4^{o}C). Plasmid DNA was isolated using Qiagen's HiSpeed™ Plasmid Maxi Purification Kit for large volume cultures or Qiagen's QIAprep™ Spin Mini Prep Kit for small volume cultures according to manufacturer's instructions. DNA was eluted into a sterile microcentrifuge tube in ddH_2O and stored at -20^{o}C.

2.4.7 Quantification

The concentration of plasmid DNA was determined by spectrophotometry at 260nm using a NanoDrop® ND-1000. 1µl of sample was pipetted onto the measurement pedestal and the concentration was generated using the NanoDrop® software.

2.4.8 Agarose Gel Electrophoresis

Agarose (to a final concentration of 0.7%) was dissolved in 1 × TAE buffer and liquefied by heating in a microwave for 2 min. The agarose solution was cooled to hand-warm temperature before the addition of 0.03% ethidium bromide. Gels were cast and allowed to set at room temperature before being submerged in 1 × TAE buffer. Samples were then diluted 1:5 in DNA sample buffer, loaded alongside 1Kb or 100bp DNA ladders (Invitrogen) depending on plasmid size and electrophoresis was performed at 100V for 30 min. Gels were visualized by UV transillumination using the ChemiGENIUS^2 Bio Imaging System (Syngene) and the GeneSnap Imaging tool (Syngene).

2.5 Site Directed Mutagenesis

Site-directed mutagenesis of two genes was performed: (1) TP53 (NCBI accession number: NM_000546) in the mammalian expression vector pcDNA3.1 (Invitrogen) and (2) eGFP C3 (Clontech) containing the Box V region of p53.

2.5.1 Primer Design

Site directed mutagenesis primers (see Table 2.5 and Table 2.6) were designed to contain the desired mutation according to guidelines set by QuikChange® Site Directed Mutagenesis Kit (Stratagene). Primers were designed to be 25 – 45 base pairs in length and have a melting temperature above 78^{o}C. Sequencing primers (see Table 2.7) were designed to anneal to specific regions of the open reading frame of the gene in order to verify presence of mutation.

Oligonucleotide primers were purchased from Sigma-Genosys and were reconstituted in ddH_2O to a final concentration of 100mM.

Table 2.5 Site directed mutagenesis primers for p53

Name	Binding Site in Sequence	Melting temperature (^{o}C)	Nucleotide Sequence Sense Primer (Nucleotides Mutated) Antisense Primer
p53 D207H	207 bp	80	5’-CGTGTGGAGTATTTGCATGAC AGAAACACTTTTCG-3’ 5’-CGAAAAGTGTTTCTGTCATG CAAATACTCCACACG-3’
p53 D207E	207 bp	80	5’-CGTGTGGAGTATTTGGAA GACAGAAACACTTTTCG-3’ 5’-CGAAAAGTGTTTCTGTCTTC CAAATACTCCACACG-3’
p53 D208N	208 bp	80	5’-GCGTGTGGAGTATTTGGAT AACAGAAACACTTTTCGAC -3’ 5’-GTCGAAAAGTGTTTCTGTT ATCCAAATACTCCACACGC -3’
p53 R209I	209 bp	81	5’-GTGGAGTATTTGGATGAC ATAAACACTTTTCGACATAGTG-3’ 5’-CACTATGTCGAAAAGTGTT TATGTCATCCAAATACTCCAC-3’
p53 H214Q	214 bp	78	5’-CAGAAACACTTTTCGACAA AGTGTGGTGGTGCCC-3’ 5’-GGGCACCACCACACTTTGTCG AAAAGTGTTTCTG-3’
p53 F270Y	270 bp	86	5’-CTGGGACGGAACAGCTAT GAGGTGCGTGTTTGTGC-3’ 5’-GCACAAACACGCACCTCATA GCTGTTCCGTCCCAG-3’
p53 A276V	276 bp	84	5’-GAGGTGCGTGTTTGTGTCTGT CCTGGGAGAGAC-3’ 5’-GTCTCTCCCAGGACAGAC ACAAACACGCACCTC-3’
p53 N288Y	288 bp	83	5’-CGCACAGAGGAAGAGTAT CTCCGCAAGAAAGGG-3’

			5’-CCCTTTCTTGCGGAGATACTC TTCCTCTGTGCG-3’
p53 N288T	288 bp	84	5’-CGCACAGAGGAAGAGACT CTCCGCAAGAAAGGG-3’ 5’-CCCTTTCTTGCGGAGAGTCTC TTCCTCTGTGCG-3’
p53 K291E	291 bp	84	5’-GAAGAGAATCTCCGCGAG AAAGGGGAGCCTCAC-3’ 5’-GTGAGGCTCCCCTTTCTCGCG GAGATTCTCTTC-3’
p53 K292I	292 bp	84	5’-GAGAATCTCCGCAAGATA GGGGAGCCTCACCAC 3’ 5’-GTGGTGAGGCTCCCCTATTTC GCGGAGATTCTC 3’
p53 K292N	292 bp	86	5’-GAGAATCTCCGCAAGAAC GGGGAGCCTCACCAC-3’ 5’-GTGGTGAGGCTCCCCGTTCTT GCGGAGATTCTC-3’

Table 2.6 Site directed mutagenesis primers to eGFP Box V

Name	**Binding Site in Sequence**	**Melting temp. (^{o}C)**	**Nucleotide Sequence Sense Primer (Nucleotides Mutated) Antisense Primer**
BoxV Ala-1	1345bp	85.8	5’CTCAGATCTCGAGGCGGCCAGCTTTGAGGTGCG3’ 5’CGCACCTCAAAGCTGGCCGCCTCGAGATCTGAG3
BoxV Ala-2	1351bp	87.8	5’CTCGAGCGGAACGCCGCTGAGGTGCGTGTTTG-3’ 5’CAAACACGCACCTCAGCGGCGTTCCGCTCGAG-3’
BoxV Ala-3	1357bp	86.0	5’GGAACAGCTTTGCGGCGCGTGTTTGTGCCTG-3’ 5’CAGGCACAAACACGCGCCGCAAAGCTGTTCC-3’
BoxV Ala-4	1363bp	82.8	5’CAGCTTTGAGGTGGCTGCTTGTGCCTGTCCTG-3’ 5’CAGGACAGGCACAAGCAGCCACCTCAAAGCTG 3’
BoxV	1369bp	82.0	5’GAGGTGCGTGTTGCTGCCTGTCCTGGG-3’

Ala-5a			5'CCCAGGACAGGCAGCAACACGCACCTC-3'
BoxV Ala-5b	1372bp	79.5	5'CGTGTTTGTGCCGCTCCTGGGAGAGAC-3' 5'GTCTCTCCCAGGAGCGGCACAAACACG-3'
BoxV Ala-6	1378bp	76.9	5'GTTTGTGCCTGTGCTGCGAGAGACTGATCTAG-3' 5'CTAGATCAGTCTCTCGCAGCACAGGCACAAAC-3'
BoxV Ala-7	1384bp	77.6	5'GCCTGTCCTGGGGCAGCCTGATCTAGATAAC-3' 5'GTTATCTAGATCAGGCTGCCCCAGGACAGGC-3'

2.5.2 Site directed mutagenesis and PCR

All mutagenesis was carried out according to protocols as described in QuikChange® Site Directed Mutagenesis Kit (Stratagene). A reaction was prepared using 10 × reaction buffer, 10mM oligonucleotides primers, 25mM dNTPs mix (Promega), 100ng template DNA and PfuTurbo DNA polymerase (Stratagene). The plasmid was denatured by temperature cycling (parameters as detailed in the manufacturer's instructions) which allowed the oligonucleotide primers containing the desired mutation to anneal. PfuTurbo DNA polymerase extended and incorporated the mutagenic primers to produce nicked circular strands. [Amendments to cycling parameters were made for annealing temperature (dependent on melting temperature of the primer) and extension time (1 min per Kb plasmid)]. The correct size of the product was confirmed by electrophoresis of 10µl of the product on a 0.7% agarose gel (see section 2.4.8). Successfully amplified products were digested with Dpn1 restriction enzyme (Invitrogen) to eliminate any remaining parental DNA template. Bacteria were transformed with the product for amplification (see sections 2.4.3 and 2.4.4). Plasmid DNA was then recovered from selected colonies using a Mini prep™ Kit (Qiagen) and DNA was sequenced (see section 2.5.3).

2.5.3 Sequence Analysis

Table 2.7 Sequencing Primers

Name	Binding Site in Sequence	Melting temperature	Nucleotide Sequence
p53 internal forward 1	420bp	70°C	5'- CTGGGCTTCTTGCATTCTGG – 3'
p53 internal forward 3	781bp	73°C	5'- GAGCCGCCTGAGGTTGGC – 3'
p53 internal reverse rev 1	61bp	68°C	5'- GCACCAGCAGCTCCTAC – 3'
eGFP forward	1219bp	70°C	5'- GACCACTACCAGCAGAACAC – 3'
eGFP reverse		53°C	5'- GCTGCAATAAACAAGTTAAC – 3'

All sequence analysis was performed by the DNA sequencing service, Wellcome Trust Clinical Research Facility, Western General Hospital. Primers were supplied at 1.6μM and plasmid DNA at 150ng/μl. Sequencing of samples was carried out using primers as detailed in Table 2.7 Sequencing Primersand where appropriate standard T7 (a forward primer which anneals to the T7 promoter region at the 5' end of the gene) and BGH (a reverse primer which anneals to the BGH polyadenylation sequence at the 3' end of the gene) primers were used along side internal sequencing primers to sequence all of the gene. Where possible sequencing reactions were completed and cleaned up in house according to ABI protocols before submitting for processing. For each 10μl sequencing reaction, 2 μl Big Dye (V3.1; Applied Biosystems) was mixed with 150ng of plasmid DNA and 1.6pmoles primer. PCR cycling parameters were used as detailed in the manufacturer's instructions. Samples were cleaned by ethanol/EDTA precipitation and submitted for sequencing. Wild-type or mutated sequences were confirmed by comparison with wild-type cDNA sequence using the Clustal W online multiple alignment programme.

2.6 In vivo Co-immunoprecipitation

2.6.1 Transient transfection of plasmid DNA

Cells were plated out into 10cm tissue dishes at 2.2 $\times 10^6$ cells per dish and allowed to grow until 70% confluent. Cells were cotransfected (using 10µl lipofectamine; as detailed in section 2.2.4) with 1µg FLAG tagged plasmid DNA encoding the protein of interest such as Chk1 or DAPK1 and up to 1µg plasmid DNA encoding the putative binding partner, EGFP-Box V gene. The concentration of transfected EGFP plasmid DNA was kept to a minimum as EGFP tag is toxic to the cell.

2.6.2 Cell lysis and Pre-clearing

Cells were harvested (see section 2.3.1) and lysed in 2 – 3 × volume 1% Triton X-100 lysis buffer (see section 2.3.1) with 1 tablet Complete® Protease Inhibitor cocktail (Roche Diagnostics) per 10ml lysis buffer. Following a 45 min incubation on ice, lysates were collected by centrifugation (13000 rpm, 10 min, 4^{o}C). Lysates were pre-cleared (agarose Sepharose® CL-4B beads) to reduce non-specific binding. 20 µl agarose beads were washed 5 times with 500 µl lysis buffer to remove ethanol. Lysates were then added to the beads and pre-cleared by incubation for 1 hour at 4^{o}C with rotation.

2.6.3 Co-immunoprecipitation of FLAG-tagged proteins

25µl M2 (anti-FLAG) agarose beads were washed sequentially with 1ml TBS (3×), 1ml 0.1M glycine pH 3.5 (2×), 1ml TBS (4×) and 1ml Triton-X 100 lysis buffer (5×). The pre-cleared lysates (see section 2.6.2) were incubated with beads for binding of FLAG-tagged proteins to beads M2 (anti-FLAG) agarose (overnight at 4^{o}C with rotation). Unbound proteins were retained for western blot analysis and the bound proteins were washed in 1ml TBS (repeat 4 ×) before elution of proteins in SDS sample buffer.

2.6.4 Coimmunoprecipitation using antibody coupled NHS beads

2.6.4.1 Coupling of antibodies to NHS (N-hydroxysuccinimide) activated beads

Where FLAG-tagged proteins were not available, antibodies to the protein of interest were crosslinked to NHS-activated Sepharose™ 4 fast flow beads (GE Healthcare) via a nucleophilic substitution reaction between the primary amine of the antibody and the carbonyl group of the NHS moiety.

Coupling: NHS activated beads were washed twice in 2 × volume ice cold 1mM HCl and twice in 2 × volume ice cold PBS. 5 µg of antibody was then added to 25µl beads, taking an aliquot of the antibody before addition. Coupling of antibody to beads was carried out for 1 hour at room temperature with rotation. An aliquot of the supernatant was taken following coupling and a Bradford assay (see section 2.3.2) was performed to determine coupling efficiency. Where 100% coupling efficiency is achieved the protein concentration of the post-coupling supernatant should be reduced to almost zero.

Washing was carried out to deactivate excess NHS active groups not coupled to the ligand and to remove any weakly bound uncoupled antibody. The wash stages were alternated between high pH (Buffer A; 0.5M ethanolamine, 0.5M NaCl; pH 8.3) and low pH (Buffer B; 0.1M acetate, 0.5M NaCl; pH 4) buffers. Beads were washed thrice in 2 × volume Buffer A, and thrice in 2 × volume Buffer B. This was repeated twice more with an incubation of 30 min at room temperature during the second wash. Antibody coupled NHS beads were pelleted and stored in PBS-NaN_3 at 4^{o}C until required.

2.6.4.2 Co-immunoprecipitation of antibody bound beads

Pre-cleared lysates (see section 2.6.2) were added to antibody bound beads (see section 2.6.4.1) and incubated overnight at 4^{o}C with rotation. Unbound lysate was retained for western blot analysis and beads were washed in 5 × volume of PBS – T (repeated 3 times more). The bound proteins were eluted with SDS sample buffer for analysis.

2.6.5 Western Blot analysis

Immunocomplexes (see section 2.6.3 and 2.6.4.2) were analysed by SDS-PAGE followed by immunoblotting (see section 2.3.4.2) with an antibody specific for the putative binding partner.

2.7 Microarray Analysis

Microarray analysis of Chk1 and DAPK1 depleted cells was performed to evaluate changes in gene expression profiles of the p53 signalling pathway. Following incubation with siRNA (see 2.2.5), cells were either harvested immediately (see section 2.3.1) or alternatively, cells were treated with X-ray damage (as described in section 2.2.6), dose/incubation time as stated in results (see section 5.2.3) before harvesting. Microarray analysis (see section 2.7.1) was performed using the Oligo GEArray® System (Superarray; Bioscience Co.).

2.7.1 Isolation of total RNA

For preparation of total RNA, RNA was extracted from cells pellets using RNeasy® Mini Kit (Qiagen) according to manufacturer's instructions. Samples were eluted into 30µl RNase free H_2O before determining concentration and purity by spectrophotometry at 260nm using the NanoDrop® ND-1000. RNA quality control was performed before proceeding to next step to ensure high quality RNA was obtained (according to manufacturer's recommendations).

2.7.2 cRNA Target Labeling for Oligo GEarray® Hybridisation

The Oligo GEarray® System (SuperArray; Bioscience Co.) was used to prepare cRNA for Oligo GEarray Hybridisation. The system employed a one-tube format, which firstly involved the synthesis of cDNA. 3µg of total RNA was used for each cDNA synthesis reaction which was carried out according to manufacturer's instructions. Subsequent cRNA synthesis and labeling was carried out according to manufacturer's instructions.

Biotinylated-UTP (Roche) was used to label cRNA and the reaction was performed overnight at 37^{o}C to ensure amplification of cRNA. Following overnight incubation, cRNA purification was performed to remove any protein or large excess of unincorporated nucleotide. The RNeasy® Mini Kit (Qiagen) protocol for RNA clean up was used and the cRNA was eluted into 50 µl 10mM Tris HCl (pH 8.0). cRNA yield was quantified by spectrophotometry at 260nm using the NanoDrop® ND-1000.

2.7.3 Oligo GEArray® Hybridization

Oligo GEArrray Hybridisation and detection of biotin-labeled cRNA was performed using the HybTube Protocol in a roller-bottle hybridization oven according to manufacturer's instructions. The array membrane was pre-hybridized in GEAhyb Hybridisation Solution for 2-3 hours at 60^{o}C with slow rotation (5 to 10 rpm). For hybridization of cRNA to the array membrane, 2 µg of biotin-labeled cRNA was added to 0.75 ml GEAhyb Hybridisation Solution and hybridized overnight at 60^{o}C with slow rotation (5 to 10 rpm).

The array membrane was then washed and processed for chemiluminescent detection using Chemiluminescent Detection Kit (Superarray; Bioscience Co.) according to manufacturer's instructions. For chemiluminescent detection, 1ml of CDP-Star chemiluminescent substrate was added to the hybridization tube and incubated for 5 min at room temperature with rotation. Membranes were placed into a plastic sheet protector, blotted dry and exposed to X-ray film (SLS), which was then developed (X-ray Imaging Equipment™, Fuji).

2.7.4 Data analysis

Detailed analysis of images was performed using the GEArray Expression Analysis Suite 2.0 (Superarray; Bioscience) software. The array image was uploaded, data extracted and analysis of the data was performed using the analysis tools available. Images are aligned to a grid either manually or automatically and the readout of signal

intensity was generated. Corrections are made for background of individually defined areas and an average of signal intensities of the 4 four replicates on each array spot. Normalisation of signal intensities between samples was performed using the control spots, which include the house-keeping genes, present on each array.

2.8 Buffers and solutions

2.8.1 SDS PAGE

2.8.1.1 Lysis Buffers:

Urea lysis buffer: 7M Urea, 0.1M DTT, 0.05% Triton-X-100, 25mM NaCl and 20mM Hepes-KOH pH 7.6

NP-40 lysis buffer: 0.8 % NP-40, 20mM Hepes pH 7.6, 0.32M KCl, 5mM DTT *, 120mM okadaic acid * and 1 × complete protease inhibitor cocktail (Roche) *

1% Triton-X-100 lysis buffer: 50mM Tris-HCl pH 7.4, 150mM NaCl, 1mM EDTA, 1% (w/v) Triton-X-100 and 10% (w/v) Glycerol

* Added fresh to a final concentration as stated

2.8.1.2 Protein quantification

Bradford Reagent: 100mg Coomassie Blue G-250, 50ml 95% ethanol, 100ml 85% phosphoric acid (made up to 1 litre with H_2O).

2.8.1.3 Preparation of gels and separation of proteins by SDS-PAGE

Separating Gel (10%): 0.272% Bis-acrylamide (National Diagnostics; Ultrapure Protogel), 0.39M Tris-HCl (pH 8.8), 0.1% SDS, 0.1% APS and 0.04% TEMED

Stacking Gel: 0.136% Bis-acrylamide, 0.13M Tris-HCl (pH 6.8), 0.1% SDS, 0.1% APS and 0.2% TEMED

Running Buffer: 192mM Glycine, 25mM Tris and 0.1% (w/v) SDS

4 × SDS sample buffer: 4% SDS, 25mM Tris (pH 6.8), 20% Glycerol, 10mM EDTA, 0.06% bromophenol blue and DTT added fresh to a final concentration of O.2M

2.8.1.4 Detection of fractionated protein by Coomassie Brilliant Blue

Fix: 50% (v/v) Methanol and 10% (v/v) Acetic Acid

Coomassie Brilliant Blue Stain: 50% (v/v) Methanol, 10% (v/v) Acetic Acid and 0.2% (w/v) Coomassie Blue R-250

Destain: 10% (v/v) Methanol and 10% (v/v) Acetic Acid

2.8.1.5 Immunoblotting

Transfer Buffer: 192mM Glycine, 25mM Tris and 20% (v/v) Methanol

10x PBS (phosphate buffered saline): 1.37M NaCl, 0.1M Na_2HPO_4 and 0.027M KCl, 0.018M KH_2PO_4 (Adjusted pH to 7.4 with HCl)

PBS – Tween: 1x PBS + 0.1% (v/v) Tween 20

10x TBS (tris buffered saline): 1.5M NaCl and 0.5M Tris (Adjusted to pH 7.4 with HCl)

TBS- Tween: 1x TBS + 0.1% (v/v) Tween 20

ECL Solution 1: 100mM Tris pH 8.5, 2.5mM Luminol Stock ,0.4mM p-Coumaric Acid

ECL Solution 2: 100mM Tris pH 8.5 and 0.02% (v/v) H_20_2

Both ECL solutions stored in dark

Stripping buffer: 62.5mM Tris (pH 6.2) and 2% SDS

2.8.2 Microbiological Techniques

2.8.2.1 Bacterial Cultures

Luria-Bertani (LB) Broth: 1% (w/v) Tryptone**,** 0.5% (w/v) Yeast Extract and 1% (w/v) NaCl (sterilised by autoclaving at 121^{o}C for 20 minutes).

LB Agar: 1% (w/v) Tryptone, 0.5% (w/v) Yeast Extract, 1% (w/v) NaCl and 1.5% (w/v) Agar, granulated (sterilised by autoclaving at 121^{o}C for 20 minutes).

Selective antibiotics used: Ampicillin at 50µg/ml for all constructs unless otherwise stated.

2.8.2.2 Preparation of competent cells

Transforming Buffer 1 (TFB I): 30mM Potassium Acetate, 100mM RbCl, 10mM $CaCl_2$, 50mM $MnCl_2$ and 15% (v/v) Glycerol (adjusted to pH 5.8 with acetic acid and sterilized by filtration)

Transforming Buffer 2 (TFB II): 10mM MOPS, 75mM $CaCl_2$, 10mM $RbCl_2$ and 15% Glycerol (adjusted to pH 6.5 with KOH and sterilized by filtration).

2.8.2.3 Agarose Gel Electrophoresis

50 × TAE (Tris-acetate-EDTA) Buffer: 2M Tris base, 5.71% acetic acid and 50mM EDTA (adjusted to pH 8.5 with KOH)

6 × DNA Sample Buffer: 30% glycerol, 0.003 % cyanol, 0.002 % bromophenol blue

3 THE ROLE OF THE P53 SER 20 SITE IN MODULATION OF P53 TRANSCRIPTIONAL ACTIVITY

3.1 Introduction

3.1.1 A role for p53 Ser 20 phosphorylation in assembly of the p53 transcription complex

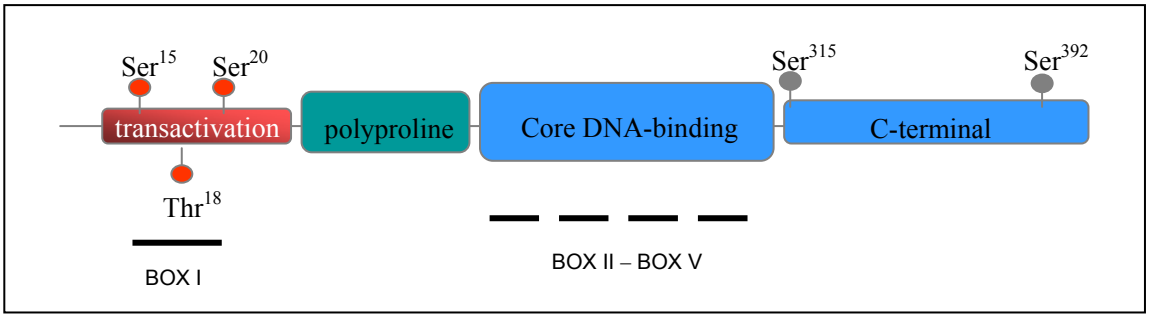

Figure 3.1 P53 is a tetrameric transcription factor.
The schematic demonstrates the four domains of p53, the location of the conserved Box-I to Box-V motifs and some of the common phosphorylation sites.

P53 is a tetrameric transcription factor (see Figure 3.1) which exhibits sequence-specific DNA binding activity mediated through its core DNA-binding domain (Lane and Hupp 2003). The p53 core domain is characterized by four evolutionary conserved sequences known as Box II – Box V domains (as demonstrated in Figure 3.1) which maintain the structural integrity of the core domain. The N-terminal transactivation domain of p53 provides a scaffold for binding of components of the transcription machinery thereby regulating transcription from p53 target genes. Modulation of the transcriptional activity of p53 depends on the docking of one of two regulatory proteins, Mdm2 or p300, which compete for binding of the N-terminal Box-I domain of p53. Mdm2 is a negative regulator which facilitates p53 degradation via the proteasome (Oren 1999). P300 is a positive regulator pathway that facilitates p53 dependent gene expression through an intramolecular mechanism (Goodman and Smolik 2000). Binding of p300 to p53 is

essential for DNA-dependent acetylation of the C-terminus of p53 which stabilizes the p53-p300-DNA complex (Dornan et al. 2003). The balance between the two regulators, Mdm2 and p300 in competing for binding of p53 regulates the specific activity of p53.

The N-terminal domain of p53 provides a scaffold for binding of components of the transcriptional machinery. The assembly of the transcription complex is initiated by phosphorylation of p53 at Serine 392 within the C-terminal phosphorylation motif by kinases such as casein kinase II (CK2) (Meek et al. 1990). The phosphorylation of this motif is thought to result in a conformational change in p53 leading to increased DNA-binding and transcriptional activity (Blaydes and Hupp 1998; Appella and Anderson 2001). Mutation of phosphoacceptor sites within this motif has been described to enhance cancer incidence in transgenic mice. An *in vivo* study showed that mice with a mutation at residue Ser389 are prone to UV-induced skin cancer (Bruins et al. 2004). Moreover lack of Ser389 phosphorylation has been shown to predispose mice to the development of 2-acetylaminofluorene-induced bladder tumours (Hoogervorst et al. 2005). Both studies therefore emphasise the importance of this motif in control of transcriptional activity of p53.

A crucial event in the activation of p53 is the phosphorylation at residues Threonine 18 and Serine 20 (Ser 20) that stabilises both the binding of the co-activator p300 (Dornan and Hupp 2001), reduces the binding of the inhibitory partner Mdm2 (Unger et al. 1999) and enhances activation of p53 target genes (Jabbur et al. 2000). A report by Jabbur and Zhang demonstrates that Asp substitution (mimics phosphorylation due to the introduction of a negative charge within the functional group) at the two phosphoaccepetor sites reduces the interaction of p53 with Mdm2 and increases the transactivation of the p53 targets, $p21^{WAF1/CIF1}$ and the apoptotic promoter, *Fas* (Jabbur and Zhang 2002). Furthermore, mutation of the Ser 20 site in mice (Ser 23) leads to the formation of spontaneous B-cell lymphoma (MacPherson et al. 2004), highlighting the importance of this site in maintaining the appropriate balance of active and inactive p53.

3.1.2 Signaling pathways target p53

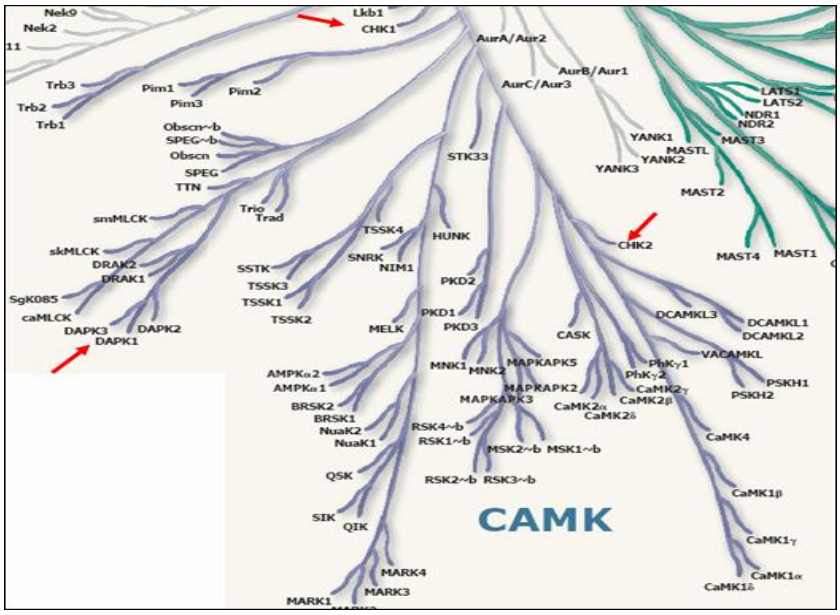

Figure 3.2 The Human Kinome.

The Calcium Calmodulin Kinase Superfamily (CAMK) form part of the phylogenetic tree known as the Human Kinome where members are related based on their kinase domains (Manning et al. 2002)

Distinct stresses activate p53. There has been a great deal of literature examining the role of p53 in the cellular responses to stresses such as DNA damage, oncogene activation and unfavourable metabolic conditions. In response to DNA damage p53 is post-translationally modified at multiple sites by kinases and acetyltransferases. DNA damage such as double strand breaks results in the activation of stress-induced signaling pathways which in turn activate cell cycle checkpoint kinases such as Chk1 and Chk2 which are recruited to phosphorylate and stimulate p53 transcriptional activity (Nyberg et al. 2002). Chk1 and Chk2 are members of the Calcium Calmodulin (CAMK) superfamily of kinases which forms a branch of the phylogenetic tree known as the Human Kinome (Figure 3.2) where members are related based on their kinase domain (Manning et al. 2002). Both Chk1 and Chk2 have been shown to phosphorylate p53 at

multiple sites in both the N- and C-termini of p53 leading to its stabilization (Ou et al. 2005). Many reports have suggested Chk2 as a putative stress induced activator of p53 (Hirao et al. 2000; Takai et al. 2002; Craig et al. 2003; Chen et al. 2005). Therefore, a hypothetical model has been proposed in which CAMK superfamily members such as checkpoint control kinases, Chk1 and Chk2; the stress activated tumour suppressor protein, death-associated protein kinase (DAPK1) and the metabolic regulator, AMP-activated protein kinase (AMPK) may all play a role in modulating p53 activity.

This was supported by data in which p53 was implicated as an essential component of metabolic cell cycle control. It has been demonstrated that glucose availability regulates cell proliferation and the metabolic sensor AMPK mediates this process. Cells treated with low glucose arrest in the G1 phase of the cell cycle and it has been shown that this arrest is p53-dependent (Jones et al. 2005). When the cell is glucose deprived, AMPK is activated leading phosphorylation of p53 at Ser15 and activation of p53. Thus, activation of p53 is required to promote cell cycle arrest which will allow the cell to survive the unfavourable glucose deprived conditions. Oncogenes such as c-myc also activate p53. Raveh and colleagues investigated whether DAPK, a tumour suppressor which sensitises cells to apoptotic signals, could affect the initial steps of oncogenesis (Raveh et al. 2001). They found that DAPK suppresses oncogene-induced transformation of primary embryonic fibroblasts by activating p53 in a $p19^{ARF}$ – dependent manner. This led to induction of apoptosis in order to eliminate the pre-malignant cells. The various reports examining the role of kinases in modulating p53 activity has led to much controversy within the field. As such, the evaluation of stress-activated p53 kinases is important in developing our understanding of the mechanisms involved in p53 activation. This report will examine the role kinases in modulation of Ser 20 phosphorylation.

3.1.3 The modulation of p53 Ser 20 phosphorylation by Calcium Calmodulin kinase superfamily members has been demonstrated in vitro

A recent report has questioned the role of Chk2 as a p53 kinase and demonstrated that p53 does not contain a classical Chk2 consensus site and that the p53 activation domain peptide fragment is not a Chk2 substrate (O'Neill et al. 2002). In a subsequent report Craig and colleagues investigated the role of Chk2 as a p53 kinase, and how Chk2 could target a protein that does not have a Chk2 consensus site (Craig et al. 2003). Two main candidate contact sites for the interaction between Chk2 and p53 were identified following a peptide scan of full length p53: Box-II and Box-V motifs of p53 core DNA-binding domain (see Figure 3.1) (Craig et al. 2003). It was shown that an N-terminal fragment of p53 which lacks the core domain is a poor substrate for Chk1 and Chk2. However, upon the addition of peptides derived from the p53 Box-II and Box-V motifs Chk1 and Chk2 stimulate *in vitro* phosphorylation of the N-terminal p53 fragment stimulated by an allosteric shift in Chk1 and Chk2. This suggested that the Box-V motif of p53 may be essential for the binding of Chk1 and Chk2 and that binding to the core domain is essential for phosphorylation of N-terminus of p53 at Threonine 18 and Serine 20 (Craig et al. 2003).

Following these results, Craig and colleagues went on to examine whether other members of the CAMK superfamily such as such as DAPK1, Chk1, DRAK and AMPK which showed homology to Chk2, could be stimulated to phosphorylate N-terminal p53 in the presence of the peptide derived from the Box-V motif of p53. They showed that there was significant stimulation of Ser 20 kinase activity in the presence of the Box-V peptide suggesting that the kinases operate in docking-dependent manner (Craig et al. 2007). The ability of these kinases to operate as activators of p53 was investigated further in this report by Craig and colleagues. They demonstrated that Ser 20 phosphorylation occured in undamaged cells and therefore established the existence of enzymes which modify Ser 20 in cycling cells (Craig et al. 2007). Furthermore, when lysates from these cells were fractionated to determine whether Ser 20 kinase activity

co-eluted with Chk1/Chk2 or DAPK1/DAPK3, the broad elution of Ser 20 kinase activity was separate from the elution of Chk1 and Chk2, however UV inducible Ser 20 kinase activity co-purified with Chk2, suggesting that Chk2 may represent the major DNA damage inducible kinase (Craig et al. 2007). They showed that DAPK1 eluted as a broad peak which correlated with the broad elution of Ser 20 kinase activity and that recombinant DAPK1 had intrinsic Ser 20 kinase activity but no Ser 15 or Thr 18 kinase activity (Craig et al. 2007), making it distinct from Chk1 and Chk2 which are dual site kinases that modify both Thr 18 and Ser 20 (Shieh et al. 2000).

3.1.4 Evaluation of DAPK1, Chk1 and Chk2 as p53 activating kinases in vivo

The identification of enzymes such as Chk1, Chk2 and DAPK1 which target Ser 20 site phosphorylation of p53 in a docking-dependent manner *in vitro* led to the investigation of these enzymes as p53-activating kinases *in vivo*. To date the identity of the main *in vivo* p53 Ser 20 kinase remains undefined and it is likely that the activation of p53 by phosphorylation at Ser 20 is cell-type and damage-type dependent. Although several reports examining the phosphorylation sites across the N- and C-termini of p53 have suggested Chk1 and Chk2 as the main p53 Ser 20 kinases *in vitro* (Hirao et al. 2000; Shieh et al. 2000; Ou et al. 2005), the role of Chk2 as a modulator of p53 has been questioned. Bunz's group examined the role of Chk2 in p53 stabilization using human colorectal cell lines in which Chk2 had been disrupted through gene targeting. They found that disruption of Chk2 did not effect p53 stabilization, phosphorylation or transcriptional activation of downstream targets (Jallepalli et al. 2003). Furthermore, Prives' group demonstrated that siRNA to Chk2 resulted in reduced expression of Chk2 but showed that p53 remained stabilized and that p53 was activated following damage (Ahn et al. 2003). Therefore further evaluation of the *in vivo* p53 activating kinases was required.

3.1.5 Identification of a novel p53 isoform

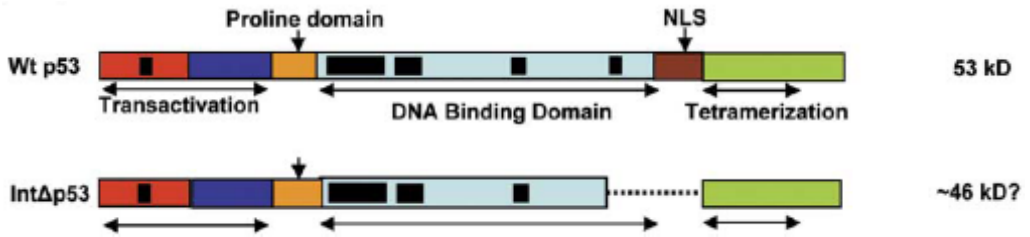

Figure 3.3 Comparison of WT p53 and the p53 ΔV isoform.
The p53 ΔV isoform lacks 66 internal amino acids (residues 257-322) which results in loss of a portion of the C-terminal end of the DNA-binding domain which includes the Box-V region (Prives and Manfredi 2005).

The recent identification of a novel isoform of p53 (Rohaly et al. 2005) may be crucial to further the investigation into the Chk1:p53 interaction. This novel p53 isoform, IntΔp53 (Figure 3.3; here after referred to as p53 ΔV) lacks 66 amino acids in the C-terminus of the DNA binding domain which is the location of the conserved Box V domain. It is an alternative splice variant which displays transcriptional activity in irradiated S phase cells only (Rohaly et al. 2005). Previous attempts at investigating the role of the Box V domain by generating point mutants or short deletions within this region of p53 have been unsuccessful as the mutant core domains were unfolded. Therefore, this isoform is potentially very useful in determining specific regions of p53 which are involved in the transcriptional activation of p53. It will allow us to investigate the roles kinase phosphorylation and docking in maintaining the integrity of p53.

3.1.6 Objectives of this chapter

The continued debate as to the identity of the main physiological p53 Ser 20 kinase(s) has led to controversy throughout the field of p53. This objective of this chapter was to investigate and to identify the *in vivo* p53 Ser 20 kinase. It is likely that different kinases will target this site in a cell-type specific and stress-specific manner. The work presented in this chapter will also set out to develop our understanding of the mechanism of CAMK regulation of p53 *in vivo*.

3.2 Results

3.2.1 Development of an in vivo p53 Ser 20 phosphorylation assay

The identification of Chk1, Chk2 and recently DAPK as p53 Ser 20 kinases *in vitro* as well as the continued debate as to the identity of the main physiological p53 Ser 20 kinase has provoked much controversy in the field. To this end, the development of an assay in which to study the stabilization of p53 by phosphorylation was crucial in order to build our understanding of the signaling pathways which control p53. A cell based transfection assay was developed to evaluate Ser 20 phosphorylation of exogenous p53 protein by specific CAMK family members. Unfortunately Ser 20 phospho-specific antibodies have low affinity precluding their use for studying endogenous p53 Ser 20 signalling pathways. Increasing amounts of p53 was transfected into H1299 cells and cell lysates were immunoblotted for levels of p53 protein and Ser 20 site phosphorylation of p53. The results (Figure 3.4; A) clearly demonstrate that transfection of p53 resulted in elevated p53 protein levels and Ser 20 site phosphorylation in a dose dependent manner (Figure 3.4; A; lanes 2 to 7). Therefore, these cells were useful models in which to study Ser 20 site phosphorylation because their endogenous Ser 20 kinase activity (activated by transfection stress) is capable of modifying at least a fraction of ectopically expressed p53 protein.

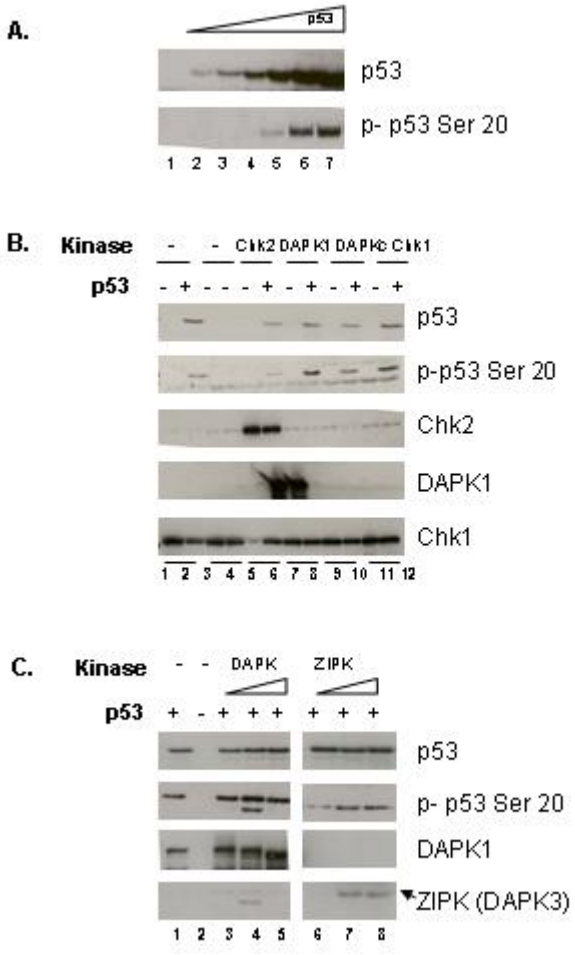

Figure 3.4 In vivo induction of Ser 20 phosphorylation of p53 by the Calcium Calmodulin kinase superfamily members.

A. Analysis of p53 phosphorylation by an endogenous Ser 20 site kinase in p53-null H1299 cells. Cells were transfected with increasing amounts (30ng to 1µg) of p53 expression vector (pcDNA 3.1p53), lysed and immunoblotted for p53 (DO12) and Ser 20 site phosphorylation of p53. B. Effects of kinase gene transfection on Ser 20 site phosphorylation of p53. H1299 cells were co-transfected with 100ng of p53 expression vector and 5µg kinase expression vectors (pDEST 12.2 Chk2, pDEST 12.2 GST DAPK1 full length, pDEST 12.2 GST DAPK1 core kinase domain and pDEST 3.2 Chk1), lysed and immunoblotted for p53 (DO12), Ser 20 site phosphorylation of p53, Chk2, DAPK1 and Chk1. C. Effects of DAPK1 and DAPK3 kinase gene transfection on Ser 20 site phosphorylation of p53. H1299 cells were transfected with 100ng of p53 and increasing amounts (1 to 5µg) of kinase expression vectors pDEST 12.2 GST DAPK1 full length or pDEST 12.2 GST ZIPK. Lysates were immunoblotted for p53 (DO12), Ser 20 site phosphorylation of p53, DAPK1 and ZIPK (DAPK3).

3.2.2 Specific Calcium Calmodulin Superfamily members stimulate p53 Ser 20 phosphorylation

The p53 null cell line, H1299 was used to investigate the *in vivo* induction of p53 Ser 20 phosphorylation by specific members of the Calcium Calmodulin Superfamily. Transfection of Chk1 and full length DAPK1 gave rise to elevated Ser 20 site phosphorylation (Figure 3.4; B; lanes 8 and 12). In contrast, transfection of Chk2 attenuated basal Ser 20 site phosphorylation (Figure 3.4; B; lanes 6) and transfection of a truncated form of DAPK1, DAPK1-core had little effect on basal Ser 20 site phosphorylation (Figure 3.4; B; lanes 10). This is associated with levels of p53 which appear to decrease following transfection of either Chk2 or DAPK core (Figure 3.4; B; lanes 6 and 10; p53 protein levels). It is therefore likely that Ser 20 phosphorylation of p53 is linked to p53 protein stability.

Members of the CAMK superfamily such as Chk1, Chk2 and DAPK1 had been shown to have phosphorylation site peptide consensus homology to the Box-I domain of p53 and a homologue of DAPK1, DAPK3 also had peptides with a striking degree of homology to the Box-I domain of p53 (Craig et al. 2007). Therefore DAPK1 and its homologue DAPK3 (also termed ZIPK) were compared for their ability to phosphorylate p53 at Ser 20 (Figure 3.4; C). DAPK1 stimulated and DAPK3 attenuated basal Ser 20 phosphorylation (Figure 3.4; C; comparing lanes 3 to 5 with lanes 6 to 8) in a similar manner to Chk2. Therefore, DAPK1 was again demonstrated as a stimulator of Ser 20 site phosphorylation of p53. This supports published data which compares the ability of DAPK1 full length, DAPK1 core and DAPK3 to modify p53-dependent transcription function (Craig et al. 2007). The transcriptional reporter assays demonstrate that full length DAPK1 stimulates and DAPK1 core and DAPK3 attenuate p53-dependent transcription function (Craig et al. 2007).

3.2.3 Chk1 induces a dose-dependent increase in p53-dependent transcription

To determine whether the stimulation of transcription correlated with increased Ser 20 site phosphorylation, a reporter assay was performed using the $p21^{WAF1}$ promoter as an indicator of p53-dependent transcription. A dose titration of p53 showed (i) the dependence of promoter activity on p53 dose and (ii) defined the range of linear relationship between p53 exogenous expression and $p21^{WAF1}$ reporter activity. The basal activity of p53 on the $p21^{WAF1}$ promoter is illustrated in Figure 3.5 and demonstrates that following addition of p53 there is significant increase in $p21^{WAF1}$ reporter activity and that this increase is p53 dose-dependent. A dose of 100ng of p53 maximises the transcriptional activity of $p21^{WAF1}$ promoter and at higher doses of p53 (200ng to 2µg) there is a decrease in transcriptional activity. From this data the optimal dose of p53 for transcriptional activation was defined as 50ng because of the high transcriptional activity.

To determine the effect of kinases on p53-dependent transcription the p53 gene was co-transfected with a titration of Chk1 or Chk2. The data (Figure 3.6) showed a dose-dependent increase in p53-dependent transcription following transfection of Chk1 and a dose-dependent attenuation of p53-dependent transcription by Chk2 (as demonstrated in Figure 3.6). This correlated with data in section 3.2.2 whereby only transfection of Chk1 but not Chk2 gave rise to elevated Ser 20 site phosphorylation. Therefore the kinase dependent increase in Ser 20 phosphorylation correlates with the kinase dependent increase in p53 transcriptional activity and the kinase dependent decrease in Ser 20 phosphorylation correlates with the kinase dependent decrease in p53 transcriptional activity.

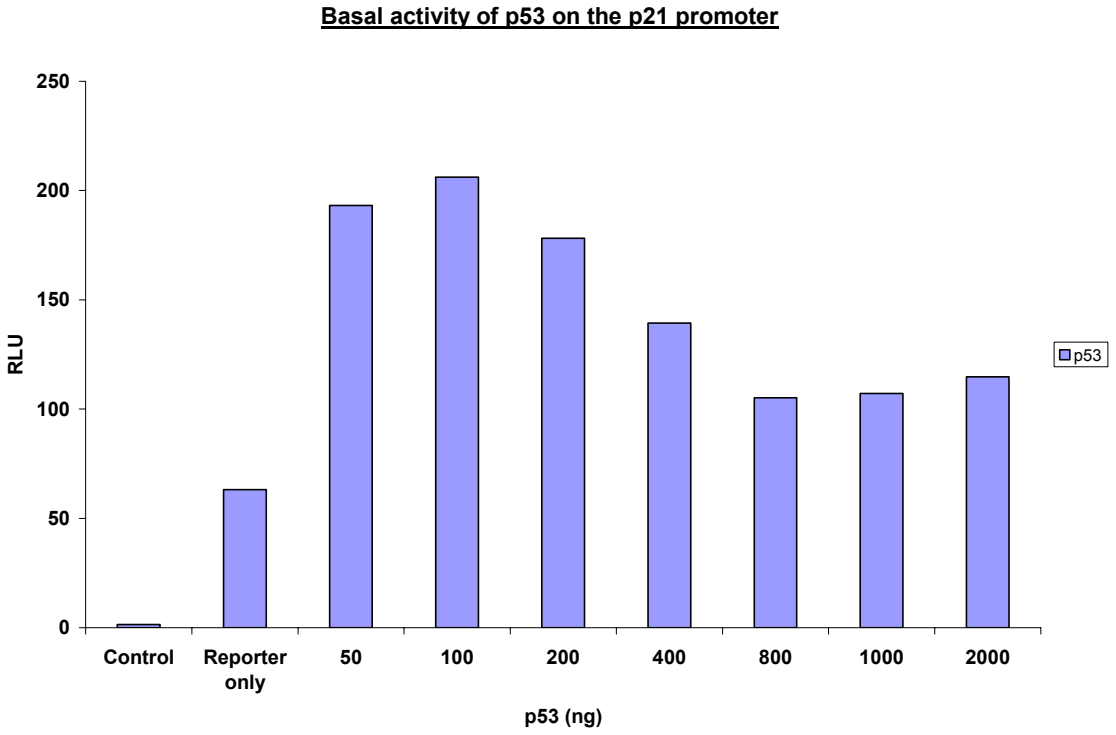

Figure 3.5 Determination of the optimal p53 dose in p53-dependent transcriptional assays.

H1299 cells were transfected with p53 (50ng to 2µg), 1µg of PGL3 $p21^{WAF1}$ luciferase reporter construct, 0.25µg pCMVβ-Gal construct and made up to a total of 4µg of transfected DNA with empty vector control. After 24 hours the cells were lysed and luciferase and β-Galactosidase activity was measured. Data shows the luciferase activity normalised to the β-Gal production represented as Relative Light Units (RLU). Activity levels of the $p21^{WAF1}$ reporter construct without p53 are represented in reporter only lane. The control lane represents the activity levels of untransfected (no DNA) control.

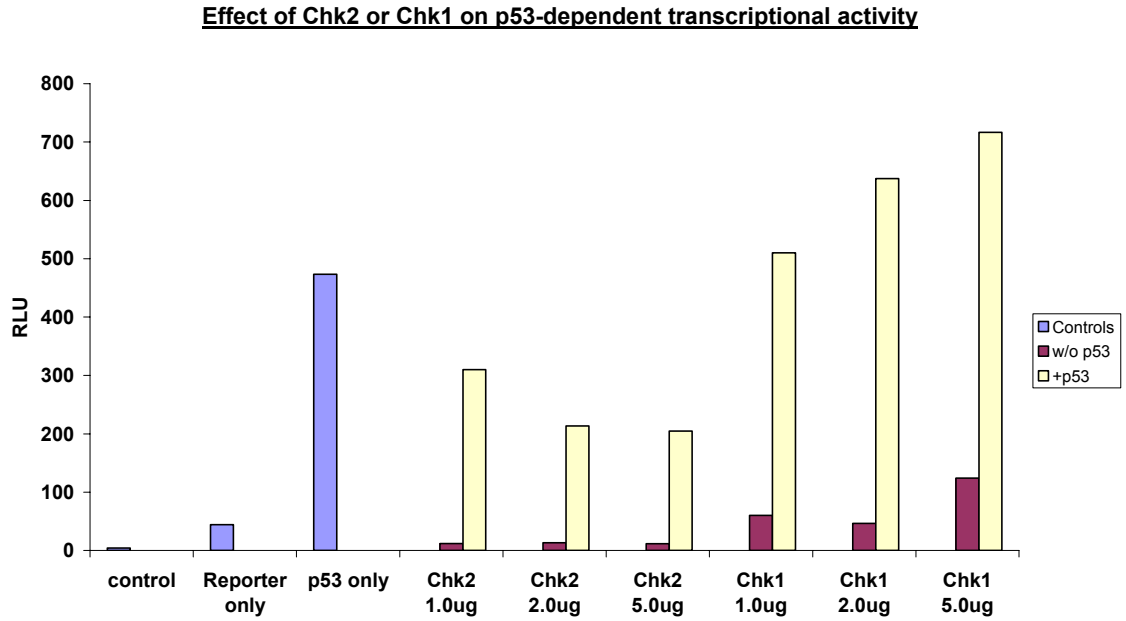

Figure 3.6 Effect of the Calcium Calmodulin superfamily gene transfection on p53-dependent reporter activity.

H1299 cells were co-transfected with p53 (50ng), a titration of Chk1 or Chk2 (from 1 to 5 µg of DNA) and reporter plasmid constructs, $p21^{WAF1}$ (1µg) and β-gal (0.25µg). After 24 hours the cells were lysed and luciferase and β-Galactosidase activity was measured. Data shows the luciferase activity normalised to the β-Gal production represented as Relative Light Units (RLU). Activity levels of the $p21^{WAF1}$ reporter construct without p53 are represented in reporter only lane. The control lane represents the activity levels of untransfected (no DNA) control.

Using two distinct transfection-based assays (p53 Ser 20 site phosphorylation and p53-dependent transcription reporter activity), it was demonstrated that only Chk1 and DAPK1 could positively affect the p53 pathway, while Chk2 and DAPK3 attenuated p53 function. Therefore, suggesting a link between Ser 20 phosphorylation and p53 activity.

3.2.4 Identification of distinct Calcium Calmodulin Kinases as the major endogenous mediators of Ser 20 phosphorylation in human tumour cells

We next set out to determine which of the three enzymes, Chk1, Chk2 or DAPK1, was the major mediator of ectopically expressed p53. H1299 cells were cotransfected with the p53 and siRNA oligonucleotides to Chk1 or Chk2. Cell lysates were immunoblotted for p53 protein, Ser 20 site phosphorylation of p53 and Chk1 protein (Figure 3.7; A). It was demonstrated that Chk1 depletion gave rise to the most pronounced attenuation of Ser 20 site phosphorylation and reduction in p53 protein levels of ectopically expressed p53 (Figure 3.7; A; lane 3). The depletion of Chk2 slightly reduced Ser 20 site phosphorylation but did not affect p53 protein levels (Figure 3.7; A; lane 4).

We then focused on determining which of the three enzymes being studied; Chk1, Chk2 or DAPK1 was the major endogenous mediator of Ser 20 phosphorylation in cells. In order to examine this, A375 cells, which express endogenous p53 and all three Calcium Calmodulin superfamily members Chk1, Chk2 and DAPK1, were used. Cell lysates were immunoblotted for changes in protein levels of the three kinases as well as p53 (Figure 3.7; B). The protein levels of each of the three kinases are significantly depleted using these siRNA oligonucleotides (Figure 3.7; B; comparing lane 1 with lanes 2 to 4 in Chk1, Chk2 and DAPK1 blots respectively). This assay demonstrated that each of the kinases could be reliably silenced without affecting the levels of the other kinases and thus validated the specificity of the siRNA oligonucleotides. Of the three manipulations only DAPK1 depletion reduced p53 protein levels (Figure 3.7; B; lane 4; p53 blot) suggesting that endogenous DAPK1 is the most effective stabilizer of p53 in A375 cells.

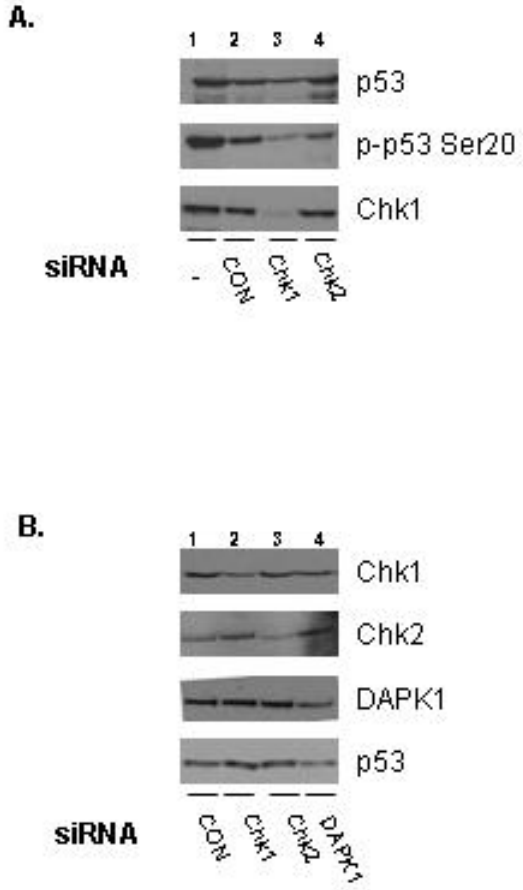

Figure 3.7 Determination of the major endogenous mediator of Ser 20 phosphorylation of ectopically expressed p53 in H1299 cells.

A. Depletion of endogenous Chk1 in H1299 using siRNA attenuates in vivo Ser 20 site phosphorylation of p53. H1299 cells were cotransfected with p53 (100ng) and 100nM siRNA control or 100nM siRNA to Chk1 or Chk2. Cells were lysed and immunoblotted for changes in p53 protein (DO12), Ser 20 site phosphorylation of p53 and Chk1 protein. B. Depletion of DAPK1 in A375 cells selectively depletes endogenous p53. A375 cells were transfected with 100nM control or 100nM siRNA to Chk1, Chk2 or DAPK1 and immunoblotted for changes in Chk1, Chk2, DAPK1 and p53 protein levels (DO12).

The two sets of data demonstrate that Chk1 depletion in H1299 cells results in loss of p53 Ser 20 phosphorylation and DAPK1 depletion in A375 cells results in loss of p53 stability. Therefore, it can be concluded that endogenous Chk1 is required for the majority of Ser 20 site phosphorylation of ectopically expressed p53 in H1299 cells and that endogenous DAPK1 is the most effective p53 protein stabilizer in A375 cells. This suggested a possible cell-specific function for the Ser 20 kinases.

3.2.5 The conserved Box-V domain of p53 is required for Ser 20 site phosphorylation of p53 by Calcium Calmodulin kinases.

We have shown that CAMK superfamily members regulate p53 *in vivo* (as described in sections 3.2.2 to 3.2.4). However, the mechanism by which this occurs in unknown. *In vitro* data suggests that the Box-V domain may be essential for the binding of CAMK members and the subsequent phosphorylation of p53 at Ser 20 (Craig et al. 2003). We therefore set out to investigate whether this mechanism occurred *in vivo*. To achieve this we used the naturally occurring alternative splice variant, p53 ΔV (see section 3.1.5) which lacks approximately 65 amino acids encompassing the Box-V docking region of p53. We examined the effect of loss of the major kinase docking site on (i) Ser 20 phosphorylation of p53 and (ii) kinase regulation of p53 activity. The Box-V docking region of p53 contains the ubiquitination signal that is required for dual site stimulation of the E3 ubiquitin ligase function of Mdm2 (Shimizu et al. 2002; Wallace et al. 2006). In light of this literature we set out to validate the p53 ΔV variant and show that it cannot be targeted by Mdm2. H1299 cells were co-transfected with Mdm2 and expression plasmids to full length p53 WT or the spliced isoform, p53 ΔV and lysates were immunoblotted with an anti-p53 antibody to identify the high-molecular-mass adducts indicative of Mdm2-mediated ubiquitination (Figure 3.8; A).

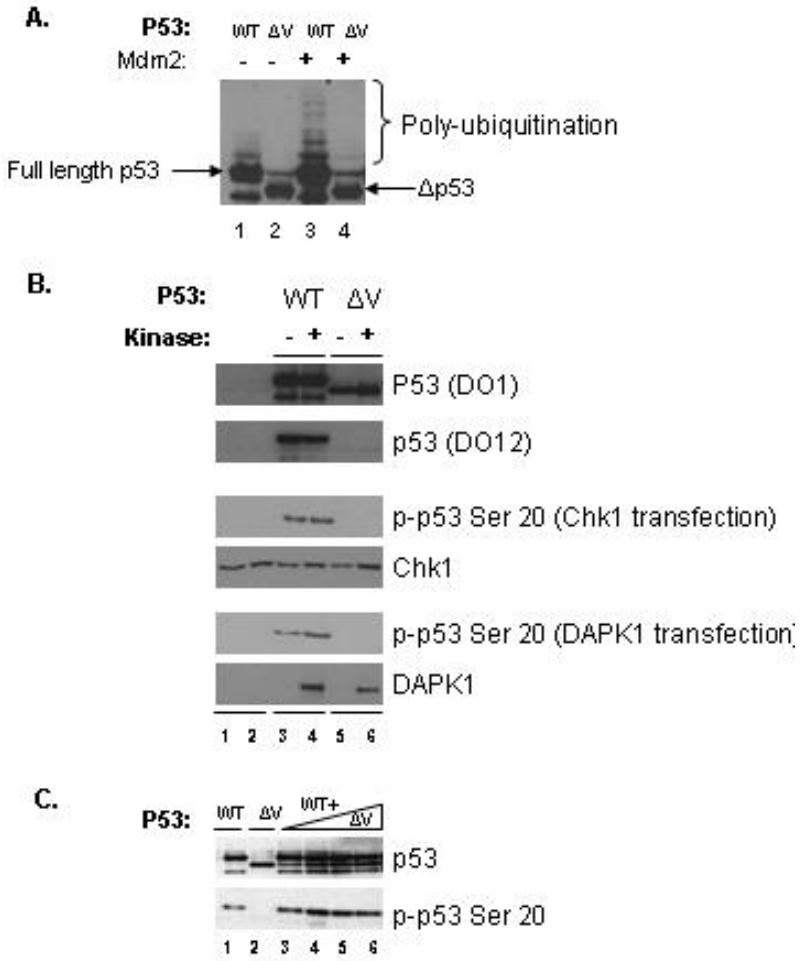

Figure 3.8 Deletion of the central region of p53 containing the Box-V domain blocks both Ser 20 site phosphorylation and ubiquitination of p53.

A. Mdm2-mediated ubiquitination is attenuated using p53 ΔV as a substrate. H1299 cells were cotransfected with 100ng p53 WT or p53 ΔV and 1μg Mdm2. Cell lysates were immunoblotted with DO1 antibody to p53 to identify high-molecular-mass adducts reflective of Mdm2-mediated ubiquitination. B. p53 ΔV is not modified at Ser 20 after kinase transfection. H1299 cells were cotransfected with 100ng p53 WT or p53 ΔV and 1μg Chk1 or DAPK1 and lysates were immunoblotted for p53 protein, evidence for deletion of the p53 central region using DO-12 antibody, Ser 20 site phosphorylation of p53, Chk1 and DAPK1. C. p53 ΔV does not compete with WT p53 phosphorylation at Ser 20. Using fixed p53, increasing amounts of p53 ΔV (0.1 to 1μg) were transfected into cells, which were lysed and immunoblotted for both p53 (DO12) and Ser 20 phosphorylation of p53.

Transfection of p53 WT or p53 ΔV alone resulted in no ubiquitination (Figure 3.8; A; lanes 1 and 2). However, when p53 WT is cotransfected with Mdm2 the resulting ubiquitination of p53 WT was clearly demonstrated (Figure 3.8; A; lane 3). Co-transfection of p53 ΔV expression plasmid and Mdm2 resulted in attenuation of Mdm2-mediated ubiquitination compared to WT p53 (Figure 3.8; A; comparing lanes 3 and 4). Therefore, the absence of the Box-V region within the p53 ΔV isoform led to attenuation of Mdm2-mediated ubiquitination, which supports a requirement of the Box-V region for Mdm2-mediated ubiquitination of p53.

To investigate the effect of loss of the Box-V region on kinase regulation, H1299 cells were transfected with expression plasmids to full length p53 or the spliced isoform, p53 ΔV and the indicated Chk1 or DAPK1 kinase expression vectors (Figure 3.8 B). To verify the deletion of the Box-V region within p53 ΔV, the DO12 antibody which binds specifically to the Box-V region of WT p53 was used (Figure 3.8; B; DO12 blot; lanes 5 and 6) and to verify the total p53 levels, the DO1 antibody was used (Figure 3.8; B; DO1 blot; lanes 3, 4, 5 and 6).

Although Ser 20 site phosphorylation of full length p53 was stimulated following transfection of Chk1 or DAPK1 (Figure 3.8; B; lanes 4 versus lane 3; Ser 20 blot), the transfected p53 ΔV exhibited no basal Ser 20 site phosphorylation (Figure 3.8; B; lane 5; Ser 20 blot) and cotransfection of Chk1 or DAPK1 did not induce Ser 20 site phosphorylation on p53 ΔV (Figure 3.8; B; lane 6 versus lane 4; Ser 20 blot). Lack of DO12 staining confirms the identity of the p53 ΔV isoform (Figure 3.8; B; lanes 5 and 6; DO12 blot). These data demonstrate that p53 ΔV was not modified at the Ser 20 site and the removal of a central region of p53 containing the Box-V domain prevented both ubiquitination and Ser 20 site phosphorylation of p53.

Furthermore, to investigate the effect of p53 WT/p53 ΔV heterotetramerisation on p53 Ser 20 phosphorylation, fixed amounts of full length p53 and increasing amounts of p53

ΔV were transfected into H1299 cells. Figure 3.8C demonstrated that transfected p53 ΔV had no basal Ser 20 site phosphorylation (Figure 3.8; C; lane 2 versus 1) and there was no dose dependent decrease in Ser 20 site phosphorylation as increasing amounts of p53 ΔV were added (Figure 3.8; C; lanes 3 to 6). Therefore, there is no evidence of Ser 20 site phosphorylation by both ΔV and WT and demonstrate that p53 ΔV does not cooperate with wild-type p53 for phosphorylation at the Ser 20 site.

3.2.6 The p53 ΔV spliced isoform is transcriptionally active

It has been reported that the p53 ΔV isoform can induce a subset of p53 targets (*p21* and *14-3-3 σ*) and that p53 ΔV exclusively associates with the p21 promoter in irradiated S-phase cells (Rohaly et al. 2005). In light of this report and the data which demonstrates that deletion of the Box-V domain prevented Ser 20 site phosphorylation of p53, a reporter assay was performed to investigate the transcriptional activity of the p53 ΔV isoform.

The data showed that as demonstrated previously (see Results 3.2.3) transfection of Chk1 stimulated p53 WT dependent transcriptional activation (Figure 3.9). The p53 ΔV protein does have intrinsic transcriptional activity suggesting that this Box-V domain deletion does not simply unfold and completely inactivate p53. However, p53 ΔV-dependent transcriptional activity was not stimulated by Chk1 transfection (Figure 3.9). Therefore, although it has been demonstrated that the removal of the central region of p53 containing the Box-V domain prevents both ubiquitination and Ser 20 site phosphorylation of p53, the p53 ΔV isoform shows some transcriptional activity. It is able to drive basal p53-dependent activity from the $p21^{WAF1}$ promoter template but in contrast to WT p53, this p53-dependent activity is not further stimulated by Chk1.

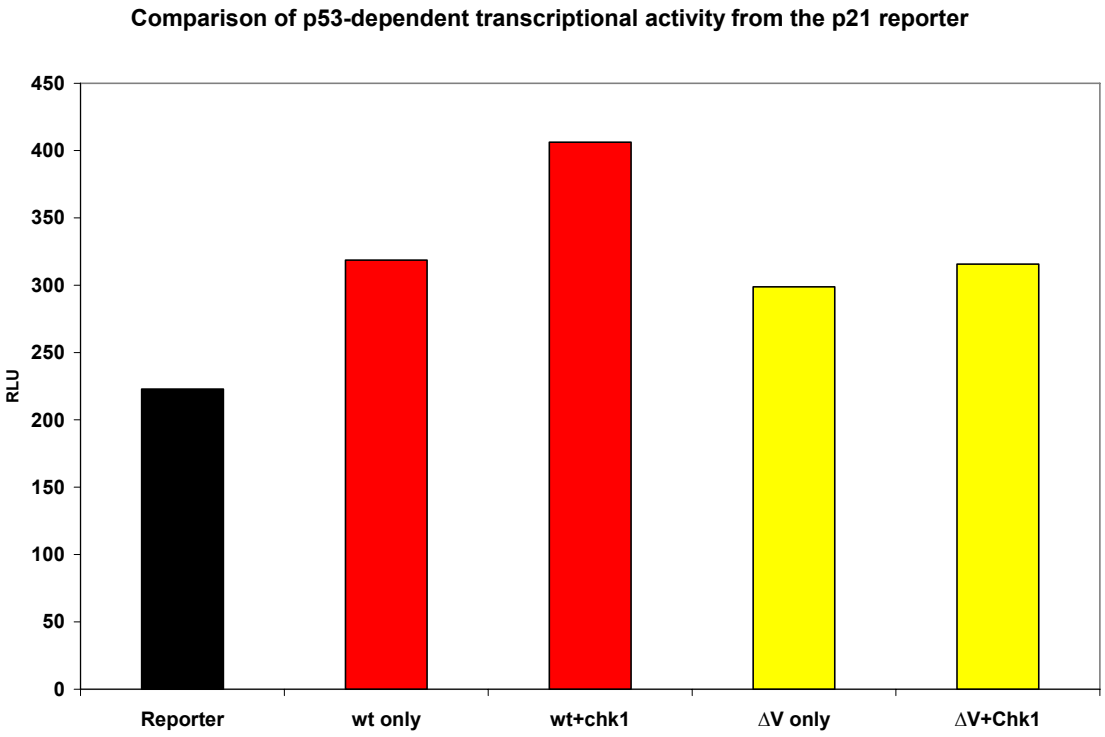

Figure 3.9 p53 ΔV-dependent transcriptional activity is not stimulated by transfection of Chk1.

H1299 were cotransfected with Chk1-encoding gene (2 µg), p53 WT or p53 ΔV (50ng) and reporter plasmid constructs; $p21^{WAF1}$-luc (1µg) and β-gal (0.25 µg). After 24 hours the cells were lysed and luciferase and β-Galactosidase activity was measured. Data shows the luciferase activity normalised to the β-Gal production represented as Relative Light Units (RLU). Activity levels of the $p21^{WAF1}$ reporter construct without p53 are represented in reporter only lane.

3.2.7 The Box-V peptide attenuates p53 Ser 20 phosphorylation

We have shown that the deletion of Box-V blocks stimulation of p53 by CAMK superfamily members suggesting that the p53 ΔV isoform lacks the CAMK docking site. In order to determine whether the CAMK members dock to Box-V *in vivo* we used Box-V peptides. It has been demonstrated using peptides derived from Box-V in *in vitro* kinase assays that the Box-V domain regulates Ser 20 phosphorylation in a docking-dependent manner (Craig et al. 2003) and that the EGFP-Box-V fusion peptide contains the ubiquitination signal for Mdm2 which can inhibit Mdm2-mediated ubiquitination of p53 *in vitro* and *in vivo* (Wallace et al. 2006). We therefore set out to investigate whether the Box-V peptide can competitively inhibit CAMK regulation of p53 Ser 20 phosphorylation and p53-dependent transcriptional activity.

H1299 cells were transfected with a titration of EGFP-control (Figure 3.10; A; lanes 2, 4, 6 and 8) or EGFP-Box-V vectors (Figure 3.10; A; lanes 3, 5, 7 and 9). The EGFP tag is toxic in the cell and increasing dose of EGFP (EGFP control or EGFP-Box-V) is decreasing levels of Ser 20 phosphorylation in this assay (Figure 3.10; A; Ser 20 blot; lanes 2 to 9). However, the data shows that there is a clear reduction of Ser 20 site phosphorylation of p53 in the presence of EGFP-Box-V relative to EGFP control (Figure 3.10; A; Ser 20 blot; compare 'C' with 'V'; lanes 2 and 3). Therefore the data has shows that the Box-V peptide specifically attenuates Ser 20 site phosphorylation of p53. This supports the hypothesis that the Box-V peptide is a competitive inhibitor of Chk1 that functions by blocking the p53 binding site on Chk1, and is consistent with the inability of p53 ΔV to function as a Chk1 substrate *in vivo*.

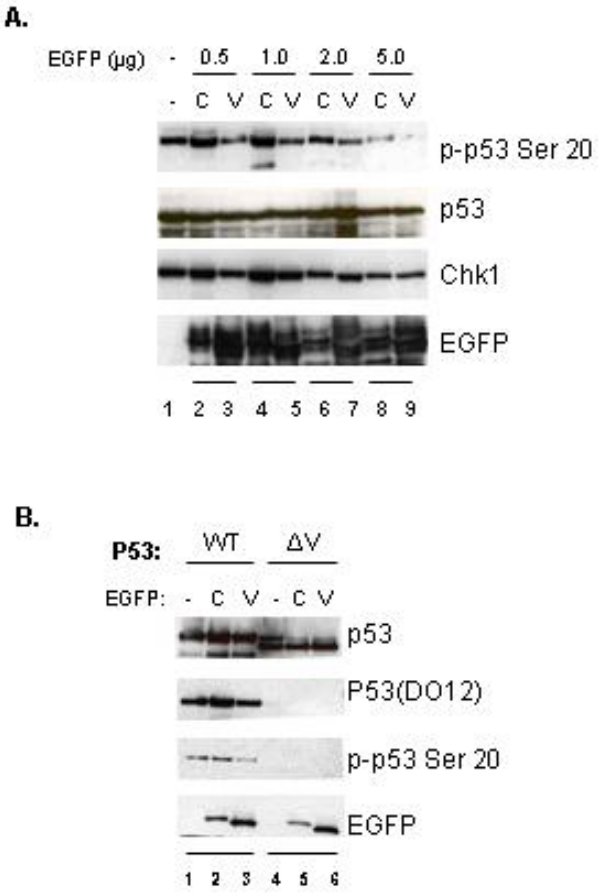

Figure 3.10 The EGFP-Box-V fusion peptide attenuates Ser 20 site phosphorylation of p53 in vivo.

A. Transfection of EGFP-Box-V attenuates Ser 20 phosphorylation of p53 WT. Chk1 (5µg) and p53 (1µg) were cotransfected into H1299 cells with increasing amounts (0.5µg to 5µg) of EGFP control (lanes 2, 4, 6 and 8) or 0.5µg to 5µg EGFP-Box-V (lanes 3, 5, 7 and 9). Cells were lysed and lysates were immunoblotted for Ser 20 site phosphorylation of p53 (DO12), p53, Chk1 and EGFP protein levels. B. EGFP- Box-V fusion peptide cannot activate p53 ΔV phosphorylation in vivo. 1µg of vectors encoding p53 WT (lanes 1 to 3) and p53 ΔV (lanes 4 to 6) were cotransfected into cells with EGFP control (lanes 2 and 5) or EGFP-Box-V (lanes 3 and 6). Cells were lysed and lysates were immunoblotted for p53 protein (DO1), evidence of deletion of the p53 central region using the DO-12 antibody, Ser 20 site phosphorylation of p53 and EGFP protein levels.

3.2.8 The Box-V peptide cannot restore p53 ΔV Ser 20 phosphorylation by endogenous Calcium Calmodulin Kinases

Deletion of the central region of p53 containing the Box-V domain (as seen in the isoform, p53 ΔV) prevents Ser 20 site phosphorylation of p53 (see results 3.2.5). It was therefore investigated whether the p53 ΔV protein could be reactivated for Ser 20 site phosphorylation *in vivo* using the EGFP-Box-V peptide fusion peptide. Vectors encoding p53 (Figure 3.10 B; lanes 1 to 3) and p53 ΔV (Figure 3.10 B; lanes 4 to 6) were cotransfected with EGFP control (Figure 3.10 B; lanes 2 and 5) or EGFP-Box-V vector (Figure 3.10 B; lanes 3 and 6). As previously shown the Box V peptide attenuated basal levels of endogenous Ser 20 site phosphorylation of full length p53 (Figure 3.10 B; Ser 20 phosphorylation immunoblot; lane 3 versus lane 2). There is no basal Ser 20 site phosphorylation of p53 ΔV (Figure 3.10 B; lane 4) as expected and following the addition of the Box-V fusion peptide, there was no reactivation of Ser 20 site phosphorylation (Figure 3.10 B; lane 6). Thus demonstrating that the EGFP-Box-V peptide fusion cannot activate p53 ΔV phosphorylation *in vivo*, under conditions where full-length p53 Ser 20 site phosphorylation is attenuated. It is likely that although the Box-V peptide may activate endogenous kinases such as Chk1, Chk1 still fails to target p53 ΔV due to lack of the binding site.

3.2.9 Chk1 stimulation of p53-dependent transcriptional activity is docking-dependent and not phosphorylation-dependent

A role for phosphorylation in p53 regulation has been suggested in reports which demonstrated that mutation of the Ser 20 site to Ala 20 can attenuate p53 activity in apoptotic and transgene-based systems (Unger et al. 1999; MacPherson et al. 2004). The importance of kinase docking over that of phosphorylation to stimulate p53 activity was previously demonstrated when a p53 Ser 20-Asp mutant marginally elevated basal p53-dependent transcription relative to WT, and was further stimulated by DAPK1 (Craig et al. 2007). In this report we have shown that the conserved Box-V domain of

p53 is required for Ser 20 site phosphorylation of p53 and kinase stimulation of p53-dependent transcription (3.2.5). It is therefore likely that Chk1 docking to the Box-V domain is required for Ser 20 site phosphorylation and transcriptional activation of p53 to take place. Docking to p53 may be a key evolutionary step and phosphorylation, may simply be a release mechanism.

To investigate this and compare the role of phosphorylation and binding on transcriptional activation of p53 a transfection-based assay was performed. Mutation of the Ser 20 site to alanine in full length and ΔV p53 was performed to examine the effects of loss of the phospho-acceptor site on basal and kinase stimulated p53-dependent transcription activity (Figure 3.11). H1299 cells were cotransfected with p53 encoding genes (p53 full length wild-type, p53 full length S20A, p53 ΔV wild-type, or p53 ΔV S20A) and Chk1 or DAPK1. The results demonstrated that for full length p53 the Ala 20 mutation did not affect basal p53-dependent transcription reporter activity (Figure 3.11; comparing p53 only columns). However, the addition of either Chk1 or DAPK1 significantly stimulated mutant but not wild-type p53-dependent transcriptional activity (Figure 3.11; comparing 'p53 + Chk1' and 'p53 + DAPK1' columns to 'p53 only' columns) suggesting that kinase activity may be required to stimulate p53 function. More strikingly, the use of the p53 ΔV wild-type and p53 ΔV S20A in this assay system demonstrated that kinase stimulation of p53 is dependent on binding to the Box-V region. The loss of the Box-V region of either ΔV or ΔV S20A p53 resulted in low basal levels of p53-dependent transcriptional activity and this activity could not be stimulated further by addition of either Chk1 or DAPK (Figure 3.11 and as demonstrated previously 3.2.6). The p53 ΔV isoform does however have lower basal transcriptional activity in this assay than previously demonstrated (section 3.2.6) and may suggest that the p53 ΔV is not consistently transcriptionally active.

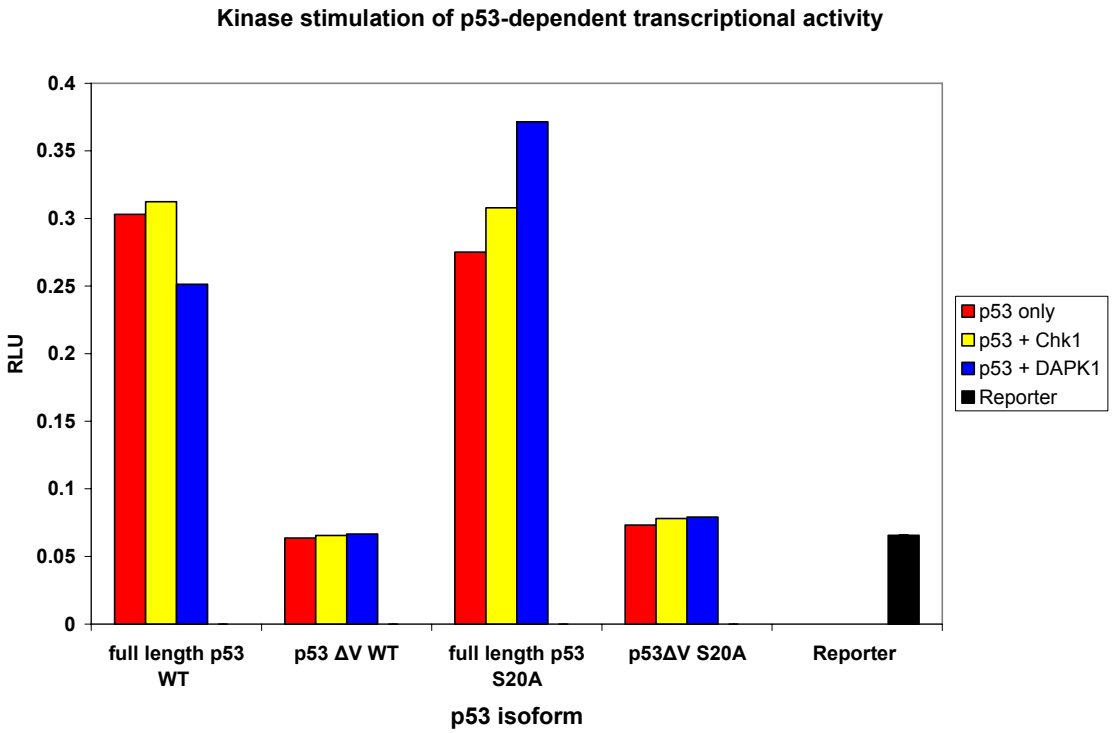

Figure 3.11 Kinase stimulation of p53-dependent transcriptional activity is docking dependent and not Ser 20 phosphorylation dependent.

H1299 cells were cotransfected with p53 encoding genes (50ng; p53 full length wild-type, p53 full length S20A, p53 ΔV wild-type, or p53 ΔV S20A) and Chk1, DAPK1 or empty vector control (2µg) expression vectors along with $p21^{WAF1}$-luc (1 µg) and REN-CMV (0.25 µg) reporters. After 24 hours the cells were lysed and luciferase and Renilla activity was measured using the dual luciferase system. Data shows the luciferase activity normalised to the Renilla production represented as Relative Light Units (RLU). Activity levels of the $p21^{WAF1}$ reporter construct without p53 are represented in reporter only lane.

Together these data demonstrate the greater contribution of kinase docking to p53 via the Box V region over kinase phosphorylation of p53 at Ser 20 and that although Ser 20 phosphorylation correlates with enhanced transactivation *in vivo*, phosphorylation is not required for this.

3.3 Discussion

The study of specific members of the Calcium Calmodulin superfamily using transfection-based technologies has allowed for the determination of a candidate kinase as the major mediator of Ser 20 site phosphorylation of p53. This study has also allowed us to delineate the mechanism of Calcium Calmodulin kinase interactions with p53 docking sites. The major observations and implications of this work are discussed in the sections below.

3.3.1 Chk1 is an endogenous modifier of p53

The identification of enzymes that phosphorylate p53 transactivation domain has been an important development in the ongoing mapping of signaling pathways that control p53-dependent transcription and consequently tumour suppression. Phosphorylation at residues Threonine 18 and Serine 20 is a crucial event in the activation of p53 that stabilises the binding of the co-activator p300 (Dornan and Hupp 2001), reduces the binding of the inhibitory partner Mdm2 (Unger et al. 1999) and enhances activation of p53 target genes (Jabbur et al. 2000).

Examination of the members of the Calcium Calmodulin superfamily of enzymes as p53 activators *in vivo* followed reports which had examined, using kinase assays, the effect of peptides derived from the Box II and Box V domains of p53 on p53 Ser 20 phosphorylation *in vitro*. These reports identified enzymes such as Chk1, Chk2 and DAPK1 which may target Ser 20 site phosphorylation of p53 in a docking-dependent manner *in vitro* (Craig et al. 2003; Craig et al. 2007) and established the existence of enzymes which modify Ser 20 in cycling cells (Craig et al. 2007). The development of the *in vivo* assay described in this work in which to investigate the Ser 20 site phosphorylation of p53 was an important tool for the research described in this study and led to identification of putative physiological Ser 20 kinase(s). The study identified Chk1 and DAPK1 as *in vivo* modifiers of Ser 20 site phosphorylation of p53, supporting

the previously reported *in vitro* data (Craig et al. 2007). Although Chk1 was identified as the most potent Ser 20 kinase in H1299 cells and that Chk1 transfection mediated the best stimulation of p53-dependent transcription reporter activity the identification of DAPK1 as a stimulator of *in vivo* Ser 20 phosphorylation of p53 was an interesting development. DAPK1 has been defined as a tumour suppressor and has been shown to be part of the cell death pathway that mediates oncogene signaling to p53 via $p19^{ARF}$ (Raveh et al. 2001). Although biological studies have shown that DAPK1 is involved in inducing myosin light chain phosphorylation (Bialik et al. 2004), autophagic vesicle formation (Inbal et al. 2002; Gozuacik and Kimchi 2004) and antagonizing FAK to activate p53-dependent apoptotic pathway (Wang et al. 2002) the physiological cell cycle substrate that mediates DAPK1-dependent activation of p53 remains undefined. The *in vivo* data presented in this report was interesting in light of a recent report which illustrated that DAPK1 could be a component of the pathway that activates p53 in gamma irradiated cells. The report demonstrated that radiation-induced p53 protein stabilization *in vivo* was attenuated in kinase domain mutants of DAPK1 (Kishino et al. 2004). This publication along side the data presented in this report may highlight a potential role for DAPK1 as a component of a genetic programme to activate p53 in irradiated cells.

The use of siRNA technology demonstrated that of the three Calcium Calmodulin kinases being studies Chk1 was the most potent endogenous mediator of Ser 20 site phosphorylation in H1299 cells and DAPK1 was identified as the most effective endogenous p53 protein stabilizer in A375 cells. Therefore, suggesting that there may be a cell-specific function for the Ser 20 site kinases. Calcium Calmodulin kinases are known to play the most dominant role in activating p53-dependent apoptosis in response to DNA damage in B cells and considering that mutation of the Ser 20 equivalent phospho-acceptor site in mice accelerates B-cell lymphoma (MacPherson et al. 2004), B cells may provide an useful model to study modification of p53. The examination of B cells and other model cell lines in which to evaluate of how distinct CAMK superfamily

members activate p53 in a cell-specific manner may provide an interesting framework in which to identify the stress activated regulators of p53.

Although the enzymes which modify p53 by phosphorylation at sites such as Ser 20 are beginning to be defined, the data has been controversial. It has been shown that Chk2 phosphorylates p53 at only Thr 18 and Ser 20 (Craig et al. 2003) whilst other *in vitro* studies have implicated both Chk1 and Chk2 in activation of p53 and have shown that these kinases can phosphorylate p53 at multiple sites in the N- and C-terminal domains leading to either stabilization or activation of p53 (Hirao et al. 2000; Shieh et al. 2000; Ou et al. 2005). Furthermore it has been shown that Chk2 deletion reduces the specific activity of p53 in cells (Takai et al. 2002). In this report we have demonstrated that Chk2 and DAPK3 are distinct from Chk1 and DAPK1 in that they lacked the ability to induce p53 Ser 20 site phosphorylation. Chk2 was the original biochemically and genetically defined Ser 20 kinase for p53 (Shieh et al. 2000; Takai et al. 2002). Although the role of Chk2 as a Ser 20 kinase has been questioned (Ahn et al. 2003; Jallepalli et al. 2003), it did seem unusual that in this assay it lacks Ser 20 kinase activity, considering the vast amounts of *in vitro* data proposing Chk2 as the Ser 20 kinase (Hirao et al. 2000; Shieh et al. 2000; Ou et al. 2005). This could be the result of several events; either Chk2 is not active in this assay or it is mainly targeting Thr 18 and therefore blocking the phospho-Ser20 epitope.

To date there have been little data examining the phosphorylation of p53 using this type of *in vivo* assay. This is likely due to the low affinity of phospho-specific antibodies making detection of phospho-epitopes difficult *in vivo*. This study was able to demonstrate how the use of a p53 null line, in which p53 could be expressed ectopically and easily detected using Ser 20 phospho-specific antibodies (which have low affinity to the endogenous p53 Ser 20 epitope) could be a useful tool in the evaluation members of the Calcium Calmodulin superfamily of kinases as putative Ser 20 site kinases. We were able to identify Chk1 and DAPK1 as putative activators of p53 and showed that

Chk1 was likely to be the main physiological Ser 20 kinase. It is worth noting however that the p53-null cell line used in these assays expresses relatively high levels of endogenous Chk1 compared with the other kinases examined in this assay. This results in little or no variation in the expression level of Chk1 between transfected and non-transfected lanes. It may have been useful in these assays to use a tagged expression vector to Chk1 to allow the detection of transfected Chk1. These assays have made a significant contribution to our understanding the mechanisms underlying p53 activation as a tumour suppressor and will be a foundation in which to clarify the role of Calcium Calmodulin kinases in the stress-activated p53 signalling pathways. Therefore we have partially resolved the controversy in the field and in that provided a framework in which to study the kinases as stress-induced p53 activators.

3.3.2 The Calcium Calmodulin kinase interaction with p53 requires the Box-V domain of p53

The Box-V domain is a binding site located in the core domain of p53 that controls covalent modification of the p53 tetramer. The identification of the novel but naturally occurring p53 isoform, p53 ΔV, (Rohaly et al. 2005) was a useful tool with which to investigate the specific regions of p53 which kinases may bind to and/or phosphorylate. The identification of this isoform, which the lacked Box-V motif, was a particularly interesting development as previous attempts at investigating the role of the Box-V domain by generating point mutants or short deletions within this region of p53 had been unsuccessful due to problems with unfolded mutant core domains. Using this isoform we have demonstrated that deletion of the Box-V domain of p53 resulted in two events; (i) loss of basal and kinase-stimulated Ser 20 site phosphorylation and (ii) attenuation of Mdm2-mediated ubiquitination of p53. Comparison of the p53 ΔV isoform and p53 WT in *in vivo* transfection based assays demonstrated that this isoform had no basal Ser 20 site phosphorylation and was not modified at Ser 20 after transfection of Chk1 or DAPK1. Furthermore, it was also demonstrated that p53 ΔV did not compete with WT

p53 for phosphorylation at Ser 20. The attenuation of Ser 20 site phosphorylation in the p53 ΔV isoform correlated with previous *in vitro* data which demonstrated that modification of p53 Ser 20 by kinases occurred by a docking dependent interaction with the Box-V motif (Craig et al. 2003).

We were also able to demonstrate using *in vivo* assays that Mdm2-mediated ubiquitination was attenuated when using the p53 ΔV isoform as a substrate. These combined data suggest that the Box-V region of p53 is a multi-protein docking site for Calcium Calmodulin superfamily members as well as Mdm2. The idea that the Box-V region may act as a multi-protein docking site correlated with literature which identified a novel Mdm2 interaction site in the core domain of p53. The report identified a site within the S9-S10 β-sheets which is flanked by the Box IV and V motifs. Mutation of this site led to increased Mdm2-dependent ubiquitination of p53 *in vitro* and increased binding of mutant p53 to RNA-Mdm2 complexes suggesting that this site may play a regulatory role in modulating Mdm2-mediated ubiquitination of p53 (Shimizu et al. 2002). The subsequent publication demonstrated that unfolding of Box-V in mutant p53 resulted in increased ubiquitination of p53 *in vivo* (Shimizu et al. 2006). Furthermore, Wallace and colleagues have reported a dual site docking mechanism by Mdm2 on the p53 tetramer which is initiated by Mdm2 occupying an allosteric pocket in the N-terminus of p53 to induce docking to the ubiquitination signal in the Box-V domain of p53 (Wallace et al. 2006). These studies along side the data which is presented in this report emphasise the requirement of the Box-V domain for both basal and kinase mediated Ser 20 site phosphorylation *in vivo* as well as for Mdm2-mediated ubiquitination of p53.

The role of the Box-V domain as a multi-protein docking site and as a site which is crucial for the phosphorylation of p53 was verified in assays which evaluated the effect of an EGFP-Box-V fusion peptide on p53 phosphorylation in cells. It had already been established that the EGFP-Box-V fusion peptide, which contains the ubiquitination

signal for Mdm2, inhibited Mdm2-mediated ubiquitination of p53 *in vitro* and in cells (Wallace et al. 2006). The data presented here demonstrated that the EGFP-Box-V fusion peptide attenuated basal and Chk1 mediated Ser 20 site phosphorylation of p53 WT. Furthermore, the EGFP-Box-V peptide fusion could not activate p53 ΔV phosphorylation *in vivo*, under conditions where full-length p53 Ser 20 site phosphorylation was attenuated. It is likely that the Box-V peptide cannot overcome the inability of p53 ΔV isoform to phosphorylate p53 at Ser 20 due to the size of the peptide versus the Box-V deletion region and it is unlikely that the peptide dynamics would be sufficient to restore the Box-V domain activity. The attenuation of Chk1 as an inducer of Ser 20 phosphorylation following the transfection of the Box-V peptide would suggest that the peptides are preventing phosphorylation by competitive inhibition resulting in the blocking of the p53 binding site on Chkl and therefore the inability of Chk1 to dock to the Box-V motif on the full-length p53 protein.

Although it was shown that the p53 ΔV variant was not modified at Ser 20 *in vivo* and that it cannot be targeted by Mdm2 due to the lack of the docking site, the p53 ΔV isoform was shown to have some transcriptional activity. It was demonstrated that the p53 ΔV isoform drove basal p53-dependent activity from a $p21^{WAF1}$ promoter template but the activity could not be stimulated further by Chk1 transfection unlike that of wild-type p53. The fact that this p53 ΔV isoforms remains transcriptionally active is interesting and demonstrates that the Box-V deletion does not simply unfold and completely inactivate p53. The isoform may be targeted at other phosphorylation sites which do not rely upon the Box-V region and resulting in its transcriptional activation. It has already been reported that the p53 ΔV isoform can induce a subset of p53 targets (*p21* and *14-3-3 σ*) and that p53 ΔV associates with the p21 promoter in irradiated S-phase cells whereas full-length p53 can only do so in other cell cycle phases (Rohaly et al. 2005). It may that the isoform has evolved the capacity to evade these cell cycle regulators during S-phase. It has also been described that mutant p53 can act in a gain-of-function manner in the apparent absence of wild-type p53 (Cadwell and Zambetti

2001). There may be a role for mutant p53 forms to exert their gain of function properties on the p53 ΔV isoform and thus accounting for the transcriptional activity of this isoform. Moreover, considering the recent literature describing a role for p63 and p73 in selectively regulating p53 transcriptional activity (Flores et al. 2002), it may be interesting to examine interactions between this isoform, p53 ΔV with full length p53 and other p53 family members such as p63 and p73.

The verification that Chk1 docking to the Box-V domain is required for *in vivo* Ser 20 site phosphorylation of p53 to take place was an important development. Although a role for phosphorylation in p53 regulation has previously been suggested (Unger et al. 1999; MacPherson et al. 2004), we proposed that kinase docking to p53 played a more dominant role than phosphorylation of p53 in the CAMK-mediated p53 regulation. Having compared the effects of Ser20A mutation with Box-V deletion on basal and kinase stimulated p53-dependent transcriptional activity, I found that; (i) p53 the Ala 20 mutation did not affect basal p53-dependent transcription reporter activity, (ii) Chk1-stimulated transcriptional activity of the Ser20A mutant is similar to WT and (iii) the addition of DAPK1 significantly stimulates the Ser20A mutant but not WT p53-dependent transcriptional activity. These results confirm previously published data in which a mutation of Ser 20 to Asp 20 marginally elevated basal p53-dependent transcription and cotransfection of DAPK1 further stimulated the Asp 20 p53 mutant as well as on Ala 20 p53 mutant (Craig et al. 2007) and suggests that kinases may be required to stimulate p53 function although loss of this phosphorylation site by mutation does not affect p53-dependent transactivation. The fact that Chk1 can stimulate transcriptional activity of the Ala 20 mutant to a similar level to that of wild-type (there is no dramatic reduction in Chk1 stimulated Ala 20 mutant transactivation activity compared to WT) does suggest that docking may be more important than phosphorylation at Ser 20 and may suggest that Chk1 could phosphorylate other sites on p53 leading to its activation. However, it was the deletion of the Box-V region in the Ala 20 mutant in this study that provided the most striking results supporting the

proposed idea. The loss of the Box-V domain resulted in complete loss of stimulation of p53 transactivation both under basal and kinase-stimulated conditions. Together these data strongly suggest that CAMK activation of p53 is docking-dependent and indicate that kinase docking may be more important than phosphorylation in CAMK-dependent regulation of p53.

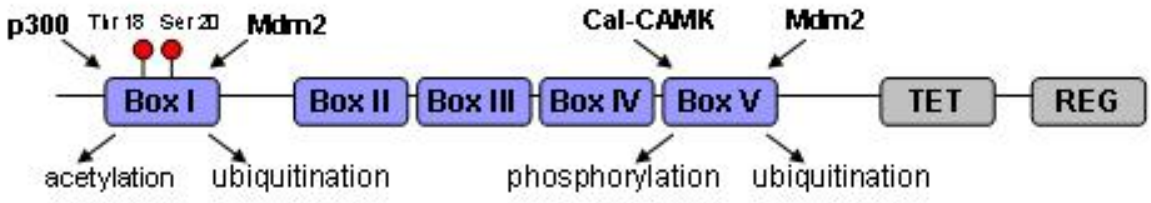

Figure 3.12 The multi-protein binding sites in the Box-I and Box-V domains of p53.
Mdm2 was the first protein to be shown to have contact sites in the Box-V domain and it is now known that the ubiquitination signal within the Box-V motif drives the dual-site binding of Mdm2 to both the Box-I and the Box-V domains to mediate C-terminal ubiquitination of p53. In this report we have shown that Calcium Calmodulin kinases (Cal-CAMK) have evolved a docking-dependent interaction with the Box-V domain which mediates phosphorylation of Ser 20 in the Box-I motif at the N-terminal of p53.

In conclusion these assays have allowed us to clarify the role of Calcium Calmodulin kinases in activation of p53 and have provided a framework in which to study the kinases as stress-induced p53 activators. We have also demonstrated (as summarized in Figure 3.12) that the Box-V region of p53 can function as a docking site for Calcium Calmodulin superfamily members as well as an Mdm2 ubiquitination signal and that protein interactions with this site controls p53 activation. These assays have made a significant contribution to elucidate the mechanisms underlying p53 tumour suppressor function.

4 THE CONSERVED P53 BOX V DOMAIN IS A CALCIUM CALMODULIN KINASE BINDING SITE

4.1 Introduction

4.1.1 Defining key domains required for p53 interactions

BOX II

^{127}SPALNKMFCQLAKTC^{141}

BOX IV

^{237}MCNSSCMGGMNRRPI^{251}

BOX V

^{267}RNSFEVRVCACPGRD^{281}

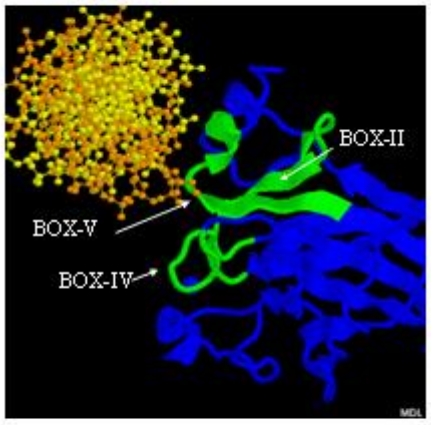

Figure 4.1 The Box peptides are adjacent in the tertiary structure of p53.
The minimal adjacent locations of the Box-II, Box-IV and Box-V peptides (in the S2 and H2 motifs) within the core domain are highlighted (Craig et al. 2003).

The identification of a Chk2 docking site in the Box-V motif of p53 (Craig et al. 2003) and as established in this report, the Box-V region of p53 is a multi-protein docking site required to activate p53 phosphorylation and ubiquitination (see section 3.2.5) has provided a basis for the continued research into kinase and p53 interactions. Figure 4.1 highlights the locations of the Box-II, Box-IV and Box-V peptides which are non-

contiguous in linear sequence but are adjacent in the tertiary structure (Craig et al. 2003).

Protein kinases such as Ser/Thr kinases and Tyr kinases play a major role in signal transduction pathways leading to the modification of protein function by phosphorylation. Protein kinases are structurally similar but differ in terms of charge and hydrophobicity of surface residues (Ubersax and Ferrell 2007). Structural characteristics of the kinase active site such as the catalytic cleft and consensus sequences determine the first level of substrate specificity. Consensus sequences are defined as amino acids situated either side of the phosphorylation site which play a significant role in kinase-substrate recognition (Kennelly and Krebs 1991). In most cases the active site of a kinase interacts with four amino acids either side of the phosphorylation site (Ubersax and Ferrell 2007). Consensus site have been determined for several kinases such as protein-kinase A (PKA), cyclin-dependent kinase (CDK) and casein-kinase 1 (CK1).

In addition to this, distal docking sites increase the affinity of a kinase for a substrate and are separate from the kinase active site, usually 50 -100 residues away from the phosphorylation site (Ubersax and Ferrell 2007). The importance of protein-kinase docking sites in the specificity of kinase interaction was highlighted in a report by Biondi and Nebreda (2003). Their studies on three families of Ser/Thr kinases demonstrated that some kinases rely upon direct docking interactions with substrates to sites distinct from the phospho-acceptor sequences (Biondi and Nebreda 2003).

The work described here sets out to determine the interaction of kinases to the Box-V domain. Binding assays were performed to investigate the *in vivo* interaction of kinases and Mdm2 with the Box-V domain of p53 which drive the modification of p53.

4.1.2 Examining the role of 'Gain of function' mutation on kinase modulation of p53 activity

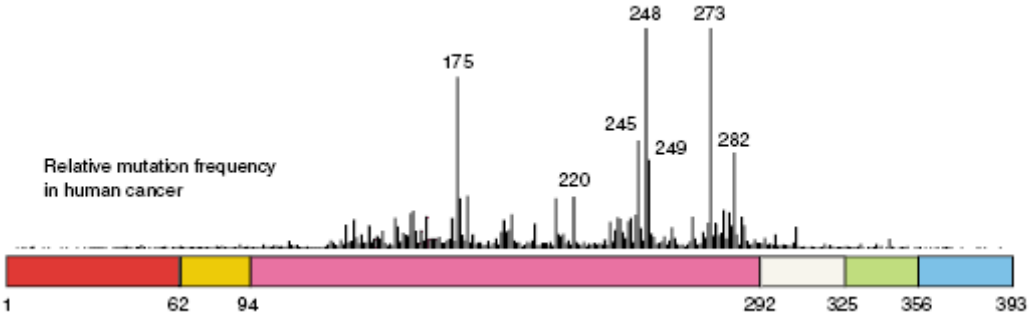

Figure 4.2 Relative mutation frequency in human cancer.
A representation of the domain structure of p53 with columns indicating the relative frequency of cancer-associated mutations for each residue according to the TP53 mutation database of the International Agency for Research on Cancer (Joerger and Fersht 2007).

P53 is a key tumour suppressor gene which characteristically protects the cell from potentially damaging cellular stress by promoting growth arrest, apoptosis and cellular senescence. The p53 tumour suppressor gene operates as one of the major barriers against cancer development. The p53 pathway is frequently impaired in human cancer and in almost 50% of all human cancers the p53 gene is mutated. Of these mutants 74% are missense point mutations that target the DNA binding core domain which result in expression of the mutant p53 protein which is DNA contact defective and conformationally impaired (Prives and Hall 1999). This therefore prevents p53-dependent transcription and tumour suppression. P53 mutations can arise sporadically or are inherited as a germline mutation in Li-Fraumeni syndrome. In many cases tumour-derived p53 mutants accumulate at a much higher level in cancer cells than wild-type p53 due to their failure to be targeted by Mdm2 for degradation (Haupt et al. 1997; Midgley and Lane 1997). As demonstrated by the diagram (Figure 4.2) which shows the relative mutation frequency in human cancer, areas where mutations occur at a markedly higher frequency than the others are known as mutation "hot-spots". For example,

mutation at codons 175, 248, 249 and 273 account for 25% of missense mutations identified in human cancers (Hainaut and Hollstein 2000). The mechanism by which p53 promotes pro-oncogenic activities has been examined in numerous reports, some suggesting that tumour derived p53 mutants have acquired novel functions which promote cancer cell growth.

The clarification of the role of p53 in carcinogenesis has been and continues to be a complex process. Following the initial discovery of p53 in 1979 as an SV40-binding protein (Lane and Crawford 1979; Linzer and Levine 1979) there has been significant development in the clarification of the role of p53 in carcinogenesis. It was subsequently classified as a proto-oncogene due to the apparent upregulation of p53 expression in proliferating cells (Milner and Milner 1981; Milner 1984; Reich and Levine 1984). The molecular cloning of the TP53 gene (Zakut-Houri et al. 1983; Zakut-Houri et al. 1985) and discovery of the sequence of the mouse wild-type TP53 gene led to the revelation that previous experiments had employed mutant p53 variants (Eliyahu et al. 1988; Finlay et al. 1988) and that wild-type p53 actually suppressed oncogene-mediated transformation (Eliyahu et al. 1989; Finlay et al. 1989). This established p53 as a bona fide tumour suppressor. These developments have provided a basis for elucidation of the various roles of p53 in carcinogenesis and have established distinct roles in which one of three events can occur; firstly, p53 loss of function, where the p53 gene mutates or there is complete loss of the gene; secondly, mutant p53 dominant-negative function, where there is promotion of tumourigenesis due to the mutant p53 inactivating WT p53 in cells by heteraoligomerisation; and finally, mutant p53 gain of function, where expression of mutant p53 in cells lacking WT p53 enhances their tumourigenic potential.

There is has been a steady increase in number of reports examining the idea of mutant gain of function and its implications as a determinant in human tumour development. In this report we will examine the molecular mechanisms of the oncogenic gain of function

nature of mutant p53 as well as the effect of this type of mutation of p53 on the interaction potential with kinases. A major molecular role of gain of function mutants is modulating the transcriptome of p53. Mutant p53 interactions with chromatin and DNA is central to transcriptome activities and in a review by Kim and Deppert (2004) it was suggested that the interaction of mutant p53 with DNA is determined by DNA structure and not specific motifs as required by WT p53. They described how mutant p53 binds to high affinity MAR elements (regulatory DNA sequences important for higher order chromatin reorganization and propagation of chromatin modification) and that binding to MAR was independent of consensus motif but increasing dependent on length of DNA (Kim and Deppert 2004). The complex interactions of mutant p53 with DNA and the mechanisms of transcriptional regulation are described by Menendez and colleagues. They describe how transcriptional regulation by mutant p53 is a consequence of the sequence-specific DNA-binding activity of WT p53 and how changes in target response elements which provide for p53 regulation of target genes can affect the expression of genes and thus the biological outcomes. They emphasise the importance of clarifying the relationship between WT or mutant p53 and target response elements to develop our understanding of the p53 master regulatory network (Menendez et al. 2007).

Models for the gain of function activity mutant p53 have been suggested. Firstly, mutant p53 has been shown to interact with other p53 family members, p63 and p73 resulting in the inhibition of the proapoptotic function of these related family members. Li and Prives described how some mutants interact with and downregulate the transcriptionally active forms of p63 and p73 which resulted in reduced apoptotic response and radioresistance in tumour cells (Li and Prives 2007). Two separate reports demonstrated that inhibition of p73 by mutant p53 abrogated apoptosis and cytotoxicity induced by anti-cancer drugs (Bergamaschi et al. 2003; Irwin et al. 2003) and that downregulation of mutant p53 enhanced chemosensitivity (Irwin et al. 2003). New *in vivo* models using knock-in mice with p53 'hot-spot' mutation at codons 172 and 270 (murine equivalent of human R175H and R273H hot-spot mutations) were made to

resemble mutation of p53 in Li-Fraumeni syndrome (Lang et al. 2004; Olive et al. 2004). They found that mutant p53 associated with p63 and p73 in tumour cells of mice (Lang et al. 2004; Olive et al. 2004) and that silencing mutant p53 resulted in increased the activity of p53 family target genes such as *p21* which was likely to be a result of the increased activity of endogenous p63 and p73 in the absence of mutant p53 (Lang et al. 2004). Thus mutant p53 may promote tumourigenesis through downregulation of its family members.

Moreover, it has been described how mutant p53 targets DNA indirectly by the interaction with other transcription factors such as NF-Y (Di Agostino et al. 2006). Under damaging conditions mutant p53 interacts with NF-Y via DNA-binding consensus sequences known as CCAAT sites (these sites are present in the regulatory regions of many key genes involved in the regulation of cell cycle). This results in the abnormal upregulation of expression of NF-Y cell cycle target genes and recruitment of p300 leading to histone acetylation (Di Agostino et al. 2006).

In addition a more direct pro-oncogenic gain of function role of mutant p53 in which mutant p53 regulates the expression of a specific set of genes has been suggested. Mutation of p53 can result in a null phenotype for the regulation of p53 target genes. However, in many cases mutation of p53 results in the gain of function phenotype as a result of the transactivation of genes which are not normally regulated by p53. For example, the *multi-drug resistance (MDR-1)* gene, was one of the first genes to be identified as upregulated by mutant p53 (Chin et al. 1992; Dittmer et al. 1993). Other studies have demonstrated that p53 mutants are involved in the upregulation of expression of numerous genes involved in cellular processes implicated in cancer progression. For example, p53 mutants such as 143A, 175H, 248W, 273H and 281G were shown to elevate the expression of EGFR (Ludes-Meyers et al. 1996) and NFKB2 was upregulated by 281G (Deb et al. 2002). Furthermore the 175H mutant can negatively regulate genes and has been shown to repress the transcription of genes such

as the CD95/Fas/Apo1 gene, which encodes a death receptor implicated in a variety of apoptotic response (Zalcenstein et al. 2003; Weisz et al. 2007).

Variation in the transactivation of p53 target genes is a characteristic of most p53 mutants which retain this gain of function activity (Rowan et al. 1996; Ryan and Vousden 1998). Recently groups have examined the consequences of missense mutations on the potential for p53 to transactivate genes through sequence-related response elements using model systems based on yeast *Saccharomyces cerevisiae* (Inga et al. 2001; Resnick and Inga 2003) and more recently in human cells (Menendez et al. 2006). A paper by the Ishioka group (Kakudo et al. 2005) constructed a yeast-based functional assay to demonstrate the variable ability of p53 gain of function mutants to transactivate specific target genes and induce apoptosis. They evaluated a group of more than 2000 p53 mutants representing all possible amino acid substitutions caused by a point mutation throughout the protein (5.9 substitutions per residue). Of these mutants 635 were shown to have increased or decreased activity for target genes compared with wild-type p53 and these were defined as "diverse" mutant p53s because of their diverse transcriptional activity for distinct p53 target genes. They hypothesised that if cellular responses such as cell cycle arrest and apoptosis are dependent on the group of p53 target genes transactivated, the ability of p53 to induce apoptosis should differ among the mutant p53s and therefore should correlate with the transactivation profile of the specific p53 target genes (Kakudo et al. 2005). To examine the hypothesis they randomly selected 30% of these mutants and evaluated their transcriptional activities and their ability to induce apoptosis. The study identified gain of function mutants which displayed apoptotic activity above WT as well as mutants with increased transcriptional activity from one or more p53 promoters. There was no significant correlation between ability to induce apoptosis and the transcriptional activity on any target gene examined indicating that it is either a pool of transactivated p53 target genes that determines the cellular response or a target gene not examined in the study (Kakudo et al. 2005).

4.1.3 Objectives of chapter

The objective of this chapter was to extend our knowledge of WT and mutant p53 interactions with kinases and Mdm2. Coimmunoprecipitation assays were used to examine kinase binding to the Box-V region of p53, and to further identify sites of interaction, mutagenesis of the Box-V region was performed. Mutation of p53 occurs in approximately half of all human tumours. In order to develop our understanding of the molecular mechanisms of the oncogenic gain of function phenotype and the molecular interactions of mutant p53 we examined the basal and kinase-stimulated transcriptional activities of specific p53 mutants. With reference to recent reports (Kakudo et al. 2005) several mutants were selected based on their increased transcriptional activity from p53 promoters and their reported frequency in human cancers. These tumour-derived p53 mutants are thought to display gain of function properties toward target genes. Mutagenesis of p53 allowed the creation of a set of mutants which could be used to investigate the effect of kinases and Mdm2 on modulation of mutant p53 activity. Using transcriptional based assays allowed us to evaluate whether the activity of these mutants can be modulated by kinases and/or Mdm2 and further identify sites of interaction between p53 and its regulatory proteins. Developing an understanding of the gain of function properties of mutant p53 and its interaction with kinases and Mdm2 is important for the development of strategies to evade this gain of function of mutant p53 and to optimise approaches aimed at p53 reactivation.

4.2 Results

4.2.1 Examination of kinase and Mdm2 binding to p53 core domain

The ability of the EGFP Box-V fusion peptide to attenuate basal and Chk1-stimulated phosphorylation of p53 at Ser 20 (see section 3.2.7) suggests that the peptide may bind to Chk1 and therefore competitively inhibiting the action of Chk1 in phosphorylating p53 at Ser 20. Furthermore the examination of Chk1 stimulated p53-dependent transcriptional activity (see section 3.2.9) demonstrated a greater contribution of kinase docking to p53 over kinase phosphorylation of p53 at Ser 20. We therefore set out to examine whether kinases and/or Mdm2 bind to the Box-V region of p53 and, if yes, to determine specific regions important for binding and to characterize the regions of interaction.

4.2.1.1 The Calcium Calmodulin Kinases bind stably to the EGFP-Box-V fusion peptide in cells

An *in-vivo* coimmunoprecipitation assay was performed to investigate whether Chk1 and EGFP-Box-V peptide form an interaction *in vivo*. FLAG-Chk1 and EGFP variants (EGFP control, EGFP-Box I or EGFP-Box V) were expressed and samples after the FLAG pull-down were immunoblotted with an anti-EGFP IgG for the respective binding fractions including control (a), empty vector (b), EGFP (c), EGFP-Box-I (d) and EGFP-Box-V (e). When EGFP-Box-V peptide was coexpressed with FLAG-Chk1, Chk1 formed a complex with the EGFP-Box-V peptide, as demonstrated by the presence of a positive band in the bound fraction (Figure 4.3; A; Blot e; lane 4). However, when EGFP-Box-I or EGFP control peptide was coexpressed with FLAG-Chk1, there was no formation of a bound complex (Figure 4.3; A; Blots c and d; lane 4). The ability of the EGFP-Box-V fusion peptide to form a stable immune complex with Chk1 in cell lysates suggests that the attenuation of p53 phosphorylation by the EGFP-Box-V fusion peptide might be attributable to its ability to bind to and inhibit Chk1.

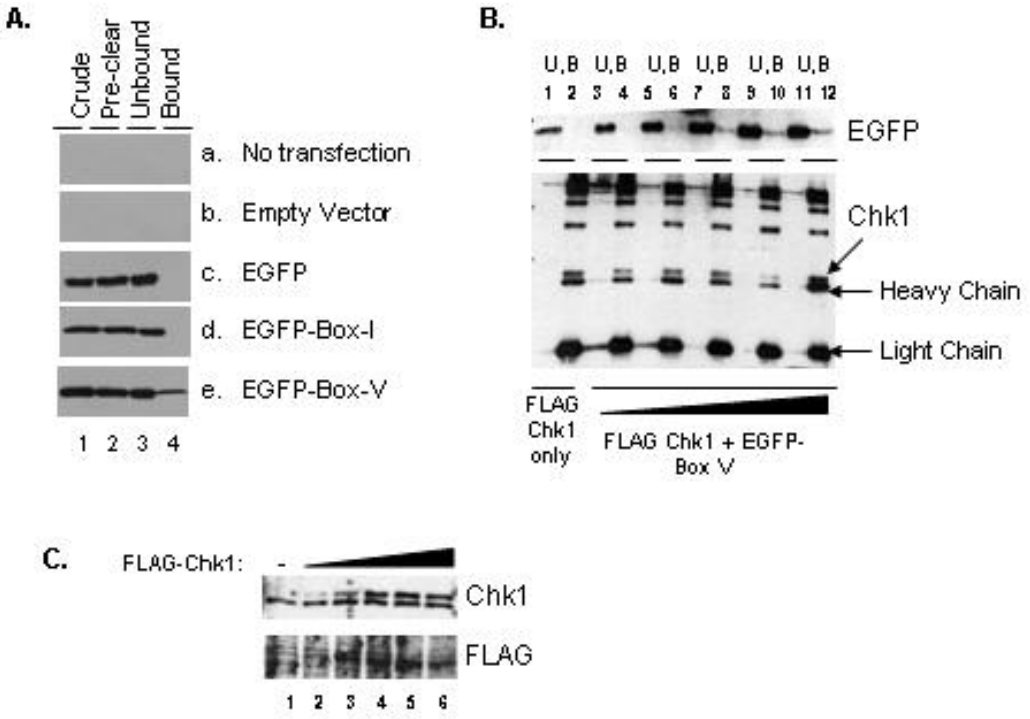

Figure 4.3 Chk1 binds stably to the EGFP-Box-V fusion peptide in cells.

A. H1299 cells were cotransfected with vectors encoding FLAG-Chk1 (1µg) and EGFP variants (0.5µg; EGFP control, EGFP-Box I and EGFP-Box V). 24 hours following transfection cells were lysed (lane 1) and lysates were precleared (lane 2) and FLAG-Chk1 was immunoprecipitated with anti-FLAG agarose beads. EGFP variants were quantified both in the unbound fraction (lane 3) and the bound fraction (lane 4). Samples after the FLAG pull-down were immunoblotted with an anti-EGFP IgG for the respective binding fractions including control (a), empty vector (b), EGFP (c), EGFP-Box-I (d) and EGFP-Box-V (e). B. H1299 cells were cotransfected with FLAG-Chk1 (1µg) and a titration of EGFP-Box-V (0.1 to 1µg). As a control, 1µg FLAG-Chk1 was transfected into cells. 24 hours following transfection cell were lysed, cell lysates were precleared and FLAG-Chk1 was subjected to immunoprecipitation with anti-FLAG agarose beads. Quantification of the EGFP-Box-V in the unbound (U; lanes 3, 5, 7, 9 and 11) or bound (B; lanes 4, 6, 8, 10 and 12) fractions after FLAG pull-down was performed by immunoblot using an anti-EGFP IgG. Protein levels of Chk1 were quantified by immunoblot under non-reducing conditions. C. Expression of transfected Chk1. FLAG-Chk1 was transfected into cells (0, 0.1, 0.2, 0.5, 1.0 and 2.0µg). Cells were lysed and lysates were immunoblotted for Chk1 (lower band is endogenous Chk1 and upper band is FLAG-tagged Chk1) and FLAG-tagged Chk1.

To further investigate and confirm the interaction between Chk1 and Box-V peptide, a coimmunoprecipitation assay was performed. The vector encoding FLAG-Chk1 was coexpressed with a titration of EGFP-Box-V into H1299 cells. Cell lysates were subjected to immunoprecipitation with anti-FLAG agarose beads followed by quantification of the EGFP-Box-V in the unbound (Figure 4.3 B; unbound; lanes 3, 5, 7, 9 and 11) or bound (Figure 4.3 B; bound; lanes 4, 6, 8, 10 and 12) fractions. Samples after FLAG pull-down were immunoblotted with an anti-EGFP IgG. Protein levels of Chk1 were quantified by immunoblot under non-reducing conditions to allow for separation of Chk1 from heavy and light chain products. The immunoblot clearly demonstrates a dose-dependent increase of EGFP-positive bands in the bound fraction (Figure 4.3 B; comparing bound fraction 'B'; lanes 4, 6, 8, 10 and 12; EGFP blot). Therefore, indicating that the Box-V fusion peptide is binding to FLAG-Chk1. However, it is evident that the majority of EGFP-Box-V peptide remains in the unbound fraction (Figure 4.3 B; comparing unbound fraction 'U'; lanes 3, 5, 7, 9 and 11; EGFP blot) and that the majority of Chk1 protein is present in the bound fraction (Figure 4.3 B; comparing bound fraction 'B'; lanes 4, 6, 8, 10 and 12; Chk1 blot). This could be a result of the finite binding capacity of the beads. It is likely that the majority of FLAG-Chk1 is binding to the anti-FLAG beads resulting in a reduced capacity for the FLAG-Chk1: EGFP-Box-V complexes to bind to the anti-FLAG beads.

To demonstrate the expression levels of untagged Chk1 and FLAG-tagged Chk1, H1299 cells were transfected with a titration (0, 0.1, 0.2, 0.5, 1.0 and 2.0μg) of FLAG-Chk1. Cells were lysed and lysates were immunoblotted for Chk1 and FLAG-tagged Chk1 (C; lanes 1 to 6). The lower band of the Chk1 blot represents endogenous Chk1 and upper band is FLAG-tagged Chk1. The level of endogenous Chk1 is demonstrated (Figure 4.3 C; lane 1) and following the addition of FLAG-Chk1 there is a dose-dependent increase in protein levels of transfected Chk1 (Figure 4.3 C; lanes 2 to 5; Chk1 and FLAG immunoblot). Therefore these results demonstrate that addition of tagged Chk1 resulted in the increasing levels of Chk1 protein in the cell.

In order to further investigate the role of other kinases such as DAPK1 in binding to the Box-V domain coimmunoprecipitation assays were performed. Vectors encoding HA-DAPK1 (the HA-DAPK vector also contains the FLAG epitope) and EGFP variants (EGFP control, EGFP-Box I or EGFP-Box V) were coexpressed in H1299 cells. Cells lysates were subjected to immunoprecipitation with anti-FLAG agarose beads. Quantification of the EGFP variant in the unbound (Figure 4.4 A; unbound (U); lanes 3, 5, 7 and 9) or bound (Figure 4.4 A; bound (B); lanes 4, 6, 8 and 10) fractions after FLAG pull-down was performed by immunoblot using an anti-EGFP IgG. The data demonstrated that when EGFP-Box-V was cotransfected with HA-DAPK1, DAPK1 formed a complex with the EGFP-Box-V peptide, as demonstrated by the presence of a positive band in the bound fraction (Figure 4.4 A; lane 10; EGFP blot). The ability of the EGFP-Box-V fusion peptide to form a stable immune complex with DAPK1 as well as Chk1 in cell lysates is a further example of a kinase interacting with the Box-V fusion peptide and therefore supports the data that the attenuation of p53 phosphorylation following the addition of the EGFP-Box-V fusion peptide (see section 3.2.7) might be attributable to its ability to bind to and inhibit kinases.

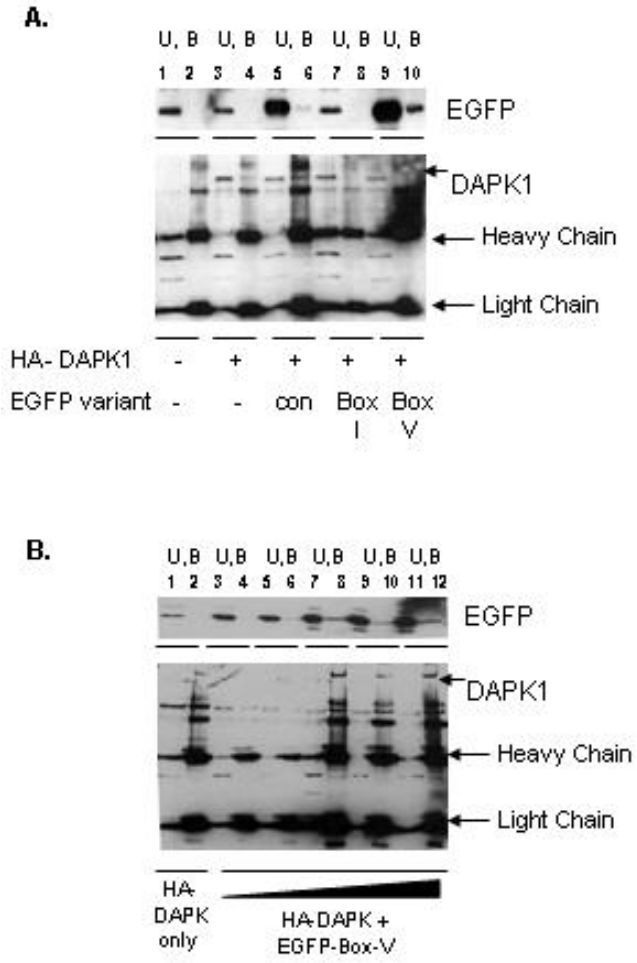

Figure 4.4 DAPK1 binds stably to EGFP-Box-V fusion peptide in cells.

A. H1299 cells were cotransfected with vectors encoding HA-DAPK1 (1µg) and EGFP variants (0.5µg; EGFP control, EGFP-Box I and EGFP-Box V). Cells were lysed, lysates were precleared and HA-DAPK1 was immunoprecipitated with anti-FLAG agarose beads. Quantification of the EGFP variant in the unbound (U; lanes 3, 5, 7 and 9) or bound (B; lanes 4, 6, 8 and 10) fractions after FLAG pull-down was performed by immunoblot using an anti-EGFP IgG. B. H1299 cells were cotransfected with the vector encoding HA-DAPK1 (1µg) and a titration of EGFP-Box-V (0 to 1µg). 24 hours following transfection cell were lysed, cell lysates were precleared and HA-DAPK1 was subjected to immunoprecipitation with anti-FLAG agarose beads followed by quantification of the EGFP-Box-V in the unbound (U; lanes 3, 5, 7, 9 and 11) or bound (B; lanes 4, 6, 8, 10 and 12) fractions by immunoblot using an anti-EGFP IgG. DAPK1 levels were quantified by immunoblot.

To further support this data and confirm the interaction between DAPK1 and Box-V peptide, the vector encoding HA-DAPK1 was coexpressed with a titration of EGFP-Box-V in H1299 cells. Cell lysates were subjected to immunoprecipitation with anti-FLAG agarose beads followed by quantification of the EGFP-Box-V in the unbound (Figure 4.4 B; unbound (U); lanes 3, 5, 7, 9 and 11) or bound (Figure 4.4 B; bound (B); lanes 4, 6, 8, 10 and 12) fractions. The data generally demonstrates a dose dependent increase of EGFP-positive bands in the bound fraction (Figure 4.4; B; comparing bound fraction 'B'; lanes 4, 6, 8, 10 and 12; EGFP blot). The reduction in EGFP-Box-V levels in lane 10 is likely to be a loading error. As demonstrated previously in FLAG-Chk1 coimmunoprecipitation assays the majority of EGFP-Box-V peptide remains in the unbound fraction (Figure 4.4; B; comparing unbound fraction 'U'; lanes 3, 5, 7, 9 and 11) and that the majority of DAPK1 protein is present in the bound fraction (Figure 4.4 B; comparing bound fraction 'B'; lanes 4, 6, 8, 10 and 12). Again this is likely be a result of the finite binding capacity of the beads in that the majority of HA-DAPK1 is binding to the beads meaning that there is a reduced capacity to allow HA-DAPK1: EGFP-Box-V complexes to bind to the anti-FLAG beads. Alternatively it could be that there is only a small proportion of EGFP expressed which binds to DAPK1 or Chk1 due to a number of factors including localization, conformation or post translational modification of DAPK1 or Chk1. However, this small proportion of binding is very significant as it confirms *in vivo* binding of Chk1/DAPK1 to the Box-V fusion peptide does occur.

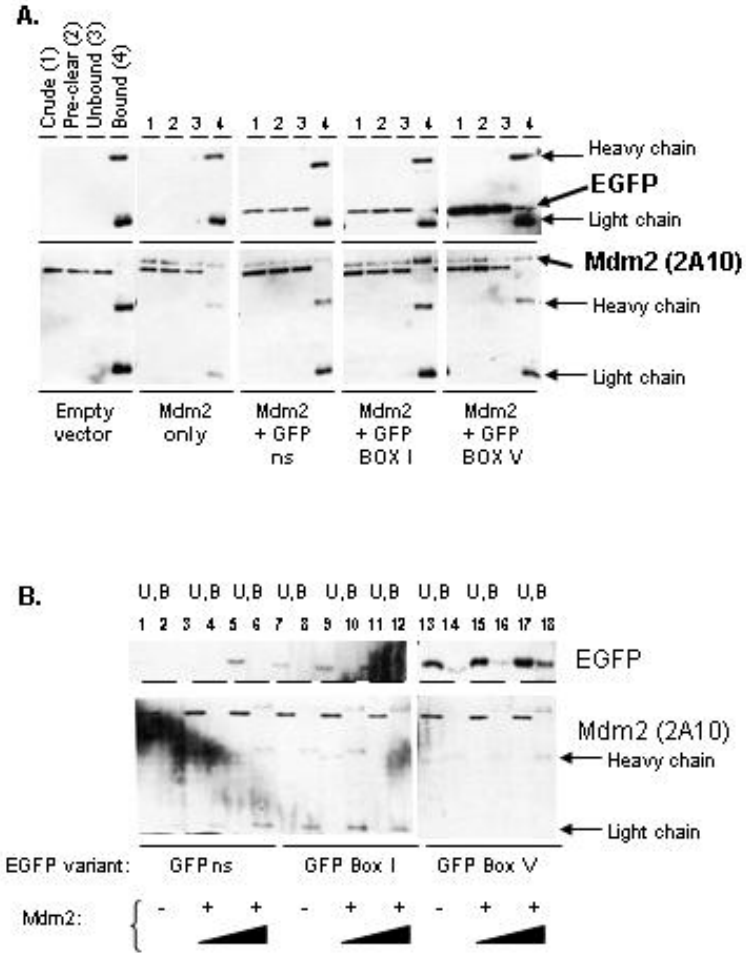

Figure 4.5 The binding of Mdm2 stabilizes the Box-V fusion peptide.

A. The vector encoding Mdm2 (1µg) was cotransfected with EGFP variants (0.5µg; EGFP control, EGFP-Box I and EGFP-Box V) into H1299 cells. 24 hours following transfection cell were lysed (lane 1), cell lysates were precleared (lane 2) and Mdm2 was subjected to immunoprecipitation using NHS-activated sepharose beads to which the anti-Mdm2 antibody, 2A10, had been previously coupled. EGFP variants were quantified both in the unbound fraction (lane 3) and the bound fraction (lane 4) by immunoblot with an anti-EGFP IgG. Mdm2 levels were shown by immunoblot. B. H1299 cells were cotransfected with a titration of the vector encoding Mdm2 (0, 1 or 2µg) and EGFP variant (0.5µg; EGFP control, EGFP-Box I or EGFP-Box V). 24 hours following transfection cells were lysed, cell lysates were precleared and Mdm2 was subjected to immunoprecipitation using 2A10 coupled NHS-activated sepharose beads. EGFP variants were quantified both in the unbound fraction (odd numbered lanes 1to17) and the

bound fraction (even numbered lanes 2 to 18) by immunoblot with an anti-EGFP IgG. Mdm2 levels were shown by immunoblot.

4.2.1.2 Binding of Mdm2 stabilizes the EGFP Box-V fusion peptide

Mdm2 negatively regulates p53 by ubiquitination and it is the Box-V docking region of p53 which contains the ubiquitination signal that is required for the dual site stimulation of the E3 ubiquitin ligase function of Mdm2 (Wallace et al. 2006). Therefore in light of the data which demonstrates the binding of kinases Chk1 and DAPK1 to the EGFP-Box-V fusion peptide in cells, Mdm2 was examined to determine whether it too formed a complex with the EGFP-Box-V fusion peptide in cells.

The vector encoding Mdm2 was coexpressed with EGFP variants (EGFP control, EGFP-Box I or EGFP-Box V) in H1299 cells. Mdm2 was subjected to immunoprecipitation using NHS-activated sepharose beads coupled with the anti-Mdm2 antibody, 2A10. EGFP variants were quantified both in the unbound fraction (lane 3) and the bound fraction (lane 4) by immunoblot with an anti-EGFP IgG. The results demonstrate that when EGFP-Box-V was cotransfected with Mdm2, similar to Chk1 and DAPK1, Mdm2 formed a complex with the EGFP-Box-V peptide, as demonstrated by the presence of a positive band in the bound fraction (Figure 4.5; A; 'Mdm2 + GFP Box-V' lane 4; EGFP blot).

To further investigate the interaction between Mdm2 and the Box-V peptide a coimmunoprecipitation assay was performed to examine the levels of stabilization of the Box-V peptide. A titration of the vector encoding Mdm2 was cotransfected with EGFP variant (EGFP control, EGFP-Box I or EGFP-Box V) into H1299 cells. EGFP variants were quantified both in the unbound fraction (Figure 4.5 B; lanes 1, 3, 5, 7, 9, 11, 13, 15 and 17) and the bound fraction (Figure 4.5 B; lanes 2, 4, 6, 8, 10, 12, 14, 16 and 18) by immunoblot with an anti-EGFP IgG. The results confirm that Mdm2 and the EGFP-Box-V peptide form a complex *in vivo* (Figure 4.5 B; comparing lanes 14, 16 and 18

with 2, 4, 6, 8, 10 and 12; EGFP blot) and demonstrate that the Box-V peptide is stabilized by transfection of increasing levels of Mdm2 (Figure 4.5 B; comparing lanes 14, 16 and 18; EGFP blot). It is likely that the binding of Mdm2 to the Box-V peptide is blocking the EGFP-Box-V degradation and leading in its stabilization.

4.2.2 Creation of p53 'Gain of function' mutants to examine kinase - p53 interaction

To develop our understanding of the sites important for p53-kinase interactions, several mutants were selected (as shown in Table 4.1) which have been reported in human cancers and have increased transcriptional activity from p53 promoters. These mutants had previously been demonstrated to have gain of function properties which included increased apoptotic activity above wild type p53 as well as increased transcriptional activity from one or more p53 promoters (Kakudo et al. 2005). The mutants were used in reporter assays to determine whether the activity of these mutants could be modulated by kinases and Mdm2 and to further define the key domains on p53 required for p53-kinase interaction.

As demonstrated by Figure 4.6 p53 'Gain of function' mutations (D208N, D207H, D207E, R209I and H214Q) were located in the 240 epitope, an exposed loop in p53 which is unfolded in mutant p53. Mutations located in the box V domain (A276V) were also been chosen to further examine the importance of the Box V domain in Chk1 docking. Other mutations were located in the extreme C-terminus of the DNA-binding domain (N288Y, K292I, N288T, K291E and K292N) which is adjacent to the Box-V region.

Table 4.1 A summary of the selected p53 mutants: transcriptional and apoptotic activity

Number	Mutant	Transcriptional Activity	Mutation Frequency in Human Tumours	Apoptotic Activity compared to WT
1	D208N	+	5	Equal or Decreased
2	D207H	+	1	Equal or Decreased
3	D207E	+	3	Equal or Decreased
4	R209I	+	1	Equal or Decreased
5	H214Q	+	4	Increased
6	N288Y	+/-	4	Equal or Decreased
7	K291E	+/-	1	Increased
8	A276V	+/-	6	Equal or Decreased
9	N288T	+	2	Equal or Decreased
10	K292I	+	2	Increased
11	K292N	+	2	Equal or Decreased

Table 4.1 Data summarised from publication (Kakudo et al. 2005) represents mutant p53 with increased (+) or mutant p53 with both decreased and increased (+/-) transcriptional activities for one or more of the eight p53 binding sequences. The TP53 mutation database (http://p53. curie.fr/) was used for mutation frequency and numbers represent the recorded frequency in human cancers. Evaluation of the ability to induce apoptosis was calculated in the subG_1 fraction after repeated FACS analysis (Kakudo et al. 2005).

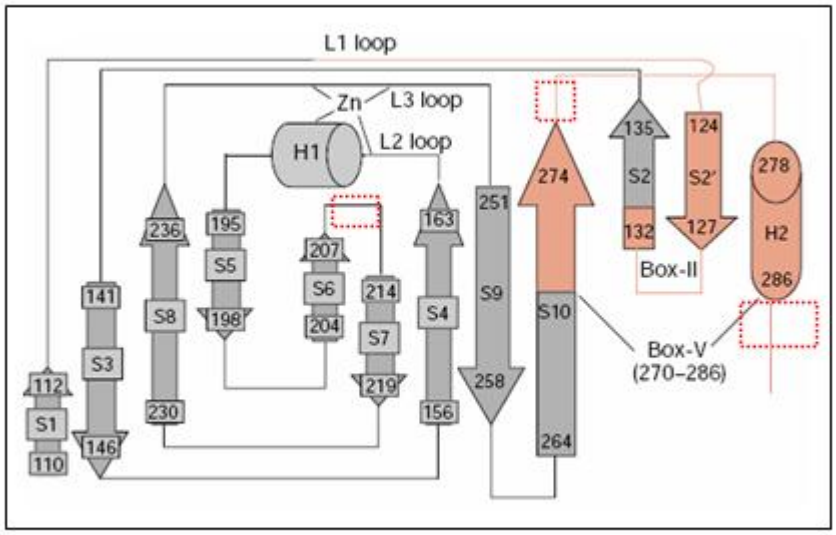

Figure 4.6 A diagram of p53 showing the location of the mutations (Craig et al. 2003).
The red dash boxes show the location of the chosen mutants which are in the: 240 epitope, an exposed loop in p53 which is unfolded in mutant p53; the extreme C-terminus of the DNA-binding domain; and the Box-V domain (chosen to further examine the importance of the Box-V domain in Chk1 docking). The Box-V peptide sequence (as well as the Box-II) are shown in red.

4.2.2.1 The p53 His175 mutant is transcriptionally activated by Chk1

It has been demonstrated that in many tumour-derived mutants a point mutation within the core domain of p53 can inactivate p53 function (Gannon et al. 1990; Kern et al. 1992). Mutation at codon 175 in p53, one of the hot-spots for mutation in human cancer, can lead to inactivation of p53 as this residue plays an important role in maintaining the structure of the DNA binding domain (Cho et al. 1994). Before examining the selected p53 'gain of function' mutants, the common tumour-derived mutant, p53 His175, was examined for its basal and kinase stimulated p53-dependent transcriptional activity (Figure 4.7).

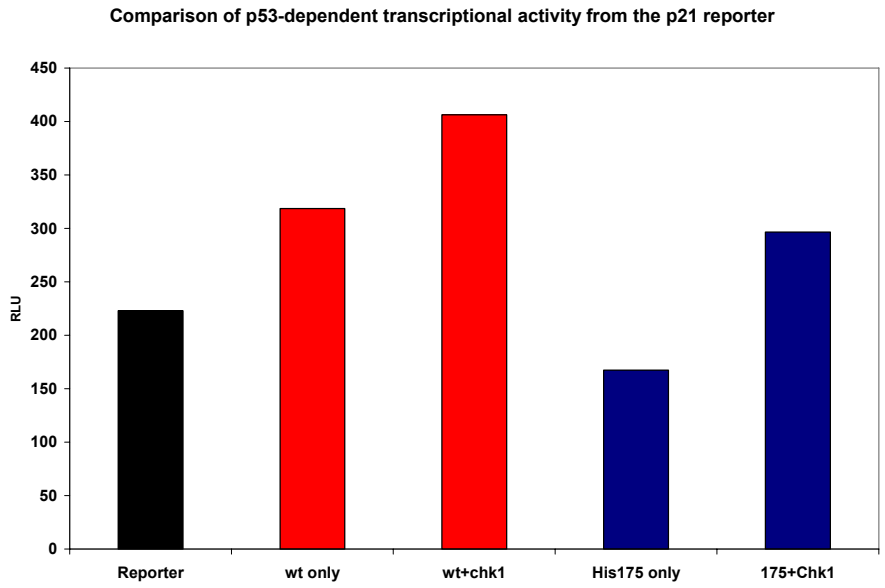

Figure 4.7 The p53His 175 isoform is transcriptionally activated by Chk1.
H1299 cells were cotransfected with Chk1-encoding gene (2 µg), p53 WT or p53 His 175 (50ng) and reporter plasmid constructs; $p21^{WAF1}$-luc and β-gal. After 24 hours the cells were lysed and luciferase and β-Galactosidase activity was measured. Data shows the luciferase activity normalised to the β-Gal production represented as Relative Light Units (RLU). Activity levels of the $p21^{WAF1}$ reporter construct without p53 are represented in reporter only lane.

The results demonstrate that the mutant encoded by the HIS175 allele induced no basal transcriptional activity from the $p21^{WAF1}$ reporter (Figure 4.7; blue column; His175 only). However, ectopic expression of Chk1 increased transcriptional activity of the transfected p53His175 (Figure 4.7; blue column; His175 + Chk1). This data examining a common tumour derived p53 mutant is potentially very interesting as it has already been demonstrated that this mutation enhances p53 ubiquitination both *in vitro* and *in vivo* (Shimizu et al. 2006). This Chk1-dependent transcriptional reactivation of the p53 HIS175 mutant suggests that Chk1, similar to Mdm2, may play an important role in modulation of p53 activity. Furthermore the data provided an interesting foundation on which to expand and develop our knowledge of the potential of kinase activation to increase or restore the activity of some p53 mutants.

4.2.2.2 Transfected of Calcium Calmodulin kinases have little effect on Ser 20 phosphorylation of ectopically expressed p53 mutants

Evaluation of kinases such as Chk1 and DAPK1 using assays such as *in vivo* Ser 20 phosphorylation and reporter based assays has identified Chk1 as a major genetic modifier of wild-type p53 (see section 3.2.4). To evaluate the basal and kinase-stimulated levels of Ser 20 phosphorylation of ectopically expressed mutant p53 compared to wild-type p53 an *in vivo* phosphorylation assay was performed. To this end, Chk1 and DAPK1 were used in the Ser 20 phosphorylation assay to investigate *in vivo* induction of mutant p53 Ser 20 phosphorylation. H1299 cells were co-transfected with wild-type or mutant p53 and Chk1 or DAPK1 expression vectors. Lysates were immunoblotted for p53 protein levels, Ser 20 site phosphorylation of p53 as well as for protein levels of Chk1 (Figure 4.8 A) and DAPK1 (Figure 4.8 B).

The western blot demonstrates that the expression levels of p53 mutants are similar to that of wild-type p53 (Figure 4.8 A and B; p53 blot). The results (Figure 4.8; A and B) indicate that although Chk1 stimulates wild-type p53 Ser 20 phosphorylation (Figure 4.8 A; comparing lanes 23 and 24). Chk1 is unable to stimulate the p53 Ser 20 activity of most of the eleven mutants (Figure 4.8 A; comparing odd numbered lanes with even numbered lanes). However, p53 mutant 8 (A276V), mutant 10 (K292I) and mutant 11 (K292N) do show some evidence of increased Ser 20 phosphorylation following the addition of Chk1 (Figure 4.8 A; Mut 8 comparing lanes 15 and 16; Mut 10 comparing lanes 19 and 20; Mut 11 comparing lanes 21 and 22; Ser 20 blot). These mutants are potentially interesting due to their location in or adjacent to the Box-V domain and were further investigated for their transcriptional activity. Following the addition of DAPK1, there was however no evidence of stimulation of either wild-type or mutant p53 Ser 20 phosphorylation (Figure 4.8 B; Ser 20 blot). The lack of stimulation of wild-type p53 Ser 20 phosphorylation following the addition of DAPK1 in this assay is likely to be the result of high level of basal p53 Ser 20 phosphorylation whereby upon addition of DAPK1 the stimulation of p53 Ser 20 phosphorylation is masked. This high basal p53

Ser 20 phosphorylation could be activated by transfection stress. These results suggest that the mutation of p53 in general results in the loss of the ability of kinases to activate Ser 20 phosphorylation of p53 and that there may be a role for kinases to phosphorylate other sites in mutant p53 leading to its activation.

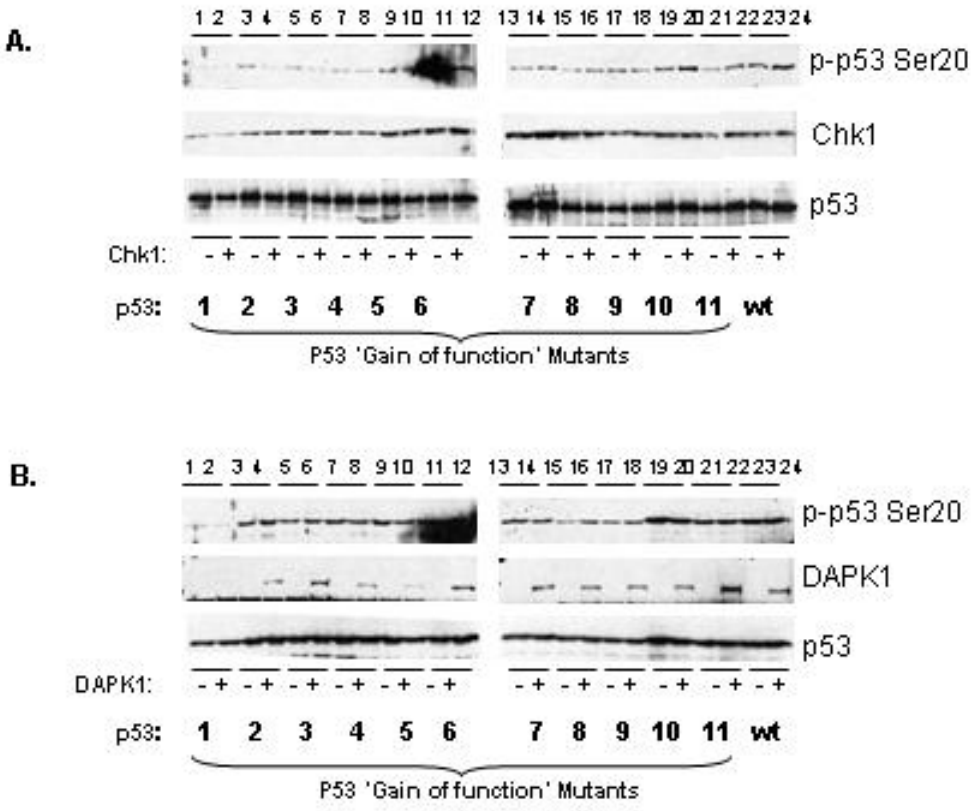

Figure 4.8 p53 mutants are not phosphorylated at Ser 20.

A and B. H1299 cells were co-transfected with 1µg of WT or mutant p53 (see Table 4.1 for details of mutants) and 1µg expression vectors to Chk1 (A) or DAPK1 (B). 24 hours following transfection cells were lysed and lysates were immunoblotted for p53 protein levels (DO12), Ser 20 site phosphorylation of p53 as well as for protein levels of Chk1 and DAPK1.

4.2.2.3 Basal transcriptional activity of the p53 mutants is promoter dependent

A preliminary gene reporter assay was performed to examine the basal and kinase stimulated transcriptional activity of the p53 mutants. H1299 cells were cotransfected with p53 expression construct and Chk1. The p53 target, p21, was used as a promoter indicator of basal and kinase stimulated p53-dependent transcription. The results demonstrated that of the p53 mutants examined in this preliminary gene reporter assay only specific mutants showed gain of function transcriptional activity above that of WT p53 and that in the main there was no significant kinase stimulated transcriptional activity towards the $p21^{WAF1}$ promoter (Figure 4.9). Mutants 1 to 5 with mutations located in the exposed 240 epitope demonstrated basal p53-dependent transcriptional activity similar to that of WT p53 whereas mutants 6 to 11 with mutations located in or adjacent to the Box-V region displayed basal p53-dependent transcriptional activity above that of WT p53 (Figure 4.9). This was potentially interesting due to the location of these mutants, adjacent to the Box-V region and suggested that some unfolding of the Box-V domain may increase p53 transcriptional activity towards $p21^{WAF1}$.

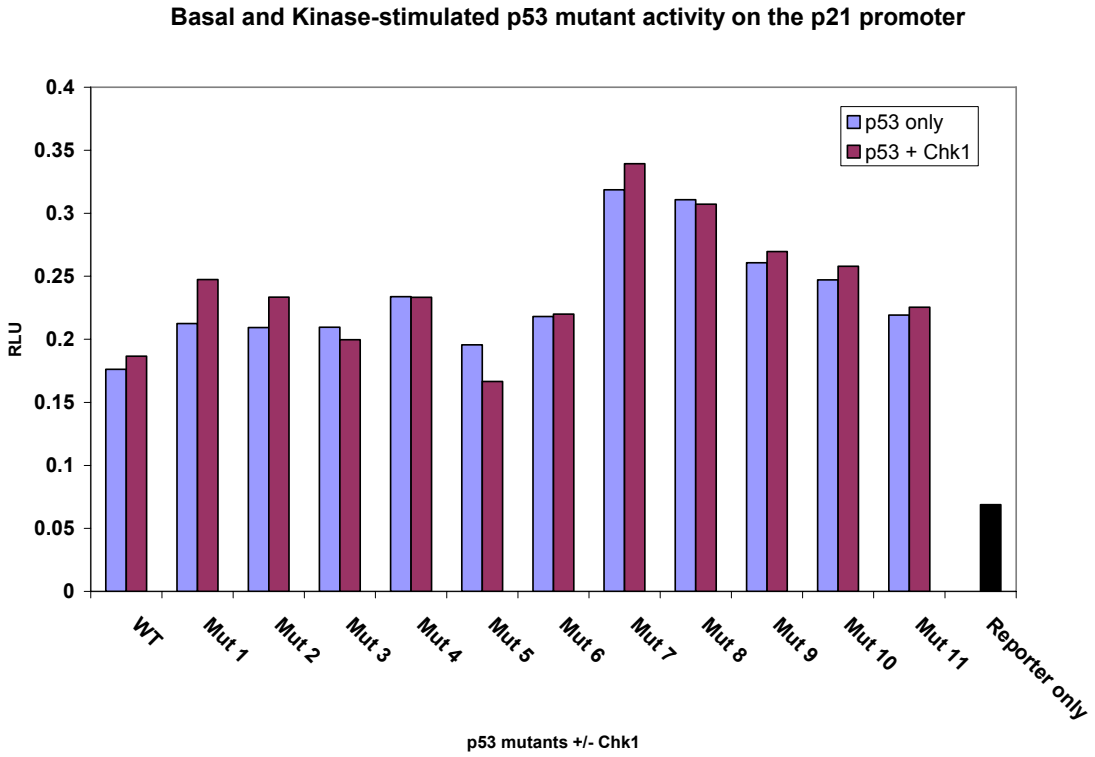

Figure 4.9 p53 mutants display some kinase stimulated p53-dependent transcriptional activity.

H1299 cells were cotransfected with 50ng of WT or mutant p53 expression construct, 2µg Chk1 and reporter plasmid constructs; $p21^{WAF1}$-luc (1µg) and REN-CMV (0.25µg). After 24 hours the cells were lysed and luciferase and Renilla activity was measured. Data shows the luciferase activity normalised to the Renilla production represented as Relative Light Units (RLU). Activity levels of the $p21^{WAF1}$ reporter construct without p53 are represented in reporter only lane.

Mutants which retain their ability to transactivate p53 target genes often show variability in the specific target genes which they are able to transactivate. For example mutants have been shown to transactivate $p21^{WAF1}$ but not BAX promoter (Rowan et al. 1996). In light of this data gene reporter assays were performed to compare and contrast the basal transcriptional activity of the p53 'Gain of function' mutants using the two common p53 target genes, *$p21^{WAF1}$* (cell cycle effector) and *BAX* (apoptotic effector). H1299 cells were cotransfected with a titration of p53 expression construct and reporter plasmid constructs; $p21^{WAF1}$-*luc* or BAX-*luc* and REN-CMV.

The results demonstrate the contrasting transactivation potential of the p53 mutants on $p21^{WAF1}$ and BAX and show that the comparative transcriptional activity of these promoters in these gene reporter assays is quite dramatic (Figure 4.10 A and B). The normalised result as represented by the Relative Light Units (RLU) is in general 10 fold lower for the BAX promoter (Figure 4.10 B) compared to the $p21^{WAF1}$ promoter (Figure 4.10 A). Examination of mutant p53-dependent transcriptional activity from the $p21^{WAF1}$ promoter demonstrates a general trend; as the transactivation activity of the mutants towards the $p21^{WAF1}$ promoter (Figure 4.10 A) decreases as p53 levels are increased (from 50ng to 500ng) suggesting that the system is more sensitive at lower levels of p53. The exceptionally high relative readings for Mutant 4 (100ng p53) and Mutant 9 (50ng p53) are due to low firefly and renilla readings which is likely the result of sample loading error and therefore not reliable and cannot be considered for analysis (Figure 4.10 A; Mutant 4, 100ng and Mutant 9, 50ng). Mutants derived from the exposed loop of p53 have similar transactivation activity toward $p21^{WAF1}$ to WT p53 (Figure 4.10 A; Mutants 1 to 5) whereas mutants 6, 7 and 8, which are located in or adjacent to the Box-V domain, show increased transactivation potential compared to WT (Figure 4.10 A). The other C-terminal mutants demonstrate a decreased transactivation potential compared to WT (Figure 4.10 A; Mutants 9, 10 and 11).

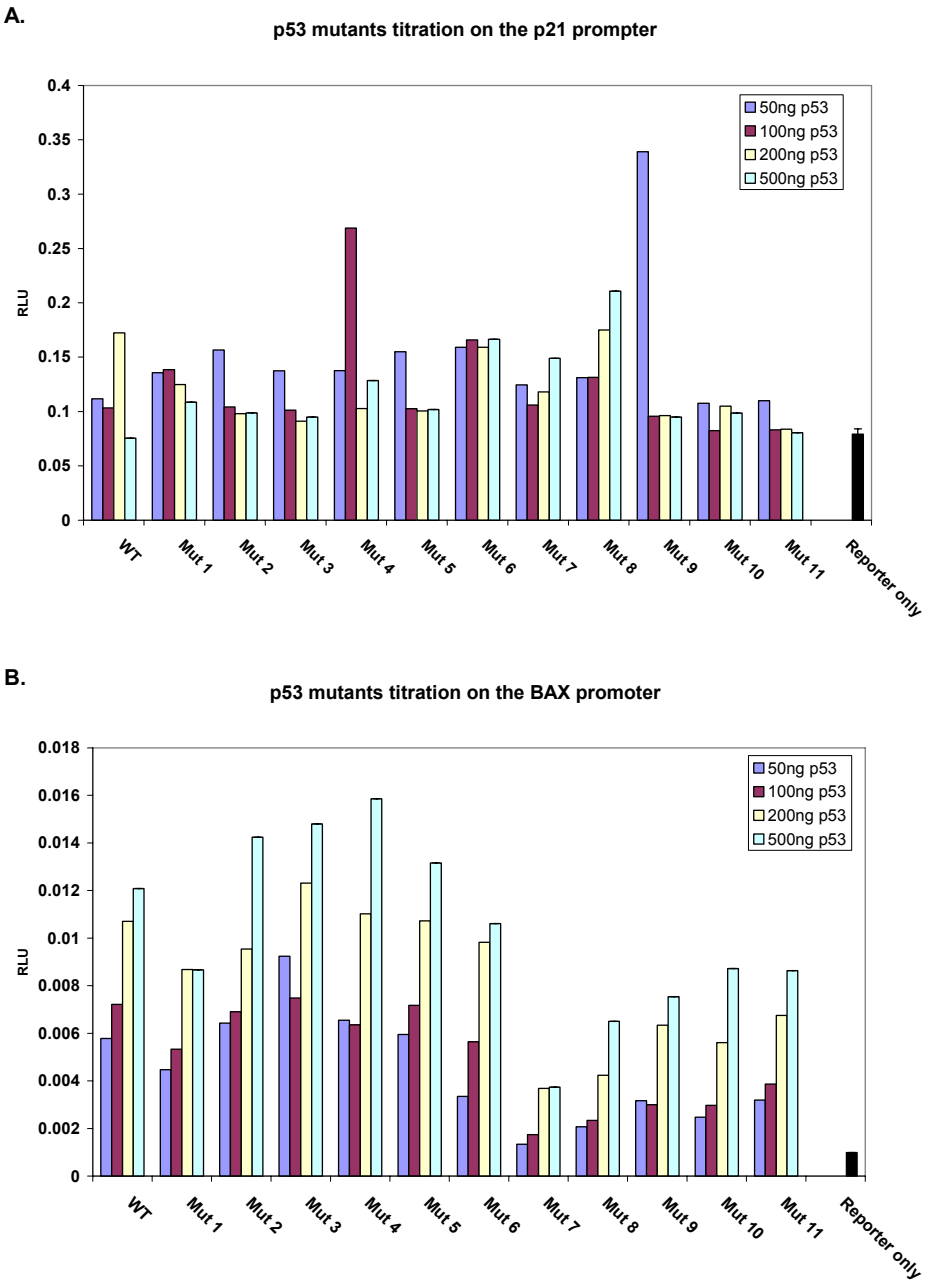

Figure 4.10 Basal transcriptional activity of p53 mutants is promoter dependent.

A & B. H1299 cells were cotransfected with a titration of WT or mutant p53 expression construct (50, 100, 200 or 500ng) and reporter plasmid constructs; $p21^{WAF1}$-luc (A; 0.14µg) or BAX-luc (B; 0.14µg) and REN-CMV (0.06µg). After 24 hours the cells were lysed and cell lysates were analyzed for their luciferase and Renilla activity. Data shows the luciferase activity normalised to

the Renilla production represented as Relative Light Units (RLU). Activity levels of the p21 reporter construct without p53 are represented in reporter only lane.

In contrast examination of mutant p53-dependent transcriptional activity from the BAX promoter demonstrates a general trend of increasing transactivation potential towards the BAX promoter (Figure 4.10 B) as levels of p53 are increased (from 50ng to 500ng). It may either be that this promoter operates more effectively at higher levels of p53, or alternatively that other cofactors may be required to stimulate the transcriptional activation of mutant p53 toward this promoter. In the main the transactivation activity of the p53 mutants on the BAX promoter remains at similar levels to WT p53 (Figure 4.10 B; comparing Mutants 1 to 6 to WT). However, it is the activity of the p53 mutants with mutations located in or adjacent to the Box-V domain which produces the most interesting result (Figure 4.10 B; comparing Mutants 6 to 11 to WT) as these mutants demonstrate a decreased transactivation potential compared to WT p53. This contrasted dramatically with the increased transactivation potential of mutants 6, 7 and 8 on the $p21^{WAF1}$ promoter. In particular mutant 7 (K292I) and mutant 8 (A276V) exhibited the most dramatic contrast in transactivation activities (Figure 4.10; comparing figures A and B; Mutants 7 and 8) and would therefore will be examined further. Overall, from these results we can conclude the p53-dependent transcriptional activity of these mutants is promoter dependent. That is, more mutants demonstrate gain of function potential towards the $p21^{WAF1}$ promoter whereas the transactivation potential of p53 mutants towards the BAX promoter is in most cases similar to WT p53. This data was consistent with data from the Ishioka group in which these mutants (K292I and A276V) showed contrasting activities on the $p21^{WAF1}$ and BAX promoters whereas other mutants such as those examined in these assays do not demonstrate such contrasting activities (Kakudo et al. 2005).

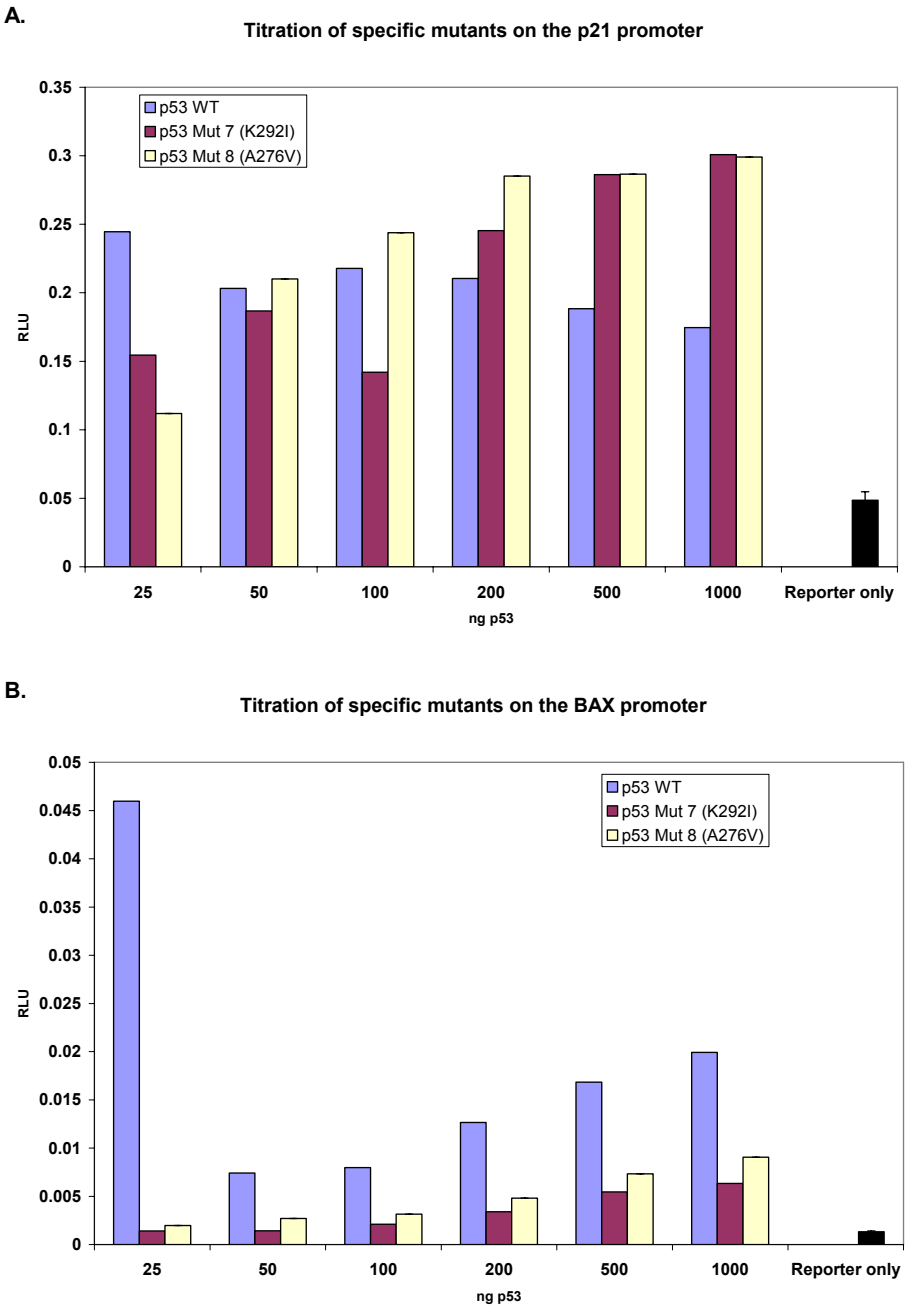

Figure 4.11 Basal transactivation activity of p53 mutants is promoter dependent.

H1299 cells were cotransfected with a titration of WT or mutant p53 expression construct (25, 50, 100, 200 or 500ng) and reporter plasmid constructs; $p21^{WAF1}$-luc or BAX-luc (0.14µg) and REN-CMV (0.06µg). After 24 hours the cells were lysed and cell lysates were analysed for their luciferase and Renilla activity. Data shows the luciferase activity normalised to the Renilla

production represented as Relative Light Units (RLU). Activity levels of the $p21^{WAF1}$ reporter construct without p53 are represented in reporter only lane.

In light of the dramatically contrasting activities of p53 mutant 7 (K292I) and mutant 8 (A276V) towards the two examined promoters ($p21^{WAF1}$ and BAX), these mutants were examined further using the gene reporter assay. To confirm previous results (Figure 4.10), we extending the titration range of the mutant p53 and firstly examined the mutant basal p53-dependent transcriptional activity on the two promoters (Figure 4.11 A and B).

Examination of specific mutants (7; K292I and 8; A276V) basal transcriptional activity from the $p21^{WAF1}$ and BAX promoters demonstrates as previously that gain of function transactivation potential is promoter dependent (Figure 4.11; comparing A and B). Mutant p53 transcriptional activity towards the $p21^{WAF1}$ promoter increases as p53 levels are increased (Figure 4.11; A; Mut 7 and Mut 8; comparing columns 25 to 1000ng p53) whereas WT p53 transcriptional activity from the $p21^{WAF1}$ promoter decreases as levels of p53 increase (Figure 4.11; A; WT p53; comparing columns 25 to 1000ng p53). This pattern of activity results in the p53 mutants demonstrating gain of function transcriptional activity as levels of p53 are increased. In contrast, mutant p53 transcriptional activity on the BAX promoter remains lower than WT p53 transcriptional activity at all levels of p53 but in general as p53 levels are increased, the transcriptional activity of all p53s toward the BAX promoter increases (Figure 4.11; B; comparing columns 25 to 1000ng p53). The exceptionally high relative readings for p53 WT (25ng) is due to low firefly and renilla readings which is likely the result of sample loading error and therefore not reliable and cannot be considered for analysis (Figure 4.11; B; p53 WT; 25ng). This data therefore supports previously demonstrated data whereby these p53 mutants, 7 and 8 demonstrated promoter specific gain of function characteristics.

4.2.2.4 P53 Mutants are not stimulated transcriptionally by addition of kinases or Mdm2

To develop and verify basal transcriptional data, the kinase and Mdm2 stimulated p53-dependent transcriptional activity was examined. Chk1 and DAPK1 were used in these gene reporter assays to examine the effect of kinases on p53 mutant transcriptional activity from both the $p21^{WAF1}$ and BAX promoters. H1299 cells were cotransfected with a fixed amount of p53 expression construct, a titration of Chk1 or DAPK1 and reporter plasmid constructs; $p21^{WAF1}$-*luc* or BAX-*luc* and REN-CMV.

The data represented in Figure 4.12 compares Chk1 and DAPK1 stimulation of p53 mutant activity from the $p21^{WAF1}$ promoter (Figure 4.12; A and B respectively) and Chk1 and DAPK1 stimulation of p53 mutant activity from the BAX promoter (Figure 4.12; C and D respectively). The data demonstrates that addition of kinases results in no stimulation of gain of function transcriptional activity of the p53 mutants on either promoter (Figure 4.12; A, B, C and D; comparing columns 0ng kinase with 50, 100, 250, 500 or 1000ng kinase). On the $p21^{WAF1}$ promoter, Mutant 7 demonstrates basal activity similar to WT p53 (Figure 4.12; A and B; comparing p53 Mut 7 to p53 WT) whereas Mutant 8 has increased basal transcriptional activity compared to WT (Figure 4.12; A and B; comparing p53 Mut 8 to p53 WT). On the BAX promoter, mutant 7 and 8 demonstrate no transcriptional activity above that of WT (Figure 4.12; C and D; comparing p53 Mut 7 and p53 Mut 8 to p53 WT) which is consistent with the data demonstrated previously Figure 4.11 B). The data point representing the effect of 100ng Chk1 on p53 Mut 7 has been removed as the relative reading is exceptionally high and lies outwith the scale of the graph (Figure 4.12; C; p53 Mut 7; 100ng Chk1). This is the result of low firefly and renilla readings which is likely the result of sample loading error.

A.

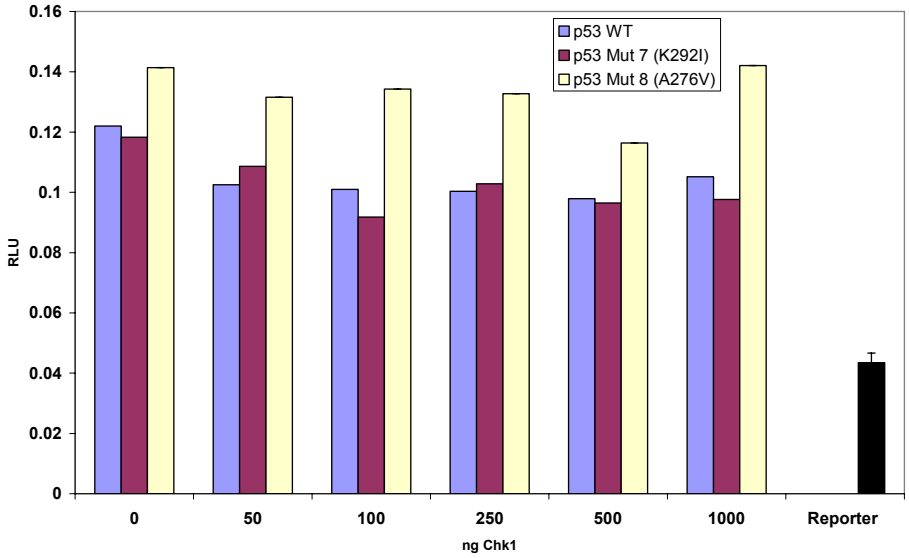
Effect of Chk1 on p53 mutant activity on the p21 promoter
p53 WT
p53 Mut 7 (K292I)
p53 Mut 8 (A276V)
RLU
0.16
0.14
0.12
0.1
0.08
0.06
0.04
0.02
0
0
50
100
250
500
1000
Reporter
ng Chk1

B.

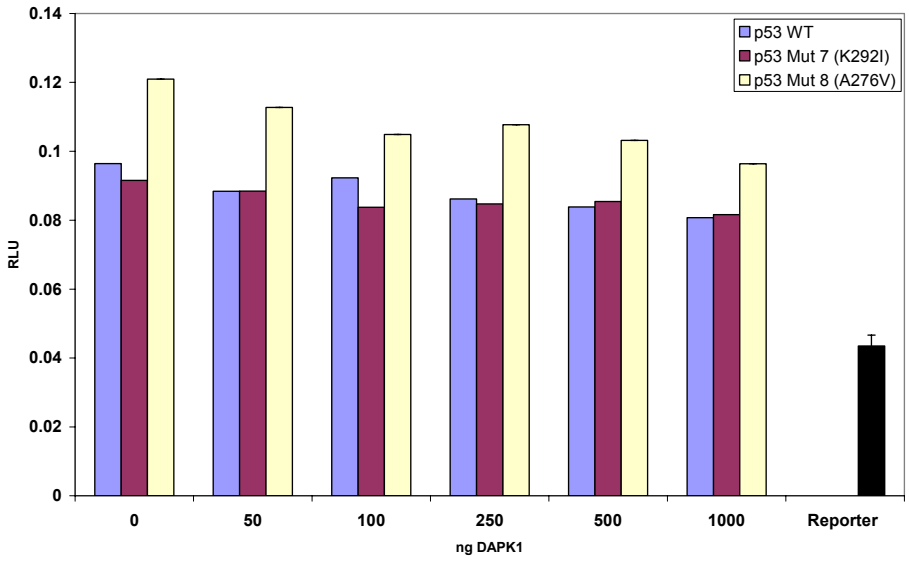
Effect of DAPK1 on p53 mutant activity on the p21 promoter
p53 WT
p53 Mut 7 (K292I)
p53 Mut 8 (A276V)
RLU
0.14
0.12
0.1
0.08
0.06
0.04
0.02
0
0
50
100
250
500
1000
Reporter
ng DAPK1

C.

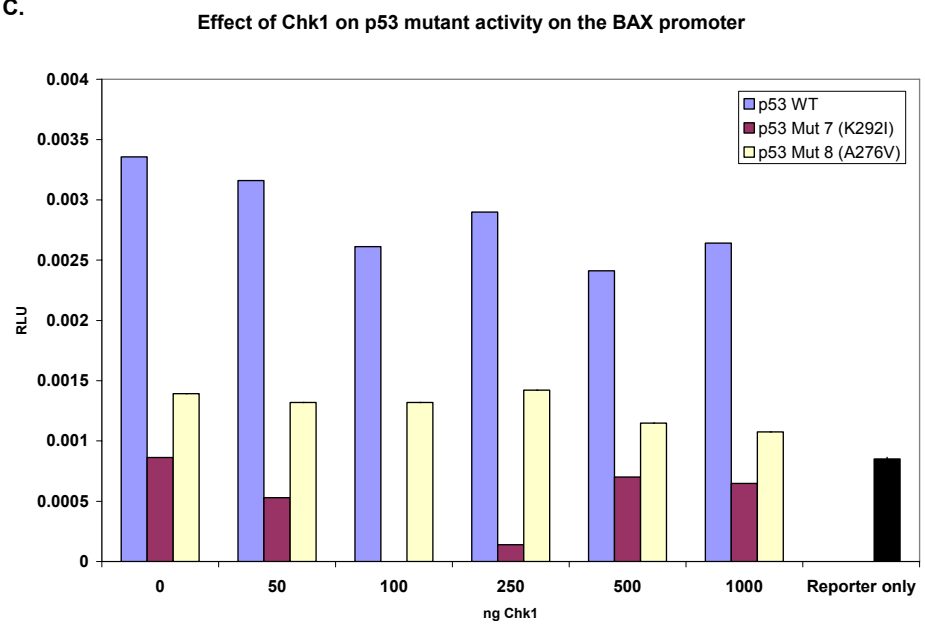

D.

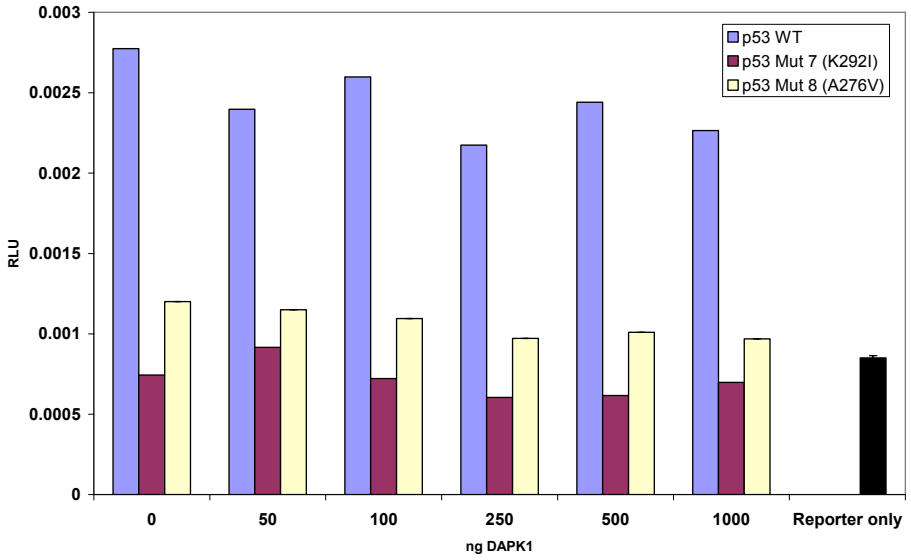

Figure 4.12 Kinases do not stimulate transactivation activity of the p53 mutants.

A and B: Effect of Chk1 (A) and DAPK1 (B) on p53 mutant activity on the $p21^{WAF1}$ promoter. H1299 cells were cotransfected with WT or mutant p53 expression construct (100ng), a titration of Chk1 or DAPK1 (50, 100, 200, 500 or 1000ng) and reporter plasmid constructs; $p21^{WAF1}$-luc (140ng) and REN-CMV (60ng). C and D: Effect of Chk1 (C) and DAPK1 (D) on p53 mutant activity on the BAX promoter (as above with 140ng BAX-luc). After 24 hours cell lysates were

analysed for their luciferase and Renilla activity (normalised data shown Relative Light Units (RLU)).

Overall, although there is no stimulation of transcriptional activity by addition of kinases it is interesting that Mutant 8 (A276V) consistently demonstrates basal transcriptional activity toward the $p21^{WAF1}$ promoter above WT. This is the only p53 mutant with a mutation actually located in the Box-V domain and it was hypothesized that this mutation may play an important role in the interaction of Mdm2 with the Box-V domain.

To address this hypothesis the assay was repeated to examine the effect of Mdm2 on p53 mutant transcriptional activity on the $p21^{WAF1}$ promoter. The results demonstrate that similar to Chk1 and DAPK1, Mdm2 does not stimulate p53-dependent transcriptional activity from the $p21^{WAF1}$ promoter (Figure 4.13). The results show that in general in this assay the transcriptional activity of both mutants remain above that of wild-type p53 (Figure 4.13; comparing Mutant 7 and Mutant 8 with WT p53). However, the addition of increasing levels of Mdm2 decreases the transactivation potential of Mutant 7 (Figure 4.13; p53 Mut 7; comparing 0ng with 50, 100, 250, 500 or 1000ng Mdm2) and may suggest that this mutant is hyper-sensitive to Mdm2 (Figure 4.13; p53 Mut 7; 1000ng Mdm2). In contrast to this result, p53 Mutant 8 (A276V) appears to be resistant to Mdm2-mediated inhibition of p53 transcriptional activity (Figure 4.13; p53 Mut 8; 1000ng Mdm2). This mutant (A276V) is located in the conserved Box-V domain, the location of the ubiquitination signal for Mdm2. The observed resistance of this mutant to Mdm2-mediated inhibition of p53 transcriptional activity may be consistent with the loss of the Mdm2 binding site.

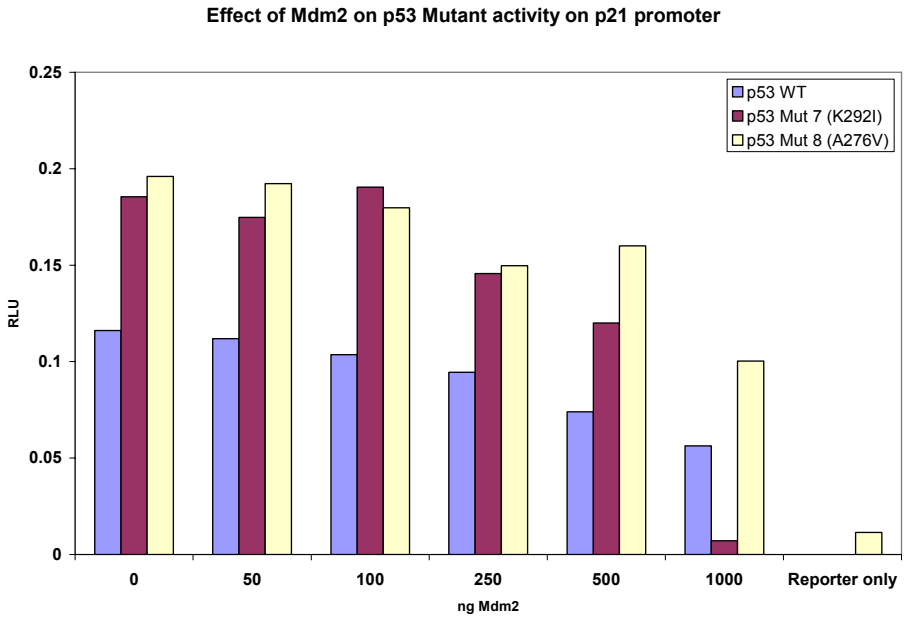

Figure 4.13 Mdm2 does not stimulate transactivation activity of the p53 mutants on p21^{WAF1} promoter.

H1299 cells were cotransfected with a fixed amount p53 expression construct (100ng), a titration of Mdm2 (50, 100, 200, 500 or 1000ng) and reporter plasmid constructs; p21^{WAF1}-luc or BAX-luc (0.14µg) and REN-CMV (0.06µg). After 24 hours the cells were lysed and cell lysates were analysed for their luciferase and Renilla activity. Data shows the luciferase activity normalised to the Renilla production represented as Relative Light Units (RLU). Activity levels of the p21^{WAF1} reporter construct without p53 are represented in reporter only lane.

Although neither kinases nor Mdm2 stimulated the transcriptional activity of the p53 mutants, Mutant 7 (K292I) and 8 (A276V) demonstrated increased basal transcriptional activity from the p21^{WAF1} promoter. The fact that these mutants contain mutations that are located in or adjacent to the Box-V region of p53 could prove particularly interesting. Therefore an approach which examined mutagenesis of the Box-V region was employed to investigate the kinase – p53 interaction in more detail.

4.2.3 Examination of specific sites of interation of kinases on p53 Box-V domain

To expand upon Box-V *in vivo* interaction data, mutagenesis of the Box-V region was also performed. The Box-V peptide was previously identified as the most potent Chk1 and Chk2 activator *in vitro* (Craig et al. 2003). This report examined the effects of individual amino acid mutations on Box-V peptide activation of Chk2 and identified mutation of amino acids to alanine at specific sites (270, 272, 273, 274 and 277) in the S10 β-sheet attenuated Chk2 activation by the Box-V peptide (Craig et al. 2003). This suggested that specific sites in the Box-V domain were important in the interaction with Chk2 and therefore should be investigated for interaction with other kinases.

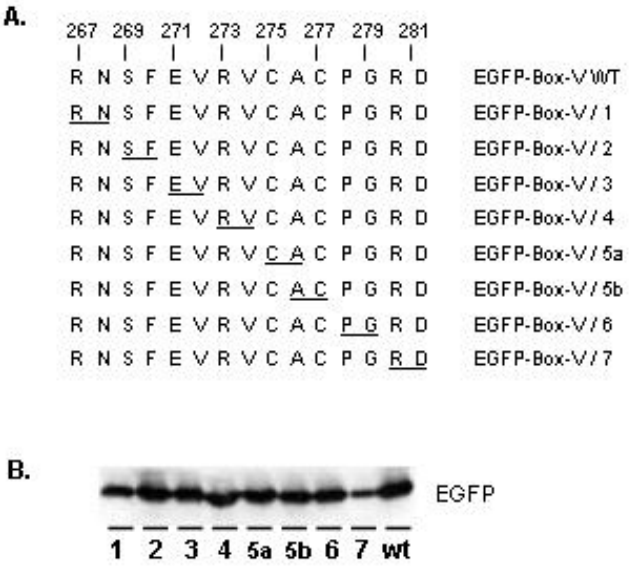

Figure 4.14 Creation of double alanine mutants to examine kinase-p53 interaction.

A. The schematic diagram shows the sequence of the EGFP-Box-V fusion peptide, the corresponding amino-acid residues, and the double alanine-mutated EGFP-Box-V derivatives (underlined). B. Expression levels of the EGFP mutants compared to WT. H1299 cells were transfected with 1μg EGFP mutant variant. After 24 hours cells were lysed and lysates were immunoblotted for levels of EGFP using the anti-EGFP IgG.

In order to investigate specific kinase binding regions within the Box-V domain, a set of double alanine mutants spanning the sequence of the Box-V peptide were prepared by site directed mutagenesis of EGFP-Box-V WT (Figure 4.14; A). This enabled us to investigate which regions of the Box-V domain kinases preferentially bind to.

4.2.3.1 DAPK1 and Chk1 have distinct but overlapping binding requirements on p53 Box-V

It has been demonstrated that the Box-V fusion peptide binds to both Chk1 and DAPK1 in cells (Figure 4.3 and Figure 4.4 respectively). In order to investigate the specific regions of the Box-V peptide which kinases may have a preferential binding capacity for, coimmunoprecipitation assays were performed using the Box-V alanine mutants. EGFP mutant and variants were quantified both in the unbound fraction (Figure 4.15 A; unbound (U); lanes 1 to 21; odd numbers) and the bound fraction (Figure 4.15 A; bound (B); lanes 2 to 22; even numbers) by immunoblot with an anti-EGFP IgG. The results demonstrate as shown previously that Chk1 forms a complex with Box-V-WT (Figure 4.15 A; lane 18; bound fraction). There were varying levels of binding of the Box-V alanine mutants to Chk1 with increased stabilization of the Box-V mutants 4, 5a and 6 (Figure 4.15 A; comparing lanes 8, 10 and 14 with lane 18; bound fraction) and reduced stabilization of the Box-V alanine mutants 1, 2, 3, 5b and 7 (Figure 4.15 A; comparing lanes 2, 4, 6 and 16 with lane 18; bound fraction). Thus, suggesting that the first six (residues 267 – 274) and last two (residues 280 and 281) amino acids of the Box-V peptide may play an important role in the binding potential of Chk1. This data is consistent with *in vitro* data which showed that amino acids residues 270, 272, 273 and 274 were important for Chk2 activation of p53 (Craig et al. 2003).

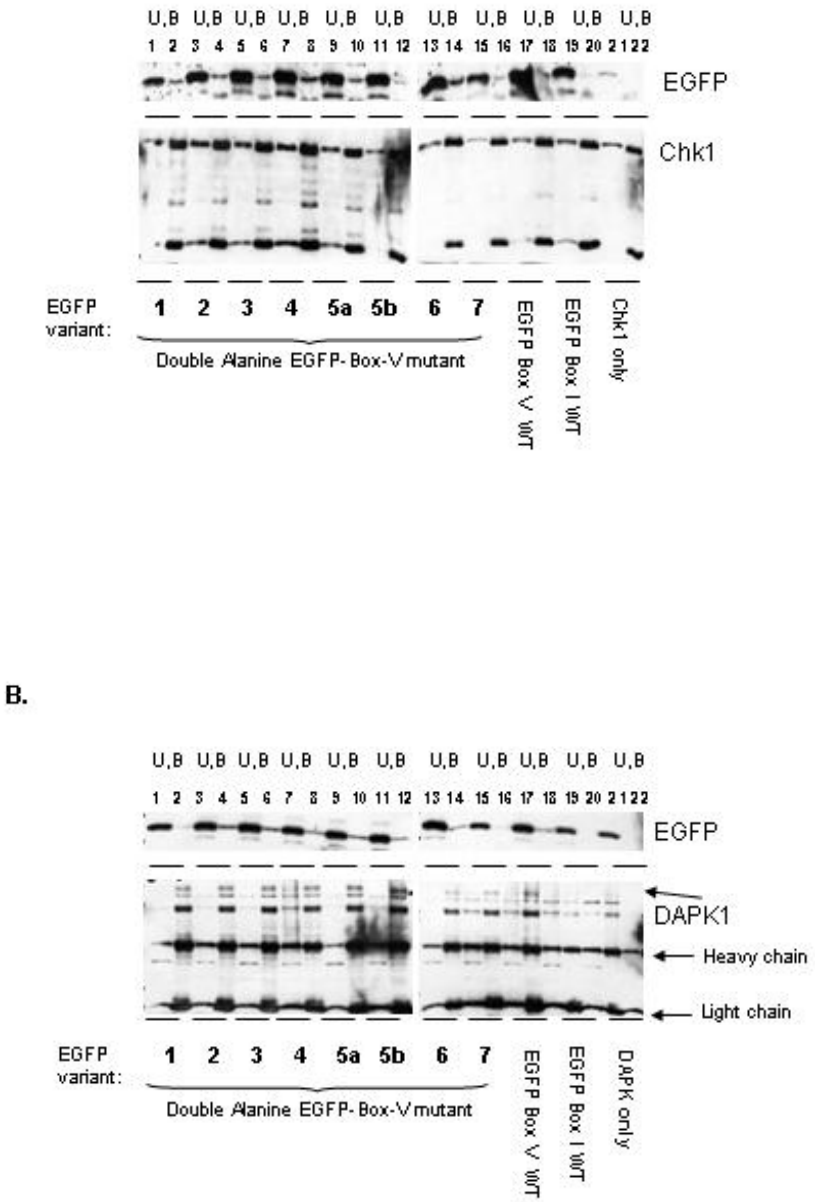

Figure 4.15 Examination of kinase binding to Box-V mutants demonstrates that binding occurs at specific sites.

(Fig 4.15) A. H1299 cells were cotransfected with vectors encoding Chk1 (1µg) and EGFP-Box-V mutants (0.5µg; EGFP-Box-V/ 1 to 7; see Figure 4.14 for details) or EGFP variants (0.5µg; EGFP-Box I and EGFP-Box V). 24 hours following transfection cells were lysed, lysates were precleared and Chk1 was subjected to immunoprecipitation using NHS-activated sepharose beads to which the anti-Chk1 antibody had been previously coupled to. EGFP mutants and variants were quantified both in the unbound fraction (U; lanes 1 to 21; odd numbers) and the bound fraction (B; lanes 2 to 22; even numbers) by immunoblot with an anti-EGFP IgG. Chk1 levels were quantified by immunoblot B. H1299 cells were cotransfected with vectors encoding HA-DAPK1 (1µg) and EGFP-Box-V mutants (0.5µg; EGFP-Box-V/ 1 to 7) or EGFP variants (0.5µg; EGFP-Box-I and EGFP-Box-V). Cells were lysed, lysates were precleared and HA-DAPK1 was immunoprecipitated with anti-FLAG agarose beads. Quantification of the EGFP mutant or variant in the unbound (U; lanes 1 to 21; odd numbers) or bound (B; lanes 2 to 22; even numbers) fractions after FLAG pull-down was performed by immunoblot using an anti-EGFP IgG. DAPK1 levels were quantified by immunoblot.

To examine the level of binding of Box-V mutants by DAPK1, H1299 cells were cotransfected with vectors encoding HA-DAPK1 and EGFP Box-V mutants (EGFP-Box-V/ 1 to 7) or EGFP variants (EGFP-Box I-WT and EGFP-Box V-WT) as controls. Cells were lysed, lysates were precleared and HA-DAPK1 was immunoprecipitated with anti-FLAG agarose beads. Quantification of the EGFP mutants and variants in the unbound (U; lanes 1 to 21; odd numbers) or bound (B; lanes 2 to 22; even numbers) fractions after FLAG pull-down was performed by immunoblot using an anti-EGFP IgG. The results demonstrate as shown previously that DAPK1 forms a complex with Box-V-WT (Figure 4.15; B; lane 18; bound fraction). There were varying levels of binding of the Box-V mutants by DAPK1. There was increased stabilization of the Box-V mutants 2, 3, 4 and 5a (Figure 4.15; B; comparing lanes 4, 6, 8 and 10 with lane 18; bound fraction) and reduced stabilization of the mutants 1, 5b, 6 and 7 when compared to Box-V-WT (Figure 4.15; B; comparing lanes 2, 12, 14 and 16 with lane 18; bound fraction). DAPK1 may therefore bind preferentially to the first two (residues 267 and 268) and last six (residues 275 - 281) amino acids as their mutation to alanine decreases the binding of DAPK1 to Box-V. The data demonstrated that the central amino acids of Box-V peptide

have a reduced binding affinity for DAPK1 suggesting that these sites are not necessarily required for binding.

4.2.3.2 The EGFP-Box-V fusion peptide binds preferentially to Mdm2

In has previously been shown that mutation of single amino acids Ser 3 and Phe 4 (residues 269 and 270 of p53 Box-V) resulted in reduced binding activity to the acid domain of Mdm2 suggesting that these sites were important in contributing to the activity of the peptide. In contrast mutation of sites Val 8, Cys 9 and Cys 11 (residues 274, 275 and 277) both increased the activity of peptides as E3-ligase inhibitors and increased binding affinity for Mdm2 suggesting that these mutations was less crucial for binding and for the resulting Mdm2 catalysed ubiquitination to take place (Wallace et al. 2006). To further investigate levels of stabilization of the Box-V peptide by Mdm2 the vector encoding Mdm2 was cotransfected with EGFP mutants (EGFP-Box-V/ 1 to 7) or EGFP variants (EGFP-Box I and EGFP-Box V) into H1299 cells. EGFP mutants and variants were quantified both in the unbound (Figure 4.16; unbound (U); lanes 1 to 21; odd numbers) or bound (Figure 4.16; bound (B); lanes 2 to 22; even numbers) fractions after FLAG pull-down was performed by immunoblot using an anti-EGFP IgG.

As previously demonstrated (Figure 4.5) the binding of Mdm2 stabilises the Box-V fusion peptide. There is increased level of stabilization when Mdm2 is coimmunoprecipitated with the Box-V alanine mutants 4, 5a, 5b and 6 (Figure 4.16; comparing lanes 8, 10, 12 and 14 with lane 18; bound fraction) and reduced levels of stabilization when Mdm2 is coimmunoprecipitated with Box-V alanine mutants 1, 2, 3 and 7 compared to Box-V WT (Figure 4.16; comparing lanes 2, 4, 6 and 16 with lane 18; bound fraction). The pattern of binding correlated with a report which used a Box-V alanine substituted library to examine the features of the Box-V region required for the inhibitory activity of Mdm2 (Wallace et al. 2006). The pattern of stabilization by Mdm2 across the Box-V peptide is also similar to that observed in the Chk1 coimmunoprecipitation assay (Figure 4.15 A), where both Mdm2 and Chk1 appear to

have reduced stabilization and thus binding affinity to mutants 1, 2, 3 and 7. Therefore, suggesting that the first six and last two amino acids of the WT Box-V peptide may play an important role in the binding potential of both Chk1 and Mdm2 and may suggest competition between Chk1 and Mdm2 for binding to the Box-V domain *in vivo*.

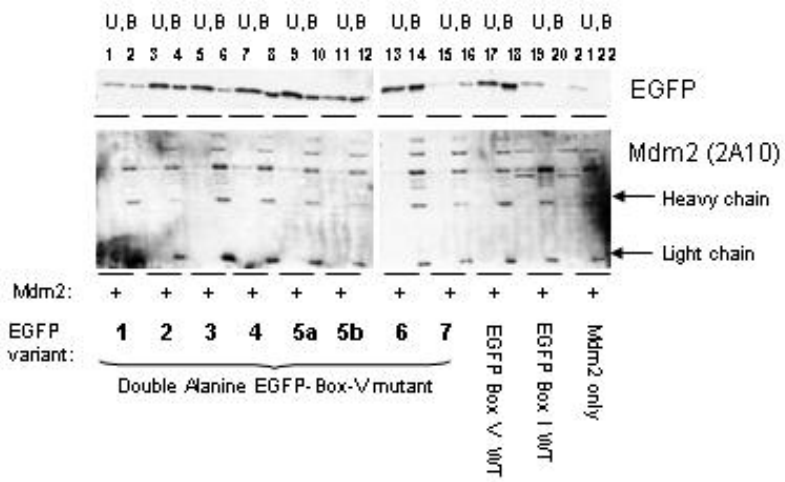

Figure 4.16 The EGFP-Box-V peptide binds preferentially to Mdm2.

The vector encoding Mdm2 (1µg) was cotransfected with EGFP-Box-V mutants (0.5µg; EGFP-Box-V/ 1 to 7) or EGFP variants (0.5µg; EGFP-Box I and EGFP-Box V) into H1299 cells. 24 hours following transfection cell were lysed and cell lysates were precleared. Mdm2 was subjected to immunoprecipitation using NHS-activated sepharose beads to which the anti-Mdm2 antibody, 2A10, had been previously coupled to. EGFP mutants and variants were quantified both in the unbound (U; lanes 1 to 21; odd numbers) or bound (B; lanes 2 to 22; even numbers) fractions after pull-down was performed by immunoblot using an anti-EGFP IgG. Mdm2 levels were quantified by immunoblot.

Table 4.2 Levels of stabilization of double alanine Box-V mutants compared to Box-V-WT

Box-V Mutant	Residues	Chk1	DAPK1	Mdm2
Box-V/1	267, 268	↔	↓	↓
Box-V/2	269, 270	↔	↑↑	↔
Box-V/3	271, 272	↔	↑↑	↓
Box-V/4	273, 274	↑↑	↔	↑
Box-V/5a	275, 276	↑	↑	↑
Box-V/5b	276, 277	↓	↔	↑
Box-V/6	278, 279	↑↑	↔	↑↑
Box-V/7	280, 281	↓	↓	↓

(↔ similar to WT; ↑ increased stabilization; and ↓ decreased stabilization above WT)

Therefore, examination of binding capacity of kinases and Mdm2 to the Box-V peptide using mutants derived from the Box-V peptide has confirmed previously described data in which Calcium Calmodulin kinases and Mdm2 bind to the Box-V peptide. The coimmunoprecipitation assays have given some insight into specific regions where kinases or Mdm2 may bind. By comparing the stabilization levels of the EGFP-Box-V mutant fusion peptide to that of EGFP-Box-V WT we have been able to define sites which may be important in contributing to the activity of the peptide. Table 4.2 summarises this data and as highlighted the sites that show decreased stabilization after mutation are the sites of interest. This may be of importance in defining the areas of interaction between p53 and kinases or Mdm2 and therefore contribute to the initiation of signals which control p53 activity.

4.3 Discussion

The objective of this chapter was to examine and extend our knowledge of interactions between kinases and p53. This involved using coimmunoprecipitation assays to examine kinase binding to the Box-V region of p53 and to characterise sites of interaction, double alanine mutants spanning the Box-V motif were made. To further define the domains required for p53: kinase interactions, a selected group of p53 'gain of function' mutants were examined for their basal and kinase stimulated transcriptional activity to different p53 targets. This allowed us to develop our understanding of the molecular mechanisms behind oncogenic gain of function, as well as expand our knowledge of the interactions of p53 mutants and whether these interactions could be modulated by kinases. This will go some way to revealing the biochemical pathways and putative targets for the treatment of cancers that display mutant p53.

4.3.1 Chk1 and Mdm2 have overlapping binding requirements on p53 Box-V

We have established that the Box-V region is a multi-protein binding site required to activate p53 phosphorylation and ubiquitination (Wallace et al. 2006; Craig et al. 2007). To further investigate this interaction between kinases and/or Mdm2 and the Box-V motif of p53 binding assays were performed *in vivo*. Using EGFP non-specific and EGFP-Box-I as controls we were able to demonstrate that both kinases of interest, Chk1 and DAPK1, bound specifically and stably to Box-V in cells. This result was validated by cotransfection of a titration of the Box-V fusion peptide and kinase of interest; which demonstrated a dose-dependent relationship between levels of transfected Box-V and the formation of FLAG-Chk1: EGFP-Box-V immune-complexes. This observation supported previous data in which the addition of the Box-V fusion peptide attenuated phosphorylation of p53 at Ser 20 (see section 3.2.7) and that this attenuation of phosphorylation may be attributable to the binding of the Box-V fusion peptide to kinases and thereby preventing the phosphorylation of p53. We have demonstrated here

that kinases do indeed bind to the Box-V fusion peptide in cells and that the Box-V domain of p53 forms a docking site for the Calcium Calmodulin kinase superfamily.

Mdm2 was the first Box-V domain binding protein to be identified (Shimizu et al. 2002) and more recently it has been shown that the Box-V region provides the ubiquitination signal for Mdm2 which is required for the dual-site docking mechanism of Mdm2 on the p53 tetramer (Wallace et al. 2006). In this report coimmunoprecipitation assays were performed as previously using EGFP non-specific and EGFP-Box-I as controls and we were able to demonstrate that Mdm2 formed a complex specifically with the Box-V peptide and not with the Box-I peptide in cells. In addition, we showed that the Box-V peptide was stabilized by transfection of increasing levels of Mdm2. The stable binding of Mdm2 is thought to prevent the degradation of the peptide and thereby stabilizing it. The fact that EGFP-Box-I did not bind to Mdm2 is this and the previous assay is surprising as it had been demonstrated *in vitro* using a peptide from the Box-I activation domain of p53 that Mdm2 was fully competent for binding to the Box-I domain of p53 (Wallace et al. 2006). It may be the case the Box-I alone is not sufficient to form the binding site and that the alternative binding site in the Box-V region may also be required. However, the ability of the EGFP-Box-V fusion peptide to form a stable immune complex with Mdm2 in cell lysates is expected and correlates with previously described data in which the Box-V domain of p53 forms part of a binding surface for Mdm2 that is involved in signaling p53 ubiquitination (see section 3.2.5)

Mutation of Box-V domain has been previously performed to investigate the role of specific residues of this docking interface on Box-V peptide activation of Chk2 (Craig et al. 2003). This report by Craig and colleagues examined the effects of individual amino acid mutations and identified mutation of amino acids to alanine at specific sites (270, 272, 273, 274 and 277) in the S10 β-sheet attenuated Chk2 activation by the Box-V peptide (Craig et al. 2003). To further investigate the interaction between the kinases/Mdm2 and Box-V region of p53 double alanine mutants spanning the Box-V

peptide region were created to determine specific sites of interaction. These results demonstrated that both Chk1 and Mdm2 showed reduced stabilization and binding affinity to mutants 1, 2, 3 and 7 and DAPK1 showed reduced stabilization and binding affinity to mutants 1, 5b, 6 and 7. Therefore, suggesting that the first six and last two amino acids of the WT Box-V peptide may play an important role in the binding potential of both Chk1 and Mdm2 and that the first two and last six amino acids of the WT Box-V peptide may play an important role in the binding potential of both DAPK1. The patterns of binding correlated with a report which used a Box-V alanine substituted library to examine the features of the Box-V region required for the inhibitory activity of Mdm2 (Wallace et al. 2006). Wallace and colleagues showed that mutation of single amino acids Ser 3 and Phe 4 resulted in reduced binding activity to the acid domain of Mdm2 suggesting that these sites were important in contributing to the activity of the peptide. In contrast mutation of sites (Val 8, Cys 9 and Cys 11) both increased the activity of peptides as E3-ligase inhibitors and increased binding affinity for Mdm2 suggesting that these mutations was less crucial for binding and for the resulting Mdm2 catalysed ubiquitination to take place (Wallace et al. 2006).

It is worth noting that in the assays examining the Box-V mutants, there is no evidence of the control Box-I forming a complex with Mdm2. As described above, this result is unexpected. It may have been useful to use more than one antibody to Mdm2 to allow detection of binding at different regions on Mdm2, although in these assays the limited availability of lysates restricted the number of analyses undertaken on one sample. As an improvement to the overall presentation of the coimmunoprecipitation data and to allow the reader to examine detail of each important band with ease, the immunoblots could have been presented in a larger format but due to the number of samples, this too has its limitations.

However, the fact that both Mdm2 and the Calcium Calmodulin kinases bind and stabilize the Box-V region, and that Chk1 and Mdm2 demonstrate similar patterns of

interaction with the Box-V peptide is potentially very interesting. This and previous published data (Shimizu et al. 2002; Wallace et al. 2006) suggest that the Box-V motif is a conformationally flexible multiprotein binding domain that controls covalent modification of the p53 tetramer. Recent studies which used nuclear magnetic resonance revealed that the acid domain of Mdm2 can bind directly to the core domain of p53 and that on binding to p53 this acid domain fragment of Mdm2 induced significant chemical shifts throughout the core domain especially within the Box-V motif (Yu et al. 2006). These data may suggest that different proteins compete with each other for binding to this specific region of p53 and that the outcome of this competition may be a factor in the regulation of p53. Considering the results from this report it is possible that the Calcium Calmodulin kinases, Chk1/DAPK1 and Mdm2 could antagonize each other through competition for the same multi-protein docking site. Results have demonstrated that the p53 mutant, p53 HIS175 can be stimulated transcriptionally by transfection of Chk1 (see section 4.2.2.1). Although it has been established that the p53 HIS175 protein is hyperubiquitinated *in vivo* due to the unfolding of the protein and thus the exposure of the Box-V motif (Shimizu et al. 2006), this transcriptional reactivation of the p53 HIS175 mutant from the $p21^{WAF1}$ reporter by Chk1 suggests that Chk1 may overcome Mdm2-mediated ubiquitination by competition for binding to the Box-V interface and drive p53 into a transactivation-competent rather than a ubiquitinated state.

Therefore, the data presented here along side previous reports highlight the potential for the Box-V domain of p53 to function both as a Calcium Calmodulin kinase docking site and an Mdm2 ubiquitination signal, which would allow cells to control p53 modulation in response to various stresses which it may encounter.

4.3.2 The role of p53 'Gain of Function' mutants

We have shown here that mutation of key contact sites on p53, specifically the Box-V domain can lead to loss of kinase binding to p53 which will likely negatively effect the activation of p53. Mutation of p53 is one of the most common events in cancer. One of three events normally occur which contribute to the progression of the cancer: p53 loss of function; mutant p53 dominant-negative function; or mutant p53 gain of function, where expression of mutant p53 in cells lacking WT p53 enhances their tumourigenic potential. This report has examined the role of the gain of function nature of mutant p53 in order to develop our understanding of the molecular mechanisms of the oncogenic gain of function phenotype and the molecular interactions of mutant p53. With reference to recent reports (Kakudo et al. 2005) a set of mutants was created to evaluate whether the activity of these mutants could be modulated by kinases and/or Mdm2 and thereby simultaneously further identify sites important for the interaction of p53 with kinases/Mdm2.

Comparison of two common p53 target genes, *p21* and *BAX* demonstrated that basal activity of the p53 mutants was promoter dependent and that p53 mutants were not stimulated transcriptionally by the addition of kinases or Mdm2. The report did however identify two potentially interesting mutations, A276V and K2921, which are found within or adjacent to the Box-V region. The p53 proteins containing these mutations demonstrate the most dramatic contrast in transactivation activities from the $p21^{WAF1}$ and BAX promoters. A more detailed examination of these specific mutants (K292I and A276V) demonstrated that gain of function transactivation potential was promoter-dependent and that these p53 mutants demonstrated $p21^{WAF1}$ promoter specific gain of function characteristics. It is likely that these mutants bind to the high affinity binding sites of the $p21^{WAF1}$ promoter but not to the low affinity binding sites on the BAX promoter. However, the data demonstrated that neither kinases nor Mdm2 further stimulated the transcriptional activity of these two p53 gain of function mutants on either promoter. It was interesting, however, that Mutant 8 (A276V), consistently

demonstrated basal transcriptional activity toward the $p21^{WAF1}$ promoter above that of WT p53 and appeared to be resistant to Mdm2-mediated inhibition of p53 transcriptional activity (Figure 4.13). This was the only p53 mutant examined that exhibited a mutation within the Box-V domain, the location of the ubiquitination signal for Mdm2. The observed resistance of this mutant to Mdm2-mediated inhibition of p53 transcriptional activity may be consistent with the loss of the Mdm2 binding site. Although in these assays this Box-V mutant p53 was not stimulated transcriptionally by kinases or Mdm2, it may nevertheless play an important role in kinase or Mdm2 interaction with the Box-V domain in a similar manner to the common tumour-derived mutant p53 His175. Indeed it is possible to imagine that mutant 8 may favour the binding of kinases rather than Mdm2, thus driving p53 into a transactivation competent state.

The recent reports demonstrating the role of the p53 core domain in binding to Mdm2 suggest that p53 mutants show alterations in their sensitivity to Mdm2 (Shimizu et al. 2006). A recent paper by the Vousden group examined the ubiquitination and degradation of mutant p53. They demonstrated that p53 mutants are ubiquitinated *in vivo* independently of Mdm2 and suggest that the chaperone-associated ubiquitin ligase (CHIP) and other E3 ligases may play more of an important role in the ubiquitination and degradation of mutant p53 (Lukashchuk and Vousden 2007). It may be that mutant 8 is activated transcriptionally towards other p53 targets which may be more sensitive to kinase stimulation of transcriptional activity or to events such as ubiquitination. A more diverse approach utilizing a range of p53 targets to examine the basal and kinase stimulated transcriptional activity of both mutant and wild-type p53 needs to be employed if we are to address these gaps of information.

Selection of the mutants for this study was based on a recent publication by the Ishioka group (Kakudo et al. 2005). They employed a yeast-based functional assay to evaluate the activity of a diverse selection of p53 mutants. Others studies have also employed yeast-based functional assays in which to investigate transcriptional activation and altered promoter selectivity of mutant p53 (Inga et al. 2001; Resnick and Inga 2003).

Most recently Menendez and colleagues investigated the relationship between changes in the p53 master regulatory network and biological outcomes using human cells as a model. They demonstrated that p53 mutations in human cells resulted in a wide range of biological outcomes because of the ability of the mutants to change the spectra of genes targeted by p53 (Menendez et al. 2006). Therefore the use of human cells will considerably contribute to the continued progression of the research examining transcriptional activation and altered promoter selectivity of mutant p53 and provide an interesting insight into p53 mutagenesis in cancer.

The affinity of p53 mutants for various p53 target sequences as well as their protein-protein interactions can be determined by the structure and energetic response of the mutant. The stability of full-length p53 is dictated by its core domain which at temperatures only slightly above body temperature will melt (Ang et al. 2006). The folding state of the mutant can be affected by mutations which reduce the thermostability of the protein. Studies have examined the folding states of mutants at low temperatures and have demonstrated that mutants can be grouped into distinct classes which correlate with the location of the mutations in the p53 structure (Bullock et al. 2000). For example, the structural hotspot mutations in the DNA-binding surface are destabilized to varying degrees and show different patterns of DNA-binding activity in their folded state (Bullock et al. 2000). Therefore, the activity of gain of function mutants may be defined by their thermodynamic stability. For example the mutants examined in detail in this study (A276V and K292I) demonstrated contrasting transcriptional activities towards the p53 target genes *p21* and *BAX*. The location of these mutations in the DNA binding domain may suggest that these mutants demonstrate varying degrees of stability which may therefore affect their ability to activate downstream targets. Examination of the thermostability of these mutants is a potentially interesting follow-up study in which to clarify the activity of these mutants, their interactions with other proteins and thus the control of p53 activity.

Knock-in mouse models provide another approach to investigating the role of p53 mutants in cancer progression. For example, development of murine model with mutation at p53 amino acid site 172 which corresponds to the R175H hot-spot mutation in human cancers to simulate Li-Fraumeni-like mutant p53, demonstrated that the mutant p53 associated with p63 and p73 in tumour cells of mice (Lang et al. 2004). They also showed that silencing mutant p53 resulted in increased the activity of p53 family target genes such as $p21^{WAF1}$ which was likely to be a result of the increased activity of endogenous p63 and p73 in the absence of mutant p53 (Lang et al. 2004). These studies proposed a means by which mutant p53 may promote tumourigenesis through downregulation of its p53 family members. With respect to continuing the investigation of the mutants examined in this study, the use of knock-in mouse models could be a potentially interesting way to clarify how interactions with other proteins may control the modulation of p53 activity.

These and other approaches have provided a basis on which to build our understanding of the activity of p53 mutants and the resulting biological outcomes. The way in which we approach the design of individual therapeutic strategies is likely to depend on individual mutation phenotypes and will therefore be complex but crucial in the treatment of many cancers. The results presented in this chapter of this report has highlighted the importance of the Box-V domain of p53 to function as a Calcium Calmodulin kinase docking site and an Mdm2 ubiquitination signal as well as highlighting the effect of specific mutations within p53 on kinase activation of p53. The role of kinases such as Chk1 and DAPK1 on activation of p53 should therefore be investigated further to determine kinase-dependent changes in p53 target gene expression.

5 IDENTIFICATION OF KINASE DRUG TARGETS FOR REACTIVATION OF THE P53 RESPONSE

5.1 Introduction

5.1.1 siRNA technology

RNA interference (RNAi) is a naturally occurring cellular defense mechanism against viral infections and transposons which utilize double stranded RNA (dsRNA) for self-propagation (Fuchs and Borkhardt 2007; Iorns et al. 2007). RNAi is a useful tool for selective transient or stable repression of gene expression and is considered a much more efficient method for gene silencing than the time consuming gene knockout in animal model systems (Fuchs and Borkhardt 2007). RNAi as a method to manipulate gene expression was first performed in *Caenorhabditis elegans* (Fire et al. 1998) and soon after performed in cultured mammalian cells to suppress the expression of endogenous and heterologous genes (Elbashir et al. 2001). The use of dsRNA in mammalian cells can however lead to the induction of interferon response and global shutdown of protein synthesis (Iorns et al. 2007). To overcome this problem short interfering RNA (siRNA) are used to silence gene expression (Iorns et al. 2007).

siRNAs are short annealing duplexes of approximately 21 nucleotides in length and are generally synthetic in origin (Martin and Caplen 2007). They can be directly added to the cell by transfection and function by binding to their complementary mRNA which leads to the degradation of the mRNA and therefore the attenuation of gene expression (Fuchs and Borkhardt 2007). Alternatively the siRNA duplexes can be generated within the cell by introducing plasmids that express short-hairpin RNA (shRNA). shRNA are precursors of siRNA which are processed within the cell by the DICER enzyme into siRNA which promote the transcript degradation by binding to their complementary mRNA (Iorns et al. 2007). Investigations utilizing both of these techniques have defined the roles for genes such as the *AURORA B* kinase in RAS transformation (Kanda

et al. 2005) and have identified *PAI1* as a critical downstream target of p53 after the induction of replicative stress (Kortlever et al. 2006).

Alternatively, RNAi libraries can be used to target multiple genes simultaneously. RNAi libraries are made up of reagents which target every single gene in the genome and are useful in elucidating phenotypes associated with loss-of-function of many individual genes simultaneously (Iorns et al. 2007). There are two types of RNA library: collections of vector based shRNA expression vectors; or libraries of siRNA (Iorns et al. 2007). Large scale screens are used in cancer research for the identification of new components in cancer relevant signaling pathways such as p53 (Fuchs and Borkhardt 2007). RNAi can also be used therapeutically to treat viral infections such as the respiratory syncytical infection, ocular and neurogenerative disease (Kim and Rossi 2007).

For the purpose of this study we will focus on using siRNA duplexes (specifically Dharmacon RNAi reagents) to study the effect of kinase depletion on activation of p53.

5.1.2 Microarray technology

The advent of microarray technology has transformed molecular biology. Previously there had been many different techniques used for the analysis of gene expression at mRNA level. These have included northern blotting, differential display, serial analysis of gene expression, and dot-blot analysis (van Hal et al. 2000). However, these techniques are in general quite limited due to low sensitivity and small sample number capability. The development of DNA microarrays which assess variation of genes in the genome and RNA microarrays which compare changes in expression of all RNA transcripts in the transcriptome has allowed the study of the entire genome and the transcriptome (Plomin and Schalkwyk 2007). Microarray technology allows the investigation of changes in transcription rates of nearly all genes of the genome in a

particular tissue or cell, as a result of different disease states, the stage of development and in response to intentional experimental perturbations (Stoughton 2005). Types of microarray include class comparison, which compares expression profiles of different tissue types; class prediction which compares normal tissues to tumour tissues; and class discovery, which aims to discover new taxonomies, groupings or clusters within a collection of samples (Manning et al. 2007).

Microarrays can be categorized as either (i) cDNA arrays in which probes are constructed with PCR products of up to a few thousand base pairs or (ii) oligonucleotides arrays which use either short (20 – 30 mer) or long (60 – 70mer) oligonucleotides (Draghici et al. 2006). The technology is based on the hybridization of mRNA to a high density array of immobilized target sequences each corresponding to a specific gene (van Hal et al. 2000). Each array contains several thousand DNA sequences which act as gene specific probes and are immobilized on a solid support such as nylon, glass or silicone (Manning et al. 2007). The process involves the reverse transcription of mRNA samples to cDNA, the incorporation of fluorescent, radioactive or chemiluminescent labeled nucleotides and the binding (hybridisation) of cDNA to the array membrane (van Hal et al. 2000; Manning et al. 2007). The emission signal of each spot on each array is a quantitative measurement which corresponds to the expression level of each gene (van Hal et al. 2000). The resulting output reading provides a 'snap-shot' of the profile of gene expression throughout the genome allowing the comparison of different groups, different time points and different tissues (Plomin and Schalkwyk 2007).

Microarrays have contributed to clarification of disease mechanisms, identified novel genes, assigned function to previously unannotated genes and enabled the grouping of genes into functional pathways (Stoughton 2005). As well as gene expression analysis, DNA microarrays have facilitated biochemical and functional genomic studies of DNA binding proteins. These technologies include ChIP-chip (or genome wide location

analysis), which utilizes chromatin immunoprecipitation of a protein followed by the microarray based detection of enriched DNA fragments to identify the *in vivo* transcription factor binding sites; Dam technology, which examines the DNA-binding site protein fused to DNA adenine methyltransferase (Dam) for identification of *in vivo* binding sites across the genome; and lastly PBM (protein-binding microarray) technology which allows high throughput characterization of DNA-binding proteins by assaying their binding to double stranded DNA microarrays (Bulyk 2006). For the purpose of this study we will focus on the use of microarrays for gene expression profiling.

Microarrays are commonly used to examine differences in expression of specific genes across samples (Manning et al. 2007). The use of microarrays to study such differences has many advantages over that of other gene expression technologies because of their relatively small size, their greater sensitivity, their requirement for a much smaller amount of starting material and the arrays have the potential for much larger sample screening (van Hal et al. 2000). The development of microarray technology has allowed for the detailed profiling of tumours where previous studies have examined only individual genes as potential targets (Nagasaki and Miki 2006). For example, breast cancers were classified based on profiles of gene expression (Perou et al. 1999) and from that the classification of cancer subtypes and prediction of therapeutic outcomes was established (Perou et al. 2000). Examination and comparison of gene expression profiles of primary carcinomas, liver metastases and carcinomatoses to normal samples identified genetic patterns associated with different stages of liver tumourigenesis (Kleivi et al. 2007). Microarray analysis was used to study effect of damage such as ionizing radiation (IR) on changes in gene expression profiles was examined in a paper by Snyder and Morgan. They used microarray analysis to confirm that genes such as *GADD45* and *CDKN1A* are consistently upregulated in response to IR and that there is also a substantial p53-independent component to the transcriptional profile following IR damage (Snyder and Morgan 2004). It is hoped that the development of gene expression

profiling along with analysis of protein expression and interactions will lead to the development of drugs targeted to specific molecules (Nagasaki and Miki 2006). Furthermore, by examining the clinical response to radiotherapy, it should be possible to identify genes linked to radiosensitivity (Snyder and Morgan 2004) .

There are however several concerns and issues associated with microarray analysis of gene expression. Although changes in the mRNA level of genes gives an insight into which genes are transcriptionally active, microarray results do not automatically translate into changes in protein expression or phenotype (Manning et al. 2007). Indeed, protein function is also controlled at the translational and post-translational levels. The transcriptional profiling of RNA has many issues. RNA is labile, is often prone to producing artifacts and in many examples RNA is too far removed from the actual cellular effectors (Hoheisel 2006). Issues such as sensitivity, accuracy, specificity and reproducibility must be carefully considered (Draghici et al. 2006). Variation in results can be influenced by several factors such as the biological samples, human variation and limitations to data analysis (Hoheisel 2006). With regard to this, results should always be viewed cautiously and should ideally always be validated using techniques such as RT-PCR.

The screening of human cancers using microarray technology has emerged as a powerful new tool in developing novel diagnostic, prognostic and therapeutic targets for cancers (Manning et al. 2007). The use of primary analytical methods such as hierarchical clustering and statistical analysis based on differential expression to examine cancer transcriptome data has allowed the clarification of several issues (Rhodes and Chinnaiyan 2005). For example, cancer can be distinguished from normal tissue using gene expression profiles; cancer subtypes often have distinct gene expression profiles; gene expression profiles of signature tumours can often predict disease recurrence and treatment response; and lastly heterogeneous cancers which can be subclassified into molecular subtypes of cancer often have distinct gene expression profiles (Rhodes and

Chinnaiyan 2005). However, other more advanced methods of analysis have uncovered important biological profiles not apparent in standard analysis methods. Methods such as 'meta-analysis', which analyses multiple sets of data to extract common gene expression patterns from independent cancer signatures and 'protein interaction networks' which elucidate the gene expression in context of the complex molecular networks using protein-protein interaction (interactome) maps have advanced the study of gene expression in cancer (Rhodes and Chinnaiyan 2005).

The role of p53 as a tumour suppressor is mainly due to its activity as a transcription factor that activates the transcription of many genes in response to cell stresses leading to growth arrest and/or apoptosis (Levine 1997). Microarray analysis has been used in several studies to address the issue of p53-dependent gene expression (Zhao et al. 2000; Kannan et al. 2001). Zhao and colleagues used the human carcinoma cell line, EB-1, containing stably transfected p53 to examine the levels of genes regulated following DNA damaging treatments such as γ radiation and UV. Cluster analysis revealed that genes could be grouped into distinct subsets and the expression of some genes was altered in a similar manner after all treatments (Zhao et al. 2000). DNA microarrays were used to identify the primary and secondary targets of p53 (Kannan et al. 2001). This group compared a human cancer cell line which expresses temperature sensitive murine p53 (H1299-ts-p53Val135) to the p53 null cell line, H1299 and used cycloheximide treatment (inhibits protein synthesis) to distinguish between primary and secondary p53 target genes. They showed that without cycloheximide there were 259 upregulated and 125 downregulated genes and upon cycloheximide treatment less than 20% of the above genes were up or down regulated. These genes were considered as primary targets (Kannan et al. 2001). Both studies go some way to clarifying the p53 targets in various cellular contexts and to clarify both the early and late response genes.

5.1.3 Objectives and Experimental Approach

The identification of Chk1 and DAPK1 as p53 activators has led to investigation of the effects of loss of these kinases on p53 signaling as well as the p53 response following IR damage. In this chapter we set out to clarify the effect of kinase depletion on the activation of p53 using siRNA technology. We then went on to combine siRNA technology and oligonucleotide microarrays which are low density gene arrays, to profile the gene expression of 113 genes involved in the human p53 signalling pathway (Superarray). This would allow us to examine the effect of kinase depletion on activation status of p53 target genes.

5.2 Results

5.2.1 Development of cell models to study the effect of loss of kinases on p53 signaling

We have previously identified, using *in vivo* assays such as transcription based reporter and siRNA putative kinases which may activate p53 by phosphorylation (see sections 3.2.1 to 3.2.4). Furthermore, we have found using coimmunoprecipitation assays that kinases and Mdm2 form an interaction with the Box-V motif of p53. In light of the identification of Chk1 and DAPK1 as p53 activators it was necessary to go on to determine the effects of loss of these kinases on p53 signaling utilizing siRNA and microarray technology.

5.2.1.1 Optimisation of siRNA technology

A preliminary transient transfection assay was set up to compare and contrast the siRNA transfection delivery reagents, Dharma*FECT*® (Dharmacon) with the nucleic acid transfection reagent, Lipofectamine™ 2000 (Invitrogen) on the depletion of endogenous kinases and the effect on p53 expression. Two tumour cell lines, A375 and A549 which express both p53 and the Calcium Calmodulin kinases (Chk1, Chk2 and DAPK1) were used to optimize the assay. A375 or A549 cells were transfected with 100nM siCONTROL or 100nM siRNA oligonucleotides to one of each of the three kinases (Chk1, Chk2 and DAPK1) using either Dharma*FECT*® Buffers 1 to 4 or Lipofectamine™ 2000 transfection delivery agents. 48 hours following transfection cells were lysed and cell lysates were immunoblotted for changes in protein levels of the three kinases as well as p53 (Figure 5.1 A; A375 and Figure 5.1 B; A549).

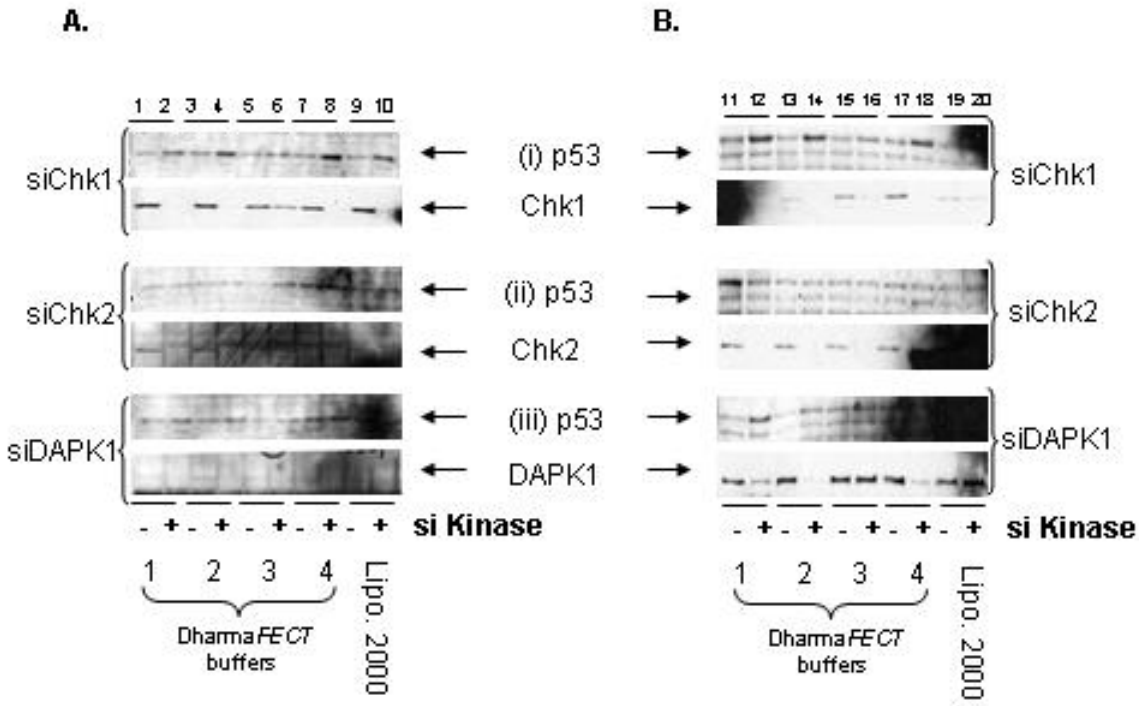

Figure 5.1 Comparison of DharmaFECT and Lipofectamine transfection delivery reagents. A375 (A) or A549 (B) cells were transfected with 100nM control or 100nM siRNA to Chk1, Chk2 or DAPK1 using 4µl DharmaFECT® Buffers 1 to 4 or Lipofectamine™ 2000 transfection delivery agents. 48 hours following transfection cells were lysed and cell lysates were immunoblotted for changes in Chk1, Chk2, DAPK1 and p53 protein levels (DO12).

Firstly, using A375 cells, the results demonstrated that the protein levels of Chk1 are significantly depleted using these siRNA oligonucleotides with either Dharma*FECT* or Lipofectamine 2000 (Figure 5.1 A; comparing odd numbered lanes (siControl) with even numbered lanes (siKinase); Chk1 blot). The only exception was when using Dharm*FECT* Buffer 3 with siRNA to Chk1 there is less of a reduction in protein levels (Figure 5.1 A; comparing lanes 5 and 6 and lanes 11 and 12; Chk1 blot). These data demonstrate that following depletion of Chk1 there is stabilization of p53 protein to varying levels dependent on transfection delivery buffer (Figure 5.1 A; siChk1;

comparing odd numbered lanes with even numbered lanes; p53 blot (i)). This is also demonstrated following depletion of DAPK1, although the stabilization is less marked (Figure 5.1 A; siDAPK1; comparing odd numbered lanes with even numbered lanes; p53 blot (iii)). Stabilisation of p53 following depletion of Chk2 is not evident is this assay (Figure 5.1 A; siChk2; comparing odd numbered lanes with even numbered lanes; p53 blot (ii)). This was a particularly interesting result and suggested that the depletion of kinases, Chk1 and DAPK1 led to the stabilization of p53 levels in these tumour cells.

A375 cells characteristically express low levels of endogenous Chk2 and DAPK1 which makes the detection of protein levels by western blot increasing difficult (Figure 5.1 A; Chk2 and DAPK1 blot). Therefore, A549 cells which characteristically express higher levels of endogenous DAPK1 as well as Chk1 and Chk2 were used to support the data demonstrated in A375 cells. The results demonstrated that the three kinases can be successfully depleted in A549 cells using the siRNA oligonucleotides with the Dharma*FECT* buffers 1, 2 and 4 and not Buffer 3 or Lipofectamine 2000 (Figure 5.1 B; comparing odd numbered lanes (siControl) with even numbered lanes (siKinase); Chk1, Chk2 or DAPK1 blots respectively). The results reflect A375 cell data in which there is stabilization of p53 following depletion of Chk1 and DAPK1 but not Chk2 (Figure 5.1 B; siChk1 and siDAPK1; comparing odd numbered lanes with even numbered lanes; p53 blot (i) and (iii) respectively).

Using the two cell lines to examine changes in protein levels of both kinases and p53 following treatment with siRNA oligonucleotides demonstrated that kinases could be successfully depleted and that depletion of Chk1 and DAPK1 led to the stabilization of p53. However, the aim of this preliminary assay was to determine the best transfection delivery buffer to use in future assays. Taking the two sets of data together it was decided the best transfection delivery buffer was Dharma*FECT* Buffer 4, based on levels of kinase depletion and p53 stabilisation.

We then went on to determine optimal incubation time for depletion of kinases. A375 cells were transfected with 100nM siControl or 100nM siRNA oligonucleotides to (i) Chk1, (ii) Chk2 and (iii) DAPK1 for either 24, 48 or 72 hours. Cells were lysed and lysates were immunoblotted for changes in protein levels of Chk1, Chk2 or DAPK1 and p53.

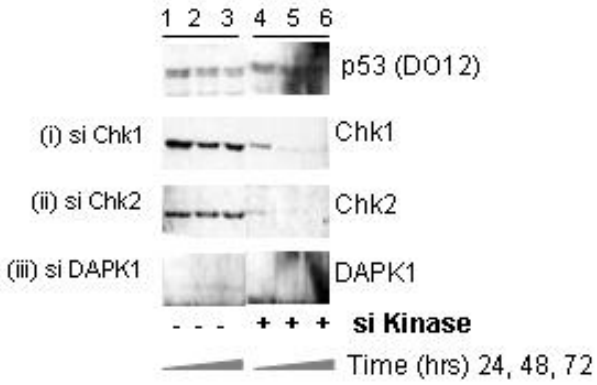

Figure 5.2 Optimisation of siRNA to determine the optimal siRNA incubation time.
A375 cells were transfected with 100nM siControl or 100nM siRNA oligonucleotides to (i) Chk1, (ii) Chk2 and (iii) DAPK1 for either 24, 48 or 72 hours. Cells were lysed and lysates were immunoblotted for changes in protein levels of the Chk1, Chk2 or DAPK1 and p53.

The results demonstrate that 24 hours following transfection of siRNA oligonucleotides there is approximately 50% depletion of kinases (Figure 5.2; comparing lanes 1 and 4; Chk1, Chk2 and DAPK1 blots). However, by 48 hours there is maximal depletion of protein levels of each of the kinases (Figure 5.2; comparing lanes 2 and 5; Chk1, Chk2 and DAPK1 blots). P53 is stabilized after Chk1 depletion (Figure 5.2; comparing lanes

1, 2 and 3 with lanes 4, 5 and 6; p53 blot). Based on these results it was determined that the protein levels of the kinases were significantly depleted from the 48hours timepoint onwards.

5.2.1.2 P53 is stabilized following damage

There has been a significant volume of literature examining the role of Calcium Calmodulin kinases in modulation of p53 activity and many reports have suggested Chk2 as a putative stress activator of p53 (Hirao et al. 2000; Takai et al. 2002; Craig et al. 2003; Chen et al. 2005). However, the role of Chk2 as a p53 kinase has been questioned in several reports (Ahn et al. 2003; Craig et al. 2003; Jallepalli et al. 2003) and in this report we have identified Chk1 and DAPK1 as putative p53 activators in cycling cells (see section 3.2.4). In this chapter of this report we have demonstrated that p53 is stabilized following depletion of Chk1 or DAPK1 but not Chk2 (Figure 5.1). However, whether p53 is active or inactive in these assays is unknown. To determine the effect of damage such as X-ray and UV on p53 stabilisation following depletion of Chk1 or DAPK1, siRNA assays were performed in conjunction with IR or UV treatment in A375 cells.

A375 cells were transfected with 100nM siControl or 100nM siRNA to Chk1 or DAPK1 for 48 hours. Cells were then treated with either X-ray (5Gy) or UV ($25J/m^2$) and incubated for 4 or 6 hours, respectively before harvesting. Firstly examining X-ray data, the results demonstrated that p53 is stabilized following depletion of Chk1 or DAPK1 (Figure 5.3 A; siChk1; comparing lanes 1 and 3; p53 blot and B; siDAPK1; comparing lanes 5 and 7; p53 blot) and that p53 is further stabilized following X-ray damage treatment (Figure 5.3 A; siChk1; comparing lane 4 with lane 2; p53 blot and B; siDAPK1; comparing lane 8 with lane 6; p53 blot).

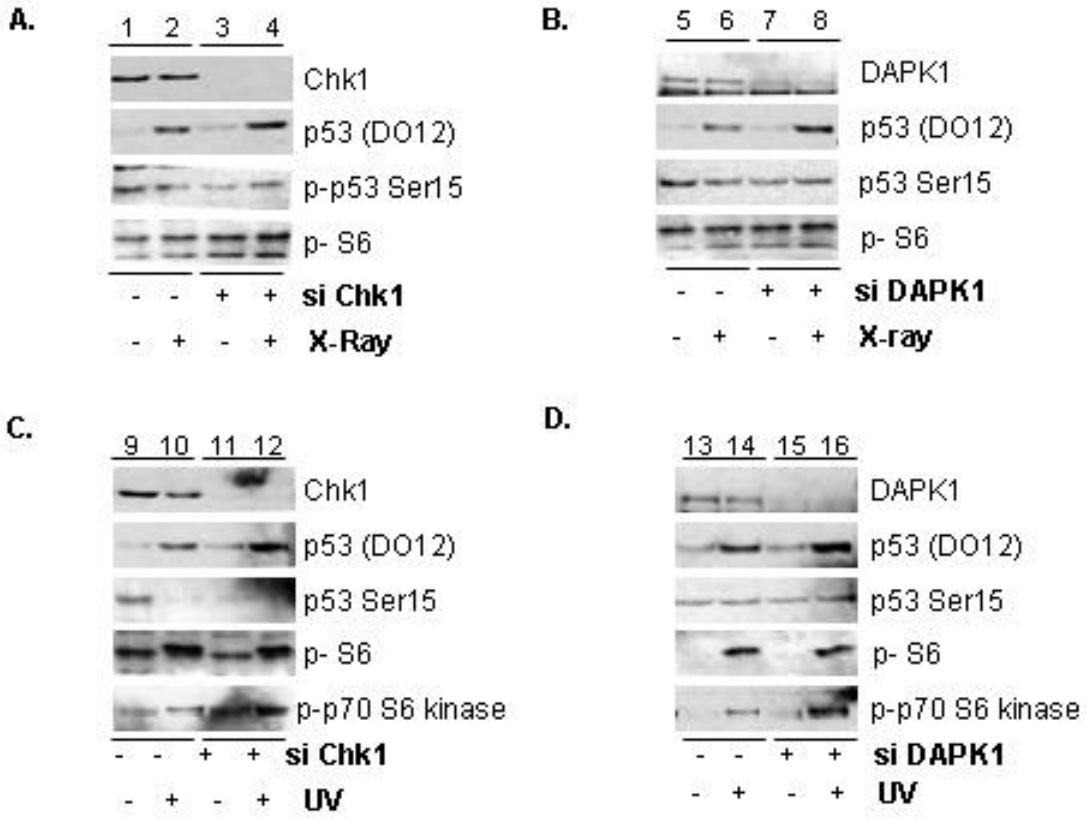

Figure 5.3 Comparison of effect damage treatments following kinase depletion on p53 stabilisation in A375 cells.

A and B. Cells were transfected with 100nM siControl or 100nM siRNA to Chk1 (A) or DAPK1 (B) for 48 hours. Cells were then treated with X-ray (5Gy) and incubated for 4 hours before harvesting. Cells were lysed and lysates were immunoblotted for changes in protein levels of p53, Chk1 or DAPK1, phospho-p53 Ser 15 and phosho S6. C and D. Cells were transfected with 100nM siControl or 100nM siRNA to Chk1 (C) or DAPK1 (D) for 48 hours. Cells were then treated with UV (25J/m2) and incubated for 6 hours before harvesting. Cells were lysed and lysates were immunoblotted for changes in protein levels of p53, Chk1 or DAPK1, phospho-p53 Ser 15, phosho-S6 ribosomal protein (Ser235/236, 2F9) and phospho-p70 S6 kinase (Thr389, 1A5).

The stabilization of p53 following damage is not dependent on Ser 15 phosphorylation in these cells (Figure 5.3 A; siChk1; comparing lanes 3 and 4; p-p53 Ser 15 blot and B; siDAPK1; comparing lanes 7 and 8; p-p53 Ser 15 blot). UV damage also stabilized p53 and depletion of kinases further stabilized p53 (Figure 5.3 C; siChk1 comparing lanes 11 and 12; p53 blot and D; siDAPK1 comparing lanes 15 and 16; p53 blot). Similar to X-ray this UV damage induced stabilization of p53 is not dependent on Ser 15 phosphorylation of p53 (Figure 5.3 C; siChk1 comparing lanes 11 and 12; p-p53 Ser 15 blot and D; siDAPK1 comparing lanes 15 and 16; p-p53 Ser 15 blot) but may be dependent on phosphorylation at other sites on p53.

Recently it has been demonstrated that DAPK1 can positively regulate mTOR (mammalian target of rapamycin) by forming an interaction with tuberous sclerosis (TSC)1/TSC2 complex in cells. This interaction neutralises TSC1/2 mediated suppression of the mTOR translation pathway leading to stimulation of mTOR as determined by changes in activity of the translational regulator, p70 S6 kinases (C. Stevens et al, in press). The kinases which are responsible for phosphorylation of ribosomal protein S6 (rpS6), S6K1 and S6K2, are direct targets of mTOR which activates these kinases through phosphorylation at specific S/T residues. Phosphorylation of T389 correlates most closely with S6K activity *in vivo* (Proud 2007). Moreover a recent report has suggested a crosstalk between p53 and mTOR signaling pathways leading to the coordinate regulation of cell growth, proliferation and death (Feng et al. 2005). Here we show here that following depletion of Chk1 or DAPK1 there is no change in S6 kinase phosphorylation (Figure 5.3 A; Chk1; comparing lanes 1 and 3; p-S6 blot and B; DAPK1; comparing lanes 5 and 7; p-S6 blot) and X-ray damage does not induce phosphorylation of S6 kinase (Figure 5.3 A; Chk1; comparing lanes 3 and 4; p-S6 blot and B; DAPK1; comparing lanes 7 and 8; p-S6 blot). Following UV damage there is increased S6 kinase phosphorylation (Figure 5.3 C; siChk1 comparing lanes 9 and 10; p-S6 blot and D; si DAPK1; comparing lanes 13 and 14; p-S6 blot) but this phosphorylation is not further increased following depletion of kinases (Figure 5.3

C; siChk1 comparing lanes 10 and 12; p-S6 blot and D; si DAPK1; comparing lanes 14 and 16; p-S6 blot). Interestingly, following UV damage there is also increased phosphorylation of the translational regulator p70 S6 kinase (Figure 5.3 C; siChk1 comparing lanes 9 and 10; p-p70 S6 kinase blot and D; siDAPK1; comparing lanes 13 and 14; p-p70 S6 kinase blot) and this p70 S6 kinase activity is increased further following depletion of kinases (Figure 5.3 C; siChk1 comparing lanes 9 and 10 with lanes 11 and 12; p-p70 S6 kinase blot and D; si DAPK1; comparing lanes 13 and 14 with lanes 15 and 16; p-p70 S6 kinase blot). Therefore although p53 stabilisation following depletion of kinases is not dependent on Ser 15 phosphorylation is these cells, there could be a role for the translational regulators, S6K1 and S6K2. As described, activated DAPK1 neutralises TSC mediated suppression of mTOR translation pathway (C. Stevens, in press). Thus following depletion of DAPK1 we would expect a decrease mTOR activity. However we have shown here that the depletion of DAPK1 leads to the increased activity of p70 S6 kinase as well as increased stabilization of p53 which may therefore suggest a crosstalk between p53 and mTOR signaling pathways.

5.2.1.3 Comparison of lysis buffers

To further investigate the mechanism of p53 stabilisation by kinase downregulation, assays were performed to compare levels of p53 stabilisation following lysis of cells using two lysis buffers, urea and NP-40. In all previous assays cells were lysed with the denaturing urea lysis buffer which is used to ensure the preservation of phospho-epitopes. NP-40 is a detergent lysis buffer which contains phosphatase inhibitors which preserve the phospho-epitopes. Firstly, to determine the effect of lysis buffer on both undamaged and damaged A375 cells, cells were treated with 25J/m^2 UV irradiation and harvested 6 hours following treatment. Cells were lysed with either urea or NP-40 lysis buffer and lysates were immunoblotted for changes in protein levels of Chk1, Chk2, DAPK1, p53, IRF1, S6 ribosomal protein or p70 S6 kinase.

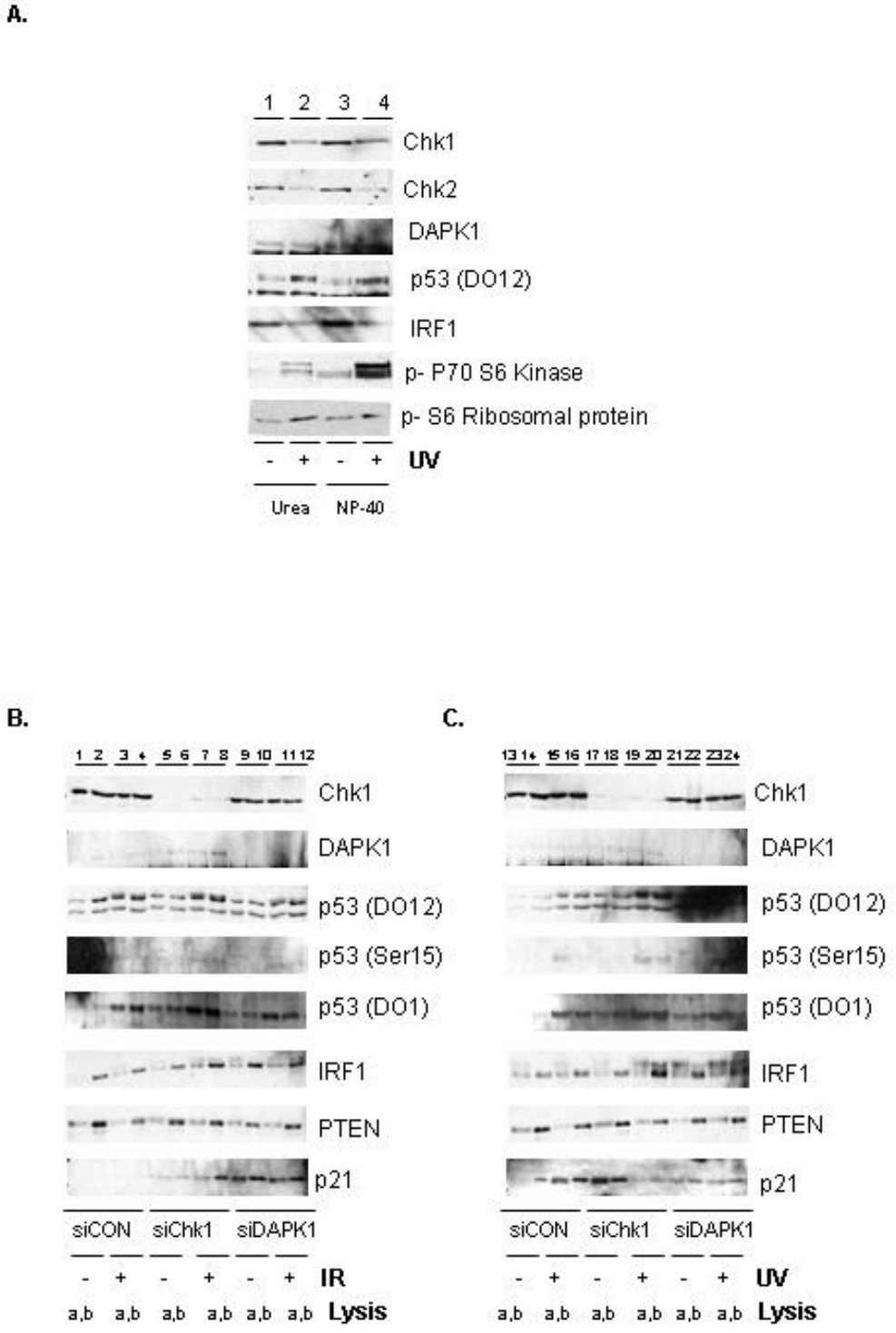

Figure 5.4 Effect of lysis buffer on p53 stabilisation.

(Figure 5.4) A. A375 cells were either undamaged or treated with 25J/m2 UV irradiation and cells were harvested 6 hours following treatment. Cells were lysed with either urea or NP-40 lysis buffer and lysates were immunoblotted for changes in protein levels of Chk1, Chk2, DAPK1, p53, IRF1 or the translational regulators S6 ribosomal protein and p70 S6 kinase. B and C. A375 cells were transfected with either 100nm siControl or 100nM siRNA to Chk1 or DAPK1 for 48hours. Following incubation with siRNA cells were either undamaged or treated with 5Gy X-ray irradiation (B) or 25J/m2 UV (C), incubated then harvested 4 or 6 hours later, respectively. Cells were then lysed with either Urea (a) or NP-40 (b) lysis buffer and cell lysates were immunoblotted for protein levels of Chk1, DAPK1, p53, IRF-1, PTEN and $p21^{WAF1}$.

In support of previous data (Figure 5.3), following UV damage Chk1 and Chk2 protein levels are reduced suggesting that these kinases are not stabilized following UV damage and this is not dependent on lysis buffer (Figure 5.4 A; comparing lanes 1 and 2; urea lysis and lanes 3 and 4; NP40 lysis; Chk1 and Chk2 blots). The protein levels of DAPK1 are unchanged following UV damage (Figure 5.4 A; comparing lanes 1 and 2; urea lysis and lanes 3 and 4; NP40 lysis; DAPK1 blot). P53 protein levels increase following damage suggesting the protein is stabilized although this stabilization of p53 is not dependent on lysis buffer (Figure 5.4 A; comparing lanes 1 and 2; urea lysis and lanes 3 and 4; NP40 lysis; p53 blot). IRF-1 (interferon regulatory factor -1), a transcriptional activator of genes involved in interferon response, is decreased following UV damage (Figure 5.4 A; comparing lanes 1 and 2; urea lysis and lanes 3 and 4; NP40 lysis; IRF1 blot). IRF-1 has been shown to modulate the expression of the cell cycle control gene, $p21^{WAF1}$, by synergising with p53 resulting in the recruitment of p300 to and subsequent acetylation of promoter bound p53 which in turn leads to increased p53-dependent $p21^{WAF1}$ promoter activity (Dornan et al. 2004). We are able to demonstrate following UV damage that the activity of the translational regulators p70 S6 kinase and S6 kinase are increased (Figure 5.4 A; comparing lanes 1 and 2; urea lysis and lanes 3 and 4; NP40 lysis; p-p70 S6 kinase and S6 kinase blots).

To compare and contrast the effect of the two lysis buffers on p53 stabilisation following kinase depletion and subsequent damage treatments, A375 cells were transfected with

either 100nM siControl or 100nM siRNA to Chk1 or DAPK1 for 48hours. The results demonstrate that following either IR (Figure 5.4 B; lanes 1 to 12) or UV (Figure 5.4 C; lanes 13 to 24) damage, p53 is stabilized as demonstrated by the p53 DO12 blots (Figure 5.4 B; IR; comparing lanes 1 and 2 with lanes 3 and 4 or UV; comparing lanes 13 and 14 with lanes 15 and 16; DO12 blot). However, p53 is not stabilized further upon Chk1 depletion and damage (Figure 5.4 B; IR; comparing lanes 7 and 8 with lanes 3 and 4; or Figure 5.4 C; UV; comparing lanes 19 and 20 with lanes 15 and 16; DO12 blot). This is also the case for DAPK1 depletion and IR damage (Figure 5.4 B; IR; lanes 11 and 12 with lanes 3 and 4) although the results are less clear for UV damage. The results also demonstrate that changing lysis buffer has no effect on p53 stabilisation (Figure 5.4 B; IR or UV; comparing odd numbered lanes with even numbered lanes; DO12 blot). Interesting the phospho-p53 Ser 15 levels increase slightly following UV (Figure 5.4 C; UV; comparing lanes 15 and 16 with lanes 13 and 14; p-p53 Ser 15 blot) and this seems to increase further following kinase depletion (Figure 5.4 C; UV; siChk1 lanes 19 and 20 and siDAPK1 lanes 23 and 24; p-p53 Ser 15 blot). This damage induced phosphorylation is less obvious following IR damage and kinase depletion (Figure 5.4 B; IR; comparing lanes 3 and 4 with lanes 7 and 8; p-p53 Ser 15 blot).

Using the DO1 antibody, which is specific to the N-terminal Box-I domain we are able to demonstrate and confirm that p53 is stabilized following damage (Figure 5.4 B; IR; comparing lanes 1 and 2 with lanes 3 and 4 or UV; comparing lanes 13 and 14 with lanes 15 and 16; DO1 blot) but this stabilization is slightly increased following depletion of Chk1 (Figure 5.4 B; IR; lanes 7 and 8 or UV; lanes 19 and 20; DO1 blot) and to a lesser extent DAPK1 (Figure 5.4 B; IR; lanes 11 and 12 or UV; lanes 23 and 24; DO1 blot). The binding of the DO1 antibody to p53 is blocked by the phosphorylation of p53 at Ser 20 (Craig et al. 1999) and these data shown here therefore suggest that there is no phosphorylation of Ser 20 following depletion of these kinases and damage.

We are also able to demonstrate that there is stabilization of IRF-1 following depletion of Chk1 and damage (Figure 5.4 B; IR; comparing lanes 7 and 8 with lanes 5 and 6 or C; UV; lanes 19 and 20 with lanes 17 and 18; IRF-1 blot) or depletion of DAPK1 and UV damage (Figure 5.4 C; UV; comparing lanes 23 and 24 with lanes 21 and 22; IRF-1 blot). Furthermore the stabilization of IRF-1 appears to be increased on lysis of cells using NP-40 lysis buffer (Figure 5.4 B; IR or UV; comparing odd numbered lanes with even numbered lanes; IRF-1 blot) suggesting that stabilization of IRF-1 may be lysis buffer dependent. The stabilization of IRF-1 may correlate with the increased expression of p21. p53 and IRF-1 have been shown to converge to regulate $p21^{WAF1}$ gene expression (Dornan et al. 2004). Following IR and Chk1 depletion there is increased p21 expression (Figure 5.4 B; IR; comparing lanes 7 and 8 with lanes 5 and 6; p21 blot) but for UV damage the data is unconvincing (Figure 5.4 C; UV; p21).

The tumour suppressor PTEN (phosphatase and tensin homologue deleted on chromosome 10) activates p53 in tumours which leads to the induction of senescence (Li and Ross 2007). We show here that PTEN is not activated following damage (Figure 5.4 B; IR; comparing lanes 3 and 4 with lanes 1 and 2 or C; UV; comparing lanes 15 and 15 with lanes 13 and 14; PTEN blot) or depletion of kinases (Figure 5.4 B and C; comparing siCON with siChk1 or siDAPK1; PTEN blot) and therefore is not involved in the stabilization of p53 is this pathway. However, PTEN, like IRF-1 is affected by the lysis buffer suggesting that the expression of this protein is dependent on the type of denaturing buffer.

Overall, we are able to demonstrate that p53 is stabilized following kinase depletion, it is further stabilized following damage such as X-ray or UV and that this stabilization is not dependent on lysis buffer used. There may be a role for IRF-1 which may coordinate with p53 to control cell cycle progression. The activity translational regulator S6 may suggest a crosstalk between p53 and mTOR signaling pathways leading to the coordinate regulation of cell growth, proliferation and death (Feng et al. 2005).

5.2.2 A cell viability assay demonstrates that depletion of kinases and subsequent damage does not result in any additional cell death

We have shown that depletion of kinases results in stabilization of p53 and that damage leads to increased stabilization of p53. To investigate the consequence of this stabilization of p53 a cell viability assay was performed. This would allow the evaluation of levels of cell proliferation and therefore allow us to determine whether depletion of kinases and subsequent damage insult was causing cell death resulting from activation of p53 pathway. The standard colourimetric assay, MTT assay, was used to measure changes in cell number and therefore determine the potential cytotoxic effects of kinase depletion and damage. A375 cells were untransfected (cells only), mock transfected (mock) or transfected with 100nM siControl or 100nM siRNA to Chk1, Chk2 and DAPK1 for 48 hours. Cells were then treated with either X-ray (5Gy) or UV (25J/m^2) and incubated for 4 or 6 hours, respectively before addition of MTT solution for 4 hours. Following incubation, DMSO was added to dissolve formazan crystals and absorbance was read at 570nm by spectrophotometry against a DMSO control.

The results are shown in the two bar graphs (Figure 5.5), the first examining the effect of kinase depletion and IR damage on cell viability (Figure 5.5 A) and the second examining the effect of kinase depletion and UV damage on cell viability (Figure 5.5 B). The results show that transfection is resulting in no reduction in cell viability (Figure 5.5; A or B; comparing mock and cells only controls) and that depletion of kinases has little or no effect on cell viability in undamaged cells (Figure 5.5; A or B; comparing siCON with siChk1, siChk1 or siDAPK1; blue bar; without IR/UV).

A.

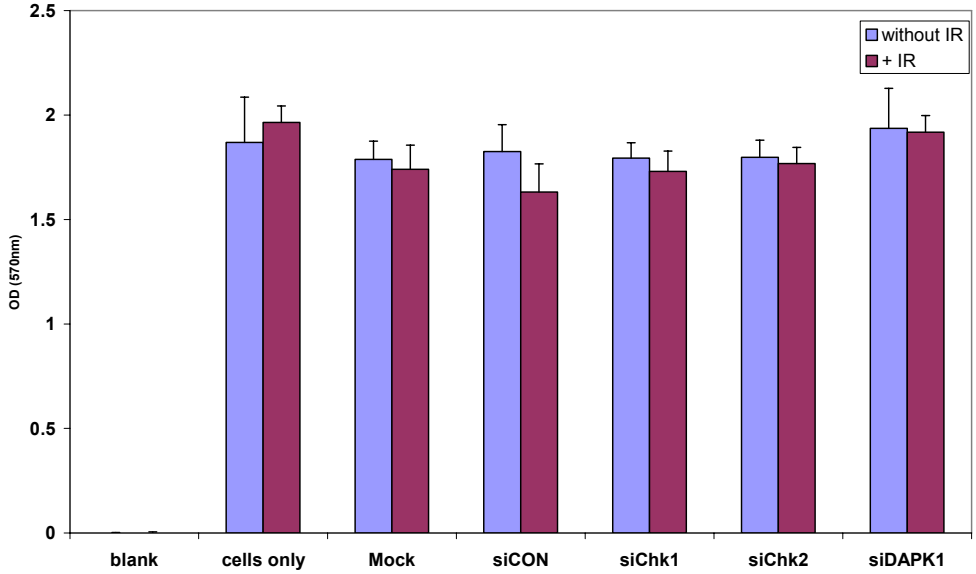

B.

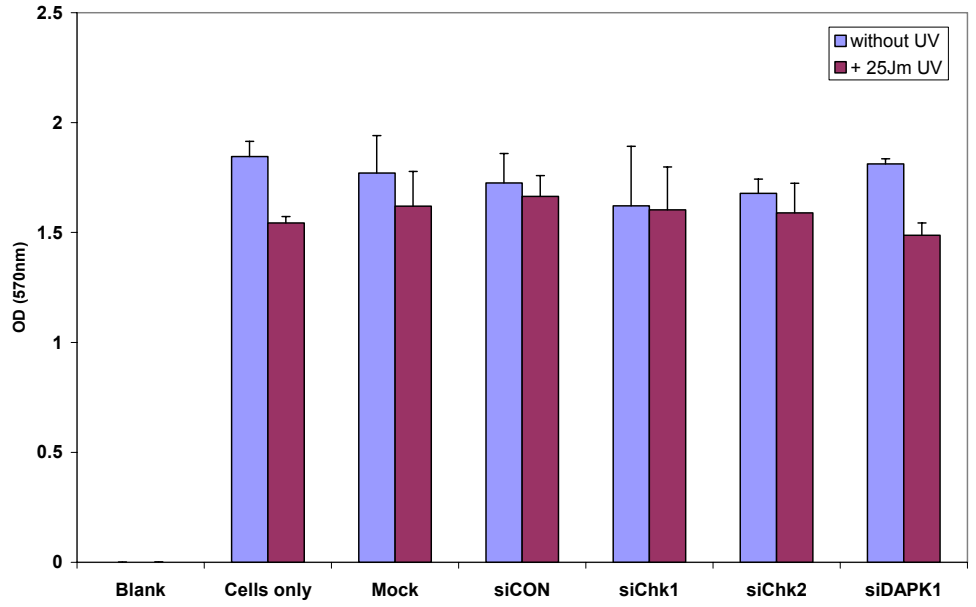

Figure 5.5 An MTT assay demonstrates that depletion of kinases and damage has no effect on cell viability.

A375 cells were transfected with 100nM siControl or 100nM siRNA to Chk1, Chk2 or DAPK1 for 48 hours. Cells were then treated with either 5Gy X-ray (A) or 25J/m^2 UV (B) and incubated for

4 or 6 hours, respectively before addition of MTT solution for 4 hours. Following incubation, DMSO was added to dissolve formazan crystals and absorbance was read at 570nm. Data was normalised using DMSO as a blank and is represented as optical density at 570nm. Each data point is the average of four replicates with error bars showing standard deviation.

The results also demonstrate that IR (5Gy X-ray) damage does not result in a reduction in cell viability in kinase depleted cells (Figure 5.5 A and B; comparing without IR, blue bars with plus IR, red bars; siChk1, siChk1 and siDAPK1) and that following UV damage in kinase depleted cells there is little effect on cell viability (Figure 5.5 C; comparing without UV, blue bars with plus UV, red bars; siChk1 and siChk1). We can conclude in the main that neither kinase depletion nor damage is affecting the viability and therefore the proliferation potential of these cells. Therefore the stabilization of p53 in these cells following kinase depletion does not result in increased cell death in this assay and that there may be other factors involved.

5.2.3 A microarray study demonstrates that silencing of kinases leads to increased activation of p53 target genes

The previous assays have demonstrated that depletion of Chk1 and DAPK1 leads to stabilization of p53. It was therefore necessary to examine the effect of blocking these kinases on the activation of the p53 signaling pathway. Microarray analysis of Chk1 and DAPK1 depleted cells was performed to evaluate the changes in gene expression profiles of 113 genes involved in the human p53 signalling pathway using the Oligo GEArray® System (Superarray; Bioscience Co.).

5.2.3.1 Microarray analysis of Chk1 or DAPK1 depleted (undamaged) cells

Firstly, oligonucleotide microarrays were used to assess the global effect of loss of Chk1 and DAPK1 in undamaged conditions. A375 cells were transfected with 100nM siControl or 100nM siRNA to Chk1 or DAPK1 for 48 hours. Labelled cRNA from kinase depleted A375 cells was assessed for changes in gene expression profile of the genes involved in the p53 signalling pathway.

The results are demonstrated in Figure 5.6 which shows the raw images of each microarray and gives an overview of the effect of depletion of Chk1 or DAPK1 kinases on upregulation of p53 signalling genes. It is apparent that there is a basal level of genes upregulated as demonstrated by the siRNA non-targetting control (Figure 5.6 A; si Con). On depletion of Chk1 there was significant upregulation of genes, indeed compared to control there are almost 4 fold more genes upregulated (Figure 5.6 B; siChk1; 70 genes upregulated) and DAPK1 depletion up to 3 fold more genes upregulated (Figure 5.6 C; siDAPK1; 56 genes upregulated). The details of each of the genes upregulated are also represented in Table 5.1 where genes have been categorized based on their function. It can be concluded from this table and the raw images that depletion of either Chk1 or DAPK1 leads to an upregulation of p53 signalling genes, some of which are upregulated at a basal level (siCon) and are present following depletion of kinases and others are

upregulated only following depletion of either Chk1 or DAPK1. This activation of the p53 signalling pathway is likely due to transfection stress.

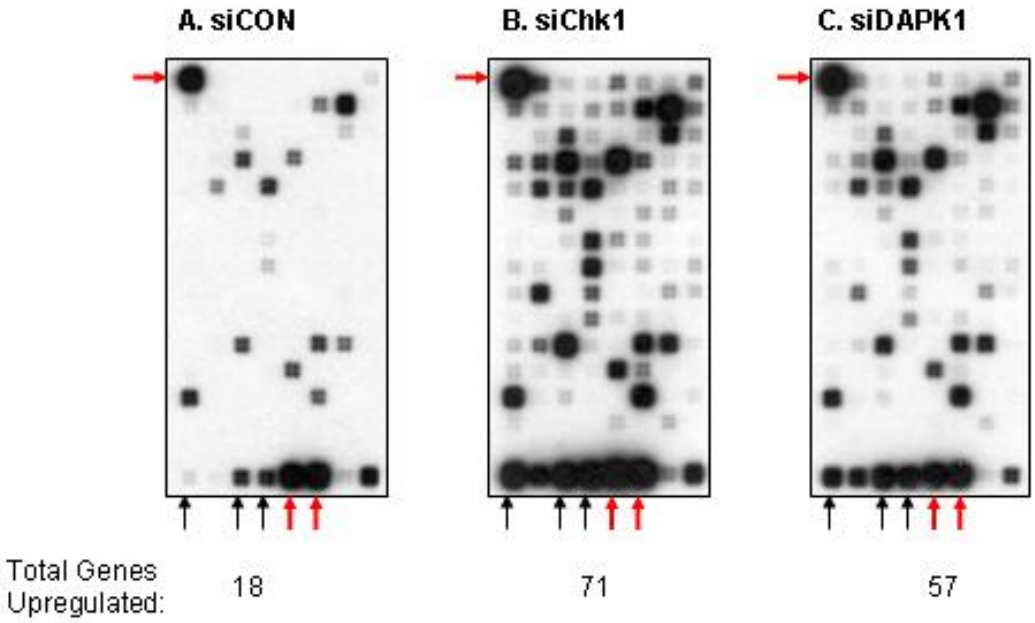

Figure 5.6 A microarray analysis of effect of kinase depletion on p53 signalling pathway. A375 cells were transfected with 100nM siControl (A) or 100nM siRNA to Chk1 (B) or DAPK1 (C) for 48 hours. Total RNA was isolated from the cells, which was then reverse transcribed into cRNA, labeled with biotin and hybridized to the Oligo GEArray® DNA Microarray, Human p53 Signaling Pathway (Superarray; Bioscience Co.). The control, house-keeping genes are indicated by arrows and the specific house-keeping genes chosen for normalization of data are indicated by the broader red arrows.

Table 5.1 Genes expressed in A375 cells following depletion of kinases

	Gene Symbol	siCON	siChk1	siDAPK1
Apoptosis	*AATF1*		X	X
	APAF1		X	X
	BAG1		X	X
	BAK1	X	X	X
	BAX		X	X
	BCL2		X	X
	BCL2A1		X	X
	BID		X	X
	BIRC5	X	X	X
	BNIP3	X	X	X
	CASP2	X	X	X
	CASP9		X	X
	CRADD		X	X
	FADD		X	X
	GADD45A		X	X
	HDAC1	X	X	X
	MCL1	X	X	X
	NFKB1		X	X
	PCBP4		X	X
	RELA	X	X	X
	TNFRSF10B	X	X	X
	TRAF4		X	X
Cell Cycle	*ATM*		X	X
	ATR		X	X
	BRCA1		X	X
	CCNG2		X	X
	CCNH	X	X	X
	CDC2		X	X
	CDC25A		X	X
	CDK4	X	X	X
	CDC7		X	X
	CDKN1A	X	X	X
	CDKN2A		X	X
	CHK1		X	
	CHK2		X	
	E2F1		X	X
	E2F3		X	
	FRAP1		X	X
	GTSE1		X	
	HK2		X	X

	KRAS		X	
	MYC		X	X
	PPM1D		X	
	PRKCA		X	
	PTEN		X	X
	PYCARD		X	
	RB1	X	X	X
	SMARCB1	X	X	X
	STAT1		X	X
	TP53		X	
	TP53BP2		X	
	TSC1		X	X
Cell Growth, Proliferentiation and Differentiation	*BAI1*		X	X
	BAP1	X	X	X
	BTG2		X	X
	CDC25C		X	X
	WDR39		X	X
	KLF6	X	X	X
	CYR61	X	X	X
	IFNB1		X	X
	JUN		X	X
	MDM4		X	X
	MYOD1		X	X
	NDRG1		X	X
	PHB		X	
	PMP22		X	X
	PPP1R13B		X	
	PTTG1	X	X	X
	SCGB3A1		X	X
	SFN	X	X	X
	SHC1		X	
Control (Housekeeping genes)	*RPS27A*	X	X	X
	GAPDH		X	X
	B2M		X	X
	HSPCB	X	X	X
	ACTB	X	X	X

Table 1.1 Genes expressed in A375 cells following depletion of Chk1 or DAPK1. Genes are categorized based on their function. 'X' represents a gene upregulated by visual assessment and a highlighted gene symbols represent genes which are upregulated (by visual assessment) under all three conditions.

.

A more detailed analysis was performed using the GEArray Expression Analysis Suite (Superarray) software which allows the user to upload the array image, extract data from the uploaded image and perform analysis of the data using the various analysis tools which are available. Images are aligned to a grid either manually or automatically and from this a readout of signal intensity is generated and corrections are made for background of individually defined areas and an average of signal intensities of the 4 four replicates on each array. Normalisation of signal intensities between samples can be performed using the control spots, which include the house-keeping genes, present on each array. House keeping genes are normally expressed consistently under most conditions and are therefore a useful normalization method to control for discrepancies between levels signal intensities due to variation in hybridisation of mRNA to the membrane. As shown in Figure 5.6, I have selected *RPS27A* and *ACTB* to use for normalization as these housekeeping genes are represented consistently across each of the samples. Each value shown in Table 5.2 represents the level of mRNA expression following background correction and normalization and is represented as relative units.

Table 5.2 demonstrates the ratio of gene intensities between the test (e.g. siChk1) and the reference (e.g. siCON) samples, which are represented as fold changes. The significance of each individual fold change is defined by applying a cut-off value where a fold change of 1.5 between reference and test sample is deemed a significant repression or induction. Upregulation of genes are shown as positive values and repression of genes as negative inverse values.

Table 5.2 Ratio of gene expression between samples (represented as fold changes)

		si Chk1 Vs siCON	siDAPK1 Vs siCON	siDAPK1 vs siChk1
Apoptosis	*AATF1*	●	■	N/A
	APAF1	●	■	N/A
	BAG1	●	■	N/A
	BAK1	10.25	4.24	-2.43
	BAX	9.17	13.99	▲1.53
	BCL2	●	■	N/A
	BCL2A1	37.35	9.3	-4.0
	BID	29.29	20.02	-1.47
	BIRC5	2.02	1.33	-1.515
	BNIP3	-3.22 *	-7.04 *	-2.17
	CASP2	5.87	3.93	-1.49
	CASP9	●	■	N/A
	CRADD	●	■	N/A
	FADD	88.81	29.83	-2.94
	GADD45A	●	■	N/A
	HDAC1	14.73	11.00	-1.33
	MCL1	4.41	3.23	-1.36
	NFKB1	769.09	163.91	-4.76
	PCBP4	●	■	N/A
	RELA	1.51	1.47	-1.03
	TNFRSF10B	●	■	N/A
	TRAF4	●	■	N/A
Cell Cycle	*ATM*	●	■	N/A
	ATR	119.04	43.93	-2.702
	BRCA1	38.69	35.5	-1.08
	CCNG2	●	■	N/A
	CCNH	3.74 *	3.18 *	-1.176
	CDC2	14.87	14.15	-1.053
	CDC25A	36.41	9.96	-5.263
	CDK4	-1.35	-1.48	-1.09
	CDC7	●	■	N/A
	CDKN1A	-2.38 *	-1.26 *	▲1.9
	CDKN2A	61.95 *	27.03	-2.273
	CHK1	●	■	N/A
	CHK2	●	■	N/A
	E2F1	110.68	29.08	-3.846
	E2F3	●	■	N/A
	FRAP1	●	■	N/A
	GTSE1	●	■	N/A
	HK2	427.72	■	N/A
	KRAS	●	■	N/A

	MYC	●	■	N/A
	PPM1D	●	■	N/A
	PRKCA	●	■	N/A
	PTEN	36.38	■	N/A
	RB1	1.23	1.11	-1.11
	SMARCB1	1.00 *	1.19	▲1.19
	STAT1	●	■	N/A
	TP53	●	■	N/A
	TP53BP2	●	■	N/A
	TSC1	●	■	N/A
Cell Growth, Proliferentiation and Differentiation	*BAI1*	●	■	N/A
	BAP1	5.25	2.03	-2.56
	BTG2	●	■	-2.12
	CDC25C	36.41	14.26	-2.564
	WDR39	●	■	N/A
	KLF6	2.57	1.8	-1.428
	CYR61	-1.05	-1.16	-1.099
	IFNB1	●	■	N/A
	JUN	●	■	N/A
	MDM4	●	■	N/A
	MYOD1	●	■	N/A
	NDRG1	54.2	32.93	-1.64
	PHB	●	■	N/A
	PMP22	52.39	30.6	-1.724
	PPP1R13B	●	■	N/A
	PTTG1	-1.55*	1.19	1.85
	SCGB3A1	●	■	N/A
	SFN	1.54	1.12	-1.37
	SHC1	●	■	N/A
Control	*RPS27A*	1.61	-2.29	-3.7
	HSPCB	-11.72	-2.14	3.0
	ACTB	-2.74	1.48	2.99

Table 1.2 Ratio of gene expression between samples (represented as fold changes). Values highlighted in grey represent genes which are upregulated in siControl; ● represents a gene which is considered absent in siChk1; ■ represents a gene which is considered absent in siDAPK1; ▲ represents a gene which is upregulated more in siDAPK1 than siChk1; and * represents a spot which is considered as bleeding, therefore value for that gene may be underestimated.

In general the fold induction of gene expression is highest following Chk1 depletion (Table 5.2, siChk1 Vs siCON). Following depletion of DAPK1 there is a similar pattern of genes induced as when Chk1 is depleted but in general the fold induction is lower than that following Chk1 depletion (Table 5.2, siDAPK1 Vs siCON). We are able to demonstrate this clearly by directly comparing the levels of fold change following DAPK1 depletion versus Chk1 depletion where the downregulation is represented as a negative inverse value (Table 5.2; siDAPK1 vs siChk1). This has highlighted two genes which are upregulated to a greater extent (more than 1.5 fold) following DAPK1 depletion, the apoptotic gene, *BAX* (*BCL2*-associated X protein) and the cell cycle gene, *CDKN1A* (cyclin-dependent kinase inhibitor 1A; p21). However the latter is likely to be an anomaly due to 'bleeding' whereby the spot signal intensity is considered to be greater than the average value of all spots, therefore underestimating the actual signal intensity (annotated in Table 5.2 by an asterix *).

Many genes are considered to be absent in all groups (control and following kinase depletion) and cannot therefore be included in calculations for fold change. These have been represented in Table 5.2 as considered absent following Chk1 depletion (● siChk1 vs siCON) or considered absent following DAPK1 depletion (■ siDAPK1 vs siCON). Some genes are upregulated at a basal level (as demonstrated in Table 5.1; siCON) and following depletion of kinases, these genes are upregulated further (Table 5.2; fold induction comparisons; siChk1 Vs siCON and siDAPK1 Vs siCON; highlighted in grey). These 14 genes have also been represented in Figure 5.7 which demonstrates the basal transcript levels of each gene as well as following depletion of kinases (represented as relative units; RU). This has highlighted several genes which show significant upregulation following depletion of one or both kinases (as calculated by fold induction; see Table 5.2). Genes include *BIRC5*, *KLF6* and *SFN*. The other genes do not demonstrate a upregulation as their fold induction is less than or equal to 1.5 (see fold induction in Table 5.2).

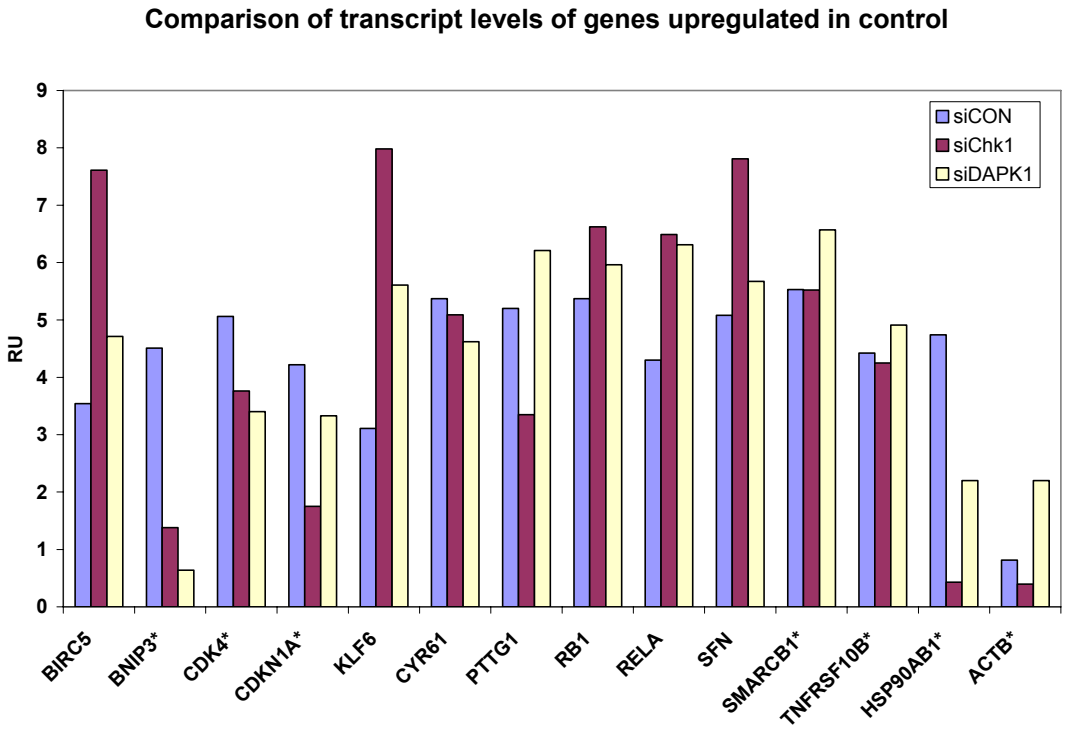

Figure 5.7 Comparison of basal and kinase stimulated transcript levels of genes.
The 14 genes which are considered to be upregulated in the control (siCON) group are shown in this graph which demonstrates the basal and kinase stimulated transcript level of each gene (represented as relative units, RU). Several genes are considered to have 'bleeding' of signal intensity in one or more groups and this has resulted in under represented transcript levels (highlighted with an asterix *).

Another 22 genes are considered to be absent in control (siCON) but present following depletion of kinases (siChk1 or siDAPK1). These upregulated genes have been represented in Table 5.2 as values of fold induction. Although considered to be absent in the control group (siCON) they do have values greater than or equal to 0.01, therefore an increase in the value following depletion of kinase has been included in this table to represent the fold change.

It is apparent that the depletion of kinases results in significant upregulation but no downregulation of p53 signalling pathway genes. To demonstrate the genes with the highest fold induction and compare the fold induction following either Chk1 or DAPK1 depletion, a figure was generated showing the upper 50% of gene fold induction (Figure 5.8 A). This demonstrates that genes such as *NFKB1*, *HK2*, *ATR* and *E2F1* are upregulated to a higher extent following depletion of kinases and are therefore likely to play a significant role following depletion of kinases. However as most of them are upregulated to a greater extent in siChk1 group they are more likely to play a role following in Chk1 depletion. At the other end of the scale the lower 50% of gene fold induction is represented in a similar figure (Figure 5.8 B) and demonstrate the genes which are upregulated to a lesser extent following depletion of kinases. At this end of the scale the comparative fold change between siChk1 and siDAPK1 is very similar suggesting that this low level induction of genes is occurring to a similar extent following depletion of either Chk1 or DAPK1.

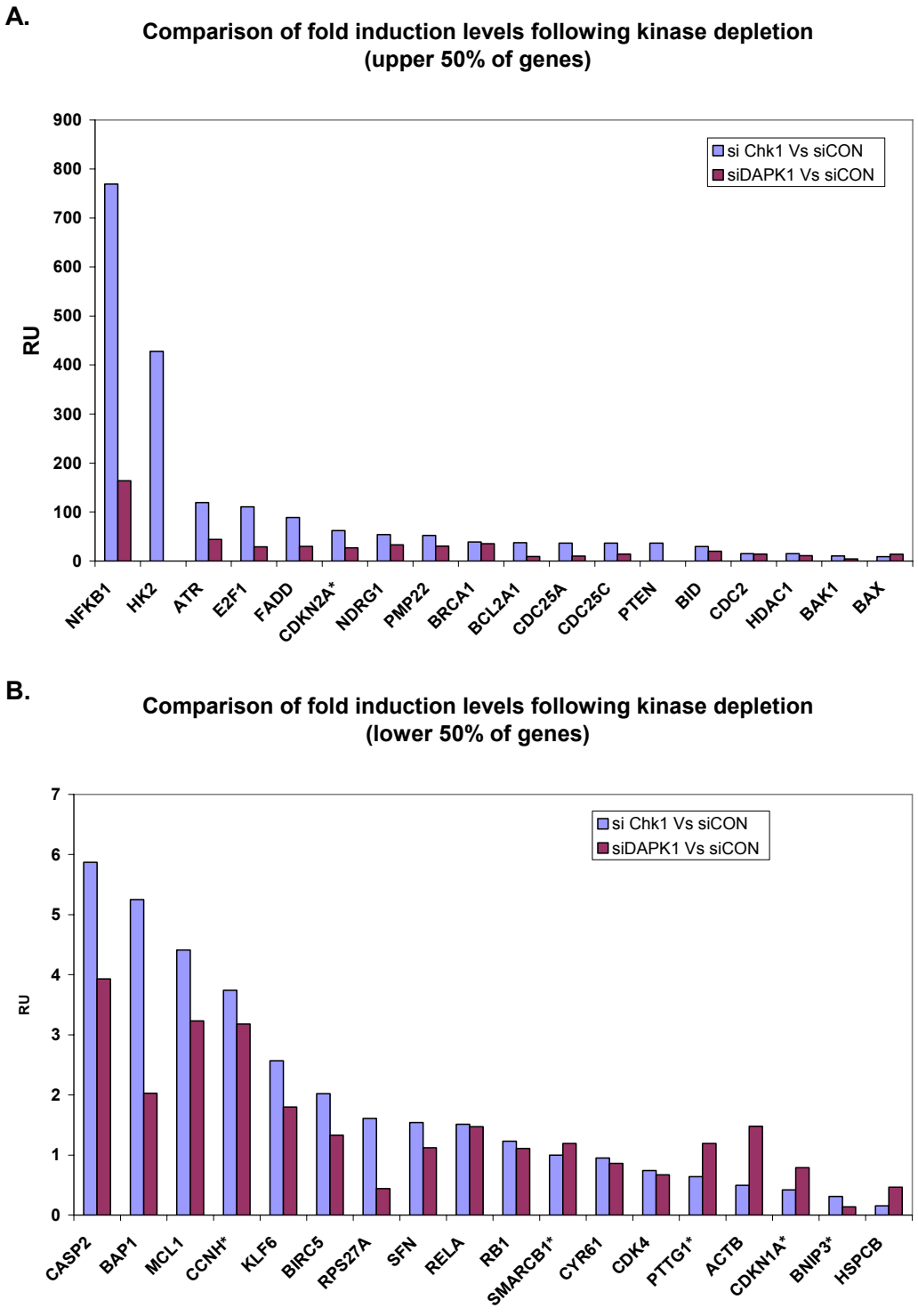

Figure 5.8 Comparison of fold induction levels following kinase depletion.
Graphs showing the upper 50% (A) and lower 50% of genes upregulated (B).

To provide an overall view of the effect of depletion of kinases on activation of p53 target genes, the Clustergram analysis tool (GEArray Expression Analysis Suite) was used to create a cluster diagram to demonstrate the microarray data. Clustergram analysis demonstrates the hierarchical clustering of genes, where genes that are more similar in terms of their expression patterns (i.e. not clustered in terms of gene function) are joined at lower heights in the dendogram and those that are less similar are joined at higher heights.

The data presented in the clustergram is based upon the colour coding of genes based on results from the entire dataset, where colours are assigned based on values in the whole dataset (Figure 5.9). This allows the expression levels of all genes to be compared across the whole dataset. Although this method is less sensitive in that genes expressed at lower levels are under represented, it allows the comparison of upregulation of the genes within a sample as well as the comparison of upregulation of the genes across the three sample groups. The clustergram therefore provides an overall picture of the effect of depletion of kinases on upregulation of p53 target genes. It demonstrates that the genes that are upregulated in siCON are also upregulated in the other samples. It also demonstrates that siChk1 has upregulated genes which are unique to this group and that genes that are upregulated in siDAPK1 are also mostly upregulated in siChk1.

Overall we have been able to demonstrate using microarray technology that depletion of either Chk1 or DAPK1 leads to significant upregulation of p53 target genes. Thus providing an insight into the pathways involved in upregulation of p53 target genes in undamaged conditions.

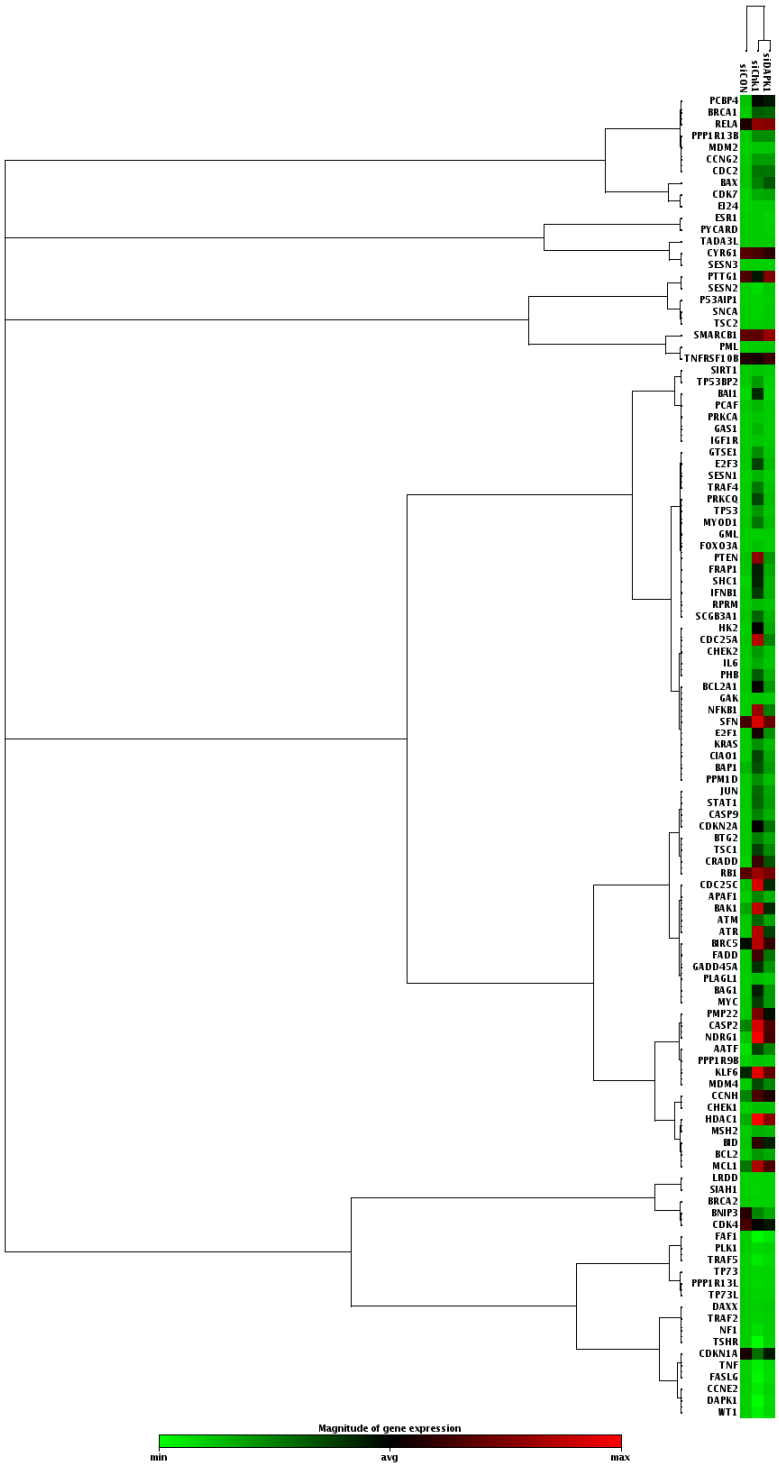
siCON
siCHK1
siDAPK1
PCBP4
BRCA1
RELA
PPP1R13B
MDM2
CCNG2
CDC2
BAX
CDK7
EI24
ESR1
PYCARD
TADA3L
CYR61
SESN3
PTTG1
SESN2
P53AIP1
SNCA
TSC2
SMARCB1
PML
TNFRSF10B
SIRT1
TP53BP2
BAI1
PCAF
PRKCA
GAS1
IGF1R
GTSE1
E2F3
SESN1
TRAF4
PRKCQ
TP53
MYOD1
GML
FOXO3A
PTEN
FRAP1
SHC1
IFNB1
RPRM
SCGB3A1
HK2
CDC25A
CHEK2
IL6
PHB
BCL2A1
GAK
NFKBI
SFN
E2F1
KRAS
CIAO1
BAP1
PPM1D
JUN
STAT1
CASP9
CDKN2A
BTG2
TSC1
CRADD
RB1
CDC25C
APAF1
BAK1
ATM
ATR
BIRC5
FADD
GADD45A
PLAGL1
BAG1
MYC
PMP22
CASP2
NDRG1
AATF
PPP1R9B
KLF6
MDM4
CCNH
CHEK1
HDAC1
MSH2
BID
BCL2
MCL1
LRDD
SIAH1
BRCA2
BNIP3
CDK4
FAF1
PLK1
TRAF5
TP73
PPP1R13L
TP73L
DAXX
TRAF2
NF1
TSHR
CDKN1A
TNF
FASLG
CCNE2
DAPK1
WT1
Magnitude of gene expression
min
avg
max

Figure 5.9 Gene expression profile following depletion of kinases demonstrates that Chk1 and DAPK1 depletion leads to upregulation of p53 target gene expression.

Clustergram analysis is used to demonstrate the correlation of genes, where genes that are more similar are joined at lower heights in the dendogram and those that are less similar are joined at higher heights. Genes are colour coded based on the entire dataset thereby allowing the comparison of genes within a sample as well as across the three groups. The colour represents the magnitude of gene expression whereby green represents low gene expression and red represents highest gene expression.

5.2.3.2 Microarray analysis of kinase depleted, X-Ray treated cells

In light of the data which demonstrated that p53 was stabilized on depletion of kinases and was further stabilized following X-ray damage (see section 5.2.1.2) and that the depletion of kinases led to upregulation of p53 target genes (see section 5.2.3.1), we set out to examine the effect of X-ray treatment on activation of p53 target genes using the same microarray technology. A375 cells were transfected with 100nM siControl or 100nM siRNA to Chk1 or DAPK1 for 48 hours. Cells were then treated with 5Gy X-ray and incubated for a further 4 hours. Labelled cRNA from kinase depleted, X-ray treated cells was then assessed for changes in gene expression profile to examine early responses of the genes involved in the p53 signalling pathway.

The results are demonstrated in Figure 5.10 which shows the raw images of each microarray and gives an overview of the effect of depletion of Chk1 or DAPK1 kinases and IR damage on upregulation of p53 signalling genes. The numbers of genes upregulated by visual assessment have been indicated in Figure 5.10 in brackets. It is apparent that there is a basal level of p53 target genes upregulated as demonstrated by the siRNA non-targeting control and following IR damage there is a significant upregulation of p53 target genes in the siControl (Figure 5.10 A; siCON; 18 genes upregulated vs B; siCON + IR; 75 genes upregulated). On depletion of either Chk1 or DAPK1 there is a significant upregulation of genes (Figure 5.10 B; siChk1; 84 genes and C; siDAPK1; 67 genes) confirming previous data as demonstrated in section 5.2.3.1. However following IR damage there is no upregulation of genes in DAPK1 depleted cells (Figure 5.10 E; siDAPK1; 67 genes versus F; siDAPK1 + IR; 67 genes) and in the case of Chk1 depleted cells there may even be some down regulation of genes following IR damage (Figure 5.10 C; siChk1; 84 genes versus F; siChk1 + IR; 75 genes). The details of each of the genes upregulated are also represented in Table 5.3 where genes have been categorized based on their function. This table highlighted some additional genes which are upregulated on kinase depletion and which were not seen previously (see Table 5.1). Overall the examination of the effect of kinase depletion and damage on

the regulation of p53 target genes by visual assessment has suggested that although there is upregulation of p53 target genes following IR damage in control, this damage insult does not result in further upregulation of p53 target genes following depletion of kinases. The results therefore suggest that the depletion of either kinase may play more of a role in the activation of p53 in undamaged conditions.

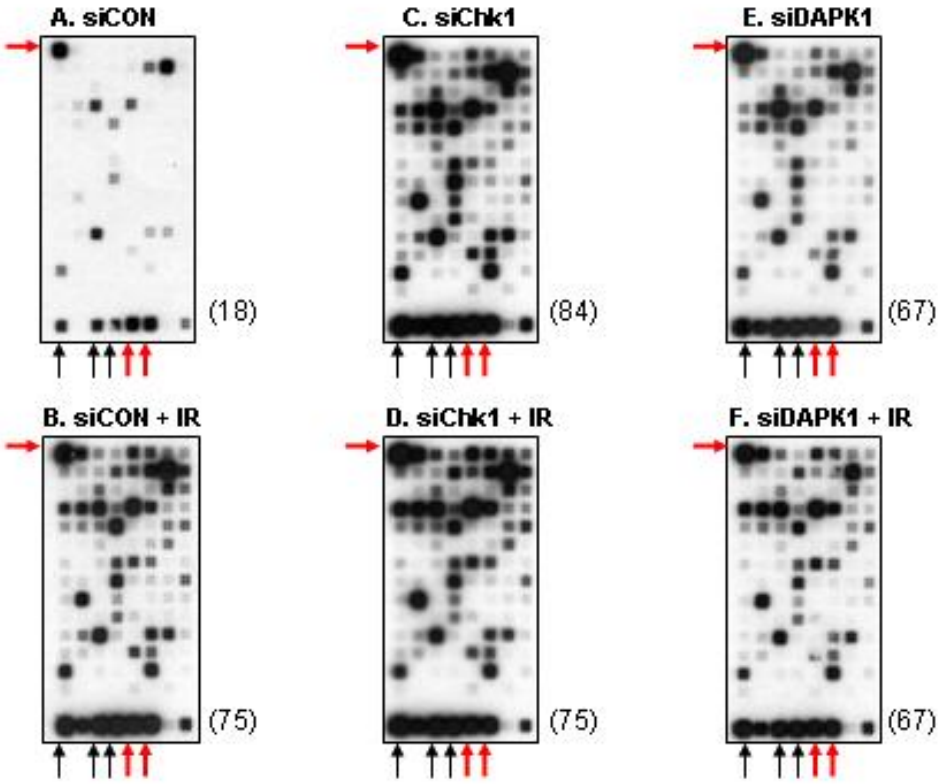

Figure 5.10 A microarray analysis of effect of X-ray damage on kinase depleted cells.
A375 cells were transfected with 100nM siControl or 100nM siRNA to Chk1 or DAPK1 for 48 hours. Cells were then treated with 5Gy X-ray and incubated for a further 4 hours. Total RNA was isolated from the cells, which was then reverse transcribed into cRNA, labeled with biotin and hybridized to the Oligo GEArray® DNA Microarray, Human p53 Signaling Pathway (OHS-027; Superarray; Bioscience Co.). The control, house-keeping genes are indicated by arrows and the specific house-keeping genes chosen for normalization of data are indicated by the broader red arrows. The numbers of genes upregulated by visual assessment is indicated in brackets.

Table 5.3 Genes expression in A375 cells following kinase depletion and IR damage

	Gene Symbol	siCON	siCON + IR	siChk1	siChk1 + IR	siDAPK	siDAPK + IR
Apoptosis	*AATF1*		X	X	X	X	X
	APAF1		X	X	X	X	X
	BAG1		X	X	X	X	X
	BAK1		X	X	X	X	X
	BAX		X	X	X	X	X
	BCL2		X	X	X	X	X
	BCL2A1		X	X	X	X	X
	BID		X	X	X	X	X
	BIRC5	X	X	X	X	X	X
	BNIP3	X	X	X	X	X	X
	CASP2	X	X	X	X	X	X
	CASP9		X	X	X	X	X
	CRADD		X	X	X	X	X
	*DAPK 1**			X			
	*DAXX**			X			
	FADD		X	X	X	X	X
	GADD45A		X	X	X	X	X
	HDAC1	X	X	X	X	X	X
	MCL1	X	X	X	X	X	X
	NFKB1		X	X	X	X	X
	PCBP4		X	X	X	X	X
	RELA	X	X	X	X	X	X
	TNFRSF10B	X	X	X	X	X	X
	TRAF4		X	X	X	X	X
Cell Cycle	*ATM*		X	X	X	X	X
	ATR		X	X	X	X	X
	BRCA1		X	X	X	X	X
	CCNG2		X	X	X	X	X
	CCNH		X	X	X	X	X
	CDC2		X	X	X	X	X
	CDC25A		X	X	X	X	X
	CDK4	X	X	X	X	X	X
	CDC7		X	X	X	X	X
	CDKN1A	X	X	X	X	X	X
	CDKN2A		X	X	X	X	X
	CHK1		X	X	X	X	X
	CHK2		X	X	X	X	X
	E2F1		X	X	X	X	X
	E2F3		X	X	X	X	X
	FRAP1		X	X	X	X	X

	GAS		X	X	X		X
	GTSE1		X	X	X	X	X
	HK2		X	X	X	X	X
	KRAS		X	X	X	X	
	*MSH2**		X	X	X		X
	MYC		X	X	X	X	X
	*PCAF **		X	X	X		X
	PPM1D		X	X	X		X
	*PPP1R9B **			X			
	PRKCA		X	X			
	PTEN	X	X	X	X	X	X
	PYCARD		X	X	X		
	RB1	X	X	X	X	X	X
	*RPRM **		X	X	X		X
	*SESN1 **		X	X	X	X	X
	*SESN2 **			X			
	SMARCB1	X	X	X	X	X	X
	STAT1			X		X	
	TP53			X	X	X	X
	TP53BP2		X	X	X	X	X
	TSC1		X	X	X	X	X
Cell Growth, Proliferentiation and Differentiation	*BAI1*		X	X	X	X	X
	BAP1		X	X	X	X	X
	BTG2		X	X	X	X	X
	CDC25C	X	X	X	X	X	X
	WDR39		X	X	X	X	X
	KLF6	X	X	X	X	X	X
	CYR61	X	X	X	X	X	X
	IFNB1		X	X	X	X	X
	*IL6 **		X	X			
	JUN		X	X	X	X	
	*MDM2 **		X	X	X		
	MDM4		X	X	X	X	X
	MYOD1		X	X	X	X	X
	NDRG1	X	X	X	X	X	X
	PHB		X	X	X	X	X
	*PML **		X	X	X		
	PMP22		X	X	X	X	X
	PPP1R13B			X			
	*PRKCQ **			X	X		
	PTTG1	X	X	X	X	X	X
	SCGB3A1		X	X	X	X	X
	SFN	X	X	X	X	X	X

	SHC1		X	X	X	X	X
Control (Housekeeping genes)	*RPS27A*	X	X	X	X	X	X
	GAPDH	X	X	X	X	X	X
	B2M		X	X	X	X	X
	HSPCB	X	X	X	X	X	X
	ACTB	X	X	X	X	X	X

Table 1.3 Gene expression in A375 cells following kinase depletion and IR damage. Genes are categorized based on their function. 'X' represents a gene upregulated by visual assessment and a highlighted gene symbols represent genes which are upregulated (by visual assessment) under all six conditions.

A more detailed analysis was performed using the GEArray Expression Analysis Suite (Superarray) software as described in section 5.2.3.1. As shown in Figure 5.10, I have selected *RPS27A* and *ACTB* to use for normalization as these housekeeping genes are represented consistently across each of the samples. Each value shown in Table 5.4 represents the level of mRNA expression following background correction and normalization and is represented as relative units. Table 5.4 demonstrates the ratio of gene intensities between the test (e.g. siCON + IR) and the reference (e.g. siCON basal) samples, which are represented as fold changes. The significance of each individual fold change is defined by applying a cut-off value where a fold change of 1.5 between reference and test sample is deemed a significant repression or induction. Genes which are considered absent in both the test and reference samples are indicated (Table 5.4; ● symbol), and genes which are considered absent across all three sample comparison groups, have been removed. Upregulation of genes are shown as positive values and repression of genes as negative inverse values.

We have already shown that the depletion of kinases leads to significant upregulation of p53 target genes (see 5.2.3.1). This microarray assay was used to demonstrate the effect of X-ray damage in kinase depleted cells on expression of p53 target genes. The results demonstrate that the highest upregulation of p53 target genes following damage occurs in the non-targeting siRNA control group (Table 5.4; siCON+IR vs siCON), suggesting that this type of damage in these cells causes significant upregulation of p53 target genes without kinase depletion. The most upregulated of these genes have been presented in Figure 5.11 which demonstrates the fold induction following damage of the upper 50% of genes upregulated. Some of the genes represented in this figure (Figure 5.11; e.g. *NFKB1*, *HK2*, *E2F1* and *PMP22*) have been previously shown to be significantly upregulated following depletion of Chk1 (see Figure 5.8 A) although the fold induction was lower in the latter case. Thus suggesting that IR damage in these cells induces the expression of similar genes to kinase depletion but the level of upregulation is higher following IR damage than kinase depletion.

Table 5.4 Ratio of gene expression between samples (represented as fold changes)

	Gene Symbol	siCON + IR Vs. siCON	siChk1 + IR Vs. siChk1	siDAPK1 + IR Vs. siDAPK1
Apoptosis	*AATF1*	94.32 *	-3.7 *	-1.02
	APAF1	5.95	1.02	3.19
	BAG1	86.06	-1.56 *	2.32
	BAK1	35.9	1.05	1.42
	BAX	77.15	-2.77	●
	BCL2	●	-1.72	●
	BCL2A1	171.21	-1.66	2.28
	BID	68.92	-2.08	-1.29
	BIRC5	4.2 *	-1.33 *	-1.64 *
	BNIP3	●	●	2.5 *
	CASP2	61.94	-2.43	-1.16
	CASP9	●	●	-2.38
	CRADD	463.14	-2.9	-1.22 *
	FADD	●	●	-2.17
	GADD45A	●	-1.72	1.41
	HDAC1	62.17	-2.5	1.09
	MCL1	9.86	-1.22	1.26
	NFKB1	975.08	-2.94	-1.49
	RELA	20.51	-1.96	1.17
	TNFRSF10B	55.98 *	-1.42 *	1.00
Cell Cycle	*ATM*	170.81	-1.2	1.37
	ATR	195.94	-2.94	1.32
	BRCA1	89.08 *	-1.58 *	2.02
	CCNG2	●	-3.7	●
	CCNH	162.45 *	-1.78 *	-1.09
	CDC2	116.70	-1.66	-1.7
	CDC25A	111.32	-4.16 *	1.4
	CDK4	2.99 *	-1.66 *	3.24 *
	CDC7	139.47	-2.12 *	1.07 *
	CDKN1A	1.32 *	-2.5 *	-2.7 *
	CDKN2A	118.97	-3.8 *	1.65 *
	CHK1	●	1.7	2.84
	CHK2	●	6.4	●
	E2F1	458.22	-1.66	1.32
	E2F3	196.78	-1.31	4.72
	HK2	497.80	-2.17	4.79
	MYC	305.47	-2.12	1.49
	PTEN	72.17	-0.18	●
	RB1	22.36	-2.32	-1.15
	SMARCB1	8.01	-2.22	1.09

Cell Growth, Proliferentiation and Differentiation	*BAI1*	739.75	2.12 *	●
	BAP1	154.90	-2.43 *	-1.85
	CDC25C	25.38	-5.26 *	-1.26 *
	WDR39	122.54	-3.44	-1.66
	KLF6	43.42	-3.44 *	-1.2
	CYR61	3.7 *	-1.96 *	1.63
	IFNB1	388.2	0.63	7.53
	NDRG1	30.08 *	-2.78 *	1.05 *
	PMP22	223.88	-3.125	-1.17
	PTTG1	2.82 *	-1.67 *	1.06
	SFN	55.87	-2.94	0.64
	SHC1	1322.18	-2.78	1.1
Control (Housekeeping genes)	*RPS27A*	1.75	-10 *	1.76 *
	HSPCB	-5.0 *	-2.86	1.345 *
	ACTB	-1.45 *	5.33	-1.08

Table 1.4 Ratio of gene expression between samples (represented as fold change). Gene symbols highlighted in grey represent genes which are upregulated at a basal level in siCONTROL; ● represents genes considered absent in both the reference and test samples; and * represents spots which are considered as bleeding, therefore value for that gene may be underestimated.

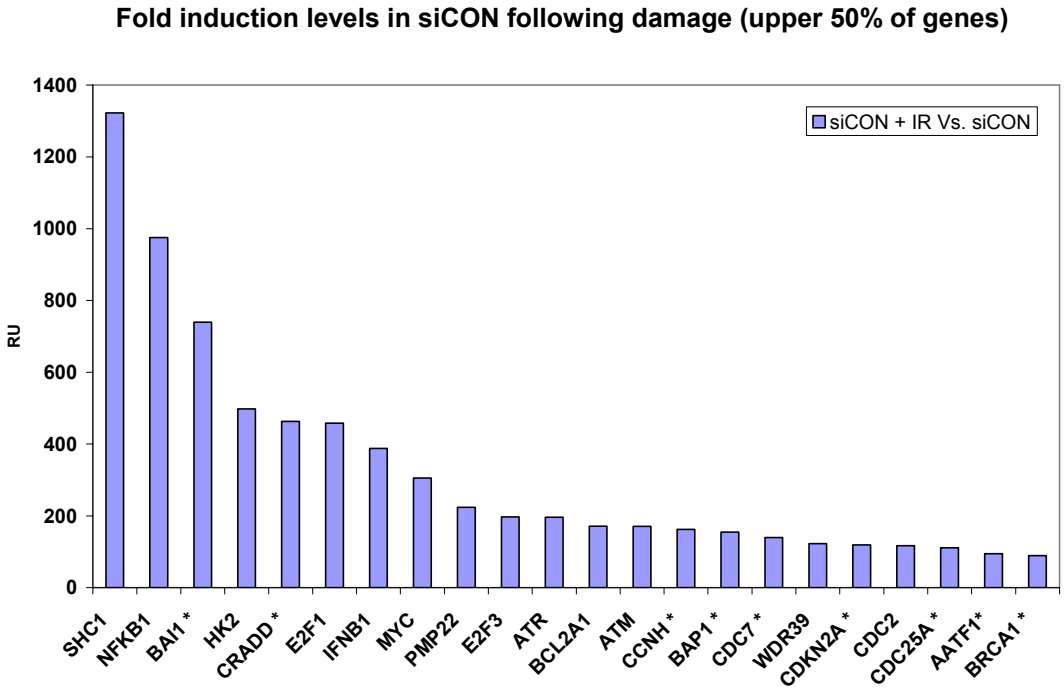

Figure 5.11 Genes upregulated following damage.

A graph representing the fold induction levels of the upper 50% of genes upregulated in non-targetting siRNA control treated cells following IR damage. An asterix (*) represents spots which are considered as bleeding, therefore value for that gene may be underestimated

Upon damage to Chk1 depleted cells, there is no significant fold change in upregulation of the majority of genes and as indicated by the negative values there is some downregulation of p53 target genes following the damage insult (Table 5.4; siChk1+IR vs siChk1). This is also true of DAPK1 depleted cells whereby for the majority of genes there is no significant fold change in upregulation of genes and many genes are found be downregulated upon damage (Table 5.4; siDAPK1+IR vs siDAPK1). In light of the fact that IR damage causes no further upregulation of p53 target genes in kinase depleted cells, analysis of fold induction between irradiated groups was not shown as there is no significant change in level of gene upregulation between groups (siControl + IR

compared to siChk1 + IR or siDAPK1 + IR). This result is also reflected in the clustergram (Figure 5.12) where these groups have been represented as most similar.

To provide an overall view of the effect of depletion of kinases on activation of p53 target genes, the Clustergram analysis tool (GEArray Expression Analysis Suite) was used to create a cluster diagram to demonstrate the microarray data as described previously (see section 5.2.3.1). The data presented in the clustergram is based upon the colour coding of genes based on results in each sample, where colours are assigned based on values of a certain sample (Figure 5.12). This allows the comparison of expression levels of all genes across all six profiles and thereby providing an overall picture of the effect of IR damage and/or kinase depletion on upregulation of p53 target genes. It demonstrates that there is a low basal level of genes upregulated in siCON treated cells and that following kinase depletion there is significant upregulation of p53 target genes. Following IR damage there is significant upregulation of genes in siCON treated cells, but kinase depleted cells are not significantly upregulated further following IR damage (Figure 5.12). As eluded to above, the way in which clustergram has grouped the samples is interesting. For instance, siCON +IR, siChk1 + IR and siDAPK1 + IR are represented as most similar; si Chk1 and siDAPK1 form a second group; and siCON is different. This would support the data whereby kinase (either Chk1 or DAPK1) depletion alone results in the most significant upregulation of genes.

Overall these data suggest that although there is upregulation of p53 target genes following IR damage in control, this damage insult on these cells following depletion of kinases does not result in further upregulation of p53 target genes. Therefore, suggesting that the depletion of either kinase may play a significant role in the activation of p53 but this damage in these cells does not lead to upregulation of any additional p53 target genes. It may be more appropriate in future studies to examine a different timepoint following IR damage to examine cell response over time.

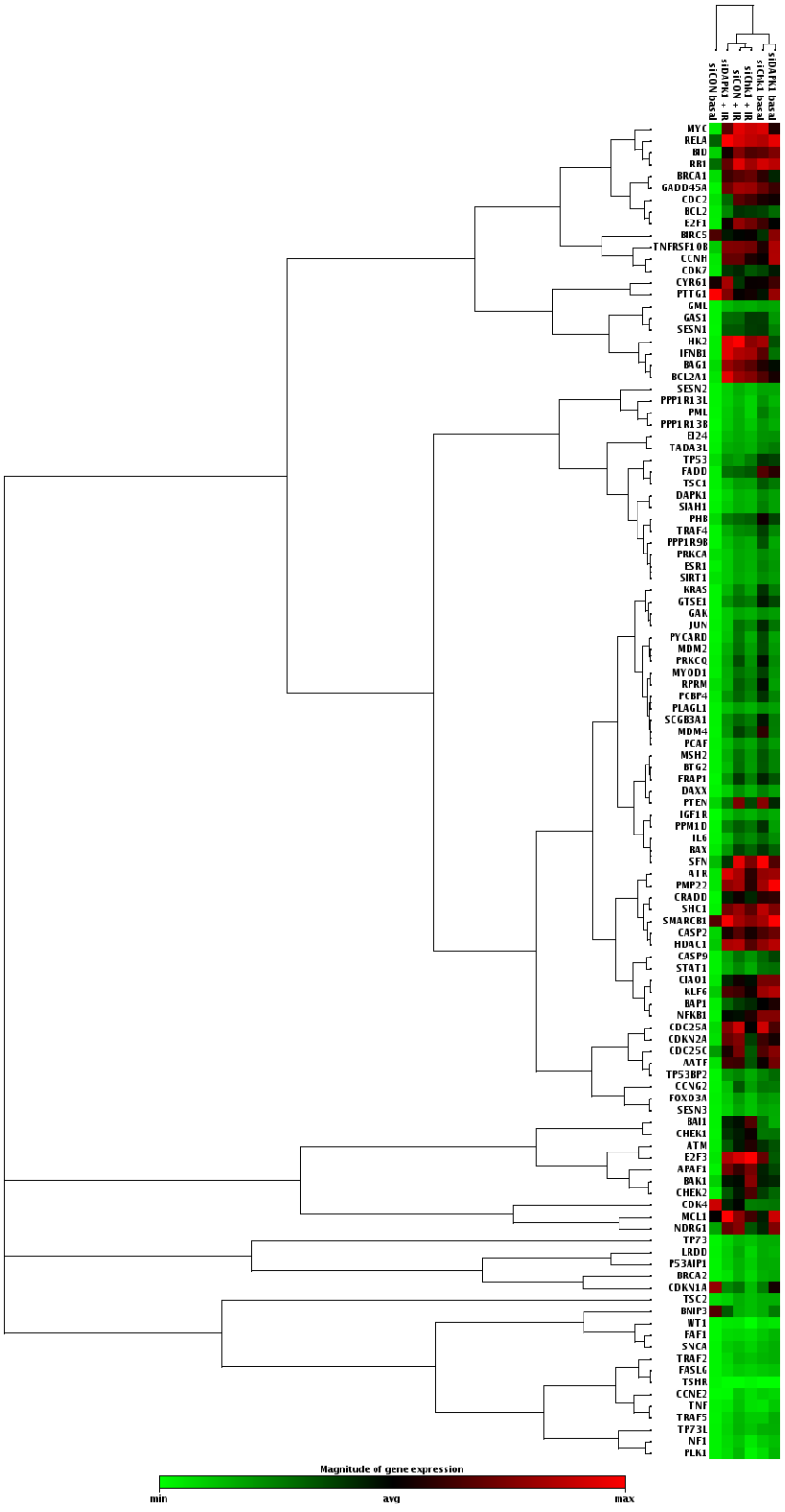
SIGN basal
SIGN TNF basal
SIGN + IR
SIGN TNF + IR
SIGN + IR
SIGN TNF + IR
SIGN basal
SIGN TNF basal
MYC
RELA
BID
RB1
BRCA1
GADD45A
CDC2
BCL2
E2F1
BRCS
TNFRSF10B
CCNH
CDK7
CYR61
PTTG1
GML
GAS1
SESN1
HK2
IFNB1
BAG1
BCL2A1
SESN2
PPP1R13L
PML
PPP1R13B
EI24
TADA3L
TP53
FADD
TSC1
DAPK1
SIAH1
PHB
TRAF4
PPP1R9B
PRKCA
ESR1
SIRT1
KRAS
GTSE1
GAK
JUN
PYCARD
MDM2
PRKCQ
MYOD1
RPRM
PCBP4
PLAGL1
SCGB3A1
MDM4
PCAF
MSH2
BTG2
FRAP1
DAXX
PTEN
IGF1R
PPM1D
IL6
BAX
SFN
ATR
PMP22
CRADD
SHC1
SMARCB1
CASP2
HDAC1
CASP9
STAT1
CIAO1
KLF6
BAP1
NFKB1
CDC25A
CDKN2A
CDC25C
AATF
TP53BP2
CCNG2
FOXO3A
SESN3
BAI1
CHEK1
ATM
E2F3
APAF1
BAK1
CHEK2
CDK4
MCL1
NDRG1
TP73
LRDD
PS3AIP1
BRCA2
CDKN1A
TSC2
BNIP3
WT1
FAF1
SNCA
TRAF2
FASLG
TSHR
CCNE2
TNF
TRAF5
TP73L
NF1
PLK1
Magnitude of gene expression
min
avg
max

Figure 5.12 Gene expression profile demonstrates that IR damage leads to upregulation of p53 target gene expression in control group only.

Clustergram analysis is used to demonstrate the correlation of genes, where genes that are more similar are joined at lower heights in the dendogram and those that are less similar are joined at higher heights. The colour coding of genes is based on results in each sample, where colours are assigned based on values of a certain sample allowing the comparison of expression levels of all genes across all six profiles. The colour represents the magnitude of gene expression whereby green represents low gene expression and red represents highest gene expression.

5.2.3.3 Microarray analysis following the combined depletion of p53 and DAPK1

In light of the data which demonstrated that kinase depletion resulted in significant upregulation of p53 target genes (see sections 5.2.3.1 and 5.2.3.2) further investigation was carried out to clarify the effect of combined depletion of DAPK1 and p53 and to elucidate the pathways which result in the activation of the p53 target genes.

Before evaluating the effect of the combined depletion of p53 and kinases on activation of p53 target genes using microarray technology western blotting was performed to confirm that RNAi was effective. A375 and A549 cells were transfected with 100nM siControl; or cotransfected with either a combination of 50nM sip53 and 50nM siRNA oligonucleotides to Chk1, Chk2 or DAPK1 to give combined total of 100nM siRNA oligonucleotides, for 48hrs. Protein levels were confirmed by immunoblotting for p53 and kinases in A375 and A549 cells.

The immunoblots confirm that siRNA oligonucleotides to p53 can deplete p53 protein levels in both A375 (Figure 5.13 B; lanes 1 to 4; p53 blot) and A549 (Figure 5.13 C; lanes 1 to 4; p53 blot) cell lines. Chk1, Chk2 and DAPK1 protein levels are also significantly depleted using the siRNA oligonucleotides in both cells (Figure 5.13 B and C; lanes 2, 5 and 6 Chk1 blot; lanes 3, 5 and 7 Chk2 blot and lanes 4, 6 and 7 DAPK1 blot respectively). In both cell lines the combined depletion of both Chk1 and DAPK1 results in the most significant stabilization of p53 (Figure 5.13 B and C; comparing lane 6 with lanes 5, 7 and 8; p53 blot). This reflects previous data in which Chk1 and DAPK1 are demonstrated to be the main p53 kinases in these cells (see section 3.2.2). In A375 cells there is evidence that the depletion of p53 alone causes a reduction in protein levels of Chk2 and DAPK1 (Figure 5.13 B; lane 1; Chk2 and DAPK1 blots) suggesting that the expression of these kinases may dependent on p53. This does not occur in A549 cells, suggesting that this may a cell specific event or is merely a transfection anomaly. The results do however confirm that combining siRNA to Chk1 and DAPK1 does result in stabilization of p53.

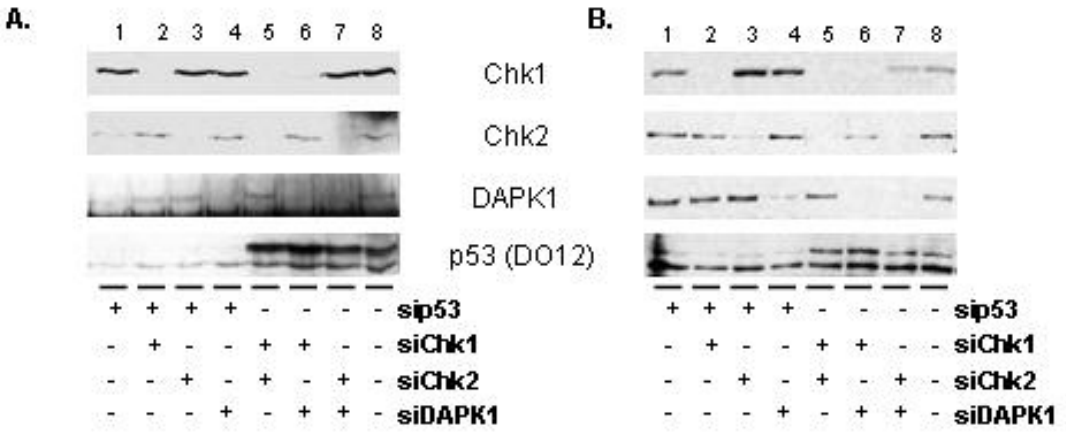

Figure 5.13 Immunoblots confirm depletion of protein levels following the comined depletion of p53 and kinases.

A and B. Evaluation of protein levels following the combined depletion of p53 and kinases. A375 (A) and A549 (B) cells were transfected with 100nM siControl; or cotransfected with either a combination of 50nM sip53 and 50nM siRNA oligonucleotides to Chk1, Chk2 or DAPK to give combined total of 100nM siRNA oligonucleotides; or a combination of 50nM siRNA oligonucleotides to Chk1, Chk2 or DAPK1 to give combined total of 100nM siRNA oligonucleotides (for 48hrs). Protein levels were confirmed by immunoblotting for p53 and kinases in both A375 and A549 cells.

Microarray analysis of A375 cells cotransfected with RNAi to DAPK1 and p53 was then performed. Labelled cRNA from kinase and p53 depleted cells was then assessed for changes in gene expression profile of p53 signalling pathway genes. The combined effect of depletion of DAPK1 and p53 are demonstrated in Figure 5.14 which shows the raw images of each microarray and gives an overview of the effect of the combined depletion on upregulation of p53 signalling genes.

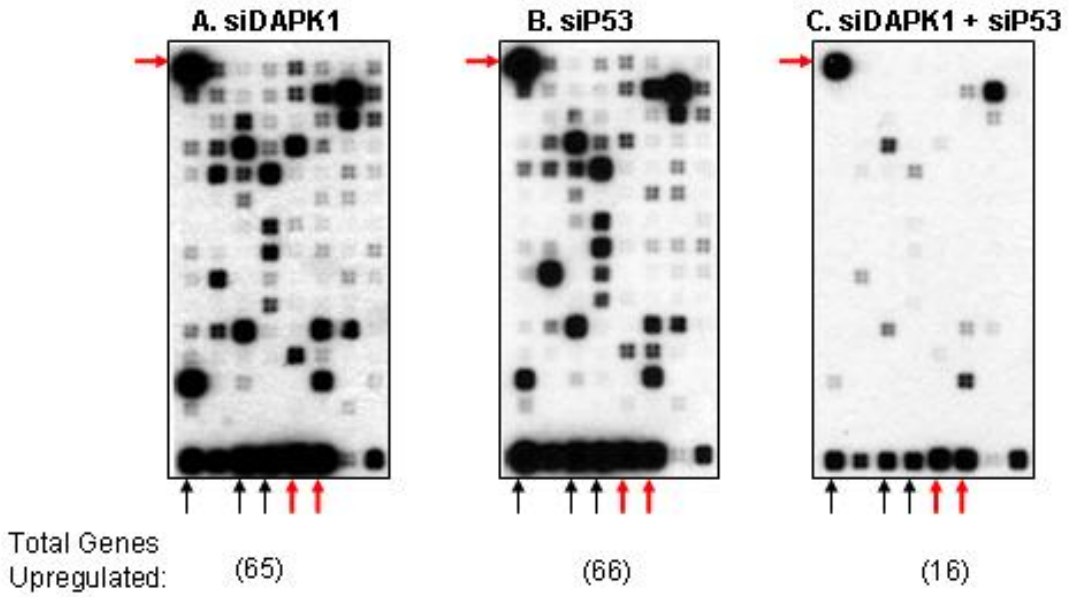

Figure 5.14 Microarray analysis of combined depletion of p53 and DAPK1 in A375 cells. A375 were transfected with 100nM siDAPK1 or cotransfected with a combination of 50nm sip53 + 50nM siCON or 50nM sip53 + 50nM siDAPK to give a combined total of 100nM siRNA oligonucleotides. Total RNA was isolated from the cells, which was then reverse transcribed into cRNA, labeled with biotin and hybridized to the Oligo GEArray® DNA Microarray, Human p53 Signaling Pathway (OHS-027; Superarray; Bioscience Co.). The control, house-keeping genes are indicated by arrows and the specific house-keeping genes chosen for normalization of data are indicated by the broader red arrows. The numbers of genes upregulated by visual assessment is indicated in brackets.

We have previously shown that non-targetting siRNA control transfected cells characteristically demonstrate low basal upregulation of p53 target genes and that depletion of DAPK1 leads significant upregulation of p53 target genes (see section 5.2.3.1). In this assay we have used siRNA to DAPK1 as a control in which to compare the effect of depletion of p53 and the combined depletion of p53 and DAPK1 on regulation of p53 target genes. The results demonstrated in Figure 5.14 show the total number of genes upregulated (shown in brackets), estimated by visual assessment. The number of upregulated genes following depletion of DAPK1 (Figure 5.14 A; 65 genes upregulated) confirms previous microarray data in which depletion of DAPK1 led to upregulation of 57 or 67 p53 target genes (Figure 5.6 C and Figure 5.10 E, respectively). Upon depletion of p53 there is a similar number of target genes upregulated, as seen following DAPK1 depletion (Figure 5.14 B; 66 genes upregulated). However, following the combined depletion of both DAPK1 and p53 there is a dramatic reduction in the number of genes upregulated (Figure 5.14 C; 16 genes upregulated). This low level of upregulation of p53 target genes has until now only been observed is the control group (Figure 5.6 A and Figure 5.10A; both show 18 genes upregulated) and suggests that the combined depletion of DAPK1 and p53 is returning the activation of p53 target genes to a basal level. The details of each of the genes upregulated are also represented in (Table 5.5) where genes have been categorized based on their function. It can be concluded from this table and the raw images that the actual genes upregulated following either DAPK1 or p53 depletion are similar and that the combined depletion of DAPK1 and p53 is resulting in the return of the number of upregulated genes to a basal level, similar to that observed following the treatment of cells with a non-targeting siRNA control. It would therefore suggest that the upregulation of genes following DAPK1 depletion is p53 dependent.

Table 5.5 Genes expressed following the combined depletion of DAPK1 and p53

	Gene Symbol	siDAPK1	sip53	siDAPK1 + sip53
Apoptosis	*AATF1*	X	X	
	APAF1	X	X	
	BAG1	X	X	
	BAK1	X	X	
	BAX	X	X	
	BCL2	X	X	
	BCL2A1	X	X	
	BID	X	X	
	BIRC5	X	X	X
	BNIP3	X	X	X
	CASP2	X	X	X
	CASP9	X	X	
	CRADD	X	X	
	FADD	X	X	
	GADD45A	X	X	
	HDAC1	X	X	X
	MCL1	X	X	X
	NFKB1	X	X	
	PCBP4	X	X	
	RELA	X	X	X
	TNFRSF10B	X	X	X
	TRAF4		X	
Cell Cycle	*ATM*	X	X	
	ATR	X	X	
	BRCA1	X	X	
	CCNG2	X	X	
	CCNH	X	X	X
	CDC2	X	X	
	CDC25A	X	X	
	CDK4	X	X	X
	CDC7	X	X	
	CDKN1A	X	X	X
	CDKN2A	X	X	
	CHK1	X	X	
	CHK2	X	X	
	E2F1	X	X	
	E2F3	X	X	
	FRAP1	X	X	
	GTSE1		X	
	HK2	X		

	KRAS	X	X	
	MSH2		X	
	MYC	X	X	
	PPM1D		X	
	PTEN	X	X	
	RB1	X	X	X
	SESN1		X	
	SMARCB1	X	X	X
	STAT1	X	X	
	TP53	X		
	TP53BP2	X	X	
	TSC1	X	X	
Cell Growth, Proliferentiation and Differentiation	*BAI1*	X	X	
	BAP1	X	X	
	BTG2	X	X	
	CDC25C	X	X	
	WDR39	X	X	
	KLF6	X	X	X
	CYR61	X	X	X
	IFNB1	X		
	IL6		X	
	JUN	X	X	
	MDM2		X	
	MDM4	X	X	
	MYOD1	X	X	
	NDRG1	X	X	X
	PHB	X	X	
	PMP22	X	X	X
	PRKCQ	X	X	
	PTTG1	X	X	X
	SCGB3A1	X	X	
	SFN	X	X	X
	SHC1	X	X	
Control (Housekeeping genes)	*RPS27A*	X	X	X
	GAPDH	X	X	X
	B2M	X	X	X
	HSPCB	X	X	X
	ACTB	X	X	X

Table 1.5 Genes expressed in A375 cells following the combined depletion of DAPK1 and p53. 'X' represents a gene upregulated by visual assessment and a highlighted gene symbols represent genes which are upregulated (by visual assessment) under all three conditions.

A more detailed analysis was performed using the GEArray Expression Analysis Suite (Superarray) software as described in section 5.2.3.1. As shown in Figure 5.14, I have selected *RPS27A* and *ACTB* to use for normalization as these housekeeping genes are represented consistently across each of the samples. Each value shown in Table 5.6 represents the level of mRNA expression following background correction and normalization and is represented as relative units. Table 5.6 demonstrates the ratio of gene intensities between the test (e.g. siDAPK1 and sip53 combined) and the reference (e.g. siDAPK1) samples, which are represented as fold changes. The significance of each individual fold change is defined by applying a cut-off value where a fold change of 1.5 between reference and test sample is deemed a significant repression or induction. Genes which are considered absent in both the test and reference samples are indicated (Table 5.6; ● symbol). A value of fold difference has been applied where the gene is considered present in the reference group (i.e. siDAPK1 or sip53) but considered absent in the test group (i.e siDAPK1 + sip53). Although considered absent, in general genes in the latter group have a value of greater than or equal to 0.01, therefore a value of fold difference has been applied (Table 5.6). Upregulation of genes are shown as positive values and repression of genes as negative inverse values.

The results demonstrate that the combined depletion of DAPK1 and p53 results in a significant downregulation of p53 target genes compared to the single depletion of DAPK1 or p53 (Table 5.6; column 1, siDAPK1 + sip53 Vs. siDAPK1 and column 2, siDAPK1 + sip53 Vs. sip53; downregulated genes represented as negative inverse values). Genes that are downregulated in siDAPK1 + sip53 compared to both individual si depletions are highlighted in grey (Table 5.6; 25 genes). This level of gene regulation following the combined depletion of DAPK1 and p53 reflects the level of gene regulation previously demonstrated in the non-targeting siRNA control (Figure 5.6 A and Figure 5.10A; both show 18 genes upregulated) and suggests that the combined loss of DAPK1 and p53 results in the loss of the cell's ability to upregulate p53 target genes to a greater extent than RNAi control.

Table 5.6 Ratio of genes expressed between samples (represented as fold changes)

	Gene Symbol	siDAPK1 + sip53 Vs. siDAPK1	siDAPK1 + sip53 Vs. sip53	sip53 Vs. siDAPK1
Apoptosis	*AATF1*	-31.9 *	-13.12 *	-2.43 *
	APAF1	●	●	N/A
	BAG1	●	●	N/A
	BAK1	●	●	N/A
	BAX	●	●	N/A
	BCL2	●	●	N/A
	BCL2A1	●	●	N/A
	BID	-142.4	-94.7	-1.5
	BIRC5	-9.47	-4.33 *	-2.1
	BNIP3	-1.15 *	1.55 *	-1.8
	CASP2	-81.5	-28.4 *	-2.87
	CASP9	●	●	N/A
	CRADD	-72.02	-49.9	-1.44
	FADD	●	●	N/A
	GADD45A	●	-165.5	■
	HDAC1	-77.1	-52.6	-1.46
	MCL1	-70.01	- 35.8 *	-1.95
	NFKB1	●	-501.1	■
	PCBP4	●	●	N/A
	RELA	-34.3	-28.7	-1.19
	TNFRSF10B	-4.09	-2.5	-1.63
	TRAF4	●	●	N/A
Cell Cycle	*ATM*	●	●	N/A
	ATR	-168.44	●	■
	BRCA1	-118.5	-61.7 *	-1.92
	CCNG2	●	●	N/A
	CCNH	-13.3	-7.06 *	-1.88
	CDC2	-112.2	-65.3	-1.72
	CDC25A	●	●	N/A
	CDK4	-2.43 *	-1.77 *	-1.37 *
	CDC7	●	-102.5	■
	CDKN1A	-36.9	-36.4	-1.01
	CDKN2A	●	●	N/A
	CHK1	●	●	N/A
	CHK2	●	●	N/A
	E2F1	●	●	N/A
	E2F3	●	●	N/A
	FRAP1	●	-212.75	■
	GTSE1	●	●	N/A
	HK2	●	●	N/A

	KRAS	●	●	N/A
	MSH2	●	●	N/A
	MYC	●	●	N/A
	PPM1D	●	●	N/A
	PTEN	-117.8	●	■
	RB1	-12.77	-11.06	-1.15
	SESN1	●	●	N/A
	SMARCB1	-5.49 *	-14.55	2.65 *
	STAT1	●	●	N/A
	TP53	●	●	N/A
	TP53BP2	●	●	N/A
	TSC1	●	●	N/A
Cell Growth, Proliferentiation and Differentiation	*BAI1*	●	●	N/A
	BAP1	-23.2 *	-18.3	-1.26 *
	BTG2	●	●	N/A
	CDC25C	-112.96	-61.02	-1.85
	WDR39	●	-286.9	■
	KLF6	-56.9	-34.2	-1.67
	CYR61	-8.54	-4.31	-1.98
	IFNB1	●	●	N/A
	IL6	●	●	N/A
	JUN	●	●	N/A
	MDM2	●	●	N/A
	MDM4	●	●	N/A
	MYOD1	●	●	N/A
	NDRG1	-15.02	-3.27 *	-4.58
	PHB	-118.5	●	■
	PMP22	-72.2	-69.8	-1.03
	PRKCQ	●	●	N/A
	PTTG1	-4.97 *	-3.71 *	-1.33 *
	SCGB3A1	-89.2	●	■
	SFN	-64.5	-30.1	-2.15
	SHC1	●	-264.8	■
Control (Housekeeping genes)	*RPS27A*	-1.49 *	-1.65 *	-0.9 *
	GAPDH	-2.55 *	7.16 *	-19.4 *
	B2M	-1.44 *	9.86 *	-14.2 *
	HSPCB	2.165 *	9.125*	-4.45 *
	ACTB	1.18 *	-0.86 *	-1.63 *

Table 1.6 Ratio of genes expressed between samples (represented as fold changes). Highlighted in grey represent genes downregulated following the combined depletion of DAPK1 and p53; ● represents a gene considered absent in both the reference and test samples; ■ represents a gene considered absent in either reference groups, siDAPK1 or sip53; N/A represents a fold difference value cannot be applied due to considered absence of gene in both

groups; * represents spots are considered ‘bleeding’, therefore gene value may be underestimated.

The fact that the depletion of p53 leads to the significant upregulation of p53 target genes is of interest. We would expect that following depletion of p53 that there would be a downregulation of some p53 target genes and upregulation of other genes as p53 acts to repress the transcription of some genes as well as activate the transcription of other genes. However, the actual genes upregulated and the level gene upregulation are similar to that seen following DAPK1 depletion (Figure 5.14 and Table 5.5). This is also demonstrated in Table 5.6 which demonstrates the fold change in the level of genes expressed between DAPK1 and p53 depleted cells (Table 5.6; column 3; sip53 vs. siDAPK1). This data shows that although the level of gene expression following p53 depletion is lower than that following DAPK1 depletion (Table 5.6; column 3; sip53 vs. siDAPK1; downregulated genes represented as negative inverse values), the fold change is in general not too large. These data suggest that although p53 is depleted, the upregulation of target genes may occur as a result of other factors causing stress within the cell.

Figure 5.15 compares the transcript levels of the 25 genes which are considered to be upregulated following the combined depletion of DAPK1 and p53 to the transcript levels following DAPK1 or p53 depletion (represented as relative units, RU). This figure demonstrates that of these 25 genes upregulated in each of the three groups, transcript levels are highest following DAPK1 depletion (Figure 5.15; siDAPK1; blue column). The only exception to this pattern is the SMARCB1 gene, which demonstrates increased transcript levels following p53 depletion but this is likely to be the result of 'bleeding' of signal intensity which reduces the value of the transcript level (Figure 5.15; sip53; red column; SMARCB1). In general the transcript levels following p53 depletion are less than two fold lower than the transcript levels following DAPK1 depletion (Figure 5.15; sip53; red column; also shown in Table 5.6). Genes such as *CDKN1A* and *RB1*, both cell cycle regulators, show similar levels of upregulation following either DAPK1 or p53 depletion suggesting that these genes may have similar roles as target genes upregulated following depletion of DAPK1 or p53. Following the combined depletion of DAPK1

and p53 transcript levels of the 25 genes are significantly reduced suggesting that there is almost complete loss in the cell's ability to induce the p53 target genes.

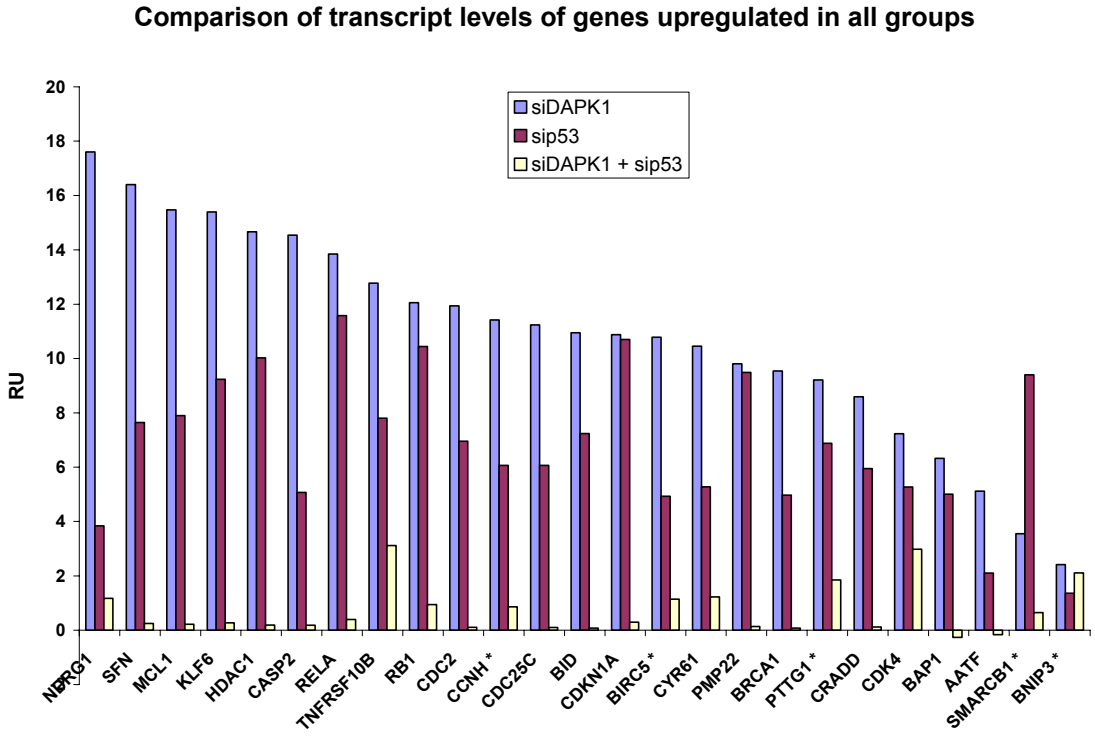

Figure 5.15 Comparison of transcript levels of genes upregulated following either single gene or combined gene depletion.

The transcript levels of the 25 genes which are considered to be upregulated following the combined depletion of DAPK1 and p53 are shown along side the transcript levels following DAPK1 or p53 depletion (represented as relative units, RU). Several genes are considered to have 'bleeding' of signal intensity in one or more groups and this has resulted in under represented transcript levels (highlighted with an asterix *).

To provide an overall view of the effect of depletion of kinases on activation of p53 target genes, the Clustergram analysis tool (GEArray Expression Analysis Suite) was used to create a cluster diagram to visualise the microarray data as described previously (see section 5.2.3.1). The data presented in the clustergram is based upon the colour coding of genes based on results from the entire dataset, where colours are assigned based on values in the whole dataset (Figure 5.16). This allows the expression levels of all genes to be compared across the whole dataset. Although this method is less sensitive in that genes expressed at lower levels are under represented, it allows the comparison of upregulation of the genes within a sample as well as the comparison of upregulation of the genes across the three sample groups and thereby provides an overall picture of the effect of the combined depletion of DAPK1 and p53 on p53 target gene expression. It demonstrates that depletion of DAPK1 or p53 leads to similar pattern of significant gene upregulation and a similar high level of gene expression (Figure 5.16; siDAPK1 or sip53; mixture of green, black and red gene expression). However, following the combined depletion of both DAPK1 and p53 there are very few genes upregulated and the level of expression is low (Figure 5.16; siDAPK1 + siP53 combined; mainly green representing low gene expression).

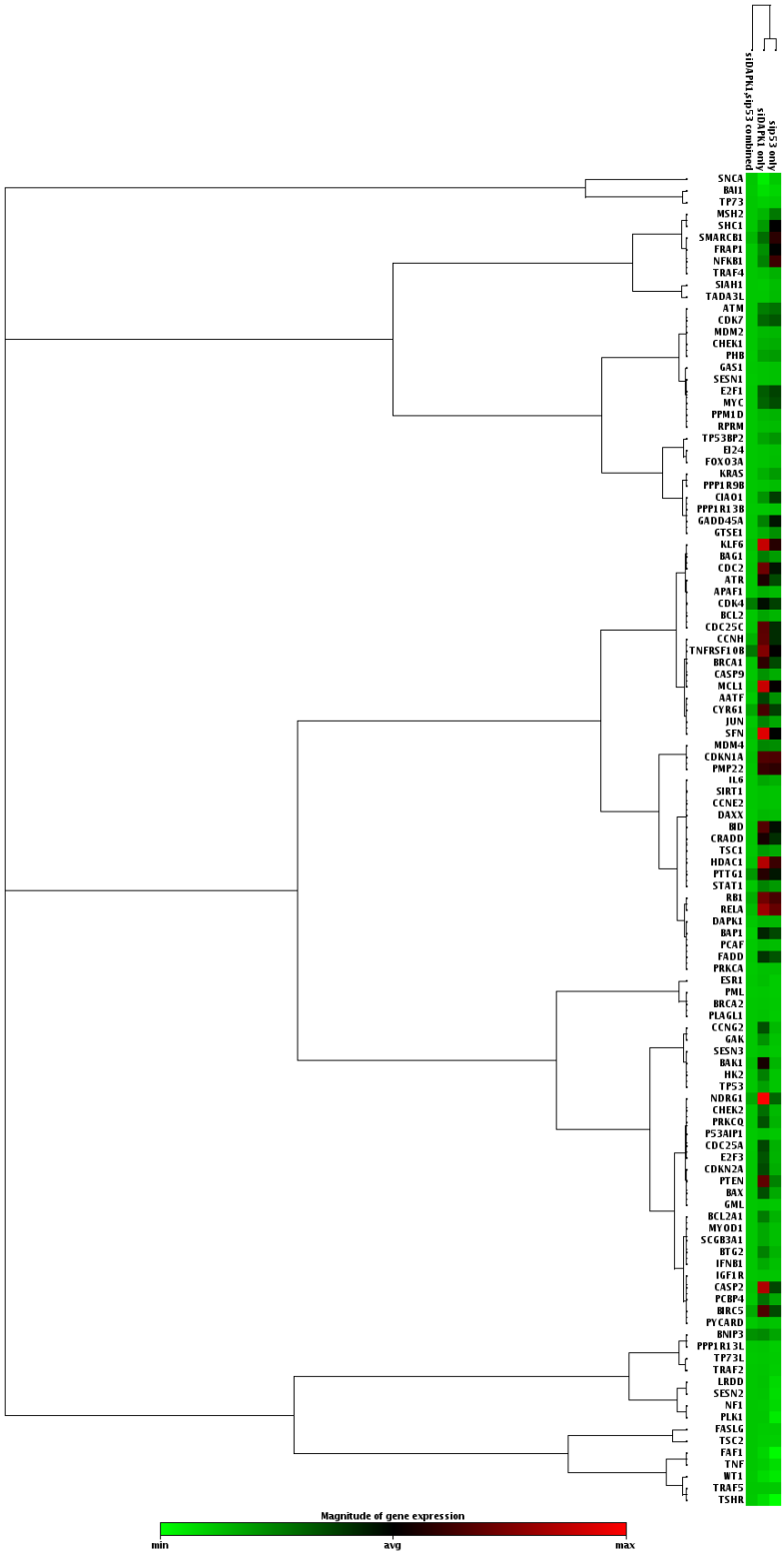
siDAPK1+p53 combined
siDAPK1 only
p53 only
SNCA
BAI1
TP73
MSH2
SHC1
SMARCB1
FRAP1
NFKB1
TRAF4
SIAH1
TADA3L
ATM
CDK7
MDM2
CHEK1
PHB
GAS1
SESN1
E2F1
MYC
PPM1D
RPRM
TP53BP2
EI24
FOXO3A
KRAS
PPP1R9B
CIAO1
PPP1R13B
GADD45A
GTSE1
KLF6
BAG1
CDC2
ATR
APAF1
CDK4
BCL2
CDC25C
CCNH
TNFRSF10B
BRCA1
CASP9
MCL1
AATF
CYR61
JUN
SFN
MDM4
CDKN1A
PMP22
IL6
SIRT1
CCNE2
DAXX
BID
CRADD
TSC1
HDAC1
PTTG1
STAT1
RB1
RELA
DAPK1
BAP1
PCAF
FADD
PRKCA
ESR1
PML
BRCA2
PLAGL1
CCNG2
GAK
SESN3
BAK1
HK2
TP53
NDRG1
CHEK2
PRKCQ
P53AIP1
CDC25A
E2F3
CDKN2A
PTEN
BAX
GML
BCL2A1
MYOD1
SCGB3A1
BTG2
IFNB1
IGF1R
CASP2
PCBP4
BRCS
PYCARD
BNIP3
PPP1R13L
TP73L
TRAF2
LRDD
SESN2
NF1
PLK1
FASLG
TSC2
FAF1
TNF
NT1
TRAF5
TSHR
Magnitude of gene expression
min
avg
max

Figure 5.16 The combined depletion of DAPK1 and p53 leads to downregulation of p53 target gene expression.

Clustergram analysis is used to demonstrate the correlation of genes, where genes that are more similar are joined at lower heights in the dendogram and those that are less similar are joined at higher heights. Genes are colour coded based on the entire dataset thereby allowing the comparison of genes within a sample as well as across the three groups. The colour represents the magnitude of gene expression whereby green represents low gene expression and red represents high gene expression.

Overall these data demonstrate that the combined depletion of DAPK1 and p53 results in loss of upregulation of p53 target genes. The fact that DAPK1 depletion results in the significant upregulation of p53 target genes and that the combined depletion with p53 causes a return to levels of gene expression previously only observed in the non-targeting control is interesting. p53 depletion alone also results in the upregulation of the same set of target p53 target genes as DAPK1 depletion suggesting that the presence of neither p53 nor DAPK1 is essential for the upregulation of these target genes. However, the presence of at least one of DAPK1 or p53 is required for upregulation of these p53 target genes, as when both p53 and DAPK1 are depleted there is significant reduction in the p53 target gene upregulation. These results suggest that the upregulation of genes following DAPK1 depletion is p53 dependent and therefore may emphasize the potential importance of DAPK1 in the p53 signalling pathway.

5.3 Discussion

In this chapter we set out to clarify the effect of kinase depletion on the activation status of p53 using gene knockdown technology. We were able to show that p53 is stabilized following kinase depletion under both damaged and undamaged conditions. We went on to combine siRNA and microarray technology to profile the effect of kinase depletion on the expression of 113 genes of the human p53 signalling pathway. Using oligonucleotides microarrays we were able to demonstrate that the depletion of Chk1 and DAPK1 led to significant upregulation of p53 target genes and that IR damage did not further upregulate these genes. Microarray analysis of the effect of the combined depletion of p53 and DAPK1 demonstrated that the silencing of both genes dramatically reduced the levels of genes upregulated by either DAPK1 or p53 depletion alone. The implications of these findings will be discussed in the two sections below.

5.3.1 A role for kinases a negative regulators of p53

Initially in this study we set out to identify kinases which may activate p53. Hypothetical models were proposed in which Calcium Calmodulin kinases such as Chk1, Chk2, DAPK1 and AMPK may play a role in modulating p53 activity. Indeed DAPK1 had been shown to suppress oncogene-induced transformation of primary embryonic fibroblasts by activating p53 in a $p19^{ARF}$ – dependent manner leading to induction of apoptosis to eliminate the pre-malignant cells (Raveh et al. 2001) and Chk1 and Chk2 were shown to phosphorylate p53 at multiple sites on p53 leading to its stabilization and activation (Ou et al. 2005). The subsequent examination of Calcium Calmodulin kinases led to the identification of Chk1 and DAPK1 as putative kinases which stimulate the Ser 20 phosphorylation of p53 (see section 3.2.2).

In this chapter we used siRNA technology to investigate the effect of depletion of these kinases on the activation status of p53. We showed that silencing Chk1 and DAPK1 resulted in the stabilization of p53 at the protein level and that this stabilization was

further enhanced following damage insult (either IR or UV) in kinase depleted cells. As A375 cells characteristically express low levels of endogenous Chk2 and DAPK, the detection of protein levels by western blot proved difficult, and led to variation in the clarity of some immunoblots. To overcome this issue, A549 cells which characteristically express higher levels of endogenous DAPK1 as well as Chk1 and Chk2, were used to support the initial data demonstrated in A375 cells. The investigation of the cause of the stabilization of p53 following depletion of kinases demonstrated that it was not dependent on Ser 15 phosphorylation in these cells, although there could be a role for phosphorylation of p53 at other sites. In light of recent literature we went on to examine the role of kinases and p53 in the signal transduction pathways that lead to mTOR activation. DAPK1 has been shown to be part of the ribosomal S6 kinase-mediated pathway that attenuates DAPK1 function (Anjum et al. 2005). Recently, it has been demonstrated that DAPK1 can positively regulate mTOR (mammalian target of rapamycin) by forming an interaction with TSC2 complex in cells. This interaction neutralises TSC1/2 mediated suppression of the mTOR translation pathway, leading to stimulation of mTOR as determined by changes in activity of mTOR targets: the translational regulators p70 S6 kinase and S6 kinase (C. Stevens et al, in press). We showed that following UV damage there was increased S6 phosphorylation but this phosphorylation was not further increased following depletion of kinases. Interestingly, following UV damage there was also increased phosphorylation of the translational regulator p70 S6 kinase and this p70 S6 kinase activity was increased further following depletion of either Chk1 or DAPK1. In light of the recent literature (C. Stevens et al, in press), we would have expected to have seen a decrease in mTOR activity following depletion of DAPK1. However we have described here that the depletion of DAPK1 led to the increased activity of p70 S6 kinase as well as increased stabilization of p53. Recent reports have suggested a crosstalk mechanism between p53 and mTOR signaling pathways leading to the coordinate regulation of cell growth, proliferation and death (Feng et al. 2005). The stabilization of p53 following kinase depletion reported here may therefore suggest crosstalk between p53 and mTOR

signaling pathways, whereby the expected activation of the mTOR pathway following DAPK1 depletion may be inhibited by the upregulation of p53 signal transduction pathways.

A cell viability assay suggested that the depletion of Chk1 or DAPK1 and the resulting activation of p53 were not leading to significant cell death or activation of cell death pathways. In light of the fact that there was no evidence of cell death, it may have been useful to follow up this issue of activation of p53 by examining for evidence of cell cycle arrest and apoptosis. The use of a technique such as flow cytometry in which data can be quantified would have been a useful method in provided information on cellular outcome following activation of p53. However, at this stage a detailed examination of the signalling pathways affected by the activation of p53 was undertaken.

We went on to examine the effect of blocking Chk1 and DAPK1 on the activation of 113 genes regulated by the p53 signaling pathway by microarray analysis. We were able to show that following depletion of Chk1 and DAPK1 there was significant upregulation of p53 target genes. This highlighted a mixture of genes such as *ATR* (involved in cell cycle arrest), *E2F1* (promotes cell proliferation), and NFκB1 (promotes inflammation) which are upregulated to a higher extent following depletion of kinases. As these genes are induced in a wide range of cell functions they are likely to play a role in maintaining a balance between cell proliferation, cell cycle arrest and apoptosis similar to that achieved in normal cells as kinase depleted cells showed no changes in overall cell viability.

Interestingly following kinase depletion and subsequent IR damage there was not much change in the expression of p53 target genes compared to kinase depletion alone suggesting that this type of damage in these cells did not induce further upregulation of genes. Only in the non-targeting control arrays was the effect of IR damage apparent where there was significant upregulation of p53 target genes. As there is such a high

level of upregulation of genes following kinase depletion, it could be that the activation of genes following the damage insult is being masked and no additional genes are being activated. Additionally, the results would therefore suggest that the depletion of kinases produces a similar response to IR damage in these cells in terms of the expression profiles of p53 target genes and would suggest that kinase depletion or IR damage induces the expression of a variety of genes involved in different cellular processes in order to achieve the desired outcome: presumably continued cell proliferation with a minimal amount of cell cycle arrest and/or apoptosis as overall cell viability was unchanged.

The significant upregulation of p53 protein and of p53 target genes following the silencing of kinases compared to a non-targeting control suggested that the presence of these kinases may have a role in the suppression of p53 and therefore may act as negative regulators of p53. The role of Chk1 as a negative regulator of p53 was suggested in a report by the Nakanishi group. They demonstrated using Chk1 null ES cells that the loss of Chk1 resulted in the activation of Chk2-p53-dependent DNA damage checkpoint (Niida et al. 2007). Furthermore, a report demonstrated that Chk1 depleted U2-OS (wild-type p53 status) exhibited activated Chk2 and increased p53 stabilisation. Although this activation was further enhanced upon replication block (hydroxyurea treatment; HU) and subsequent release, the enhanced activation was demonstrated to be independent of Chk2 or p53 status of the cells (Cho et al. 2005). However, the activation of Chk2 and p53 in Chkl depleted cells without treatment could support previously described data (Niida et al. 2007) and the microarray data which has been presented in this report. This could suggest a role for Chk2 in the activation of p53 following the loss of Chk1, whereby a feedback loop results in the activation of Chk2 following depletion of Chk1 to promote the activation of p53 and subsequent apoptotic or cell cycle pathways. In support of this hypothesis, Chk2 was upregulated at the gene level following Chk1 depletion in both sets of microarray data presented here.

Similarly, it may be possible that DAPK2 and DAPK3 are upregulated following DAPK1 depletion.

Although DAPK1 and Chk1 depletion led to significant upregulation of p53 targets, we have previously shown DAPK1 as well as Chk1 to stimulate phosphorylation of p53 (see section 3.2.2). These results may suggest a dual function role for kinases with Chk1 and DAPK1 acting either as survival factors or as inducers of cell cycle arrest and apoptosis. The former role as a survival factor in suppressing p53 activation would support recent literature whereby DAPK1 was shown to form a multi-protein survival complex with cathepsin B and this complex negatively regulated TNFR-1 dependent cell death pathways (Lin et al. 2007). Furthermore, DAPK1 has been shown to form a complex with TSC2 in cells leading to the stimulation of growth-promoting mTOR translational pathways (C. Stevens et al, in press). The latter role of DAPK1 in phosphorylation and activation of p53 is consistent with the original studies on the involvement of DAPK1 in apoptotic pathways. Indeed, DAPK1 has been shown to be part of the cell death pathway that mediates oncogene signaling to p53 via $p19^{ARF}$ (Raveh et al. 2001), inducing myosin light chain phosphorylation and membrane blebbing associated with cytoplasmic changes during apoptosis (Bialik et al. 2004), stress induced autophagic vesicle formation (Inbal et al. 2002; Gozuacik and Kimchi 2004) and antagonizing FAK to activate p53-dependent apoptotic pathway (Wang et al. 2002).

The suggestion that DAPK1 may act as a survival factor led us to examine the effect of the combined depletion of DAPK1 and p53 in A375 cells. Interestingly following the single depletion of p53, virtually the same p53 target genes were upregulated as following DAPK1 depletion suggesting that p53 may play a similar role in the activation of target genes as DAPK1. We were also able to show that the combined depletion of p53 and DAPK1 resulted in the blocking of upregulation of p53 target genes. The level of gene upregulation following combined depletion was similar to that seen in the non-targetting control group. This suggests that the presence of both p53 and DAPK1 in this

cell system suppresses the activation of p53 target genes. Therefore, upon targeted depletion of either p53 or DAPK1 there is significant stimulation of p53 target genes but the combined depletion blocks this stimulation suggesting that the loss of both is detrimental to reactivation of the p53 response. The role of kinases such as DAPK1 and Chk1 as putative drug targets for reactivation of the p53 response will be discussed in the following section (5.3.2).

The study of gene expression using microarray technology is a useful way in which to determine the activation status of signaling pathways and putative target genes. In this study we have been able to use microarray technology to investigate the effect of kinase depletion on activation of p53 which has led to the identification of putative kinase drug targets, namely Chk1 and DAPK1, for reactivation of the p53 response. However, we must consider the implications of these results and future investigations. It is always necessary to validate microarray data by way of techniques such as reverse transcribed PCR (RT-PCR). Oligonucleotide microarrays are often less sensitive at detecting the range of transcript abundance. A report by Draghici and colleagues discusses the issues of accuracy (or sensitivity), the precision (or reproducibility) and specificity (ability to bind to specific sequence) of microarray technology and suggests that the expression and magnitude of gene expression is often less sensitive in oligonucleotides microarrays than RT-PCR (Draghici et al. 2006). As discussed in the introduction (section 5.1.2), there have been several studies examining p53-dependent gene expression by microarray analysis (Zhao et al. 2000; Kannan et al. 2001). However, as the function of protein coding genes is carried out by the protein product it is important to study the expression of genes at protein level. A recent report used 2D gel electrophoresis to examine p53-dependent expression at the protein level and to identify novel proteins. They were able to separate approximately 5800 protein spots, of which 115 showed substantial expression changes upon p53 activation and 55 spots were identified by mass spectrometry. Many of the proteins identified by mass spectrometry had no previous connection to p53 and were shown to have different functions such as mRNA

processing, translation, redox regulation and apoptosis (Rahman-Roblick et al. 2007). Therefore further work is required to validate the data presented here by using techniques such as RT-PCR and furthermore examine the expression of genes at protein level by using techniques such as 2D gel electrophoresis. As a first step in this validation approach, we have shown that the levels of p53 protein are increased following depletion of Chk1 and/or DAPK1.

5.3.2 Kinase drug targets for reactivation of the p53 response

Microarrays have been successfully applied to the identification of drug targets, drug development and treatment validation (Manning et al. 2007). A report described how the cellular effects of potent inhibitor compounds of human cyclin-dependent kinase 2 (CDK2) were characterized in yeast on a genome wide scale by monitoring changes in mRNA levels in treated cells with the use of oligonucleotide probe arrays (Gray et al. 1998). Furthermore, gene expression analysis can be used as a method for drug validation and identification of secondary drug targets. A report used gene expression analysis to identify pathways that were altered by a immunosuppressant drug (FK506) in use in the clinic and demonstrated that the drug had off-target effects (Marton et al. 1998). Around half of all tumours carry mutation in p53 which results in loss of ability to activate p53-induced cell cycle arrest and apoptosis. In this report we have demonstrated that the depletion of kinases such as Chk1 and DAPK1 led to the upregulation of p53 target genes. Upon validation, the implication of this data could be signigicant and could provide a platform on which to develop specific kinase inhibitors to Chk1 and DAPK1 to allow reactivation of the p53 response and therefore the induction of cell cycle arrest and apoptosis to prevent progression of tumours that contain mutations in p53. Several reports have examined different methods in which to reactivate p53. Small molecules such as PRIMA-1 (proline-rich membrane anchor-1), which suppresses growth of cells expressing mutant p53, have been identified. These can restore wild-type function to mutant p53 and may be forerunners in the development

of anti-cancer drugs (Bykov et al. 2003). Others studies have examined the *in vivo* activation of p53 by small molecule inhibitors (Nutlin-3) of the negative regulator of p53, Mdm2 (Vassilev et al. 2004). More recently, a report has suggested how the combined use of Mdm2 and Mdm4 antagonists in cancer cells expressing WT-p53 may allow the increased activation of p53 (Toledo and Wahl 2007).

Several reports have examined the roles of kinases such as Chk1 as therapeutic targets for cancer treatment. Cell cycle checkpoint abrogation has been proposed as a method to sensitise cancer cells to DNA damaging agents (Dixon and Norbury 2002; Zhou and Bartek 2004). In normal cells DNA damage leads to p53 dependent cell cycle arrest in G1 whereas tumour cells, deficient in p53, rely on checkpoints to mediate arrest in S or G2 phase. Therefore targeting cell cycle checkpoints would only abrogate cell cycle blocks in tumour cells, as normal cells would still arrest in G1, and promote mitotic catastrophe and apoptosis of tumour cells (Dixon and Norbury 2002; Zhou and Bartek 2004). A report by Xiao and colleagues compared three kinases involved in cell cycle checkpoint control to determine the main kinase(s) responsible for cell cycle arrest of mammalian cells. They showed that downregulation of Chk1, but not Chk2 or MK2, abrogated stress induced G2 arrest, which led to mitotic catastrophe or apoptosis. The double inhibition of Chk1 and Chk2 was no better than Chk1 inhibition alone, therefore suggesting that Chk1 was the only relevant checkpoint kinase as a target for cancer treatments (Xiao et al. 2006). More recently a report described how the inhibition of Chk1 was used to activate p53 to promote the elimination of tumour cells. The depletion of Chk1 preferentially killed tetraploid colon cancer cells in their normal model, abolished spindle assembly checkpoint and caused premature and abnormal mitosis leading to the activation of p53 and p53-regulated transcripts, Puma and BBC-3 (Vitale et al. 2007). Therefore, several reports have investigated the role of small molecule inhibitors designed to known negative regulators of p53 (Mdm2) as well as to kinases as putative anti-cancer therapies which abrogate cell cycle blocks specifically in tumour cells and promote the reactivation of p53 which leads to increased apoptosis and

mitotic catastrophe. The data presented in this report supports the recent literature with regard to the targeting of Chk1 to reactivate the p53 pathway (Xiao et al. 2006; Vitale et al. 2007). In addition to this data we propose another member of the Calcium Calmodulin superfamily of kinases, DAPK1 as a putative drug target for reactivation of the p53 pathway. Although DAPK1 was originally shown to be implicated in cell death pathways, it is now becoming apparent that DAPK1 may act as a survival factor (Lin et al. 2007). This data presented here would also support a role for DAPK1 as a survival factor and a potential target for design of therapies to treat human cancers.

6 SUMMARY, CONCLUSIONS AND FUTURE DIRECTIONS

6.1 Defining the role of Calcium Calmodulin Kinases in modulation of p53 activity

Protein phosphorylation is the most widespread type of post-translational modification which occurs in signal transduction (Ubersax and Ferrell 2007). Protein kinases are key signaling enzymes which play a major role in the regulation of multiple cellular responses. Therefore the clarification of the role of p53 phosphorylation by protein kinases is essential to the development of our understanding of the signaling pathways crucial to the activation of p53.

A crucial event in the activation of p53 is the phosphorylation at residues Threonine 18 and Serine 20 (Ser 20) that both stabilises the binding of the co-activator p300 and reduces the binding of the inhibitory partner Mdm2. These phosphorylation events therefore enhance activation of p53 target genes. The identification of enzymes that phosphorylate the p53 transactivation domain at residues such as Thr 18 or Ser 20 has been an important development in the ongoing mapping of signaling pathways that control p53-dependent transcription and consequently tumour suppression.

In this report we examined specific members of the Calcium Calmodulin kinase (CAMK) superfamily and their role in modulation of p53 activity. Using transcription-based assays and a newly developed *in vivo* Ser 20 phosphorylation assay we showed that Chk1 and DAPK1 but not Chk2 phosphorylated p53 at Ser 20, which led to transcriptional activation of p53. Verification of these results using siRNA technology demonstrated that Chk1 was the most potent endogenous mediator of Ser 20 site phosphorylation in H1299 cells, and DAPK1 was identified as the most effective endogenous p53 protein stabilizer in A375 cells, thus suggesting a cell-specific function

for these kinases. These results have contributed significantly to the clarification of the role of Calcium Calmodulin kinases in the stress-activated p53 signalling pathways, partially resolving the controversy in the field as to the identity of the main p53 Ser 20 kinases *in vivo* (Ahn et al. 2003; Jallepalli et al. 2003). Indeed, our work suggests that Chk1 and DAPK1, rather than Chk2 were the main Ser 20 kinases. However, in order to investigate the role of other members of the CAMK superfamily it would be necessary to employ a wide scale screening approach. The use of a p53 null line, in which p53 can be expressed ectopically and easily detected using Ser 20 phospho-specific antibodies would be a useful tool to continue the evaluation members of the Calcium Calmodulin superfamily of kinases as putative Ser 20 site kinases. It has been shown that mutation of the Ser 20 equivalent phospho-acceptor site in mice accelerates B-cell lymphoma (MacPherson et al. 2004) therefore B cells may provide a useful model in which to study modification of p53. Cell models could be developed in order to evaluate how distinct CAMK superfamily members activate p53 in a cell-specific manner and may provide an interesting framework in which to identify the stress activated regulators of p53.

Moreover, a recent report described a technique for detecting the specific activity of Ser/Thr kinases in cells through the introduction of expression vectors encoding modified substrate kinase fusion proteins (Suda et al. 2008). They fused p53 with individual kinase domains of Chk1, Cdk5 and DYRK3 and showed that phosphorylation of p53 Ser 15 and Ser 20 sites could be significantly induced by the catalytic activity of kinases such as Chk1 contained within fusion proteins. To verify the data they used a kinase-inactive mutant and showed that the mutation blocked phosphorylation of p53, thereby showing that the Ser15/Ser20 activity was dependent on the catalytic activity of the fused target kinase (Suda et al. 2008). This type of system may be useful in the elucidation of the sites within p53 which specific kinases such as Chk1 phosphorylate. It also could be used as a screening method in which to examine the role of other related CAM kinases as well as kinases from other families such as CK1 (casein kinase 1) and TK (tyrosine kinases) in modulation of p53 activity.

6.2 Calcium Calmodulin kinases & Mdm2 have overlapping binding requirements on p53 Box-V

Our studies examining the interaction of kinases with p53 demonstrated the requirement of the Box-V domain of p53 for kinase-docking and subsequent kinase-mediated phosphorylation of the Box-I domain. The previously identified naturally occurring p53 isoform, p53 ΔV, (Rohaly et al. 2005) was a useful tool with which to investigate the specific regions of p53 which kinases may bind to and/or phosphorylate. Using this isoform we were able to demonstrate that deletion of the Box-V domain of p53 resulted in two events; (i) loss of basal and kinase-stimulated Ser 20 site phosphorylation and (ii) attenuation of Mdm2-mediated ubiquitination of p53. These combined data suggest that the Box-V region of p53 is a multi-protein docking site for Calcium Calmodulin superfamily members as well as Mdm2. The idea that the Box-V region may act as a multi-protein docking site correlated with literature which identified a novel Mdm2 interaction site in the core domain of p53 (Shimizu et al. 2002) and that this interaction site was necessary for a dual site docking mechanism of Mdm2 on the p53 tetramer (Wallace et al. 2006).

The clarification that the Box-V region is a multi-protein binding site required to activate p53 phosphorylation and ubiquitination led to further investigation examining the interaction between kinases and/or Mdm2 and the Box-V motif of p53. Binding assays performed *in vivo* demonstrated that Chk1, DAPK1 and Mdm2 form an interaction with the Box-V domain and that this interaction required distinct residues in the Box-V protein. We showed that Chk1 and Mdm2 appeared to have overlapping requirements for binding to the Box-V domain. This suggested that the Calcium Calmodulin kinases, Chk1/DAPK1 and Mdm2 may antagonize each other through competition for the same multi-protein docking site. Supporting this idea was the result which demonstrated that the p53 mutant, p53 HIS175 could be stimulated transcriptionally by transfection of Chk1. Although it has been established that the p53 HIS175 protein is hyperubiquitinated *in vivo* due to the unfolding of the protein and thus

the exposure of the Box-V motif (Shimizu et al. 2006), this transcriptional reactivation of the p53 HIS175 mutant from the $p21^{WAF1}$ reporter by Chk1 suggests that Chk1 may overcome Mdm2-mediated ubiquitination by competition for binding to the Box-V interface and drive p53 into a transactivation-competent rather than a ubiquitinated state. The idea that different proteins compete with each other for binding to this specific region of p53 resulting in the regulation of p53 reflected recent data which used nuclear magnetic resonance to show that on binding to p53 the acid domain fragment of Mdm2 induced significant chemical shifts throughout the core domain of p53 especially within the Box-V motif (Yu et al. 2006). A technique such as this which uses immobilized peptide arrays could be employed to examine the binding of other CAM kinases to p53 and identify specific binding sites in the p53 Box-V domain. It would also be useful to verify the binding results using immunofluorescence whereby colocalisation of the protein and Box-V domain could be examined in cells.

The clarification of the protein interactions with the Box-V site and the resulting control of p53 activation have made a significant contribution to this field. However, we should continue to investigate which other proteins interact with this site to further elucidate the mechanisms underlying p53 tumour suppressor function.

6.3 The role of 'Gain of function' mutation on kinase modulation of p53 activity

Mutation of key contact sites on p53 such as the Box-V domain can have a detrimental effect on the activation of p53 (Craig et al. 2003; Wallace et al. 2006). However, some mutations can result in a gain of function phenotype and interactions of proteins with these p53 mutants can positively stimulate p53 (Kim and Deppert 2004; Li and Prives 2007; Menendez et al. 2007). In this report we examined the gain of function nature of mutant p53 in order to develop our understanding of the molecular mechanisms of the oncogenic gain of function phenotype and the molecular interactions of mutant p53.

Based upon results from a recent paper (Kakudo et al. 2005), a set of mutants was created to evaluate whether the activity of these mutants could be modulated by kinases and/or Mdm2 and thereby simultaneously further identify sites important for the interaction of p53 with kinases/Mdm2. We identified two potentially interesting mutations, A276V and K2921, which are found within or adjacent to the Box-V region. A detailed examination of these mutants (K292I and A276V) demonstrated that gain of function transactivation potential was $p21^{WAF1}$ promoter-dependent but that kinases did not further stimulate the transcriptional activity on either the $p21^{WAF1}$ or BAX promoters suggesting that these sites play an important role in kinase docking. Interestingly the A276V mutant appeared to be resistant to Mdm2-mediated inhibition of p53 transcriptional activity. This mutation lies within the Box-V domain, the location of the ubiquitination signal for Mdm2. The observed resistance of this mutant to Mdm2-mediated inhibition of p53 transcriptional activity may be consistent with the loss of the Mdm2 binding site and would suggest that mutation of this site may play an important role in Mdm2 interaction with the Box-V domain. It may be possible that the A276V mutant favours the binding of kinases rather than Mdm2, thus driving p53 into a transactivation competent state.

Although this transcriptional data provides insight into interactions of the p53 mutants, it would have been useful to perform these assays in triplicate to allow for formal statistical analysis to be applied. This would allow for validation of the data and clarify any doubt surrounding reproducibility.

To further investigate the role of these mutants in the potential stimulation of p53 activity, we could employ techniques such as yeast-based functional assays. These simple assays can be used to predict the transcriptional behaviour of mutant p53 in higher eukaryotes. For example, Campomenosi and colleagues employed a yeast based assay in which they examined a selection of mutants and investigated the promoter specific transactivation potential of each mutant, thus allowing the categorization of

mutants based on their transcriptional behaviour (Campomenosi et al. 2001). In light of the data which shows that p21 can protect against cell killing by chemotherapeutic drugs in some settings (Waldman et al. 1997), this type of assay would allow the proper classification of mutants which may have valuable clinical applications in the treatment of cancers. Indeed, tumours containing p53 mutants with gain of function p21 transactivation potential may display resistance to chemotherapeutic agents. It would therefore be of clinical value to identify such tumours and either select an appropriate treatment regime to minimise drug resistance or combine chemotherapeutics with a p21-targeting agent.

Further investigation could also focus on the development of mouse models in which to clarify the role of mutant p53 in cancer progression. For example, a report described the development of a murine model with mutation at p53 amino acid site 172 (corresponds to the human R175H hot-spot mutation) to simulate Li-Fraumeni-like mutant p53 and demonstrated that the mutant p53 associated with p63 and p73 in tumour cells of mice (Lang et al. 2004). They also showed that silencing mutant p53 resulted in increased activity of p53 target genes such as $p21^{WAF1}$ which was likely to be a result of the increased activity of endogenous p53 family members p63 and p73 (Lang et al. 2004). These studies proposed a means by which mutant p53 may promote tumourigenesis through downregulation of its family members. With respect to continuing the investigation of the mutants examined in this study, the use of knock-in mouse models could be a potentially interesting and a highly informative way to clarify how interactions with other proteins such as CAM kinases may control the modulation of p53 activity.

The experimental approaches outlined above could provide a basis on which to build our understanding of the activity of p53 mutants and the resulting biological outcomes. The way in which we approach the design of individual therapeutic strategies is likely to depend on individual mutation phenotypes and will therefore be complex but crucial in the treatment of many cancers.

6.4 The identification of kinase drug targets for reactivation of the p53 response

In the final results chapter of this report set we set out to clarify the effect of kinase depletion on activation of p53. Using gene knockdown technology we demonstrated that p53 is stabilized at the protein level following Chk1 and DAPK1 depletion under both damaged and undamaged conditions. Moreover, using gene expression microarrays which profile gene expression of the p53 signalling pathway we were able to demonstrate that the depletion of Chk1 and DAPK1 led to significant upregulation of p53 target genes. Further microarray analysis of the effect of the combined depletion of p53 and DAPK1 demonstrated that the silencing of both genes dramatically reduced the level of p53 target genes upregulated. This suggests that the upregulation of genes following DAPK1 depletion was p53-dependent. These results could have significant implications, some of which are discussed in the following sections.

6.4.1 A role for kinases as negative regulators of p53

The significant upregulation of p53 target genes following the silencing of Chk1 and DAPK1 compared to a non-targeting control suggested that the presence of these kinases may have a role in the suppression of p53 and therefore may act as negative regulators of p53. The role of Chk1 as a negative regulator was supported by recent literature which showed that Chk1 depletion led to activation of p53 and Chk2 (Cho et al. 2005; Niida et al. 2007). Together these results could suggest a role for Chk2 in the activation of p53 following the loss of Chk1, whereby a feedback loop results in the activation of Chk2 following Chk1 depletion to promote the activation of p53. This proposed pathway of interaction is shown in Figure 6.1. It would be interesting to test this hypothesis by studying the activation status of proteins such as other members CAMK superfamily which may be involved in the signaling pathways which activate p53 following loss of kinases. It may be that several kinases are able to compensate for the loss of each other whereby loss of Chk1 for example may activate many additional

kinases which in turn activate p53. Mammalian cell culture models in which kinases such as Chk1 are depleted by siRNA and cells are selected to generate a stable inducible kinase knockdown cell line would be a useful system to study the interactions between different kinases signaling pathways.

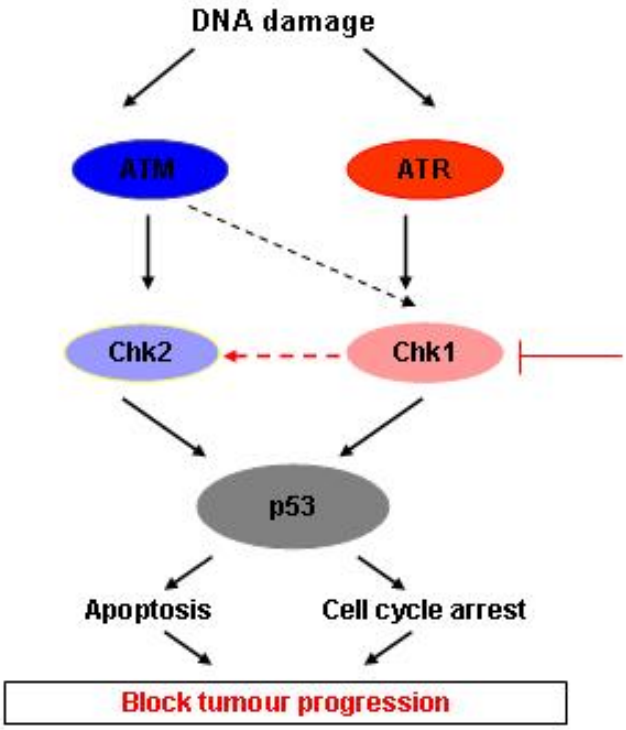

Figure 6.1 A proposed mechanism for the activation of p53 following Chk1 depletion. Upon damage the activation of checkpoint kinases occurs through ATM and ATR which lead to the activation of p53. Upon depletion of Chk1, there may be a crosstalk between pathways whereby Chk2 is activated to allow subsequent activation of p53 leading to senescence and cell death.

In addition to the potential role of Chk1 and DAPK1 as negative regulators of p53, we have also shown DAPK1 as well as Chk1 to stimulate phosphorylation of p53 leading to its transcriptional activation (see sections 3.2.2 and 3.2.3). These results, although contradictory, agree with the current controversy in the field and may suggest an overall role for kinases such as DAPK1 as survival factors which supports recent literature (Lin et al. 2007). This role in which kinases such as DAPK1 both activate and repress p53 to promote survival could have several implications. DAPK1 may be able to 'sense' the varying cellular conditions conditions or cellular environment and promote either activation or repression of p53, as appropriate, by phosphorylation at different residues to ensure the survival of the cell. For example, DAPK1 normally represses p53 when there is no damage to ensure that the cell can go on dividing as normal. However, upon damage DAPK1 phosphorylates p53 which ensures that the damaged cells are either eliminated or arrested until the damage is repaired. This prevents the propagation of mutated cells and ensures the survival of the tissue as a whole.

6.4.2 Development of drug targets

The disruption of normal signal transduction pathways is a key feature in the development and progression of cancer. Kinases are therefore therapeutically important drug targets. Upon targeted depletion of either Chk1 or DAPK1 there was significant stimulation of p53 target genes, which suggests that kinases such as DAPK1 and Chk1 could be exploited as putative drug targets for reactivation of the p53 response. Upon validation, using techniques such as flow cytometry, the implication of this data could be significant and could provide a platform on which to develop specific kinase inhibitors to allow reactivation of the p53 response and therefore the induction of cell cycle arrest and apoptosis to prevent progression of tumours. Several reports have examined the roles of kinases such as Chk1 as therapeutic targets for cancer treatment (Xiao et al. 2006; Vitale et al. 2007). In light of these reports, as well as the data we have presented here, further investigation should focus on the development of kinases inhibitors which

promote the reactivation of p53 to advance the elimination of the tumour. Several reports, such as the use of the Mdm2 inhibitor Nutlin-3 to activate the p53 pathway (Vassilev et al. 2004), have shown the valuable role of small molecule inhibitors. Development of small molecule inhibitors to kinases has already been successful in some cases such as the tyrosine kinase inhibitor gleevec (or imatinib) which has been used in the clinic to treat certain types of cancer. Several other kinase inhibitors are currently being developed as anti-cancer agents (Zhou and Bartek 2004). The data presented here suggests that there would be therapeutic value in developing small molecule inhibitors to kinases (such as Chk1 and DAPK1) involved in the p53 signalling pathway.

6.5 Conclusion

The activation of p53 is crucial step in the pathway which controls tumour progression. It is therefore unsurprising that the p53 pathway is compromised in most human cancers. The identification of Chk1 and DAPK1 as key modifiers of the p53 signalling pathway *in vivo* has been a crucial development in field. Investigations have allowed the elucidation of the role of specific regions within p53 for the complex docking-dependent interactions of kinases and/or Mdm2 with p53. The identification of Chk1 and DAPK1 as suppressors of p53 was a surprising but significant development in the study of p53. This finding may result in the development of anti-cancer drugs targeted to Chk1 or DAPK, with the aim of reactivating the p53 pathway, and thereby inhibiting tumour progression.

7 REFERENCES

Agarwal, M. L., W. R. Taylor, et al. (1998). "The p53 network." J Biol Chem **273**(1): 1-4.

Ahn, J., M. Urist, et al. (2003). "Questioning the role of checkpoint kinase 2 in the p53 DNA damage response." J Biol Chem **278**(23): 20480-9.

Ahn, J., M. Urist, et al. (2004). "The Chk2 protein kinase." DNA Repair (Amst) **3**(8-9): 1039-47.

Alarcon, R., C. Koumenis, et al. (1999). "Hypoxia induces p53 accumulation through MDM2 down-regulation and inhibition of E6-mediated degradation." Cancer Res **59**(24): 6046-51.

Allen, J. B., Z. Zhou, et al. (1994). "The SAD1/RAD53 protein kinase controls multiple checkpoints and DNA damage-induced transcription in yeast." Genes Dev **8**(20): 2401-15.

Ang, H. C., A. C. Joerger, et al. (2006). "Effects of common cancer mutations on stability and DNA binding of full-length p53 compared with isolated core domains." J Biol Chem **281**(31): 21934-41.

Anjum, R., P. P. Roux, et al. (2005). "The tumor suppressor DAP kinase is a target of RSK-mediated survival signaling." Curr Biol **15**(19): 1762-7.

Antoni, L., N. Sodha, et al. (2007). "CHK2 kinase: cancer susceptibility and cancer therapy - two sides of the same coin?" Nat Rev Cancer **7**(12): 925-36.

Appella, E. and C. W. Anderson (2001). "Post-translational modifications and activation of p53 by genotoxic stresses." Eur J Biochem **268**(10): 2764-72.

Arienti, K. L., A. Brunmark, et al. (2005). "Checkpoint kinase inhibitors: SAR and radioprotective properties of a series of 2-arylbenzimidazoles." J Med Chem **48**(6): 1873-85.

Asher, G. and Y. Shaul (2005). "p53 proteasomal degradation: poly-ubiquitination is not the whole story." Cell Cycle **4**(8): 1015-8.

Baker, S. J., E. R. Fearon, et al. (1989). "Chromosome 17 deletions and p53 gene mutations in colorectal carcinomas." Science **244**(4901): 217-21.

Baker, S. J., S. Markowitz, et al. (1990). "Suppression of human colorectal carcinoma cell growth by wild-type p53." Science **249**(4971): 912-5.

Banin, S., L. Moyal, et al. (1998). "Enhanced phosphorylation of p53 by ATM in response to DNA damage." Science **281**(5383): 1674-7.

Barak, Y., T. Juven, et al. (1993). "mdm2 expression is induced by wild type p53 activity." Embo J **12**(2): 461-8.

Bartek, J., J. Falck, et al. (2001). "CHK2 kinase--a busy messenger." Nat Rev Mol Cell Biol **2**(12): 877-86.

Bartek, J., C. Lukas, et al. (2004). "Checking on DNA damage in S phase." Nat Rev Mol Cell Biol **5**(10): 792-804.

Bartek, J. and J. Lukas (2003). "Chk1 and Chk2 kinases in checkpoint control and cancer." Cancer Cell **3**(5): 421-9.

Bell, D. W., J. M. Varley, et al. (1999). "Heterozygous germ line hCHK2 mutations in Li-Fraumeni syndrome." Science **286**(5449): 2528-31.

Benchimol, S., P. Lamb, et al. (1985). "Transformation associated p53 protein is encoded by a gene on human chromosome 17." Somat Cell Mol Genet **11**(5): 505-10.

Bensaad, K., A. Tsuruta, et al. (2006). "TIGAR, a p53-inducible regulator of glycolysis and apoptosis." Cell **126**(1): 107-20.

Bergamaschi, D., M. Gasco, et al. (2003). "p53 polymorphism influences response in cancer chemotherapy via modulation of p73-dependent apoptosis." Cancer Cell **3**(4): 387-402.

Bergstralh, D. T. and J. P. Ting (2006). "Microtubule stabilizing agents: their molecular signaling consequences and the potential for enhancement by drug combination." Cancer Treat Rev **32**(3): 166-79.

Bialik, S., A. R. Bresnick, et al. (2004). "DAP-kinase-mediated morphological changes are localization dependent and involve myosin-II phosphorylation." Cell Death Differ **11**(6): 631-44.

Bialik, S. and A. Kimchi (2004). "DAP-kinase as a target for drug design in cancer and diseases associated with accelerated cell death." Semin Cancer Biol **14**(4): 283-94.

Bialik, S. and A. Kimchi (2006). "The Death-Associated Protein Kinases: Structure, Function, and Beyond." Annu Rev Biochem.

Biondi, R. M. and A. R. Nebreda (2003). "Signalling specificity of Ser/Thr protein kinases through docking-site-mediated interactions." Biochem J **372**(Pt 1): 1-13.

Blandino, G. and M. Dobbelstein (2004). "p73 and p63: why do we still need them?" Cell Cycle **3**(7): 886-94.

Blasina, A., I. V. de Weyer, et al. (1999). "A human homologue of the checkpoint kinase Cds1 directly inhibits Cdc25 phosphatase." Curr Biol **9**(1): 1-10.

Blaydes, J. P. and T. R. Hupp (1998). "DNA damage triggers DRB-resistant phosphorylation of human p53 at the CK2 site." Oncogene **17**(8): 1045-52.

Bode, A. M. and Z. Dong (2004). "Post-translational modification of p53 in tumorigenesis." Nat Rev Cancer **4**(10): 793-805.

Bottger, A., V. Bottger, et al. (1997). "Molecular characterization of the hdm2-p53 interaction." J Mol Biol **269**(5): 744-56.

Bottger, A., V. Bottger, et al. (1997). "Design of a synthetic Mdm2-binding mini protein that activates the p53 response in vivo." Curr Biol **7**(11): 860-9.

Bourdon, J. C., K. Fernandes, et al. (2005). "p53 isoforms can regulate p53 transcriptional activity." Genes Dev **19**(18): 2122-37.

Bourke, E., H. Dodson, et al. (2007). "DNA damage induces Chk1-dependent centrosome amplification." EMBO Rep **8**(6): 603-9.

Brown, A. L., C. H. Lee, et al. (1999). "A human Cds1-related kinase that functions downstream of ATM protein in the cellular response to DNA damage." Proc Natl Acad Sci U S A **96**(7): 3745-50.

Bruins, W., E. Zwart, et al. (2004). "Increased sensitivity to UV radiation in mice with a p53 point mutation at Ser389." Mol Cell Biol **24**(20): 8884-94.

Bullock, A. N., J. Henckel, et al. (2000). "Quantitative analysis of residual folding and DNA binding in mutant p53 core domain: definition of mutant states for rescue in cancer therapy." Oncogene **19**(10): 1245-56.

Bulyk, M. L. (2006). "DNA microarray technologies for measuring protein-DNA interactions." Curr Opin Biotechnol **17**(4): 422-30.

Buscemi, G., P. Perego, et al. (2004). "Activation of ATM and Chk2 kinases in relation to the amount of DNA strand breaks." Oncogene **23**(46): 7691-700.

Bykov, V. J., G. Selivanova, et al. (2003). "Small molecules that reactivate mutant p53." Eur J Cancer **39**(13): 1828-34.

Cadwell, C. and G. P. Zambetti (2001). "The effects of wild-type p53 tumor suppressor activity and mutant p53 gain-of-function on cell growth." Gene **277**(1-2): 15-30.

Campomenosi, P., P. Monti, et al. (2001). "p53 mutants can often transactivate promoters containing a p21 but not Bax or PIG3 responsive elements." Oncogene **20**(27): 3573-9.

Carling, D. (2004). "The AMP-activated protein kinase cascade--a unifying system for energy control." Trends Biochem Sci **29**(1): 18-24.

Carrassa, L., M. Broggini, et al. (2004). "Chk1, but not Chk2, is involved in the cellular response to DNA damaging agents: differential activity in cells expressing or not p53." Cell Cycle **3**(9): 1177-81.

Ceskova, P., H. Chichger, et al. (2006). "On the mechanism of sequence-specific DNA-dependent acetylation of p53: the acetylation motif is exposed upon DNA binding." J Mol Biol **357**(2): 442-56.

Chan, H. M. and N. B. La Thangue (2001). "p300/CBP proteins: HATs for transcriptional bridges and scaffolds." J Cell Sci **114**(Pt 13): 2363-73.

Chehab, N. H., A. Malikzay, et al. (1999). "Phosphorylation of Ser-20 mediates stabilization of human p53 in response to DNA damage." Proc Natl Acad Sci U S A **96**(24): 13777-82.

Chen, C., S. Shimizu, et al. (2005). "Chk2 regulates transcription-independent p53-mediated apoptosis in response to DNA damage." Biochem Biophys Res Commun **333**(2): 427-31.

Chen, C. H., W. J. Wang, et al. (2005). "Bidirectional signals transduced by DAPK-ERK interaction promote the apoptotic effect of DAPK." Embo J **24**(2): 294-304.

Chen, C. R., W. Wang, et al. (2005). "Dual induction of apoptosis and senescence in cancer cells by Chk2 activation: checkpoint activation as a strategy against cancer." Cancer Res **65**(14): 6017-21.

Chen, D., N. Kon, et al. (2005). "ARF-BP1/Mule is a critical mediator of the ARF tumor suppressor." Cell **121**(7): 1071-83.

Chen, J., X. Wu, et al. (1996). "mdm-2 inhibits the G1 arrest and apoptosis functions of the p53 tumor suppressor protein." Mol Cell Biol **16**(5): 2445-52.

Chen, L. and J. Chen (2003). "MDM2-ARF complex regulates p53 sumoylation." Oncogene **22**(34): 5348-57.

Chen, P., C. Luo, et al. (2000). "The 1.7 A crystal structure of human cell cycle checkpoint kinase Chk1: implications for Chk1 regulation." Cell **100**(6): 681-92.

Chen, Y. and Y. Sanchez (2004). "Chk1 in the DNA damage response: conserved roles from yeasts to mammals." DNA Repair (Amst) **3**(8-9): 1025-32.

Chen, Z., L. C. Trotman, et al. (2005). "Crucial role of p53-dependent cellular senescence in suppression of Pten-deficient tumorigenesis." Nature **436**(7051): 725-30.

Chen, Z., Z. Xiao, et al. (2006). "Selective Chk1 inhibitors differentially sensitize p53-deficient cancer cells to cancer therapeutics." Int J Cancer **119**(12): 2784-94.

Chin, K. V., K. Ueda, et al. (1992). "Modulation of activity of the promoter of the human MDR1 gene by Ras and p53." Science **255**(5043): 459-62.

Chini, C. C. and J. Chen (2003). "Human claspin is required for replication checkpoint control." J Biol Chem **278**(32): 30057-62.

Cho, S. H., C. D. Toouli, et al. (2005). "Chk1 is essential for tumor cell viability following activation of the replication checkpoint." Cell Cycle **4**(1): 131-9.

Cho, Y., S. Gorina, et al. (1994). "Crystal structure of a p53 tumor suppressor-DNA complex: understanding tumorigenic mutations." Science **265**(5170): 346-55.

Cohen, O., E. Feinstein, et al. (1997). "DAP-kinase is a Ca2+/calmodulin-dependent, cytoskeletal-associated protein kinase, with cell death-inducing functions that depend on its catalytic activity." Embo J **16**(5): 998-1008.

Cohen, O., B. Inbal, et al. (1999). "DAP-kinase participates in TNF-alpha- and Fas-induced apoptosis and its function requires the death domain." J Cell Biol **146**(1): 141-8.

Collado, M. and M. Serrano (2005). "The senescent side of tumor suppression." Cell Cycle **4**(12): 1722-4.

Craig, A., M. Scott, et al. (2003). "Allosteric effects mediate CHK2 phosphorylation of the p53 transactivation domain." EMBO Rep **4**(8): 787-92.

Craig, A. L., J. P. Blaydes, et al. (1999). "Dephosphorylation of p53 at Ser20 after cellular exposure to low levels of non-ionizing radiation." Oncogene **18**(46): 6305-12.

Craig, A. L., L. Burch, et al. (1999). "Novel phosphorylation sites of human tumour suppressor protein p53 at Ser20 and Thr18 that disrupt the binding of mdm2 (mouse double minute 2) protein are modified in human cancers." Biochem J **342 (Pt 1)**: 133-41.

Craig, A. L., J. A. Chrystal, et al. (2007). "The MDM2 ubiquitination signal in the DNA-binding domain of p53 forms a docking site for calcium calmodulin kinase superfamily members." Mol Cell Biol **27**(9): 3542-55.

Crighton, D., S. Wilkinson, et al. (2006). "DRAM, a p53-induced modulator of autophagy, is critical for apoptosis." Cell **126**(1): 121-34.

Deb, D., M. Scian, et al. (2002). "Hetero-oligomerization does not compromise 'gain of function' of tumor-derived p53 mutants." Oncogene **21**(2): 176-89.

Deiss, L. P. and A. Kimchi (1991). "A genetic tool used to identify thioredoxin as a mediator of a growth inhibitory signal." Science **252**(5002): 117-20.

Di Agostino, S., S. Strano, et al. (2006). "Gain of function of mutant p53: the mutant p53/NF-Y protein complex reveals an aberrant transcriptional mechanism of cell cycle regulation." Cancer Cell **10**(3): 191-202.

Di Stefano, V., G. Blandino, et al. (2004). "HIPK2 neutralizes MDM2 inhibition rescuing p53 transcriptional activity and apoptotic function." Oncogene **23**(30): 5185-92.
Dittmer, D., S. Pati, et al. (1993). "Gain of function mutations in p53." Nat Genet **4**(1): 42-6.
Dixon, H. and C. J. Norbury (2002). "Therapeutic exploitation of checkpoint defects in cancer cells lacking p53 function." Cell Cycle **1**(6): 362-8.
Dornan, D., M. Eckert, et al. (2004). "Interferon regulatory factor 1 binding to p300 stimulates DNA-dependent acetylation of p53." Mol Cell Biol **24**(22): 10083-98.
Dornan, D. and T. R. Hupp (2001). "Inhibition of p53-dependent transcription by BOX-I phospho-peptide mimetics that bind to p300." EMBO Rep **2**(2): 139-44.
Dornan, D., H. Shimizu, et al. (2003). "The proline repeat domain of p53 binds directly to the transcriptional coactivator p300 and allosterically controls DNA-dependent acetylation of p53." Mol Cell Biol **23**(23): 8846-61.
Dornan, D., H. Shimizu, et al. (2003). "DNA-dependent acetylation of p53 by the transcription coactivator p300." J Biol Chem **278**(15): 13431-41.
Dornan, D., I. Wertz, et al. (2004). "The ubiquitin ligase COP1 is a critical negative regulator of p53." Nature **429**(6987): 86-92.
Draghici, S., P. Khatri, et al. (2006). "Reliability and reproducibility issues in DNA microarray measurements." Trends Genet **22**(2): 101-9.
Eckner, R., M. E. Ewen, et al. (1994). "Molecular cloning and functional analysis of the adenovirus E1A-associated 300-kD protein (p300) reveals a protein with properties of a transcriptional adaptor." Genes Dev **8**(8): 869-84.
Efeyan, A. and M. Serrano (2007). "p53: guardian of the genome and policeman of the oncogenes." Cell Cycle **6**(9): 1006-10.
el-Deiry, W. S., S. E. Kern, et al. (1992). "Definition of a consensus binding site for p53." Nat Genet **1**(1): 45-9.
Elbashir, S. M., J. Harborth, et al. (2001). "Duplexes of 21-nucleotide RNAs mediate RNA interference in cultured mammalian cells." Nature **411**(6836): 494-8.
Eliyahu, D., N. Goldfinger, et al. (1988). "Meth A fibrosarcoma cells express two transforming mutant p53 species." Oncogene **3**(3): 313-21.
Eliyahu, D., D. Michalovitz, et al. (1989). "Wild-type p53 can inhibit oncogene-mediated focus formation." Proc Natl Acad Sci U S A **86**(22): 8763-7.
Esser, C., M. Scheffner, et al. (2005). "The chaperone-associated ubiquitin ligase CHIP is able to target p53 for proteasomal degradation." J Biol Chem **280**(29): 27443-8.
Fakharzadeh, S. S., S. P. Trusko, et al. (1991). "Tumorigenic potential associated with enhanced expression of a gene that is amplified in a mouse tumor cell line." Embo J **10**(6): 1565-9.
Feijoo, C., C. Hall-Jackson, et al. (2001). "Activation of mammalian Chk1 during DNA replication arrest: a role for Chk1 in the intra-S phase checkpoint monitoring replication origin firing." J Cell Biol **154**(5): 913-23.
Feng, Z., W. Hu, et al. (2007). "The regulation of AMPK beta1, TSC2, and PTEN expression by p53: stress, cell and tissue specificity, and the role of these gene

products in modulating the IGF-1-AKT-mTOR pathways." Cancer Res **67**(7): 3043-53.
Feng, Z., H. Zhang, et al. (2005). "The coordinate regulation of the p53 and mTOR pathways in cells." Proc Natl Acad Sci U S A **102**(23): 8204-9.
Finlan, L. and T. R. Hupp (2004). "The N-terminal interferon-binding domain (IBiD) homology domain of p300 binds to peptides with homology to the p53 transactivation domain." J Biol Chem **279**(47): 49395-405.
Finlay, C. A., P. W. Hinds, et al. (1989). "The p53 proto-oncogene can act as a suppressor of transformation." Cell **57**(7): 1083-93.
Finlay, C. A., P. W. Hinds, et al. (1988). "Activating mutations for transformation by p53 produce a gene product that forms an hsc70-p53 complex with an altered half-life." Mol Cell Biol **8**(2): 531-9.
Fire, A., S. Xu, et al. (1998). "Potent and specific genetic interference by double-stranded RNA in Caenorhabditis elegans." Nature **391**(6669): 806-11.
Flores, E. R., K. Y. Tsai, et al. (2002). "p63 and p73 are required for p53-dependent apoptosis in response to DNA damage." Nature **416**(6880): 560-4.
Fuchs, B., D. O'Connor, et al. (1995). "p53 phosphorylation mutants retain transcription activity." Oncogene **10**(4): 789-93.
Fuchs, U. and A. Borkhardt (2007). "The application of siRNA technology to cancer biology discovery." Adv Cancer Res **96**: 75-102.
Gannon, J. V., R. Greaves, et al. (1990). "Activating mutations in p53 produce a common conformational effect. A monoclonal antibody specific for the mutant form." Embo J **9**(5): 1595-602.
Ghosh, J. C., T. Dohi, et al. (2006). "Activated checkpoint kinase 2 provides a survival signal for tumor cells." Cancer Res **66**(24): 11576-9.
Goodman, R. H. and S. Smolik (2000). "CBP/p300 in cell growth, transformation, and development." Genes Dev **14**(13): 1553-77.
Gorina, S. and N. P. Pavletich (1996). "Structure of the p53 tumor suppressor bound to the ankyrin and SH3 domains of 53BP2." Science **274**(5289): 1001-5.
Gozuacik, D. and A. Kimchi (2004). "Autophagy as a cell death and tumor suppressor mechanism." Oncogene **23**(16): 2891-906.
Gozuacik, D. and A. Kimchi (2006). "DAPk protein family and cancer." Autophagy **2**(2): 74-9.
Gozuacik, D. and A. Kimchi (2007). "Autophagy and cell death." Curr Top Dev Biol **78**: 217-45.
Gray, N. S., L. Wodicka, et al. (1998). "Exploiting chemical libraries, structure, and genomics in the search for kinase inhibitors." Science **281**(5376): 533-8.
Gu, W. and R. G. Roeder (1997). "Activation of p53 sequence-specific DNA binding by acetylation of the p53 C-terminal domain." Cell **90**(4): 595-606.
Hainaut, P. and M. Hollstein (2000). "p53 and human cancer: the first ten thousand mutations." Adv Cancer Res **77**: 81-137.
Hardie, D. G., D. Carling, et al. (1998). "The AMP-activated/SNF1 protein kinase subfamily: metabolic sensors of the eukaryotic cell?" Annu Rev Biochem **67**: 821-55.

Haupt, S., M. Berger, et al. (2003). "Apoptosis - the p53 network." J Cell Sci **116**(Pt 20): 4077-85.
Haupt, Y., Y. Barak, et al. (1996). "Cell type-specific inhibition of p53-mediated apoptosis by mdm2." Embo J **15**(7): 1596-606.
Haupt, Y., R. Maya, et al. (1997). "Mdm2 promotes the rapid degradation of p53." Nature **387**(6630): 296-9.
Hawley, S. A., J. Boudeau, et al. (2003). "Complexes between the LKB1 tumor suppressor, STRAD alpha/beta and MO25 alpha/beta are upstream kinases in the AMP-activated protein kinase cascade." J Biol **2**(4): 28.
Hawley, S. A., M. Davison, et al. (1996). "Characterization of the AMP-activated protein kinase kinase from rat liver and identification of threonine 172 as the major site at which it phosphorylates AMP-activated protein kinase." J Biol Chem **271**(44): 27879-87.
Hermeking, H., C. Lengauer, et al. (1997). "14-3-3 sigma is a p53-regulated inhibitor of G2/M progression." Mol Cell **1**(1): 3-11.
Hirao, A., Y. Y. Kong, et al. (2000). "DNA damage-induced activation of p53 by the checkpoint kinase Chk2." Science **287**(5459): 1824-7.
Hoheisel, J. D. (2006). "Microarray technology: beyond transcript profiling and genotype analysis." Nat Rev Genet **7**(3): 200-10.
Hollstein, M., K. Rice, et al. (1994). "Database of p53 gene somatic mutations in human tumors and cell lines." Nucleic Acids Res **22**(17): 3551-5.
Honda, R., H. Tanaka, et al. (1997). "Oncoprotein MDM2 is a ubiquitin ligase E3 for tumor suppressor p53." FEBS Lett **420**(1): 25-7.
Hong, S., R. V. Pusapati, et al. (2006). "Oncogenes and the DNA damage response: Myc and E2F1 engage the ATM signaling pathway to activate p53 and induce apoptosis." Cell Cycle **5**(8): 801-3.
Hoogervorst, E. M., W. Bruins, et al. (2005). "Lack of p53 Ser389 phosphorylation predisposes mice to develop 2-acetylaminofluorene-induced bladder tumors but not ionizing radiation-induced lymphomas." Cancer Res **65**(9): 3610-6.
Hupp, T. R., D. P. Lane, et al. (2000). "Strategies for manipulating the p53 pathway in the treatment of human cancer." Biochem J **352 Pt 1**: 1-17.
Hupp, T. R., D. W. Meek, et al. (1992). "Regulation of the specific DNA binding function of p53." Cell **71**(5): 875-86.
Hupp, T. R., D. W. Meek, et al. (1993). "Activation of the cryptic DNA binding function of mutant forms of p53." Nucleic Acids Res **21**(14): 3167-74.
Iliakis, G., Y. Wang, et al. (2003). "DNA damage checkpoint control in cells exposed to ionizing radiation." Oncogene **22**(37): 5834-47.
Imamura, K., T. Ogura, et al. (2001). "Cell cycle regulation via p53 phosphorylation by a 5'-AMP activated protein kinase activator, 5-aminoimidazole- 4-carboxamide-1-beta-D-ribofuranoside, in a human hepatocellular carcinoma cell line." Biochem Biophys Res Commun **287**(2): 562-7.
Inbal, B., S. Bialik, et al. (2002). "DAP kinase and DRP-1 mediate membrane blebbing and the formation of autophagic vesicles during programmed cell death." J Cell Biol **157**(3): 455-68.

Inbal, B., O. Cohen, et al. (1997). "DAP kinase links the control of apoptosis to metastasis." Nature **390**(6656): 180-4.
Inga, A., P. Monti, et al. (2001). "p53 mutants exhibiting enhanced transcriptional activation and altered promoter selectivity are revealed using a sensitive, yeast-based functional assay." Oncogene **20**(4): 501-13.
Inoki, K., T. Zhu, et al. (2003). "TSC2 mediates cellular energy response to control cell growth and survival." Cell **115**(5): 577-90.
Iorns, E., C. J. Lord, et al. (2007). "Utilizing RNA interference to enhance cancer drug discovery." Nat Rev Drug Discov **6**(7): 556-68.
Irwin, M. S., K. Kondo, et al. (2003). "Chemosensitivity linked to p73 function." Cancer Cell **3**(4): 403-10.
Jabbur, J. R., P. Huang, et al. (2000). "DNA damage-induced phosphorylation of p53 at serine 20 correlates with p21 and Mdm-2 induction in vivo." Oncogene **19**(54): 6203-8.
Jabbur, J. R. and W. Zhang (2002). "p53 Antiproliferative function is enhanced by aspartate substitution at threonine 18 and serine 20." Cancer Biol Ther **1**(3): 277-83.
Jackson, M. W., M. K. Agarwal, et al. (2004). "Limited role of N-terminal phosphoserine residues in the activation of transcription by p53." Oncogene **23**(25): 4477-87.
Jallepalli, P. V., C. Lengauer, et al. (2003). "The Chk2 tumor suppressor is not required for p53 responses in human cancer cells." J Biol Chem **278**(23): 20475-9.
Jin, S. and A. J. Levine (2001). "The p53 functional circuit." J Cell Sci **114**(Pt 23): 4139-40.
Joerger, A. C. and A. R. Fersht (2007). "Structure-function-rescue: the diverse nature of common p53 cancer mutants." Oncogene **26**(15): 2226-42.
Johnson, C. R., P. E. Morin, et al. (1995). "Thermodynamic analysis of the structural stability of the tetrameric oligomerization domain of p53 tumor suppressor." Biochemistry **34**(16): 5309-16.
Jones, R. G., D. R. Plas, et al. (2005). "AMP-activated protein kinase induces a p53-dependent metabolic checkpoint." Mol Cell **18**(3): 283-93.
Kakudo, Y., H. Shibata, et al. (2005). "Lack of correlation between p53-dependent transcriptional activity and the ability to induce apoptosis among 179 mutant p53s." Cancer Res **65**(6): 2108-14.
Kamijo, T., J. D. Weber, et al. (1998). "Functional and physical interactions of the ARF tumor suppressor with p53 and Mdm2." Proc Natl Acad Sci U S A **95**(14): 8292-7.
Kanda, A., H. Kawai, et al. (2005). "Aurora-B/AIM-1 kinase activity is involved in Ras-mediated cell transformation." Oncogene **24**(49): 7266-72.
Kannan, K., N. Amariglio, et al. (2001). "DNA microarrays identification of primary and secondary target genes regulated by p53." Oncogene **20**(18): 2225-34.
Kastan, M. B., Q. Zhan, et al. (1992). "A mammalian cell cycle checkpoint pathway utilizing p53 and GADD45 is defective in ataxia-telangiectasia." Cell **71**(4): 587-97.

Katsuragi, Y. and N. Sagata (2004). "Regulation of Chk1 kinase by autoinhibition and ATR-mediated phosphorylation." Mol Biol Cell **15**(4): 1680-9.
Kennelly, P. J. and E. G. Krebs (1991). "Consensus sequences as substrate specificity determinants for protein kinases and protein phosphatases." J Biol Chem **266**(24): 15555-8.
Keramaris, E., A. Hirao, et al. (2003). "Ataxia telangiectasia-mutated protein can regulate p53 and neuronal death independent of Chk2 in response to DNA damage." J Biol Chem **278**(39): 37782-9.
Kern, S. E., J. A. Pietenpol, et al. (1992). "Oncogenic forms of p53 inhibit p53-regulated gene expression." Science **256**(5058): 827-30.
Khanna, K. K., K. E. Keating, et al. (1998). "ATM associates with and phosphorylates p53: mapping the region of interaction." Nat Genet **20**(4): 398-400.
Kim, D. H. and J. J. Rossi (2007). "Strategies for silencing human disease using RNA interference." Nat Rev Genet **8**(3): 173-84.
Kim, E. and W. Deppert (2004). "Transcriptional activities of mutant p53: when mutations are more than a loss." J Cell Biochem **93**(5): 878-86.
Kimchi, A. (1998). "DAP genes: novel apoptotic genes isolated by a functional approach to gene cloning." Biochim Biophys Acta **1377**(2): F13-33.
Kishino, M., K. Yukawa, et al. (2004). "Deletion of the kinase domain in death-associated protein kinase attenuates tubular cell apoptosis in renal ischemia-reperfusion injury." J Am Soc Nephrol **15**(7): 1826-34.
Kissil, J. L., E. Feinstein, et al. (1997). "DAP-kinase loss of expression in various carcinoma and B-cell lymphoma cell lines: possible implications for role as tumor suppressor gene." Oncogene **15**(4): 403-7.
Kleivi, K., G. E. Lind, et al. (2007). "Gene expression profiles of primary colorectal carcinomas, liver metastases, and carcinomatoses." Mol Cancer **6**: 2.
Kortlever, R. M., P. J. Higgins, et al. (2006). "Plasminogen activator inhibitor-1 is a critical downstream target of p53 in the induction of replicative senescence." Nat Cell Biol **8**(8): 877-84.
Koumenis, C., R. Alarcon, et al. (2001). "Regulation of p53 by hypoxia: dissociation of transcriptional repression and apoptosis from p53-dependent transactivation." Mol Cell Biol **21**(4): 1297-310.
Kubbutat, M. H., S. N. Jones, et al. (1997). "Regulation of p53 stability by Mdm2." Nature **387**(6630): 299-303.
Kubbutat, M. H., R. L. Ludwig, et al. (1998). "Regulation of Mdm2-directed degradation by the C terminus of p53." Mol Cell Biol **18**(10): 5690-8.
Lambert, P. F., F. Kashanchi, et al. (1998). "Phosphorylation of p53 serine 15 increases interaction with CBP." J Biol Chem **273**(49): 33048-53.
Lane, D. P. (1992). "Cancer. p53, guardian of the genome." Nature **358**(6381): 15-6.
Lane, D. P. and L. V. Crawford (1979). "T antigen is bound to a host protein in SV40-transformed cells." Nature **278**(5701): 261-3.
Lane, D. P. and T. R. Hupp (2003). "Drug discovery and p53." Drug Discov Today **8**(8): 347-55.

Lang, G. A., T. Iwakuma, et al. (2004). "Gain of function of a p53 hot spot mutation in a mouse model of Li-Fraumeni syndrome." Cell **119**(6): 861-72.
Latonen, L. and M. Laiho (2005). "Cellular UV damage responses--functions of tumor suppressor p53." Biochim Biophys Acta **1755**(2): 71-89.
Lavin, M. F. and N. Gueven (2006). "The complexity of p53 stabilization and activation." Cell Death Differ **13**(6): 941-50.
Lee, J. H. and T. T. Paull (2004). "Direct activation of the ATM protein kinase by the Mre11/Rad50/Nbs1 complex." Science **304**(5667): 93-6.
Lee, J. S., K. M. Collins, et al. (2000). "hCds1-mediated phosphorylation of BRCA1 regulates the DNA damage response." Nature **404**(6774): 201-4.
Leng, R. P., Y. Lin, et al. (2003). "Pirh2, a p53-induced ubiquitin-protein ligase, promotes p53 degradation." Cell **112**(6): 779-91.
Leu, J. I., P. Dumont, et al. (2004). "Mitochondrial p53 activates Bak and causes disruption of a Bak-Mcl1 complex." Nat Cell Biol **6**(5): 443-50.
Levine, A. J. (1997). "p53, the cellular gatekeeper for growth and division." Cell **88**(3): 323-31.
Li, L., J. Liao, et al. (2001). "A TSG101/MDM2 regulatory loop modulates MDM2 degradation and MDM2/p53 feedback control." Proc Natl Acad Sci U S A **98**(4): 1619-24.
Li, L. and A. H. Ross (2007). "Why is PTEN an important tumor suppressor?" J Cell Biochem **102**(6): 1368-74.
Li, M., C. L. Brooks, et al. (2004). "A dynamic role of HAUSP in the p53-Mdm2 pathway." Mol Cell **13**(6): 879-86.
Li, M., C. L. Brooks, et al. (2003). "Mono- versus polyubiquitination: differential control of p53 fate by Mdm2." Science **302**(5652): 1972-5.
Li, M., D. Chen, et al. (2002). "Deubiquitination of p53 by HAUSP is an important pathway for p53 stabilization." Nature **416**(6881): 648-53.
Li, Y. and C. Prives (2007). "Are interactions with p63 and p73 involved in mutant p53 gain of oncogenic function?" Oncogene **26**(15): 2220-5.
Lill, N. L., S. R. Grossman, et al. (1997). "Binding and modulation of p53 by p300/CBP coactivators." Nature **387**(6635): 823-7.
Lin, J., J. Chen, et al. (1994). "Several hydrophobic amino acids in the p53 amino-terminal domain are required for transcriptional activation, binding to mdm-2 and the adenovirus 5 E1B 55-kD protein." Genes Dev **8**(10): 1235-46.
Lin, W. C., F. T. Lin, et al. (2001). "Selective induction of E2F1 in response to DNA damage, mediated by ATM-dependent phosphorylation." Genes Dev **15**(14): 1833-44.
Lin, Y., C. Stevens, et al. (2007). "Identification of a dominant negative functional domain on DAPK-1 that degrades DAPK-1 protein and stimulates TNFR-1-mediated apoptosis." J Biol Chem **282**(23): 16792-802.
Linzer, D. I. and A. J. Levine (1979). "Characterization of a 54K dalton cellular SV40 tumor antigen present in SV40-transformed cells and uninfected embryonal carcinoma cells." Cell **17**(1): 43-52.

Linzer, D. I., W. Maltzman, et al. (1979). "The SV40 A gene product is required for the production of a 54,000 MW cellular tumor antigen." Virology **98**(2): 308-18.
Liu, G. and X. Chen (2006). "Regulation of the p53 transcriptional activity." J Cell Biochem **97**(3): 448-58.
Liu, Q., S. Guntuku, et al. (2000). "Chk1 is an essential kinase that is regulated by Atr and required for the G(2)/M DNA damage checkpoint." Genes Dev **14**(12): 1448-59.
Llambi, F., F. C. Lourenco, et al. (2005). "The dependence receptor UNC5H2 mediates apoptosis through DAP-kinase." Embo J **24**(6): 1192-201.
Lopez-Girona, A., K. Tanaka, et al. (2001). "Serine-345 is required for Rad3-dependent phosphorylation and function of checkpoint kinase Chk1 in fission yeast." Proc Natl Acad Sci U S A **98**(20): 11289-94.
Lou, Z., K. Minter-Dykhouse, et al. (2003). "MDC1 is coupled to activated CHK2 in mammalian DNA damage response pathways." Nature **421**(6926): 957-61.
Lu, H. and A. J. Levine (1995). "Human TAFII31 protein is a transcriptional coactivator of the p53 protein." Proc Natl Acad Sci U S A **92**(11): 5154-8.
Lu, X. and D. P. Lane (1993). "Differential induction of transcriptionally active p53 following UV or ionizing radiation: defects in chromosome instability syndromes?" Cell **75**(4): 765-78.
Ludes-Meyers, J. H., M. A. Subler, et al. (1996). "Transcriptional activation of the human epidermal growth factor receptor promoter by human p53." Mol Cell Biol **16**(11): 6009-19.
Lukashchuk, N. and K. H. Vousden (2007). "Ubiquitination and degradation of mutant p53." Mol Cell Biol **27**(23): 8284-95.
Ma, J., J. D. Martin, et al. (2006). "A second p53 binding site in the central domain of Mdm2 is essential for p53 ubiquitination." Biochemistry **45**(30): 9238-45.
MacPherson, D., J. Kim, et al. (2004). "Defective apoptosis and B-cell lymphomas in mice with p53 point mutation at Ser 23." Embo J **23**(18): 3689-99.
Maltzman, W. and L. Czyzyk (1984). "UV irradiation stimulates levels of p53 cellular tumor antigen in nontransformed mouse cells." Mol Cell Biol **4**(9): 1689-94.
Manning, A. T., J. T. Garvin, et al. (2007). "Molecular profiling techniques and bioinformatics in cancer research." Eur J Surg Oncol **33**(3): 255-65.
Manning, G., D. B. Whyte, et al. (2002). "The protein kinase complement of the human genome." Science **298**(5600): 1912-34.
Martin, S. E. and N. J. Caplen (2007). "Applications of RNA interference in mammalian systems." Annu Rev Genomics Hum Genet **8**: 81-108.
Marton, M. J., J. L. DeRisi, et al. (1998). "Drug target validation and identification of secondary drug target effects using DNA microarrays." Nat Med **4**(11): 1293-301.
Martoriati, A., G. Doumont, et al. (2005). "dapk1, encoding an activator of a p19ARF-p53-mediated apoptotic checkpoint, is a transcription target of p53." Oncogene **24**(8): 1461-6.
Matoba, S., J. G. Kang, et al. (2006). "p53 regulates mitochondrial respiration." Science **312**(5780): 1650-3.

Matsuoka, S., M. Huang, et al. (1998). "Linkage of ATM to cell cycle regulation by the Chk2 protein kinase." Science **282**(5395): 1893-7.
May, P. and E. May (1999). "Twenty years of p53 research: structural and functional aspects of the p53 protein." Oncogene **18**(53): 7621-36.
Maya, R., M. Balass, et al. (2001). "ATM-dependent phosphorylation of Mdm2 on serine 395: role in p53 activation by DNA damage." Genes Dev **15**(9): 1067-77.
Meek, D. W. (2004). "The p53 response to DNA damage." DNA Repair (Amst) **3**(8-9): 1049-56.
Meek, D. W., S. Simon, et al. (1990). "The p53 tumour suppressor protein is phosphorylated at serine 389 by casein kinase II." Embo J **9**(10): 3253-60.
Menendez, D., A. Inga, et al. (2007). "Changing the p53 master regulatory network: ELEMENTary, my dear Mr Watson." Oncogene **26**(15): 2191-201.
Menendez, D., A. Inga, et al. (2006). "The biological impact of the human master regulator p53 can be altered by mutations that change the spectrum and expression of its target genes." Mol Cell Biol **26**(6): 2297-308.
Michael, D. and M. Oren (2002). "The p53 and Mdm2 families in cancer." Curr Opin Genet Dev **12**(1): 53-9.
Michael, D. and M. Oren (2003). "The p53-Mdm2 module and the ubiquitin system." Semin Cancer Biol **13**(1): 49-58.
Midgley, C. A. and D. P. Lane (1997). "p53 protein stability in tumour cells is not determined by mutation but is dependent on Mdm2 binding." Oncogene **15**(10): 1179-89.
Milner, J. (1984). "Different forms of p53 detected by monoclonal antibodies in non-dividing and dividing lymphocytes." Nature **310**(5973): 143-5.
Milner, J. and S. Milner (1981). "SV40-53K antigen: a possible role for 53K in normal cells." Virology **112**(2): 785-8.
Minsky, N. and M. Oren (2004). "The RING domain of Mdm2 mediates histone ubiquitylation and transcriptional repression." Mol Cell **16**(4): 631-9.
Moll, U. M. and O. Petrenko (2003). "The MDM2-p53 interaction." Mol Cancer Res **1**(14): 1001-8.
Momand, J., H. H. Wu, et al. (2000). "MDM2--master regulator of the p53 tumor suppressor protein." Gene **242**(1-2): 15-29.
Momand, J., G. P. Zambetti, et al. (1992). "The mdm-2 oncogene product forms a complex with the p53 protein and inhibits p53-mediated transactivation." Cell **69**(7): 1237-45.
Nagasaki, K. and Y. Miki (2006). "Gene expression profiling of breast cancer." Breast Cancer **13**(1): 2-7.
Ng, C. P., H. C. Lee, et al. (2004). "Differential mode of regulation of the checkpoint kinases CHK1 and CHK2 by their regulatory domains." J Biol Chem **279**(10): 8808-19.
Nieminen, A. L., S. Qanungo, et al. (2005). "Mdm2 and HIF-1alpha interaction in tumor cells during hypoxia." J Cell Physiol **204**(2): 364-9.
Niida, H., Y. Katsuno, et al. (2007). "Specific role of Chk1 phosphorylations in cell survival and checkpoint activation." Mol Cell Biol **27**(7): 2572-81.

Nyberg, K. A., R. J. Michelson, et al. (2002). "Toward maintaining the genome: DNA damage and replication checkpoints." Annu Rev Genet **36**: 617-56.

O'Neill, T., L. Giarratani, et al. (2002). "Determination of substrate motifs for human Chk1 and hCds1/Chk2 by the oriented peptide library approach." J Biol Chem **277**(18): 16102-15.

Oe, T., N. Nakajo, et al. (2001). "Cytoplasmic occurrence of the Chk1/Cdc25 pathway and regulation of Chk1 in Xenopus oocytes." Dev Biol **229**(1): 250-61.

Oliner, J. D., K. W. Kinzler, et al. (1992). "Amplification of a gene encoding a p53-associated protein in human sarcomas." Nature **358**(6381): 80-3.

Olive, K. P., D. A. Tuveson, et al. (2004). "Mutant p53 gain of function in two mouse models of Li-Fraumeni syndrome." Cell **119**(6): 847-60.

Oren, M. (1999). "Regulation of the p53 tumor suppressor protein." J Biol Chem **274**(51): 36031-4.

Oren, M., N. C. Reich, et al. (1982). "Regulation of the cellular p53 tumor antigen in teratocarcinoma cells and their differentiated progeny." Mol Cell Biol **2**(4): 443-9.

Ou, Y. H., P. H. Chung, et al. (2005). "p53 C-terminal phosphorylation by CHK1 and CHK2 participates in the regulation of DNA-damage-induced C-terminal acetylation." Mol Biol Cell **16**(4): 1684-95.

Pabla, N., S. Huang, et al. (2008). "ATR-Chk2 Signaling in p53 Activation and DNA Damage Response during Cisplatin-induced Apoptosis." J Biol Chem **283**(10): 6572-83.

Perou, C. M., S. S. Jeffrey, et al. (1999). "Distinctive gene expression patterns in human mammary epithelial cells and breast cancers." Proc Natl Acad Sci U S A **96**(16): 9212-7.

Perou, C. M., T. Sorlie, et al. (2000). "Molecular portraits of human breast tumours." Nature **406**(6797): 747-52.

Plomin, R. and L. C. Schalkwyk (2007). "Microarrays." Dev Sci **10**(1): 19-23.

Prives, C. and P. A. Hall (1999). "The p53 pathway." J Pathol **187**(1): 112-26.

Prives, C. and J. J. Manfredi (2005). "The continuing saga of p53--more sleepless nights ahead." Mol Cell **19**(6): 719-21.

Proud, C. G. (2007). "Signalling to translation: how signal transduction pathways control the protein synthetic machinery." Biochem J **403**(2): 217-34.

Rahman-Roblick, R., U. J. Roblick, et al. (2007). "p53 targets identified by protein expression profiling." Proc Natl Acad Sci U S A **104**(13): 5401-6.

Raveh, T., G. Droguett, et al. (2001). "DAP kinase activates a p19ARF/p53-mediated apoptotic checkpoint to suppress oncogenic transformation." Nat Cell Biol **3**(1): 1-7.

Reich, N. C. and A. J. Levine (1984). "Growth regulation of a cellular tumour antigen, p53, in nontransformed cells." Nature **308**(5955): 199-201.

Resnick, M. A. and A. Inga (2003). "Functional mutants of the sequence-specific transcription factor p53 and implications for master genes of diversity." Proc Natl Acad Sci U S A **100**(17): 9934-9.

Rhodes, D. R. and A. M. Chinnaiyan (2005). "Integrative analysis of the cancer transcriptome." Nat Genet **37 Suppl**: S31-7.

Rodriguez, R. and M. Meuth (2006). "Chk1 and p21 cooperate to prevent apoptosis during DNA replication fork stress." Mol Biol Cell **17**(1): 402-12.

Rohaly, G., J. Chemnitz, et al. (2005). "A novel human p53 isoform is an essential element of the ATR-intra-S phase checkpoint." Cell **122**(1): 21-32.

Rotter, V., O. N. Witte, et al. (1980). "Abelson murine leukemia virus-induced tumors elicit antibodies against a host cell protein, P50." J Virol **36**(2): 547-55.

Rowan, S., R. L. Ludwig, et al. (1996). "Specific loss of apoptotic but not cell-cycle arrest function in a human tumor derived p53 mutant." Embo J **15**(4): 827-38.

Ryan, K. M. and K. H. Vousden (1998). "Characterization of structural p53 mutants which show selective defects in apoptosis but not cell cycle arrest." Mol Cell Biol **18**(7): 3692-8.

Sablina, A. A., P. M. Chumakov, et al. (2001). "p53 activation in response to microtubule disruption is mediated by integrin-Erk signaling." Oncogene **20**(8): 899-909.

Saito, S., A. A. Goodarzi, et al. (2002). "ATM mediates phosphorylation at multiple p53 sites, including Ser(46), in response to ionizing radiation." J Biol Chem **277**(15): 12491-4.

Sakaguchi, K., J. E. Herrera, et al. (1998). "DNA damage activates p53 through a phosphorylation-acetylation cascade." Genes Dev **12**(18): 2831-41.

Sancar, A., L. A. Lindsey-Boltz, et al. (2004). "Molecular mechanisms of mammalian DNA repair and the DNA damage checkpoints." Annu Rev Biochem **73**: 39-85.

Saville, M. K., A. Sparks, et al. (2004). "Regulation of p53 by the ubiquitin-conjugating enzymes UbcH5B/C in vivo." J Biol Chem **279**(40): 42169-81.

Schwartz, M. F., J. K. Duong, et al. (2002). "Rad9 phosphorylation sites couple Rad53 to the Saccharomyces cerevisiae DNA damage checkpoint." Mol Cell **9**(5): 1055-65.

Sengupta, S. and C. C. Harris (2005). "p53: traffic cop at the crossroads of DNA repair and recombination." Nat Rev Mol Cell Biol **6**(1): 44-55.

Shaulsky, G., N. Goldfinger, et al. (1990). "Nuclear accumulation of p53 protein is mediated by several nuclear localization signals and plays a role in tumorigenesis." Mol Cell Biol **10**(12): 6565-77.

Shaulsky, G., N. Goldfinger, et al. (1991). "Nuclear localization is essential for the activity of p53 protein." Oncogene **6**(11): 2055-65.

Shaw, R. J., M. Kosmatka, et al. (2004). "The tumor suppressor LKB1 kinase directly activates AMP-activated kinase and regulates apoptosis in response to energy stress." Proc Natl Acad Sci U S A **101**(10): 3329-35.

Shelton, D. N., E. Chang, et al. (1999). "Microarray analysis of replicative senescence." Curr Biol **9**(17): 939-45.

Shieh, S. Y., J. Ahn, et al. (2000). "The human homologs of checkpoint kinases Chk1 and Cds1 (Chk2) phosphorylate p53 at multiple DNA damage-inducible sites." Genes Dev **14**(3): 289-300.

Shieh, S. Y., M. Ikeda, et al. (1997). "DNA damage-induced phosphorylation of p53 alleviates inhibition by MDM2." Cell **91**(3): 325-34.

Shimizu, H., L. R. Burch, et al. (2002). "The conformationally flexible S9-S10 linker region in the core domain of p53 contains a novel MDM2 binding site whose mutation increases ubiquitination of p53 in vivo." J Biol Chem **277**(32): 28446-58.

Shimizu, H., D. Saliba, et al. (2006). "Destabilizing missense mutations in the tumour suppressor protein p53 enhance its ubiquitination in vitro and in vivo." Biochem J **397**(2): 355-67.

Shohat, G., T. Spivak-Kroizman, et al. (2001). "The pro-apoptotic function of death-associated protein kinase is controlled by a unique inhibitory autophosphorylation-based mechanism." J Biol Chem **276**(50): 47460-7.

Snyder, A. R. and W. F. Morgan (2004). "Gene expression profiling after irradiation: clues to understanding acute and persistent responses?" Cancer Metastasis Rev **23**(3-4): 259-68.

Soussi, T., C. Caron de Fromentel, et al. (1990). "Structural aspects of the p53 protein in relation to gene evolution." Oncogene **5**(7): 945-52.

Soussi, T. and P. May (1996). "Structural aspects of the p53 protein in relation to gene evolution: a second look." J Mol Biol **260**(5): 623-37.

Stapleton, D., K. I. Mitchelhill, et al. (1996). "Mammalian AMP-activated protein kinase subfamily." J Biol Chem **271**(2): 611-4.

Stein, R. W., M. Corrigan, et al. (1990). "Analysis of E1A-mediated growth regulation functions: binding of the 300-kilodalton cellular product correlates with E1A enhancer repression function and DNA synthesis-inducing activity." J Virol **64**(9): 4421-7.

Stevens, C., L. Smith, et al. (2003). "Chk2 activates E2F-1 in response to DNA damage." Nat Cell Biol **5**(5): 401-9.

Stewart, G. S., B. Wang, et al. (2003). "MDC1 is a mediator of the mammalian DNA damage checkpoint." Nature **421**(6926): 961-6.

Stewart, Z. A., L. J. Tang, et al. (2001). "Increased p53 phosphorylation after microtubule disruption is mediated in a microtubule inhibitor- and cell-specific manner." Oncogene **20**(1): 113-24.

Stoughton, R. B. (2005). "Applications of DNA microarrays in biology." Annu Rev Biochem **74**: 53-82.

Suda, M., T. Ishii, et al. (2008). "A cell-based screening method for specifically detecting kinase activity." Anal Bioanal Chem **390**(1): 343-8.

Sykes, S. M., H. S. Mellert, et al. (2006). "Acetylation of the p53 DNA-binding domain regulates apoptosis induction." Mol Cell **24**(6): 841-51.

Syljuasen, R. G., C. S. Sorensen, et al. (2005). "Inhibition of human Chk1 causes increased initiation of DNA replication, phosphorylation of ATR targets, and DNA breakage." Mol Cell Biol **25**(9): 3553-62.

Takai, H., K. Naka, et al. (2002). "Chk2-deficient mice exhibit radioresistance and defective p53-mediated transcription." Embo J **21**(19): 5195-205.

Takai, H., K. Tominaga, et al. (2000). "Aberrant cell cycle checkpoint function and early embryonic death in Chk1(-/-) mice." Genes Dev **14**(12): 1439-47.
Tao, W. and A. J. Levine (1999). "P19(ARF) stabilizes p53 by blocking nucleo-cytoplasmic shuttling of Mdm2." Proc Natl Acad Sci U S A **96**(12): 6937-41.
Tereshko, V., M. Teplova, et al. (2001). "Crystal structures of the catalytic domain of human protein kinase associated with apoptosis and tumor suppression." Nat Struct Biol **8**(10): 899-907.
Thut, C. J., J. L. Chen, et al. (1995). "p53 transcriptional activation mediated by coactivators TAFII40 and TAFII60." Science **267**(5194): 100-4.
Thut, C. J., J. A. Goodrich, et al. (1997). "Repression of p53-mediated transcription by MDM2: a dual mechanism." Genes Dev **11**(15): 1974-86.
Toledo, F. and G. M. Wahl (2007). "MDM2 and MDM4: p53 regulators as targets in anticancer therapy." Int J Biochem Cell Biol **39**(7-8): 1476-82.
Tominaga, K., H. Morisaki, et al. (1999). "Role of human Cds1 (Chk2) kinase in DNA damage checkpoint and its regulation by p53." J Biol Chem **274**(44): 31463-7.
Towler, M. C. and D. G. Hardie (2007). "AMP-activated protein kinase in metabolic control and insulin signaling." Circ Res **100**(3): 328-41.
Trigiante, G. and X. Lu (2006). "ASPP [corrected] and cancer." Nat Rev Cancer **6**(3): 217-26.
Ubersax, J. A. and J. E. Ferrell, Jr. (2007). "Mechanisms of specificity in protein phosphorylation." Nat Rev Mol Cell Biol **8**(7): 530-41.
Unger, T., T. Juven-Gershon, et al. (1999). "Critical role for Ser20 of human p53 in the negative regulation of p53 by Mdm2." Embo J **18**(7): 1805-14.
van Hal, N. L., O. Vorst, et al. (2000). "The application of DNA microarrays in gene expression analysis." J Biotechnol **78**(3): 271-80.
Vassilev, L. T., B. T. Vu, et al. (2004). "In vivo activation of the p53 pathway by small-molecule antagonists of MDM2." Science **303**(5659): 844-8.
Vitale, I., L. Galluzzi, et al. (2007). "Inhibition of Chk1 Kills Tetraploid Tumor Cells through a p53-Dependent Pathway." PLoS ONE **2**(12): e1337.
Vousden, K. H. (2002). "Activation of the p53 tumor suppressor protein." Biochim Biophys Acta **1602**(1): 47-59.
Vousden, K. H. and D. P. Lane (2007). "p53 in health and disease." Nat Rev Mol Cell Biol **8**(4): 275-83.
Waldman, T., Y. Zhang, et al. (1997). "Cell-cycle arrest versus cell death in cancer therapy." Nat Med **3**(9): 1034-6.
Wallace, M., E. Worrall, et al. (2006). "Dual-site regulation of MDM2 E3-ubiquitin ligase activity." Mol Cell **23**(2): 251-63.
Walworth, N., S. Davey, et al. (1993). "Fission yeast chk1 protein kinase links the rad checkpoint pathway to cdc2." Nature **363**(6427): 368-71.
Wang, B., S. Matsuoka, et al. (2002). "53BP1, a mediator of the DNA damage checkpoint." Science **298**(5597): 1435-8.
Wang, G. L. and G. L. Semenza (1995). "Purification and characterization of hypoxia-inducible factor 1." J Biol Chem **270**(3): 1230-7.

Wang, W. J., J. C. Kuo, et al. (2002). "DAP-kinase induces apoptosis by suppressing integrin activity and disrupting matrix survival signals." J Cell Biol **159**(1): 169-79.
Wang, X., T. Arooz, et al. (2001). "MDM2 and MDMX can interact differently with ARF and members of the p53 family." FEBS Lett **490**(3): 202-8.
Wang, X., D. Michael, et al. (2002). "p53 Activation by nitric oxide involves down-regulation of Mdm2." J Biol Chem **277**(18): 15697-702.
Watson, I. R. and M. S. Irwin (2006). "Ubiquitin and ubiquitin-like modifications of the p53 family." Neoplasia **8**(8): 655-66.
Weisz, L., M. Oren, et al. (2007). "Transcription regulation by mutant p53." Oncogene **26**(15): 2202-11.
Wu, X., J. H. Bayle, et al. (1993). "The p53-mdm-2 autoregulatory feedback loop." Genes Dev **7**(7A): 1126-32.
Wu, X. and J. Chen (2003). "Autophosphorylation of checkpoint kinase 2 at serine 516 is required for radiation-induced apoptosis." J Biol Chem **278**(38): 36163-8.
Wu, X., S. R. Webster, et al. (2001). "Characterization of tumor-associated Chk2 mutations." J Biol Chem **276**(4): 2971-4.
Xiao, Z., J. Xue, et al. (2006). "Differential roles of checkpoint kinase 1, checkpoint kinase 2, and mitogen-activated protein kinase-activated protein kinase 2 in mediating DNA damage-induced cell cycle arrest: implications for cancer therapy." Mol Cancer Ther **5**(8): 1935-43.
Xu, Y. (2003). "Regulation of p53 responses by post-translational modifications." Cell Death Differ **10**(4): 400-3.
Xue, W., L. Zender, et al. (2007). "Senescence and tumour clearance is triggered by p53 restoration in murine liver carcinomas." Nature **445**(7128): 656-60.
Yang, A., M. Kaghad, et al. (2002). "On the shoulders of giants: p63, p73 and the rise of p53." Trends Genet **18**(2): 90-5.
Yu, G. W., S. Rudiger, et al. (2006). "The central region of HDM2 provides a second binding site for p53." Proc Natl Acad Sci U S A **103**(5): 1227-32.
Zachos, G., E. J. Black, et al. (2007). "Chk1 is required for spindle checkpoint function." Dev Cell **12**(2): 247-60.
Zachos, G., M. D. Rainey, et al. (2003). "Chk1-deficient tumour cells are viable but exhibit multiple checkpoint and survival defects." Embo J **22**(3): 713-23.
Zachos, G., M. D. Rainey, et al. (2005). "Chk1-dependent S-M checkpoint delay in vertebrate cells is linked to maintenance of viable replication structures." Mol Cell Biol **25**(2): 563-74.
Zakut-Houri, R., B. Bienz-Tadmor, et al. (1985). "Human p53 cellular tumor antigen: cDNA sequence and expression in COS cells." Embo J **4**(5): 1251-5.
Zakut-Houri, R., M. Oren, et al. (1983). "A single gene and a pseudogene for the cellular tumour antigen p53." Nature **306**(5943): 594-7.
Zalcenstein, A., P. Stambolsky, et al. (2003). "Mutant p53 gain of function: repression of CD95(Fas/APO-1) gene expression by tumor-associated p53 mutants." Oncogene **22**(36): 5667-76.

Zhao, H. and H. Piwnica-Worms (2001). "ATR-mediated checkpoint pathways regulate phosphorylation and activation of human Chk1." Mol Cell Biol **21**(13): 4129-39.
Zhao, R., K. Gish, et al. (2000). "Analysis of p53-regulated gene expression patterns using oligonucleotide arrays." Genes Dev **14**(8): 981-93.
Zhou, B. B. and J. Bartek (2004). "Targeting the checkpoint kinases: chemosensitization versus chemoprotection." Nat Rev Cancer **4**(3): 216-25.
Zou, L. and S. J. Elledge (2003). "Sensing DNA damage through ATRIP recognition of RPA-ssDNA complexes." Science **300**(5625): 1542-8.